



HAL
open science

Contributions to analysis and prevention of power system blackouts

Dang Toan Nguyen

► **To cite this version:**

Dang Toan Nguyen. Contributions to analysis and prevention of power system blackouts. Automatic. Institut National Polytechnique de Grenoble - INPG, 2008. English. NNT: . tel-00352414

HAL Id: tel-00352414

<https://theses.hal.science/tel-00352414>

Submitted on 13 Jan 2009

HAL is a multi-disciplinary open access archive for the deposit and dissemination of scientific research documents, whether they are published or not. The documents may come from teaching and research institutions in France or abroad, or from public or private research centers.

L'archive ouverte pluridisciplinaire **HAL**, est destinée au dépôt et à la diffusion de documents scientifiques de niveau recherche, publiés ou non, émanant des établissements d'enseignement et de recherche français ou étrangers, des laboratoires publics ou privés.

INSTITUT POLYTECHNIQUE DE GRENOBLE

N° attribué par la bibliothèque

|_|_|_|_|_|_|_|_|_|_|_|_|_|_|_|

THESE

pour obtenir le grade de

Docteur De L'Institut Polytechnique De Grenoble

Spécialité : » Automatique- Productique »

préparée au laboratoire GIPSA-LAB

dans le cadre de l'**Ecole Doctorale**

« Electronique, Electrotechnique, Automatique, Télécommunication, Signal »

présentée et soutenue publiquement

par

Dang Toan NGUYEN

Le 12 Novembre 2008

TITRE

Contribution à l'analyse et à la prévention des blackouts
de réseaux électriques

DIRECTEUR DE THÈSE

Didier GEORGES

JURY

M.	Dugard Luc	, Président
M.	Thomas Jean Luc	, Rapporteur
Mme.	Polit Monique	, Rapporteur
M.	Lam Du Son	, Examineur
M.	Tran Quoc Tuan	, Examineur
M.	Georges Didier	, Directeur de thèse

Acknowledgements

This dissertation was implemented under the educational cooperation between the French Embassy in Vietnam and Electricity of Vietnam (EVN). Over the years, the author has had the opportunity to be indebted to many people and organizations. The author is especially grateful to some people and organizations as below.

The author would like to send special thanks to **Prof. Dugard Luc** - Directeur de recherche - Gipsa-Lab - Grenoble INP for accepting to be the president of the Jury of the author's defense ceremony.

The author would like to express his gratitude to **Prof. Jean-Luc Thomas** - Chaise d'Electrotechnique - CNAM, Paris for accepting to be the first reviewer of the Jury. Prof Jean-Luc Thomas has not only given many kind and appropriate comments about the dissertation, but also supported the author with many excellent documents; one of them had been conducted by himself. Without the kind help and agreement of Prof Jean-Luc Thomas, the author would never have a chance to defend his dissertation.

The author would like to send special thanks to **Prof. Polit Monique** - Université de Perpignan for accepting to be the second reviewer of the Jury. Prof. Polit Monique has provided many useful and kind suggestions about the dissertation. The author would never forget the kindness and help of Prof Polit Monique.

The author is greatly indebted to **Dr Lam Du Son** - the vice President of Electricity of Vietnam (EVN) for accepting to be the examiner of the Jury and many good questions and kind comments about the dissertation. Without the help and support of Dr Lam Du Son, the author would never have a chance to do his PhD in France.

The author would like to express his deep gratitude to his countryman **Dr. Tran Quoc Tuan**, G2Lab - Grenoble INP, who has been accepted to be the examiner, and his family for many contributions, consistent encouragements and support. Without the zeal help and support of Dr. Tran Quoc Tuan, the author would not have been able to write and finish this dissertation. The author would never forget the whole-hearted guidelines, invaluable advice, practical and rational discussions of Dr. Tran Quoc Tuan throughout his studying time at Institut Polytechnique de Grenoble.

The author would like to express his profound gratitude, the most sincere appreciation and special thanks to his supervisor **Prof. Didier Georges** - Gipsa-Lab - Grenoble INP for his constant moral support, invaluable advice, many useful discussions, continuous encouragement and sense of responsibility. The author is greatly indebted to Prof. Didier Georges for his kindness, help, many orientations throughout the study time at Institut Polytechnique de Grenoble) - France.

It is the author's pleasure to thank the **Electricity of Vietnam (EVN)** for continuously and fully financial support during the years of studies. The author also wishes to express the deep gratitude to the **French Embassy** in Vietnam, Les services de la vie étudiant - **CROUS-Grenoble** for their huge contributions during time of studies in France. Without their support of providing accommodation, health care, administrative and social services, the author would not have been being diligent and peaceful in his studying.

The author would like to express his gratitude and special thanks to the secretaries, librarians, technicians and staffs of **Le Département Automatique de GIPSA-lab** for their administrative and technical help from the beginning till the last day of his studying in France. The author would like to send many thanks to his friends, colleagues in the laboratory for their encouragement, discussions and fun, especially some colleagues: **Mr Nguyen Hai Binh, Mr Trinh Do Hieu, Mr. Irfan Ahmad** and **Mr. Marouane Alma**.

The author acknowledges the support of **Dr. Le Anh Tuan** - a lecturer of Department of Energy and Environment - Division of Electric Power Engineering, Chalmers University of Technology, Gothenburg, Sweden, **Mr. John Diazdeleon**- an engineer of American Superconductor Inc, **Mr. Patrick Dolan**- an engineer of PJM electric system for their devoted help and document support, useful guidelines in solving the problems of using the software PSS/E. The author also would like to thank to **Dr. Le Thanh Luong** who has provided useful suggestions and excellent documents support for making the final presentation.

The author would like to send special thanks to his junior **Mr. Nguyen Quang Tuan** for spending a lot of time and efforts to comment and correct English versions of the dissertation as well as the final presentation. Many thanks are reserved for Mr Tuan's help, encouragement, sharing difficulties and joyfulness during the author's living time in Grenoble- France.

The author would like to express his gratitude and special thanks to his classmate - a good friend - **Mr Tran Quoc Dung** - an electrical engineering of Power Transmission company no 1- Electricity of Vietnam. Without whole-heater help, continuous support and useful discussions of Mr Tran Quoc Dung, the author would neither be able to use proficiently the software PSS/E nor finish his work. Mr Tran Quoc Dung also sent the author many useful and practical documents and technical brochures.

The author wishes to send special thanks to his closest friend **Mr. Vu Xuan An** - an electrical engineer of Electricity of Vietnam-who has been always beside the author since he was a student- for his consistent encouragements, useful suggestions, sharing difficulties and document support. Many thanks are reserved for other friends of the author for their help, sharing difficulties, encouragement and silently huge contributions.

The author is greatly indebted to his beloved girlfriend - **Ms. Le Thu Ha** - for taking care, spiritual contributions, wholehearted encouragements and sharing difficult moments during studying time in France with the author. Part of this work is dedicated to the author's beloved girlfriend, who has been enduring the author over the years.

Last and overall, the author would like to thank with extreme gratitude to the author's **beloved parents** for all difficulties, hardships and tears they have undergone in educating and bringing their son. Extreme thanks are also sent to the **beloved sister** and **brother** of the author for their encouragements, affection and sacrifice. This work is totally dedicated to his beloved parents and his family.

Grenoble-France, September 2008

NGUYEN DANG TOAN

Abstract

The electrical power system plays an important role as the major economic infrastructure in any country. As the recent increase in economic and environment pressures, the power systems become large-scale, more complex and operating closer to their stability limit. Some power system blackouts occurred around the world in recent years are consequence of stated situation. The main objective of this dissertation is to provide some solutions to prevent power systems from blackout. Some major analyses of past blackout phenomena were firstly investigated in order to understand the main causes and mechanisms. From these analyses, it is established that the major reasons for power system blackouts are directly related to the stability problems, such as angle and voltage stability. In order to prevent power system from blackout caused by small signal stability, a novel energy approach based on controllability and observability gramians has been proposed. The method was applied to choosing the optimal selection of control inputs/outputs in order to add damping torque to prevent power system oscillations. The results could be applied to large-scale power systems in order to build a new control structure with robustness properties. In this dissertation, this energy approach was also applied to prevent transient stability. The approach employs a heuristic method combination with controllability gramians to choose generators, which are used to redispatch power generation output in order to improve transient stability by increasing critical clearing time. Finally, major factors influenced on voltage collapse have been taken into account through long-term dynamic simulation. One preventive control strategy based on optimal power flow has also been proposed. The main goal of this method is to maintain the system's voltage in a desirable range. From the correction point of view, some major discussions of undervoltage load shedding based on the assumption of using intelligent and directly controlled load have been given.

Keywords: Power system blackout, small signal stability, controllability and observability gramians, transient stability, voltage collapse, undervoltage load shedding.

Table of Contents

Acknowledgements	iii
Abstract.....	v
Table of Contents	vii
List of Figures.....	xi
List of Tables	xv
Abbreviations	xvii
Résumé en Français	- 1 -
Chapter 1 INTRODUCTION	1
1.1 MOTIVATION OF THE DISSERTATION	1
1.2 OBJECTIVES OF THE DISSERTATION	2
1.2.1 Contribution to Investigation of Major Power System Blackouts.....	2
1.2.2 Contribution to Improving Small Signal Stability.....	2
1.2.3 Contribution to Improving Transient Stability	3
1.2.4 Contribution to Improving Voltage Stability and Voltage Collapse Prevention.....	3
1.3 ORGANIZATION OF THE DISSERTATION	4
1.4 LIMITATIONS AND SCOPE OF THE DISSERTATION	4
Chapter 2 POWER SYSTEM BLACKOUTS: PHENOMENA, MECHANISMS, CAUSES AND SOLUTIONS.....	5
2.1 INTRODUCTION.....	5
2.2 ANALYSIS OF POWER SYSTEM BLACKOUTS	5
2.2.1 Investigation of Recent Power System Blackouts.....	5
2.2.2 Causes of Power System Blackouts	12
2.2.3 Mechanisms of Power System Blackouts.....	13
2.2.4 Power System Stability	16
2.3 ANGLE STABILITY.....	17
2.3.1 Angle Stability Definitions.....	17
2.3.2 Methods for Angle Stability Analysis	18
2.3.3 Preventive Methods for Angle Stability Improvement.....	30
2.4 VOLTAGE STABILITY	31
2.4.1 Voltage Stability Definitions.....	31
2.4.2 Voltage Collapse Scenarios.....	33
2.4.3 Methods for Voltage Stability Analysis	34
2.4.4 Preventive and Corrective Methods to Prevent Voltage Collapse.....	37
2.5 MAJOR SUGGESTIONS FOR Preventions of POWER SYSTEM BLACKOUTS.....	41

2.6 CONCLUSIONS	43
Chapter 3 AN ENERGY APPROACH TO OPTIMAL PLACEMENT OF CONTROLLERS/SENSORS FOR IMPROVEMENT OF ANGLE STABILITY	45
3.1 INTRODUCTION.....	45
3.2 CONTROLLABILITY AND OBSERVABILITY GRAMIANS	48
3.2.1 Gramians Definitions	48
3.2.2 Balanced Realization for Model Reduction of Linearized Power System	49
3.3 PROCEDURE FOR OPTIMAL SELECTION OF CONTROLLERS AND SENSORS IN POWER SYSTEM	51
3.4 TWO APPLICATIONS	53
3.4.1 A Two-Area Power System.....	53
3.4.2 A “39 Bus New England Power System”	66
3.5 CONCLUSIONS	72
Chapter 4 TRANSIENT STABILITY AND PREVENTION CONTROL	75
4.1 INTRODUCTION.....	75
4.2 TRANSIENT STABILITY TIME-DOMAIN SIMULATION.....	77
4.2.1 Active Power Output of Generator near a Fault.....	78
4.2.2 Fault Locations	79
4.2.3 Fault Clearing Time.....	80
4.3 NEW PREVENTION METHOD FOR TRANSIENT STABILITY	81
4.3.1 Some Recalls on Controllability and observability gramians	81
4.3.2 Redispatch Generation Output to Improve Critical Clearing Time.....	82
4.4 APPLICATION.....	85
4.5 CONCLUSIONS	92
Chapter 5 DYNAMIC SIMULATION, PREVENTIVE AND CORRECTIVE METHODS TO PREVENT VOLTAGE COLLAPSE	93
5.1 INTRODUCTION.....	93
5.2 DYNAMIC SIMULATION OF VOLTAGE COLLAPSE.....	94
5.2.1 Factors Influencing on Voltage Collapse of “BPA Power System”	94
5.2.2 Dynamic Simulation of Voltage Collapse for “Nordic Power System”	108
5.3 PREVENTIVE METHOD FOR VOLTAGE COLLAPSE.....	115
5.3.1 Voltage Collapse Indicator	115
5.3.2 Secondary Voltage Control to Avoid Risk of Voltage Collapse	117
5.3.3 Dynamic Simulation.....	130
5.4 CORRECTIVE METHOD BY USING UNDERVOLTAGE LOAD SHEDDING	131

5.4.1 Choosing Thresholds for UVLS Relay.....	134
5.4.2 Choosing Amount of Load Shed.....	137
5.4.3 Choosing Time for Activation and Time Steps of UVLS	139
5.4.4 Validation of UVLS by Dynamic Simulation	140
5.5 CONCLUSIONS	144
Chapter 6 CONCLUSIONS AND PERSPECTIVES	145
6.1 CONCLUSIONS	145
6.1.1 Major Suggestions to Preventing Power System Blackouts.....	145
6.1.2 Contribution to Improving Small Signal Stability.....	146
6.1.3 Contribution to Improving Angle Transient Stability	146
6.1.4 Contribution to Improving Voltage Stability	146
6.2 PERSPECTIVES.....	147
6.2.1 Perspectives Concerning the Research.....	147
6.2.2 General Perspectives	148
Appendix A The Branch and Bound Method for Integer Programming.....	149
Appendix B The “Two-Area Power System” and “39 Bus New England Power System”	153
Appendix C The “BPA Power System” and “Nordic Power System”.....	159
Bibliography	163
Personal Publications.....	175

List of Figures

Figure 2-1: Frequency of the European power system before and after the split [18].	10
Figure 2-2: Map of under-frequency load shedding in the French power system [19].	11
Figure 2-3: General causes of power system blackouts.	13
Figure 2-4: Typical mechanisms of power system blackout.	15
Figure 2-5: Classification of power system stability.	16
Figure 2-6: Total Power of California-Oregon Interconnection observed in the blackout in USA, August 10, 1996 [22].	18
Figure 2-7: Rotor angle responses to a transient disturbance [2].	18
Figure 2-8: Single machine infinite bus (SMIB).	22
Figure 2-9: System representation with generator represented by classical model.	22
Figure 2-10: Power-angle varies to a step change in mechanical power input.	23
Figure 2-11: Single machine infinite bus (SMIB) and equivalent circuit.	25
Figure 2-12: System response to a fault: stable case and unstable case.	25
Figure 2-13: Voltage collapse during the blackout in USA, August 14, 2003 [15].	32
Figure 2-14: Main methods for voltage stability analysis.	35
Figure 3-1: Thyristor excitation system with PSS [2].	46
Figure 3-2: Wide-Area Protection and Control with PMUs [20], [81].	47
Figure 3-3: The “Two area power system” [2].	54
Figure 3-4: Full eigenvalues and critical eigenvalues of “Two-area power system”.	56
Figure 3-5: Distribution of Hankel singular values of reduced “Two-area power system”.	59
Figure 3-6: Frequency response of original and reduced of “Two-area power system”.	60
Figure 3-7: Expected controllability gramian overall scenarios.	61
Figure 3-8: Expected controllability gramian overall scenarios.	62
Figure 3-9: Static excitation system with a standard PSS.	62
Figure 3-10: Power output of G3 with different placements of a PSS.	63
Figure 3-11: Angle of G3 with different placements of a PSS.	64
Figure 3-12: Power output of G3 with different placements of two PSSs.	65
Figure 3-13: Angle of G3 with different placements of two PSSs.	65
Figure 3-14: The “39 Bus New England power system”.	66
Figure 3-15: Distribution of Hankel singular values of reduced “39 bus New England power system”.	67
Figure 3-16: Frequency response of original and reduced of “39 bus New England power system”.	68
Figure 3-17: Relative angles of G2, G8, and G9 respectively in case of fault at the line 25-26.	70
Figure 3-18: Relative angles of G2, G8, and G9 respectively in case of fault at the line 16-17.	72

Figure 4-1: Different contingencies of “39 bus New England system”.	77
Figure 4-2: Internal angle of G9 with different active power output.	78
Figure 4-3: Internal angle of G9 with different fault locations.	80
Figure 4-4: Internal angle of G9 with different fault clearing time (FCT).	81
Figure 4-5: Rescheduling power generation with the smallest CCT.	83
Figure 4-6: Quasi-linear relationship between CCT and active power output.	84
Figure 4-7: CCT with respect to power output of G6.	86
Figure 4-8: CCT with respect to power output of G9.	86
Figure 4-9: Angle of G6 before and after redispatching with FCT equal to the threshold.	88
Figure 4-10: Angle of G9 before and after redispatching with FCT equal to the threshold.	88
Figure 4-11: Angle of G2 after redispatching with FCT equal to the threshold.	89
Figure 4-12: Angle of G8 after redispatching with FCT equal to the threshold.	89
Figure 4-13: Angle of G10 after redispatching with FCT equal to the threshold.	90
Figure 4-14: Angle of G3 after redispatching with FCT equal to the threshold.	90
Figure 4-15: Angle of G4, G5 after redispatching with FCT equal to the threshold.	91
Figure 4-16: Angle of G7 before and after redispatching with FCT equal to the threshold.	91
Figure 5-1: The “BPA power system”.	95
Figure 5-2: Dynamic complex load model (CLOAD type).	98
Figure 5-3: Voltage profile at bus 11 for cases A, B and C.	98
Figure 5-4: Model for load tap changer transformer regulating secondary voltage.	99
Figure 5-5: Voltage profile of bus 11 for both case C and D.	101
Figure 5-6: Voltage profile at bus 10 and bus 11 in case D.	101
Figure 5-7: Block diagram and Inverse time characteristic of MAXEX2.	102
Figure 5-8: Influence of ULTC and OEL with respect to voltage collapse.	105
Figure 5-9: Voltage profiles of buses 11 for both cases E and F.	105
Figure 5-10: Case G-Influence of Motor load with respect to voltage collapse.	107
Figure 5-11: The “Nordic power system”.	108
Figure 5-12: Scenario 1-Voltage profile of bus 4043 with respect to different cases.	110
Figure 5-13: Scenario 1-Reactive power of generator at bus 4042 with respect to different cases.	110
Figure 5-14: Scenario 2-Voltage profile of bus 41 with respect to different cases.	111
Figure 5-15: Scenario 2-Reactive power output of G4042 with respect to different cases.	112
Figure 5-16: Scenario 3-Voltage profile of bus 46 with respect to different cases.	113
Figure 5-17: Scenario 4-Voltage profile of buses 41, 42, 43, and 46.	114
Figure 5-18: Scenario 4-Reactive power output of G4041, G4042, G4047, and G4051.	114
Figure 5-19: Voltage and L_indicator with different reactive power injected at bus 11 of “39 Bus New England power system”.	117
Figure 5-20: Voltage and L_indicator with respect to different K_{load} .	117

Figure 5-21: Tap modeling for load-flow calculation.	122
Figure 5-22: Principle of method to maintain voltage profile.	123
Figure 5-23: The 30 bus IEEE power system.	124
Figure 5-24: Voltages of the “30 bus IEEE power system” before and after re-adjustment.	125
Figure 5-25: L_indicator of the “30 bus IEEE power system” before and after re-adjustment.	126
Figure 5-26: Voltages of the “30 bus IEEE power system” before and after re-adjustment.	126
Figure 5-27: L_indicator of the “30 bus IEEE power system” before and after re-adjustment.	127
Figure 5-28: Voltage profile of the “Nordic power system” before and after re-adjustment.	129
Figure 5-29: L_indicator of the “Nordic power system” before and after re-adjustment.	129
Figure 5-30: Scenario 1: Voltage profile of bus 4043 before and after adjustment.	130
Figure 5-31: Scenario 2: Voltage profile of bus 4043 before and after adjustment.	131
Figure 5-32: Threshold voltage magnitude for setting UVLS relay.	134
Figure 5-33: Voltage profile of bus 42 when applying the rule C. W. Taylor [58].	135
Figure 5-34: Voltage profile of bus 42 when applying rule of authors in [116].	136
Figure 5-35: Voltage profile of bus 41 when applying rule of authors in [116].	137
Figure 5-36: Centralized UVLS scheme.	138
Figure 5-37: New UVLS scheme with direct load control context.	138
Figure 5-38: Scenario 1-Voltage profile of bus 41 with the proposed UVLS scheme.	140
Figure 5-39: Scenario 2-Voltage profile of bus 46 with the proposed UVLS scheme.	141
Figure 5-40: Scenario 3-Voltage profile of bus 42 with the proposed UVLS scheme.	142
Figure 5-41: Scenario 4-Voltage profile of bus 41 with the proposed UVLS scheme.	142
Figure 5-42: Scenario 5-Voltage profile of buses 41, 42, 43 with the proposed UVLS scheme.	143
Figure A-6-1: Principle of Branch and Bound method.	150
Figure B-6-2: Bloc diagram of the EXST1 model.	155
Figure B-6-3: Bloc diagram of the STAB1 power system stabilizer model.	155

List of Tables

Table 3-1: Some generated scenarios for “Two area power system”.....	54
Table 3-2: Critical eigenvalues, damping coefficient, oscillation frequency and the maximum normalized participation factor for each scenario of “Two area power system”.	57
Table 3-3: Critical eigenvalues and four maximum normalized participation factors for each scenario of “Two area power system”.....	58
Table 3-4: Index values according generator selection.....	60
Table 3-5: Index values according to generators selection.....	61
Table 3-6: Some generated scenarios for “39 bus New England system”.	67
Table 3-7: Index values according to generator selection.....	68
Table 4-1: Active power output of G9.	78
Table 4-2: Different locations of fault.....	79
Table 4-3: Different fault clearing time.....	80
Table 4-4: Initial conditions of power output.....	85
Table 4-5: CCT for contingencies.....	85
Table 4-6: New power output and total amount of shifted power.....	87
Table 4-7: Controllability gramian of generators.....	87
Table 4-8: Weighted factor and corresponding new power output of candidate generators.....	87
Table 5-1: Voltage and reactive power output of initial condition.....	95
Table 5-2: Cases study and typical scenario.....	95
Table 5-3: Typical values for exponents of load model [3].	97
Table 5-4: Generators with reactive power output limit.....	109
Table 5-5: Controlled variables before and after adjustment for the “30 bus IEEE power system”... ..	125
Table 5-6: List of controlled variables before and after adjustment for the “Nordic power system”. ..	128
Table B-1: Bus data of the “Two area power system”.	153
Table B-2: Generators load flow data of the “Two area power system”.....	153
Table B-3: Branch data of the “Two area power system”.....	153
Table B-4: Generators dynamic data of the “Two area power system”.	154
Table B-5: Excitation dynamic data of the “Two area power system”.	154
Table B-6: PSS data of the “Two area power system”.....	155
Table B-7: Bus data of the “39 bus New England System”.	156
Table B-8: Generators load flow data of the “39 bus New England System”.....	157
Table B-9: Branch data of the “39 bus New England System”.....	157
Table B-10: Transformer data of the “39 bus New England System”.	157
Table B-11: Power system stabilizers data of the “39 bus New England System”.....	158

List of figures

Table C-12: Bus data of the “BPA power system”	159
Table C-13: Generators load flow data of the “BPA power system”	159
Table C-14: Branch data of the “BPA power system”	159
Table C-15: Transformer data of the “BPA power system”	160
Table C-16: Generators dynamic data of the “BPA power system”	160
Table C-17: Excitation dynamic data of the “BPA power system”	160

Abbreviations

BPA	Bonneville Power Administration
CCT	Critical Clearing Time
CIGRE	Conseil International des Grands Réseaux Électriques or : International Council on Large Electric systems
COI	Centre of Inertia
EPRI	Electric Power Research Institute
E.ON Netz	A Transmission System Operator in Germany
ESM	Energy System Management
FACTS	Flexible AC Transmission System
FCT	Fault Clearing Time
GENCLS	Classical Generator Model
GENROE	Round Rotor Generator Model
GENSAL	Salient Pole Rotor Generator Model
HVDC	High Voltage Direct Current
HYGOV	Hydro Turbine-Governor Model
IEEE	Institute of Electrical and Electronics Engineers
MAXEX2	Over-Excitation Limiter Model
OEL	Over Excitation Limiter
OLTC1	Under-Load Tap Changer model
OMIB	One Machine Infinite Bus
PMU	Phasor Measurement Unit
PSS	Power System Stabilizer
PTI	Power Technology Inc.
RTCA	Real Time Contingency Analysis
RWE TSO	A transmission system operator in Germany - RWE Transportnetz Strom
SE	State Estimator
SEXS	Simplified Excitation System
SIME	Single Machine Equivalent
SMIB	Single Machine Infinite Bus
SSS	Small Signal Stability

Abbreviation

STAB1	Speed Sensitive Stabilizer Model
SVC	Static Var Compensator
TCSC	Thyristor Controlled Series Compensator
TEF	Transient Energy Function
TenneT	The transmission system operator in Netherlands
UEP	Unstable Equilibrium Point
ULTC	Under Load Tap Changer
UVLS	Under Voltage Load Shedding
WAMS	Wide Area Measurement Systems
WAPC	Wide Area Protection and Control

Résumé en Français

CHAPITRE 1 : INTRODUCTION

1.1 MOTIVATION DE LA THÈSE

Les réseaux électriques jouent un rôle important pour le développement économique de tous les pays. Cependant, un réseau électrique fait face à certains problèmes critiques tels que l'épuisement rapide des ressources naturelles, l'augmentation continue de la demande d'électricité, les problèmes d'environnement, et la pression économique. La présence de la génération décentralisée et de la déréglementation de la production électrique sont des facteurs qui conduisent à des réseaux électriques plus complexes et à plus grande échelle. Toutes ces difficultés amènent les réseaux électriques à leur limite de capacité. Il en résulte que les réseaux électriques sont plus vulnérables aux perturbations de différentes natures. Quelques blackouts électriques ayant eu des conséquences graves et qui se sont produits aux USA et dans les pays européens sont une illustration évidente de cette problématique.

Bien que les pannes de réseaux électriques soient devenues un souci depuis et pour des décennies, elles se produisent rarement et aucune n'est identique aux autres. Cependant leurs conséquences peuvent être énormes du point de vue économique et du point de vue de la sécurité énergétique. Par exemple, le blackout électrique qui s'est produit aux Etats-Unis en août 2003, a eu d'énormes conséquences : 65 GW de charge ont été déconnectés et il a fallu presque 30 heures pour rétablir totalement le système. Le blackout électrique qui s'est produit en Italie en septembre 2003, a eu pour conséquences que 27 GW ont été déconnectés et le coût économique a été estimé à environ 50 milliards de dollars.

Les causes de blackouts électriques sont généralement multiples. Elles sont le résultat final d'une cascade de phénomènes dynamiques compliqués; parfois les erreurs humaines ont pu amplifier la panne du système. Par conséquent, les chercheurs et les opérateurs de réseaux électriques se concentrent sur le moyen d'éliminer les causes premières des blackouts. L'objectif est de trouver des solutions pour empêcher que la plupart de problèmes graves puissent se produire à l'avenir.

Cette thèse a pour objectif de proposer quelques contributions afin de prévenir certaines situations pouvant conduire aux blackouts électriques.

1.2 OBJECTIFS DE LA THÈSE

1.2.1 Analyse des blackouts importants des réseaux électriques survenus dans le passé

Cette thèse est premièrement consacrée à l'étude des blackouts électriques importants qui se sont produits dans le monde ces dernières années. Une analyse des principales causes de ces blackouts est résumée. Des solutions déjà proposées pour étudier et prévenir les blackouts électriques sont récapitulées. Cette analyse est non seulement utile pour étudier les blackouts électriques passés mais elle est également essentielle pour développer les stratégies préventives et correctives à l'avenir.

1.2.2 Amélioration de la stabilité en présence de petites perturbations

L'instabilité face aux petites perturbations est reconnue comme une des causes principales des blackouts électriques. Afin d'éviter les pannes causées par les problèmes de stabilité limitée, plusieurs solutions ont été développées comme, l'installation de stabilisateurs de tension, l'utilisation de dispositifs d'électronique de puissance comme les FACTS. Un des problèmes les plus difficiles pour améliorer la stabilité en présence de petites perturbations est le choix d'un placement optimal des dispositifs de commande et de mesure. Dans cette thèse, une approche originale basée sur les gramiens de commandabilité et d'observabilité est proposée et appliquée à quelques exemples de réseaux. Les résultats peuvent être étendus aux grands réseaux électriques afin d'établir de nouvelles stratégies de commande robuste pour la conduite des réseaux.

1.2.3 Amélioration de la stabilité transitoire

La stabilité transitoire est un facteur particulièrement difficile à étudier en raison de ses caractéristiques complexes et non linéaires, qui sont représentées par des équations intégral-différentielles fortement non linéaires avec une évolution temporelle très rapide. La stabilité transitoire est souvent la cause initiale d'autres problèmes de stabilité tels que l'instabilité en présence de petites perturbations, ou l'instabilité de tension. En réalité, l'instabilité transitoire peut être évitée en appliquant correctement des actions préventives. Dans cette thèse, une nouvelle méthode préventive basée sur une approche énergétique est présentée. La méthode utilise une combinaison de méthodes heuristiques basées sur les gramiens de commandabilité et d'observabilité comme critère de choix des générateurs pour la redistribution de puissance afin d'augmenter le temps d'élimination critique de défauts (le TEC).

1.2.4 Amélioration de la stabilité de tension – méthodes préventive et corrective

L'instabilité de tension a été identifiée comme une des causes principales des blackouts électriques dans le passé. Avec la présence de la déréglementation de la production électrique, les contraintes environnementales ont limité le développement ou la réhabilitation des réseaux de transport; la gestion de la production, particulièrement la gestion de la puissance réactive, devient plus difficile qu'avant. Pour ces raisons, les réseaux se trouvent plus près de leur limite de stabilité. Cela peut provoquer un risque élevé d'instabilité de tension. En analysant les blackouts électriques passés, on observe que les effondrements de tension sont liés aux phénomènes dynamiques à long terme en fonction de différents facteurs. Dans cette thèse, ces facteurs importants, causes de l'effondrement de tension, ont été identifiés par la simulation dynamique à long terme. Nous proposons une stratégie préventive basée sur l'optimisation du plan de tension. En ce qui concerne les actions correctives, quelques stratégies de délestage ont été également étudiées.

CHAPITRE 2 : BLACKOUTS SUR LES RÉSEAUX ÉLECTRIQUES : CAUSES, MÉCANISMES ET SOLUTIONS

2.1. ANALYSES DES BLACKOUTS SUR LES RÉSEAUX ÉLECTRIQUES

2.1.1 Investigation de quelques blackouts récents

Pendant les deux dernières décennies, plusieurs blackouts électriques ont été rapportés dans le monde entier. De nombreuses causes telles que les conditions atmosphériques critiques, des dysfonctionnements des systèmes de conduite et de surveillance sont à l'origine de ces événements catastrophiques. Le critère de sécurité basé sur une contingence (le critère N-1) n'est pas respecté. Le dysfonctionnement des dispositifs de protection est également un facteur qui conduit à cette situation. Dans le contexte de la déréglementation, la faible coordination entre les centres de conduite, peut provoquer une faible coordination des actions correctives... etc. Par ailleurs, ces phénomènes sont amplifiés par des phénomènes dynamiques compliqués. Voici la liste de blackouts électriques étudiés :

France (19 décembre 1978), Belgique (4 août 1982), Suède (27 décembre 1983), Floride USA (17 mai 1985), Tokyo au Japon (23 juillet 1987), France (12 janvier 1987), Finlande (Août 1992), Western Systems Coordination Council (WSCC-USA) (juillet 1996), North American Electricity Reliability Council (NERC-USA) (14 août 2003), Suède/Danemark (23 septembre 2003), Italie (28 septembre 2003), Grèce (12 juillet 2004), les pays européens (4 Novembre 2008- L'enquête réalisée par la Commission de Régulation de L'énergie (CRE) a été menée avec l'appui technique de Monsieur Jean-Luc Thomas, Professeur Titulaire de la Chaire d'Électrotechnique au Conservatoire national des arts et métiers (CNAM) (Références : [1-19]).

2.1.2 Mécanisme typique des blackouts

Le mécanisme ou l'enchaînement d'événements conduisant aux blackouts électriques est directement lié aux processus de perte de stabilité; cette instabilité se manifeste principalement à travers l'instabilité angulaire, l'instabilité de fréquence et l'effondrement de tension. Le mécanisme typique des blackouts électriques peut être généralement décrit par la figure ci-dessous :

Dans cette thèse, nous nous intéressons principalement à l'instabilité angulaire et à l'effondrement de tension.

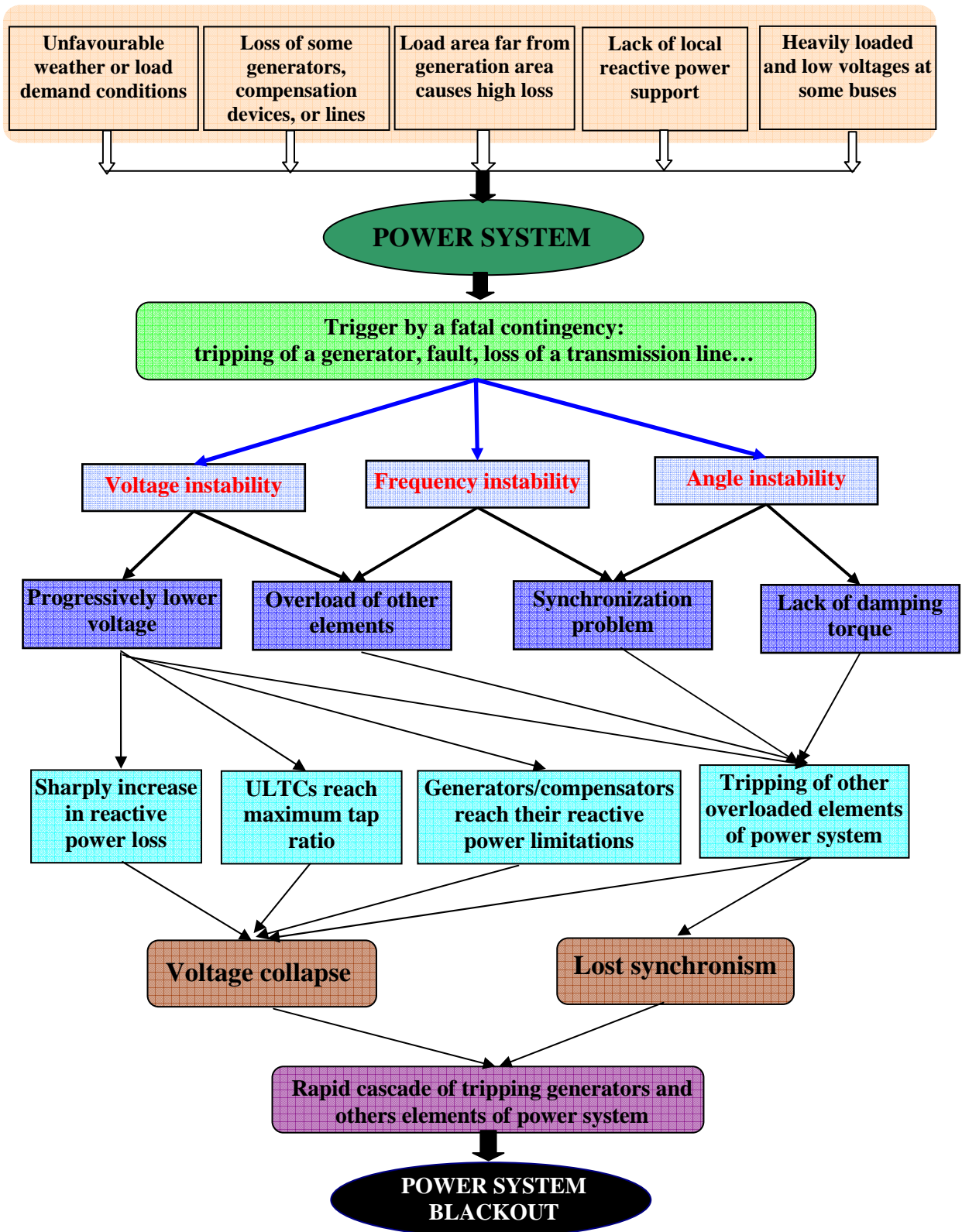


Figure 2-1 : Mécanisme typique de blackout électrique sur les réseaux.

2.2. STABILITÉ ANGULAIRE

2.2.1 Définitions de la stabilité angulaire

La stabilité angulaire est définie comme la capacité des générateurs synchrones d'un réseau à maintenir le synchronisme après avoir été soumis à une ou des perturbations. L'instabilité se traduit par des oscillations angulaires de certains générateurs menant à la perte de leur synchronisme avec les autres générateurs.

La stabilité angulaire est classifiée dans deux catégories : la stabilité des angles de rotor aux petites perturbations et la stabilité des angles de rotor aux grande perturbations, encore appelée stabilité transitoire (Référence : [1]).

2.2.2 Méthode d'étude de la stabilité angulaire

2.2.2.1 Stabilité en présence de petites perturbations

Pour cette étude, les perturbations sont normalement considérées suffisamment petites pour que la linéarisation des équations d'état du réseau puisse s'appliquer. Les méthodes traditionnelles sont basées sur l'analyse des valeurs propres, des vecteurs propres et du facteur de participation. Le facteur de participation est traditionnellement employé pour déterminer le placement optimal des systèmes de stabilisation.

Une analyse complète des valeurs propres des systèmes est souvent difficile si bien qu'il faut employer des techniques de réduction de modèle qui ne considèrent qu'une petite fraction de tous les modes de système. Plusieurs méthodes efficaces ont été rapportées dans la littérature, comme l'analyse modale sélective (SMA), la méthode d'Arnoldi, la méthode du spectre dominant Eigensolver et l'algorithme d'AESOPS développé par l'EPRI (Références : [1, 20-26])

2.2.2.2 Stabilité transitoire

Pour traiter les grands problèmes de stabilité transitoire angulaire, les méthodes traditionnelles consistent à résoudre les équations afin de déterminer la zone stable ou les marges de la stabilité. Quelques méthodes importantes sont le critère d'égalité des aires, la simulation temporelle par des méthodes numériques d'intégration, les méthodes directes utilisant une fonction d'énergie (méthode de Lyapounov), la combinaison entre le critère d'égalité des aires et la simulation temporelle (méthode SIME) (Références : [1, 27-31]).

2.2.3 Méthodes préventives

2.2.3.1 Méthode pour prévenir l'instabilité en présence de petites perturbations

La stabilité en présence de petites perturbations est liée directement à l'atténuation insuffisante des oscillations de réseaux, par conséquent, des méthodes employées pour empêcher l'instabilité en présence de petites perturbations consistent à ajouter un couple d'atténuation des oscillations. Le système de stabilisation (PSS) est considéré comme le dispositif important utilisé pour amortir les oscillations de puissance. Les approches traditionnelles sont basées sur l'analyse de sensibilité des valeurs propres, en particulier des vecteurs propres, et des facteurs de participation. Le choix optimal de PSS est classiquement déterminé en employant des facteurs de participation de quelques modes critiques. Les systèmes de transport flexible à C.A. (FACTS), ou le courant continu à haute tension (CCHT)

sont également considérés pour atténuer les oscillations de puissance (Références : [1, 31-40]).

2.2.3.2 Méthode préventive pour l'instabilité transitoire

Les différentes méthodes suivantes sont utilisées pour la prévention de l'instabilité transitoire (Référence : [1])

- Fermeture rapide des valves
- Méthodes pour augmenter les couples électriques
- Systèmes de régulation de tension performants
- Utilisation des systèmes de transport flexible (FACTS)...

2.3 STABILITÉ DE TENSION

2.3.1 Définitions de stabilité de tension

2.3.1.1 Stabilité de tension

La stabilité de tension est la capacité du réseau de maintenir la tension à tous les noeuds du réseau après avoir été soumis à une perturbation d'une condition de fonctionnement initiale donnée.

La stabilité de tension peut être encore divisée en sous-problèmes : stabilité transitoire de tension et stabilité de tension aux petites perturbations. Le délai pour le problème de l'instabilité de tension peut varier de quelques secondes à des dizaines de minutes. Par conséquent, la stabilité de tension peut être un phénomène à court terme ou à long terme. Dans cette thèse, nous nous sommes concentrés principalement sur le phénomène d'effondrement de tension à long terme (Références : [1-2, 20, 41]).

2.3.1.2 Instabilité de tension ou effondrement de tension

L'instabilité de tension provient de la tentative de charge dynamique de reconstituer la puissance qui dépasse la capacité des systèmes de transmission et de génération.

L'effondrement de tension est le processus par lequel la séquence d'opérations accompagnant l'instabilité de tension mène à un blackout électrique ou à des tensions anormalement basses dans une partie significative du réseau.

2.3.2 Scénarios d'effondrement de tension

Il y a beaucoup de scénarios pour menant à l'effondrement de tension : variation des charges (effondrement à long terme de tension), des pannes de réseau (effondrement transitoire de tension).

2.3.3 Méthodes d'étude de l'effondrement de tension

Le problème de la stabilité de tension a été étudié et analysé depuis des décennies. Cependant, la suite récente de blackouts électriques sérieux dus à l'effondrement de tension ces dernières années montre qu'il s'agit toujours d'un problème pour les chercheurs et les compagnies d'exploitation des réseaux. En particulier, beaucoup de recherches se sont concentrées sur les aspects suivants (Références : [1-2, 41-44]) :

- **Outils et techniques** : les propositions sont le choix des outils et les techniques appropriés qui peuvent être employés pour comprendre le mécanisme du problème de stabilité de tension et pour prendre des décisions de planification basées sur des simulations plus fiables. L'analyse de flux de puissance, l'analyse quasi-statique et l'analyse de stabilité transitoire sont les outils principaux qui peuvent être choisis pour faire l'analyse statique et dynamique du réseau.
- **Modélisation** : La sélection des modèles et des scénarios ou des situations de pannes appropriés pour la simulation qui est associée à l'effondrement de tension est très importante. L'interaction de la charge du système et de l'équipement tel que des dispositifs de protection de générateur, des systèmes d'excitation, des transformateur réglage en charge, de compensation de shunt et de délestage joue un rôle important dans ce processus.
- **Indicateurs** : Des indicateurs pourraient être employés pour aider des opérateurs à déterminer si l'état de système est sécurisé ou dangereux. En plus, ils pourraient être considérés comme critères pour l'évaluation de sécurité de système.
- **Stratégie de commande** : une méthodologie préventive et corrective complète est nécessaire pour éviter l'effondrement de tension. Dans les cas pour lesquels le critère de stabilité de tension n'est pas engagé, des mesures de conduite doivent être définies et prises pour améliorer la stabilité du réseau.

Beaucoup de méthodes proposées pour éviter l'effondrement de tension ont été mentionnées dans la littérature. Ces méthodes peuvent être classifiées dans deux catégories principales en tant que méthodes statiques et méthodes dynamiques comme le montre la Figure. 2-2

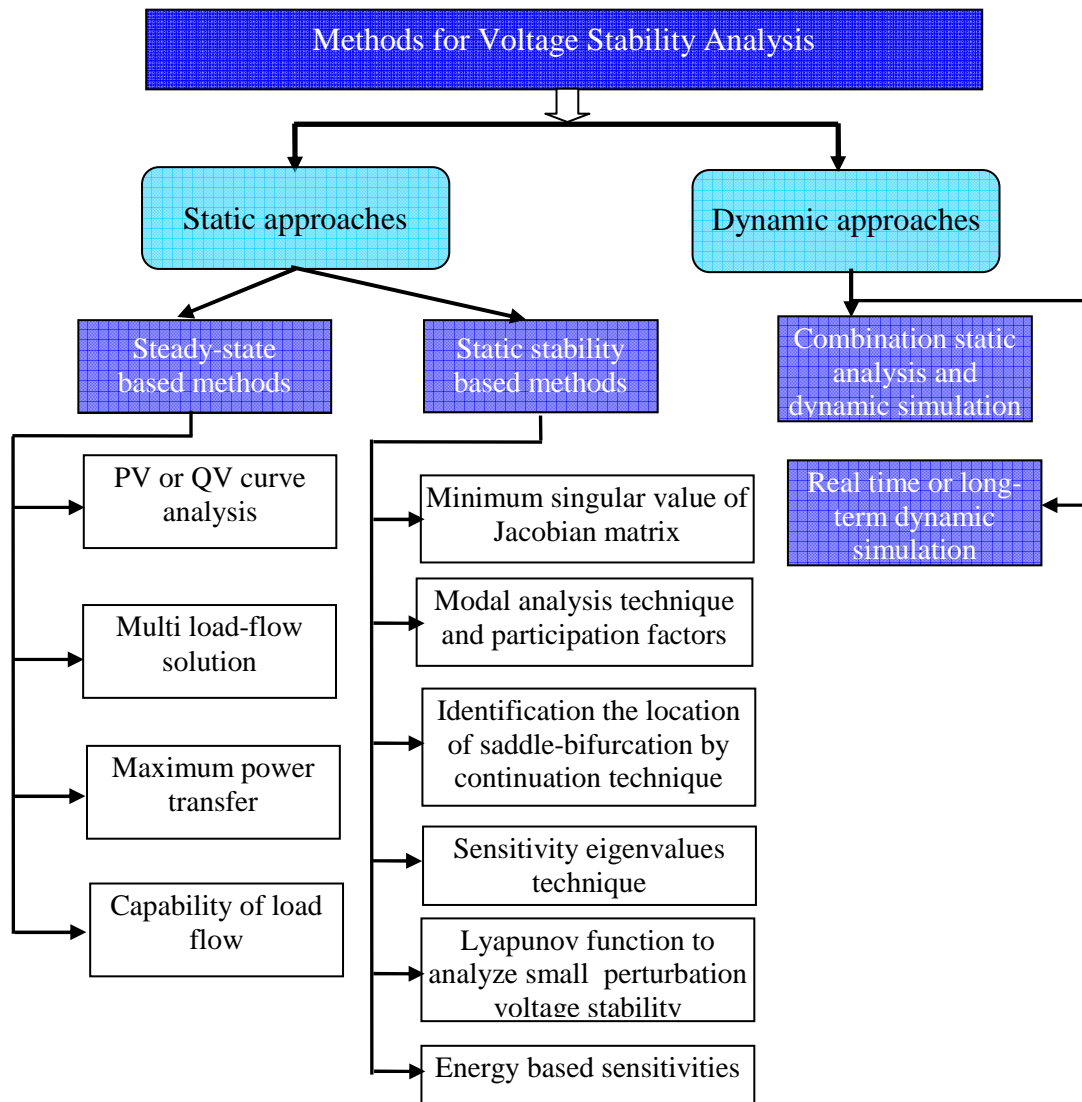


Figure 2-2: Techniques majeures pour étudier écoulement de tension.

2.3.4 Méthodes préventive et corrective d'effondrement de tension

Pour éviter l'effondrement de tension, la plupart des compagnies électriques ont défini des stratégies raisonnables de conduite ou des directives strictes auxquelles les opérateurs doivent se conformer dans les situations urgentes. Les dispositifs de conduite préventive et corrective donnent les valeurs de consigne optimales. Les différentes mesures correctives peuvent être appliquées pour augmenter la stabilité de tension du système. Certaines des stratégies possibles de conduite sont (Références : [1-2, 41-74]).

1. Réglage secondaire de tension : Cette stratégie de réglage secondaire de tension de générateur concerne la stratégie de réglage de puissance réactive, la compensation réactive par les capacité shunt, et l'ajustement des prises de transformateur réglable en charge.
2. Répartition de puissance active des groupes
3. Contrôle urgent de réglage
4. Délestage des charges.

CHAPITRE 3 : APPROCHE ÉNERGÉTIQUE POUR LE PLACEMENT OPTIMAL DES DISPOSITIFS DE CONTRÔLE OU CAPTEURS AFIN D'AMÉLIORER LA STABILITÉ ANGULAIRE

3.1 INTRODUCTION

Les réseaux électriques font face au problème des oscillations dues au manque d'atténuation de couple aux rotors des générateurs. L'atténuation insuffisante de couple peut causer des blackouts électriques critique, voir par exemples : les blackouts électriques en Suède/au Danemark et sur le réseau américain WSCC-USA. Les dispositifs (par exemple : PSS, ou FACTS) sont utilisés généralement non seulement pour atténuer des oscillations du réseau mais aussi pour améliorer également les performances du réseau. Des capteurs sont installés dans le réseau pour mesurer les signaux désirés. Ils sont utiles pour la surveillance, la protection et pour la conduite du réseau. Le PMU ou l'unité de mesure de phase offrent beaucoup d'avantages tels que l'estimation d'état linéaire, les véritables mesures simultanées et la surveillance dynamique. L'accroissement du nombre de mesures contribue à rendre les réseaux plus contrôlables. Cependant, ces dispositifs sont normalement très chers et limités dans la quantité disponible, c'est pourquoi ces dispositifs ne sont pas installés partout dans le réseau. Pour cette raison, le problème de choix de placement optimal de ces dispositifs est très important et intéressant (Références : [12, 15, 33, 78-79]).

Le problème du placement optimal des dispositifs comme les PSS, ou les FACTS ou bien les capteurs, par exemple les PMU, a déjà fait l'objet d'études dans le passé. La plupart des approches existantes sont des méthodes algébriques basées sur l'analyse de sensibilité des valeurs propres en utilisant les vecteurs propres et les facteurs de participation. Le choix optimal des contrôleurs/des capteurs est classiquement déterminé en employant des facteurs de participation de quelques modes critiques. Ces méthodes ont plusieurs inconvénients. Premièrement, la détermination des modes critiques peut être problématique en cas de systèmes à grande échelle parce que le mode critique peut ne pas être unique. En outre, la définition des modes critiques dépend également des modes d'oscillation locale ou inter-région. Deuxièmement, l'approche de facteur de participation est qu'elle traite seulement les états et n'inclut pas les comportements d'entrée/sortie. Cette approche ne peut pas effectivement identifier un emplacement optimal de contrôleur et un signal de retour en l'absence d'information sur l'entrée/sortie, qui est plus important quand le feedback de la sortie est utilisée (Références : [1, 22, 31-33, 80-82]).

Afin d'éviter ces inconvénients, dans ce chapitre, nous proposons une approche énergétique pour le choix optimal de localisations de contrôleurs/capteurs basé sur l'utilisation des gramiens de commandabilité et d'observabilité, combinée avec une technique de réduction de modèle par réalisation équilibrée. Pour prendre en considération l'effet des changements du réseau, nous proposons une approche stochastique basée sur des scénarios qui prennent en compte l'occurrence des situations défectueuses, telles que des lignes de transmission qui déclenchent, des changements de charges, avec l'objectif d'introduire une robustesse de la décision. Cette approche est fondée sur la maximisation d'un indicateur qui est défini comme l'espérance de la trace des gramiens de commandabilité et d'observabilité sur l'ensemble des scénarios.

L'idée principale est de choisir les contrôleurs (équivalents aux entrées) correspondant à l'énergie minimum requise pour commander les modes les plus significatifs du système et pour choisir le placement des capteurs correspondant au rendement maximum d'énergie des capteurs afin d'améliorer la stabilité aux petites perturbations du réseau. Cette approche peut être considérée comme l'élément d'un procédé d'optimisation à définir de nouveaux systèmes de contrôle dans le cadre de l'amélioration de sécurité des réseaux (par exemple : le choix optimal de PSSs pour améliorer la stabilité angulaire).

3.2 GRAMIENS DE COMMANDABILITE ET D'OBSERVABILITÉ

Considérons un système décrit sous la forme d'une représentation d'état :

$$\begin{aligned} \dot{x}(t) &= A.x(t) + B.u(t) \\ y &= C.x(t) \end{aligned} \quad (3.2-1)$$

Où : $A \in \mathbb{R}^{n \times n}$, $B \in \mathbb{R}^{n \times m}$, $C \in \mathbb{R}^{p \times n}$ and $x \in \mathbb{R}^n$. Nous supposons que le système décrit par l'équation (3.2-1) est contrôlable et observable. Les fonctions transitoires de commandabilité et d'observabilité d'un système linéaire sont définies respectivement :

$$\begin{aligned} L_c(X, T) &= \min_{u, x(0)=X} \frac{1}{2} \int_{-T}^0 \|u(\tau)\|^2 d\tau, x(-T) = 0 \\ L_o(X, T) &= \frac{1}{2} \int_0^T \|y(\tau)\|^2 d\tau, x(0) = X, u \equiv 0 \end{aligned} \quad (3.2-2)$$

Nous rappelons le résultat bien connu suivant (Références : [83-84])

Theorème 1 : Les fonctions transitoires de commandabilité et d'observabilité sont données par :

$$\begin{aligned} L_c(X, T) &= \frac{1}{2} X^T W_c^{-1}(T) X \\ L_o(X, T) &= \frac{1}{2} X^T W_o(T) X \end{aligned} \quad (3.2-3)$$

où : $W_c(T) = \int_{-T}^0 e^{At} B B^T e^{A^T t} dt$, $W_o(T) = \int_0^T e^{A^T t} C^T C e^{At} dt$ sont les gramiens transitoires de commandabilité et d'observabilité sur l'horizon T respectivement. Si le système dans l'équation (3.2-1) est asymptotiquement stable autour de l'origine, où $T \rightarrow \infty$: $\lim_{T \rightarrow \infty} W_c(T) = \bar{W}_c$ et $\lim_{T \rightarrow \infty} W_o(T) = \bar{W}_o$. Alors \bar{W}_c et \bar{W}_o sont obtenus comme solutions uniques définies positives des équations de Lyapunov suivantes :

$$\begin{aligned} A W_c + W_c A^T + B B^T &= 0 \\ A^T W_o + W_o A + C^T C &= 0 \end{aligned} \quad (3.2-4)$$

Puisque la matrice de commandabilité W_c dépend de la matrice d'entrée de commande B, l'énergie de commande peut être affectée en choisissant correctement cette matrice d'entrée de commande tandis que la matrice d'observabilité W_o dépend de la matrice de sortie C,

l'énergie de sortie des capteurs peut être affectée en choisissant correctement cette matrice de sorties. A partir des équations (3.2-1) et (3.2-2), on suggère qu'afin de réduire au minimum l'énergie d'entrée de commande, nous devons minimiser $(W_C)^{-1}$ ou maximiser W_C dans le sens d'une norme donnée de matrice. Afin de maximiser l'énergie de sortie des capteurs, nous devons maximiser W_O dans le sens d'une norme donnée de matrice (par exemple, la trace (W_C) ou la trace (W_O) pourrait être utilisée car une norme afin de calculer l'énergie).

3.3 PROCÉDÉ POUR LE CHOIX OPTIMAL DES CONTRÔLEURS ET DES CAPTEURS DANS LES RESEAUX ELECTRIQUES

L'utilisation de la méthode de grammiens de commandabilité et d'observabilité pour le choix optimal placement des contrôleurs/des capteurs a été proposée dans littérature. Cependant, aucun de ces auteurs n'a proposé un algorithme spécifique pour le placement optimal des contrôleurs/des capteurs pour les réseaux électriques. Dans cette section, nous proposons une approche énergétique utilisant des grammiens de commandabilité et d'observabilité pour le choix optimal des contrôleurs/des capteurs dans les réseaux électriques. L'approche consiste en sélection des contrôleurs qui fournit des signaux de commande additionnels d'entrée dans le but d'augmenter la robustesse vis-à-vis des perturbations. Elle prend en considération également l'influence de tous les contrôleurs existants dans le réseau. Le problème est alors de déterminer un ensemble d'entrées de commande M parmi les m entrées possibles liées aux générateurs du réseau afin de maximiser la commandabilité globale du système. Le problème du placement optimal des capteurs consiste à déterminer un ensemble de P capteurs parmi le n états possibles du réseau.

L'algorithme est récapitulé comme suit :

1. Produire d'un ensemble de N scénarios indépendants ω_i avec la probabilité d'occurrence $p(\omega_i)$, $i=1.., N$ (assez grand). Ces scénarios peuvent être choisis en se basant sur des situations typiques de fonctionnement de réseau électrique en question. On élimine les configurations instables en vérifiant des conditions stables de la matrice A .
2. Pour chaque scénario ω_i , $i=1, \dots, N$, effectuer la linéarisation autour de l'état d'équilibre correspondant du réseau pour obtenir l'espace d'état comme dans (3.2 1). Pour chaque scénario ω_i et chaque configuration de commande d'entrées α_i et de mesures β_i , nous mettons le système sous forme de réalisation équilibrée pour obtenir le système réduit comme suit :

$$\begin{aligned} \dot{x}^{\omega_i} &= A^{\alpha\beta}(\omega_i)x^{\omega_i} + \sum_{j=1}^m \alpha_j B_j^{\beta}(\omega_i)u_j = A^{\alpha\beta}(\omega_i)x^{\omega_i} + B^{\alpha\beta}(\omega_i)u \\ y^{\beta} &= C^{\beta}(\omega_i)x^{\omega_i} \end{aligned} \quad (3.3-1)$$

3. Le système défini par (3.3-1) a ses grammiens de commandabilité et d'observabilité qui satisfont $W_C = W_O = \Sigma^{\alpha\beta}$, où α_i est égal à 1 quand la commande d'entrée u_i est autrement choisie égale à 0, β est un vecteur de configuration de capteur : β_i est égal à 1 quand l'état $x_i(\omega_i)$ est mesuré, autrement égal à 0. α et β remplissent des conditions : $\sum_{i=1}^m \alpha_i = M$ et $\sum_{i \in I} \beta_i = P$.

4. Pour chaque scénario ω_i , calculer les grammiens de commandabilité et d'observabilité du système équilibré (Référence : [86]) : $\Sigma^{\alpha,\beta}(\omega_i)$ ce qui satisfait une de ces deux équations de Lyapunov :

$$(A^{\alpha\beta}(\omega_i)) \cdot (\Sigma^{\alpha\beta}(\omega_i)) + (\Sigma^{\alpha\beta}(\omega_i)) \cdot (A^{\alpha\beta}(\omega_i))^T + (B^{\alpha\beta}(\omega_i)) \cdot (B^{\alpha\beta}(\omega_i))^T = 0$$

or

(3.3-2)

$$(A^{\alpha\beta}(\omega_i))^T \cdot (\Sigma^{\alpha\beta}(\omega_i)) + (\Sigma^{\alpha\beta}(\omega_i)) \cdot (A^{\alpha\beta}(\omega_i)) + (C^{\beta}(\omega_i))^T \cdot (C^{\beta}(\omega_i)) = 0$$

5. Pour chaque scénario ω_i , calculer une mesure de l'énergie en utilisant la trace du gramien :

$$E(\omega_i) = \text{trace}(\Sigma^{\alpha\beta}(\omega_i))$$
(3.3-3)

6. Le choix optimal des contrôleurs/des capteurs est obtenu en résolvant le problème d'optimisation suivant :

$$\max_{\substack{\alpha_i \in \{0,1\}, i=1,\dots,m \\ \beta_i \in \{0,1\}, i \in I}} \left(E_{\omega}(X) = \frac{1}{N} \sum_{i=1}^N p(\omega_i) E(\omega_i) \right)$$
(3.3-4)

Où $E_{\omega}(X) = \frac{1}{N} \sum_{i=1}^N p(\omega_i) X(\omega_i)$ est l'espérance moyenne de tous les scénarios ω_i . (Pour

des cas simples, $p(\omega_i)$ pourrait être considéré égal à 1 qui signifie que tous les scénarios ont la même probabilité d'occurrence).

Quand les scénarios et le nombre de configurations contrôleurs/capteurs sont relativement petits (disons, $n < 20$), une solution optimale peut être trouvée par l'énumération des solutions. Cependant, en traitant le système à grande échelle, le placement optimal des contrôleurs/des capteurs est habituellement un problème d'optimisation fortement combinatoire. Pour résoudre ce problème combinatoire de grande taille, des solutions efficaces sous-optimales peuvent être obtenues en employant des méthodes telles que la méthode du recuit simulé, les algorithmes génétiques ou la méthode « Branch and Bound » (Références : [84-96]).

3.4 APPLICATIONS

L'utilisation de cette méthode est appliquée pour choisir l'emplacement optimal de configurations contrôleurs/capteurs afin d'amortir des oscillations des réseaux électriques. Deux réseaux sont utilisés : un système à deux régions et le "39 Bus New England". Le programme PSS/E est utilisé pour le calcul de répartition des charges et effectue la linéarisation du système correspondant à chaque scénario. Le programme Matlab est utilisé pour effectuer la réduction d'ordre et pour calculer la matrice gramien réduit $\Sigma^{\alpha\beta}$ dans l'équation (3.3-2). Dans la présente partie, nous nous limitons à quelques scénarios; donc le problème optimal (3.3-4) peut être résolu en employant une méthode d'énumération (Références : [97-98]).

3.4.1 Réseau système à deux régions

Le réseau système à deux régions est utilisé couramment pour des études fondamentales des oscillations de réseau électrique. Le diagramme de système est présenté sur la Figure 3-1 :

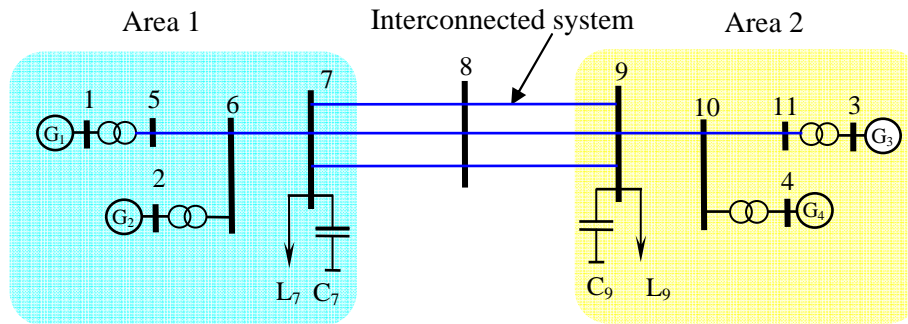


Figure 3-1: Réseau système à deux régions

Afin d'illustrer facilement l'approche, nous considérons seulement quelques scénarios comme dans le Tableau 3-1.

Tableau 3-1: Quelques scénarios pour le « réseausystème à deux régions ».

Scénario	Puissance de zone 1 à zone 2 (MW)	No de Ligne	Production / charge (MW)	
			Area 1	Area 2
1	0	1	1400/1367	1400/1367
2	100	1	1400/1267	1400/1467
3	200	1	1400/1167	1400/1567
4	400	1	1422/967	1428/1767
5	0	2	1400/1367	1400/1367
6	300	2	1400/1067	1400/1667
7	400	2	1400/967	1400/1767
8	600	2	1400/767	1400/1967
9	400	2	1600/1157	1570/1917
10	600	2	1605/947	1533/2067

Le problème est de choisir quelques emplacements de contrôleurs/capteurs à installer dans ce réseau avec le but d'améliorer ses performance et sécurité. Une application typique consiste à choisir de façon optimale le placement d'un PSS (*power system stabilizer*) pour amortir l'oscillation du réseau.

3.4.1.1 Choix optimal de l'emplacement de configurations contrôleurs/capteurs par la méthode proposée

Dans le premier cas, le problème est de choisir l'emplacement optimal d'un ensemble de contrôleurs/capteurs pour un générateur parmi quatre générateurs. Dans le deuxième cas, le problème est de choisir l'emplacement optimal d'un ensemble de contrôleurs/capteurs pour deux générateurs parmi quatre générateurs du réseau.

Pour chaque scénario dans le Tableau 3-1, nous considérons deux signaux de commande d'entrée; la consigne de puissance mécanique et la consigne de tension terminale (ΔP_{mec} et

ΔV_{ref}), et trois quantités de sorties qui peuvent être mesurées par des dispositifs de mesure; puissance active (P), puissance réactive (Q) et tension terminale (E_{ter}) qui correspondent à chaque générateur respectivement. La tension au nœud 8 (V_{bus_8}) est prise comme un signal mesuré. Le système dynamique original inclut 40 variables d'état.

Cas 1 : Choix de l'emplacement optimal de configurations contrôleurs/capteurs pour un générateur

Pour le premier cas, la valeur $E(\omega_i)$ pour chaque scénario i (avec $T = \infty$) est indiquée dans le Tableau 3-2. Dans ce cas, une solution énumérative peut être obtenue sans besoin d'employer une méthode d'optimisation en nombres entiers.

Tableau 3-2: Valeurs des indicateurs selon le générateur choisi

Scénarios	E(ω_i) correspondent avec les entrées et sorties des générateurs				Nombres correspondant de commandabilités/observabilités des variables d'état			
	G1	G2	G3	G4	G1	G2	G3	G4
1	295	402	305	426	18	18	18	18
2	306	471	291	387	18	18	18	18
3	322	512	279	363	18	18	18	18
4	868	4070	710	2488	16	18	18	16
5	301	420	318	453	18	18	18	18
6	320	451	277	347	18	18	18	18
7	315	461	275	321	18	18	18	18
8	1802	2753	1591	1518	18	18	18	18
9	381	758	303	396	18	18	18	18
10	4945	13121	4062	6304	18	18	18	18
Eω	986	2342	841	1300				

Nous pouvons voir que le choix des entrées/des sorties de G2 mène aux valeurs maximum de l'indicateurs E (X). Ceci signifie que si nous devons ajouter un ensemble de contrôleurs/capteurs sur un des générateurs du réseau afin d'améliorer la performance du réseau, l'endroit optimal est à G2.

Cas 2 : Choix de l'emplacement optimal de configurations contrôleurs/capteurs pour deux générateurs

Les valeurs $E(\omega_i)$ pour chaque scénario quand l'horizon transitoire est égal à $T = \infty$ sont indiquées dans le Tableau 3-3. Les résultats prouvent que quand nous choisissons les générateurs G2 et G4, nous obtenons la valeur maximum de l'indicateur. Ceci signifie que si nous devons déterminer la localisation de deux configurations contrôleurs/capteurs dans l'ensemble nombres générateurs du réseau pour améliorer la performance du réseau, les endroits optimaux sont à G2 et à G4.

Tableau 3-3: Valeurs des indicateurs selon le générateur choisi.

Scénario	E(ω_i) correspondant avec les entrées et sorties des générateurs					
	G1,G2	G1,G3	G1,G4	G2,G3	G2,G4	G3,G4
1	708	602	727	713	831	744
2	786	599	712	764	872	696
3	844	606	715	793	901	655
4	5093	1590	3556	4936	6621	3356
5	731	622	760	743	878	784
6	780	603	689	734	824	636
7	786	595	663	742	819	611
8	4582	3396	3352	4364	4353	3132
9	1151	691	850	1074	1243	731
10	18224	9015	11418	17315	19587	10457
Eω	3369	1832	2344	3218	3693	2180

3.4.1.2 Validation par simulation dynamique

Afin d'illustrer l'efficacité de cette méthode, nous considérons l'installation d'un PSS standard pour les générateurs

La Figure 3-2 présente une comparaison de l'atténuation d'oscillation de puissance correspondant aux trois placements possibles d'un PSS à G1, G2, G3. Cette simulation a été faite pour le scénario 4 en appliquant un défaut triphasé d'une durée de 5ms au noeud 7, la durée de simulation est 30s. La figure est tracée pour la puissance active de G3 correspondant au défaut. On observe sur la figure que le placement d'un PSS à G2 (la Ligne Verte) donne de meilleurs résultats d'atténuation des oscillations en comparaison avec les autres cas.

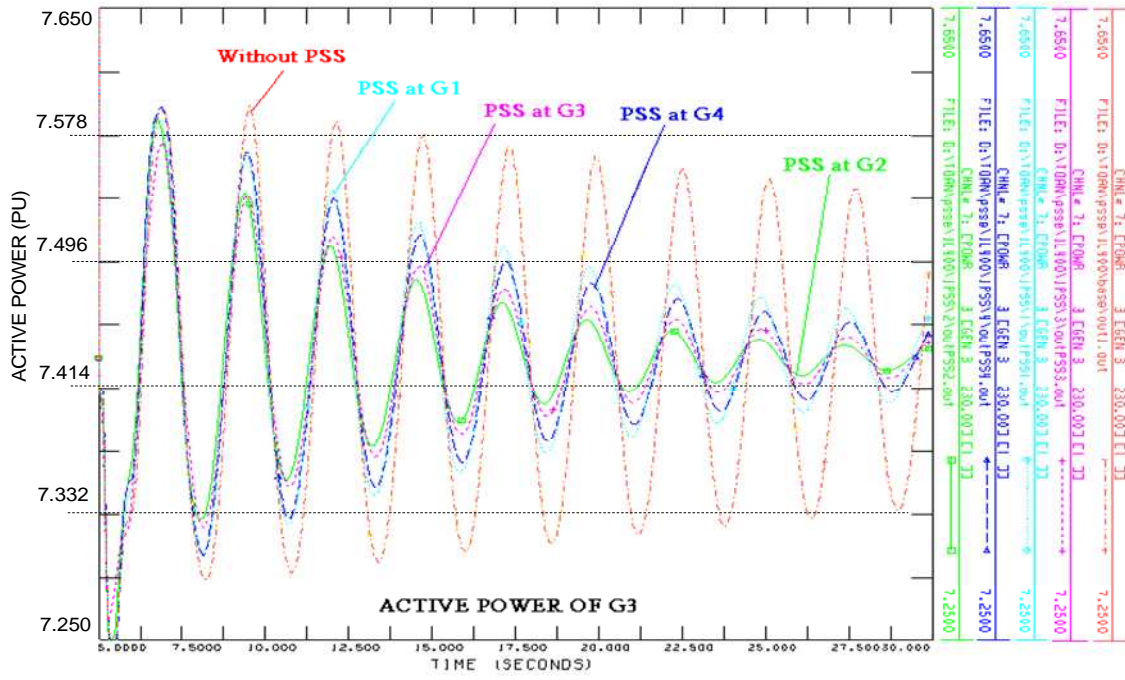


Figure 3-2: Puissance de générateur G3 avec les différents placements de PSS.

CHAPITRE 4 : STABILITÉ TRANSITOIRE ET ACTIONS PRÉVENTIVES

4.1 INTRODUCTION

La stabilité transitoire est un phénomène très complexe et difficile. La stabilité transitoire est le résultat de système aux défauts qui ont des caractéristiques fortement non linéaires et d'évolution temporelle rapide. Il est nécessaire de comprendre et d'analyser des mécanismes de stabilité transitoire afin de trouver les solutions efficaces.

Le problème de stabilité transitoire peut être évité en appliquant des actions préventives ou correctives. Du point de vue préventif, en ce qui concerne le contrôle de stabilité transitoire, quelques méthodes de contrôle peuvent être considérées comme l'identification de zones instables, la détermination du temps critique d'élimination de défaut et la détermination de marge de stabilité afin de pouvoir appliquer les actions préventives. Le critère d'égalité des aires donne une compréhension claire pour déterminer le temps critique d'élimination de défaut et la marge de stabilité. Cependant, cette méthode est seulement appliquée à un système simple d'une machine raccordée à un noeud infini (SMIB : Single Machine Infinite Bus). Les méthodes de simulation dans le domaine temporel peuvent identifier le temps critique d'élimination de défaut (TEC) pour les différentes situations de pannes mais elles ne peuvent pas identifier la zone stable et/ou la marge de la stabilité. Les méthodes basées sur la fonction d'énergie transitoire (TEF Transient Energy Fonction) peuvent être utilisées. Dans ces méthodes, l'énergie transitoire critique est associée aux points d'équilibre instables après que le défaut ait été identifié. Si l'énergie transitoire après le défaut, (c.-à-d., défaut éliminé) est inférieure à cette énergie critique, le système est stable ; autrement, il est instable. Cependant, un des problèmes les plus difficiles est l'identification de la trajectoire et de l'énergie critique. Une autre méthode basée sur une machine équivalente (SIME : Single Machine Equivalent) est développée. Cette méthode est réellement une combinaison entre les méthodes de simulation temporelle et le critère d'égalité des aires (Références : [1, 28, 31]).

Dans ce chapitre, plusieurs simulations dans le domaine temporel ont été effectuées avec les différents scénarios.

Le développement de méthodes qui permettent d'améliorer la stabilité transitoire de réseau est aussi un des problèmes majeurs des compagnies d'exploitation des réseaux. Les méthodes basées sur l'approche heuristique pourraient s'appliquer pour les grands réseaux électriques avec moins de calcul et plus simplement. L'une d'entre elles est de redistribuer les puissances des groupes afin d'augmenter le temps critique d'élimination de défaut. L'idée de cette méthode est qu'il est nécessaire de repousser le réseau dans un domaine plus stable face à certains défauts grave qui se produisent.

Dans ce chapitre, nous présentons une nouvelle méthode préventive basée sur la fonction d'énergie en utilisant une combinaison de méthode heuristique avec le gramien de commandabilité. Cet indicateur est utilisé comme la mesure afin de choisir les générateurs les plus efficaces pour redistribuer la puissance pour d'augmenter le temps critique d'élimination de défaut (Références : [99-111]).

4.2 NOUVELLE MÉTHODE PRÉVENTIVE POUR AMÉLIORER LA STABILITÉ TRANSITOIRE

4.2.1 Gramien de commandabilité et observabilité

Un système linéarisé dans l'espace d'état est utilisé :

- Du point de vue préventif : Afin de prévenir un système instable face aux perturbations, l'énergie transitoire est proportionnelle à la trace de W_C^{-1} comme déjà présentée au chapitre 3. Le système est moins sensible à la perturbation. Si l'énergie transitoire est plus grande. Pour pousser le réseau dans une zone plus stable, il faut donc maximiser l'énergie transitoire proportionnelle à la trace de W_C^{-1} , ou bien minimiser W_C au sens d'une norme donnée de matrice.
- Pour les grands réseaux électriques, des gramien de commandabilité/observabilité pourraient être employés pour la réduction d'ordre de système dans l'espace d'état (méthode de Moore – Référence : [86]).

4.2.2 Redistribution de puissance des groupes pour améliorer le temps critique d'élimination de défaut

Des méthodes de redistribution de puissance des groupes afin d'augmenter le temps critique d'élimination de défaut (TEC) ont été proposées dans les littérature. Pour voir l'évolution de la stabilité des machines, l'angle de rotor des générateurs est utilisé. C'est pourquoi, dans la présente partie, l'évolution de l'angle de rotor pour les défauts les plus critiques comme un court-circuit triphasé sur les lignes très proches des générateurs est étudiée. En outre, comme discuté ci-dessus, le temps d'élimination de défaut (TED) est un facteur important qui influence la stabilité transitoire. La valeur maximum de TED telle que le réseau reste stable est le TEC.

Dans ce chapitre, nous proposons une méthode qui permet d'augmenter le TEC par la redistribution de puissance des groupes en utilisant le gramien de commandabilité.

L'algorithme se résume comme suit.

1. Pour un réseau donné, déterminer le TEC des générateurs pour les différents défauts triphasés sur toutes les lignes et tous les nœuds du réseau (contingencies en anglais)
2. Pour les TEC obtenus, arranger ces valeurs dans l'ordre décroissant. Fixer une valeur cible de TEC. Le problème est de redistribuer les puissances des groupes pour qu'on obtienne les TEC supérieurs à cette valeur cible
3. Pour une valeur cible de TEC, les générateurs sont divisés en deux groupes :
 - a. Les générateurs qui ont le TEC inférieur à la valeur cible seront choisis comme les candidats pour réduire la puissance fournie – groupe a
 - b. Les générateurs qui ont le TEC entre la valeur cible et 1.3 fois la valeur cible restent inchangés en terme de puissance fournie – groupe b
 - c. Les générateurs qui ont le TEC supérieur à 1.3 fois de la valeur cible sont les candidats pour augmenter la puissance fournie – groupe c; il faut noter que la totalité de puissance augmentée par cette étape doit être égale à la totalité de puissance réduite par l'étape a).

4. La quantité de puissance à réduire est calculée par une relation linéaire entre le TEC et la puissance active fournie par des groupes :

$$\operatorname{tg} \alpha_i = \frac{TEC_{i2} - TEC_{i1}}{P_{i1} - P_{i2}} = \frac{(TEC_{i\text{-desired}} - TEC_{i1})}{P_{i1} - P_{i\text{-desired}}} \quad (4.2-1)$$

$$P_{i\text{-desired}} = P_{i1} - \frac{(TEC_{i\text{-desired}} - TEC_{i1})}{\operatorname{tg} \alpha_i} \quad (4.2-2)$$

$$P_{\text{shifted}} = \sum_{i=1}^N (P_{i1} - P_{i\text{-desired}}) \quad (4.2-3)$$

où :

Pour un générateur i : P_{i1} , P_{i2} , TEC_{i1} , TEC_{i2} , sont calculés par des simulations afin de construire cette relation linéaire entre le TEC et la puissance active fournie. Il faut avoir deux simulations pour obtenir cette relation.

P_{i1} est la puissance active initiale du générateur i

$TEC_{i\text{-cible}}$ est la valeur cible de TEC

N est le nombre des générateurs à réduire la puissance.

La Figure 4-1 donne une démonstration pour obtenir cette relation linéaire.

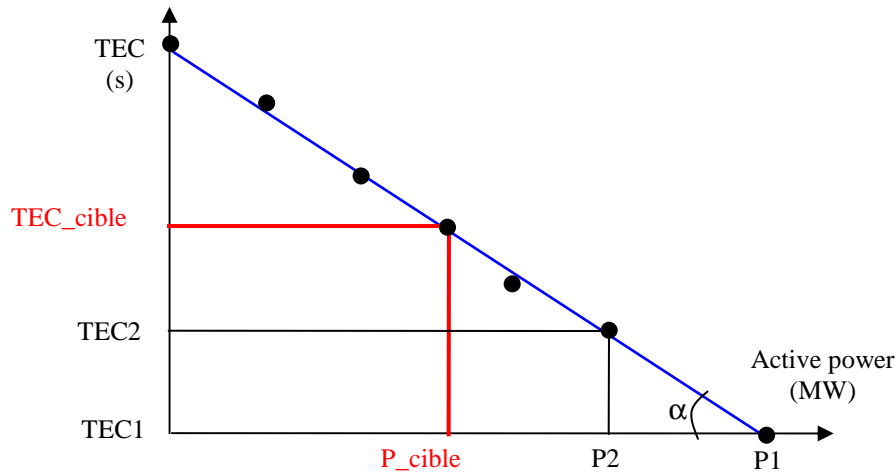


Figure 4-1: Relation linéaire entre le TEC et la puissance active fournie.

5. Afin d'assurer l'équilibre entre la production et la demande, un ou des générateurs dans le groupe c sont les candidats pour prendre la totalité des puissances réduites par les générateurs du groupe a . Les générateurs qui ont les valeurs les plus petites de gramien de commandabilité ($\min \operatorname{trace}(W_c)$) sont sélectionnés. La répartition de puissance pour chaque générateur est déterminée par un facteur de proportionnalité correspondant à la quantité de puissance à augmenter :

$$W_i = \frac{1/W_{c-i}}{\sum_{i=1}^n 1/W_{c-i}} \quad (4.2-4)$$

Où n est le nombre des générateurs du groupe c (dont la puissance sera augmentée).

6. Vérifier la limite de puissance (P_{max}) des générateurs et effectuer les simulations pour assurer que les TEC sont supérieurs à TEC cible.

4.3 APPLICATION

Afin de démontrer l'intérêt de la méthode proposée, un modèle réseau de New England de 39 noeuds est utilisé. L'état initial des générateurs du réseau est donné dans le Tableau 4-1 et Table 4-2 :

Tableau 4-1: Condition initiale des générateurs

Générateur	Puissance/ Pmax (MW)	Générateur	Puissance/ Pmax (MW)
G2	541/700	G7	560/700
G3	650/750	G8	540/700
G4	632/750	G9	830/900
G5	508/700	G10	250/350
G6	650/750		

Tableau 4-2: Les TEC des générateurs avec la plus grave panne

Générateur	G2	G3	G4	G5	G6	G7	G8	G9	G10
TEC	0.18	0.17	0.13	0.13	0.11	0.18	0.2	0.088	0.20

En se basant sur les valeurs TEC calculées pour les différentes situations de pannes (Table 4-2), la valeur cible de TEC est choisie à 130 ms. Les générateurs G6 et G9 sont les candidats pour réduire la puissance. Les puissances à réduire pour ces deux générateurs sont présentées dans le Tableau 4-3. Les générateurs G2, G8 et G10 sont les générateurs dont il faut augmenter la puissance.

Tableau 4-3: Nouvelle valeur de puissance et puissance à réduire pour les générateurs G6 et G8

Générateur	Puissance après la réduction (MW)	Puissance à réduire (MW)	Puissance totale à réduire (MW)
G6	607	43	156
G9	697	113	

Le générateur qui a les plus petites valeurs de trace de gramien de commandabilité est la plus stable car il a l'énergie stabilisante la plus grande. Le tableau 4-4 présente les valeurs de gramien de commandabilité des générateurs.

Tableau 4-4: Gramien de commandabilité des générateurs.

Générateur	Trace de $(W_C) \times 10^3$	Générateur	Trace de $(W_C) \times 10^3$
G2	0.4390	G7	0.6317
G3	0.5051	G8	0.4620
G4	0.5820	G9	1.0841
G5	0.6466	G10	0.2047
G6	0.5715		

Enfin le facteur de redistribution et la puissance à augmenter pour les générateurs G2, G8 et G10 sont présentés sur le Tableau 4-5. Dans ce cas, aucun générateur dépasse la limite de puissance active autorisée (P_{max}).

Table 4-5: Facteur de redistribution et puissance à augmenter pour les générateurs G2, G8 et G10.

Générateur	W_i	Puissance à augmenter	Puissance après l'augmentation
G2	0.244	38.1	≈ 579
G8	0.236	36.2	≈ 576
G10	0.520	81.7	≈ 331

Afin de valider la méthode proposée, une simulation temporelle est effectuée. Une valeur de TEC de 130ms est choisie comme la valeur cible pour les situations de pannes. L'action préventive ici est la redistribution de puissance avec la méthode présentée ci-dessus. Les figures 4-2 et 4-3 présentent l'évolution des angles rotoriques des générateurs G6 et G9, respectivement, sans action préventive et avec l'action préventive. On constate qu'avec l'action préventive, les générateurs sont plus stables.

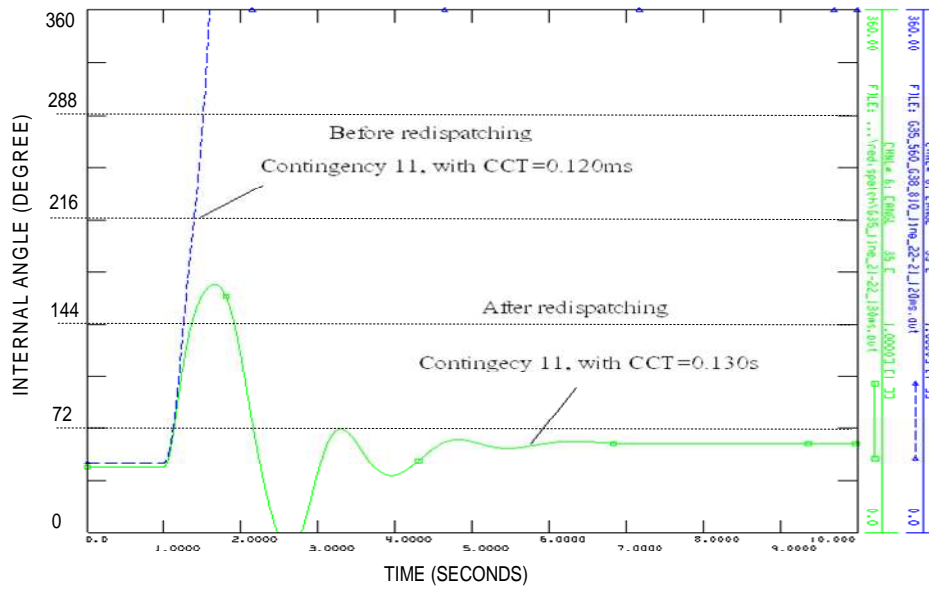


Figure 4-2: Angle rotorique du générateur G6 sans et avec action préventive

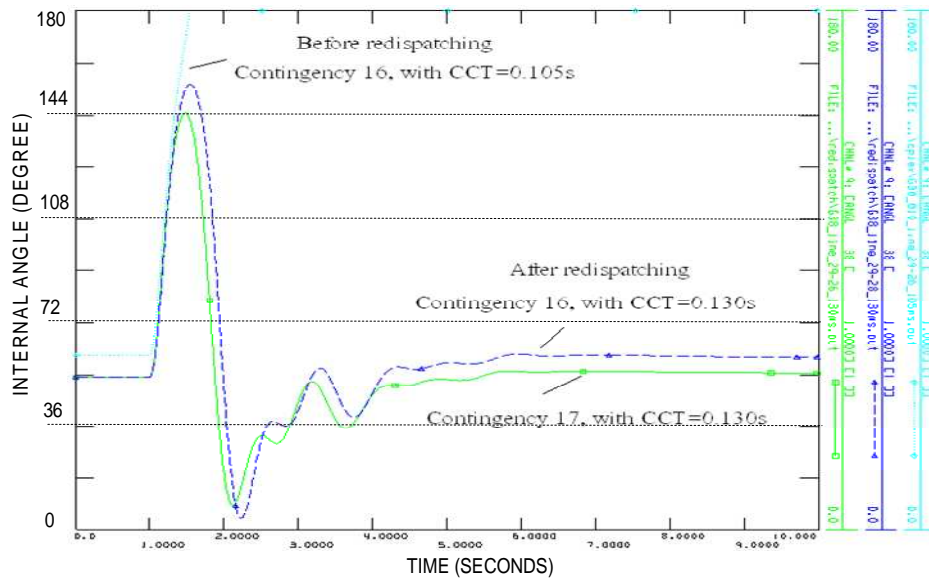


Figure 4-3: Angle rotorique du générateur G9 sans et avec action préventive

CHAPITRE 5 : SIMULATION DYNAMIQUE, MÉTHODES PRÉVENTIVES ET CORRECTIVES POUR LA PRÉVENTION D'EFFONDREMENT DE TENSION

5.1 INTRODUCTION

L'effondrement de tension est l'une de causes importantes des blackouts électriques récents des réseaux électriques. Par conséquent, la compréhension profonde du mécanisme d'effondrement de tension ainsi que des facteurs qui ont des influences directes sur l'effondrement de tension sont des considérations essentielles pour les opérateurs et les chercheurs. Le phénomène d'effondrement de tension est lié aux phénomènes dynamiques et compliqués des éléments dynamiques du réseau tels que les générateurs, les actions des dispositifs de protection, les charges... etc. Par conséquent, pour une meilleure compréhension de ces phénomènes, la simulation dynamique devrait être utilisée. Elle permet principalement de fournir plus d'informations sur le comportement dynamique des dispositifs du réseau pendant l'analyse de stabilité de tension. En particulier, nous pouvons observer non seulement la variation du profil de tension aux noeuds mais également les séquences de l'activation des dispositifs de contrôle automatiques de tension au cours de la simulation. Comme le montre l'analyse des blackouts électriques récemment survenus sur les réseaux électriques, les phénomènes d'effondrement de tension sont généralement liés à des phénomènes à long terme (quelques minutes).

Dans ce chapitre, nous limitons notre étude aux phénomènes dynamiques à long terme de la stabilité de tension en employant le logiciel PSS/E (Power System Simulator for Engineering). Les comportements dynamiques des dispositifs du réseau comme les générateurs, les limiteurs de courant des systèmes d'excitation (OverExcitation Limiter -OEL), les transformateurs réglables en charge (UnderLoad Tap Changer-ULTC), les différents types de charge, etc, sont étudiés en employant les modèles standard de la bibliothèque de PSS/E. Le réseau BPA (Bonneville Power Administration) et le réseau Nordique ont été utilisés pour l'étude (Références : [1-2, 68]).

Pour avoir une compréhension des mécanismes et des facteurs de l'effondrement de tension, il est nécessaire de trouver un plan raisonnable de conduite contre l'effondrement de tension avec des actions préventives et curatives.

Les actions préventives sont mises en oeuvre avant l'effondrement de tension afin de maintenir une grande marge de stabilité et ainsi éviter. En régime permanent, la relation des variables du réseau est représentée par des équations de répartition de puissance (loadflow). Pour un réseau donné, si des paramètres, comme la topologie du réseau, le plan de production et la charge sont connus, des équations de calcul de répartition sont résolues pour déterminer l'état du réseau (déphasage et module de tension). Pour les réseaux de transport d'énergie, les équations de calcul de répartition peuvent être représentées par des équations couplées, c'est-à-dire que la tension dépend fortement de la puissance réactive. Quand la puissance réactive est injectée sur un noeud de charge, la tension sur ce noeud est augmentée. Quand la tension sur un ou plusieurs noeuds du réseau dépasse les valeurs autorisées (V_{max} et V_{min}), les opérateurs doivent effectuer les actions de conduite afin de restaurer un plan de tension normal par des moyens comme : l'enclenchement des condensateurs de shunt, le changement

des réglages des transformateurs, ou le changement de tension terminale des générateurs... Par conséquent, une stratégie préventive de conduite doit être construite afin d'assurer un bon plan de tension pour les différentes situations de pannes.

Dans ce chapitre, nous proposons une stratégie de réglage secondaire de tension basée sur un calcul d'optimisation (OPF : optimal power flow) afin d'éviter le risque d'effondrement de tension. Les variables de contrôle sont : la tension terminale des générateurs, les prises des transformateurs, la puissance réactive des condensateurs. Une relation entre la variation de tension et la variation des variables de contrôle est établie par les matrices de sensibilité. Une fonction objectif est ensuite construite et minimisée par la programmation quadratique pour maintenir un bon plan de tension (Références : [112-115]).

Pour les actions correctives, il y a plusieurs méthodes pour éviter l'effondrement de tension comme présenté au chapitre 2. Cependant, afin de maintenir la tension du réseau dans les limites admissibles face à une perturbation grave, une méthode corrective rapide est proposée. Cette action est basée sur le délestage de charge quand la tension est trop basse (UVLS : under voltage load shedding) comme le proposent C.W. Taylor et D. Lefebvre (Références : [57, 116]).

5.2 SIMULATION DYNAMIQUE D'EFFONDREMENT DE TENSION

5.2.1 Facteurs de l'effondrement de tension

Dans cette section, des facteurs de l'effondrement de tension ont été étudiés en employant la simulation dynamique sur le réseau BPA et le réseau nordique. L'influence des modèles de charge statiques et dynamiques sur l'effondrement de tension a été discutée en détail.

Les charges dynamiques jouent un rôle important sur l'effondrement de tension; en particulier, la charge de moteur à induction. L'influence des transformateurs réglable en charge (ULTC) et la limite de courant des systèmes d'excitation (OEL) sont des causes directes pour l'effondrement de tension. L'impact des ULTCs et des OELs ainsi que le comportement dynamique des dispositifs de protection pendant la simulation dynamique à long terme ont été également étudiés.

Quelques scénarios de l'étude de l'effondrement de tension ont été simulés pour deux réseaux : BPA et Nordique réseaux électriques. Différents facteurs dynamiques ont été observés. A partir des résultats d'analyse des facteurs qui ont influencé l'effondrement de tension pour le réseau BPA et le réseau nordique, nous constatons :

- une baisse de tension et une augmentation des pertes sur le réseau quand une ligne ou un générateur est déclenché.
- La dynamique de restauration de charge aux nœuds de charge et les transformateurs réglables en charge sont des facteurs défavorables, puisqu'ils visent à reconstituer la charge quand le plan de tension est très bas.
- Après que les limiteurs d'excitation aient été activés, les générateurs ne sont pas capables de fournir la puissance réactive pour compenser les pertes supplémentaires dans le réseau, et par conséquent ils ne peuvent plus maintenir constante la tension terminale.

D'autres mécanismes peuvent causer ou jouer un rôle significatif dans des phénomènes d'effondrement de tension la protection de lignes, la réponse des systèmes de régulation de vitesse, les limites des dispositifs FACTS et l'augmentation rapide de charge. Comme cela est illustré ci-dessus, les effondrements de tension sont souvent des événements en cascades, avec beaucoup de facteurs, qui amènent à un blackout total du réseau (Références : [112,117, 122-123]).

5.3 MÉTHODES PRÉVENTIVES POUR ÉVITER L'EFFONDREMENT DE TENSION

5.3.1 Indicateur d'effondrement de tension

L'indicateur d'effondrement de tension aide les opérateurs connaître l'état actuel du réseau et la distance du réseau au point d'effondrement. Beaucoup d'indicateurs sont mentionnés au chapitre 2. Toutefois pour les actions préventives, nous présentons ici le indicateur L proposé par P. Kessel et H. Glavitsch (Référence : [124]). Même cet indicateur est statique et basé sur les données de calcul de répartition, il ne peut pas donc refléter le comportement dynamique du réseau. Toutefois cet indicateur se calcule rapidement et il est bon pour la prévision d'état du réseau. L'indicateur de risque d'instabilité de tension sur chaque nœud du réseau est défini comme suit :

$$L_j = \left| 1 + \frac{V_{0j}}{V_j} \right| = \left| 1 - \frac{\sum_{i \in \alpha_G} F_{ji} V_j^*}{V_j} \right| \quad (5.3-1)$$

L'indicateur global est déterminé par :

$$L = \max\{L_j\}, j \in \alpha_L \text{ et } 0 < L < 1 \quad (5.3-2)$$

où : α_G est le nombre des noeuds de génération, α_L est le nombre des noeuds de charge, et F_{ij} est le facteur de participation de charge $[F] = -[Y_{LL}]^{-1} [Y_{LG}]$.

En employant cet indicateur statique, les opérateurs du réseau connaissent la distance du réseau au point d'effondrement. Un ensemble de calculs du power-flow peut être réalisé afin de fournir les informations pour déterminer l'indicateur L sur la trajectoire de calcul. Ce procédé ne reflète pas les comportements dynamiques du réseau mais il donne une image assez précise avec un temps de calcul rapide pour prévenir l'effondrement de tension.

5.3.2 Réglage secondaire de tension pour améliorer la stabilité de tension

Dans une situation de forte charge ou après une perturbation, les tensions de quelques noeuds du réseau peuvent dépasser leurs limites ; s'il n'y a pas d'actions de conduite convenables, le réseau peut rencontrer un risque d'instabilité de tension ou même un effondrement de tension. Par conséquent, une stratégie de contrôle de tension est nécessaire pour maintenir rapidement les tensions à leurs limites admissibles. Pour la stratégie de réglage de tension secondaire que nous proposons ici, les variables de contrôle sont : la puissance réactive des condensateurs de shunt, les réglages des transformateurs, et la tension terminale des générateurs.

Nous proposons la minimisation des variations des variables de contrôle :

$$M \min_{\Delta V_G, \Delta Q_C, \Delta T_L} \{C_1(\Delta V_G)^2 + C_2(\Delta Q_C)^2 + C_3(\Delta T_L)^2\} \quad (5.3-3)$$

Où

- $\Delta V_G, \Delta Q_C, \Delta T_L$ sont les variations de tension terminale des générateurs, de puissance réactive des condensateurs, des prises des transformateurs, respectivement
- $C_1 \geq 0, C_2 \geq 0, C_3 \geq 0$, sont les coefficients de pondération des variables de contrôle.

Avec les contraintes définies par les matrices de sensibilité :

$$\begin{cases} \begin{bmatrix} (\Delta V_L)_{\min} \\ \left(\frac{\Delta Q_G}{V_G}\right)_{\min} \end{bmatrix} \leq \begin{bmatrix} S_{V_L V_G} & S_{V_L Q_C} & S_{V_L T_L} \\ S_{Q_G V_G} & S_{Q_G Q_C} & S_{Q_G T_L} \end{bmatrix} \begin{bmatrix} \Delta V_G \\ \Delta Q_C \\ \Delta T_L \end{bmatrix} \leq \begin{bmatrix} (\Delta V_L)_{\max} \\ \left(\frac{\Delta Q_G}{V_G}\right)_{\max} \end{bmatrix} \\ (\Delta V_G)_{\min} \leq \Delta V_G \leq (\Delta V_G)_{\max} \\ (Q_C)_{\min} \leq Q_C \leq (Q_C)_{\max} \\ (\Delta T_L)_{\min} \leq \Delta T_L \leq (\Delta T_L)_{\max} \end{cases} \quad (5.3-4)$$

où :

$$\begin{cases} (\Delta V_G)_{\min} = (V_G)_{\min} - V_G^0 \\ (\Delta V_L)_{\min} = (V_L)_{\min} - V_L^0 \\ (\Delta T_L)_{\min} = (T_L)_{\min} - T_L^0 \\ (\Delta Q_G)_{\min} = (Q_G)_{\min} - Q_G^0 \end{cases} \quad \text{et} \quad \begin{cases} (\Delta V_G)_{\max} = (V_G)_{\max} - V_G^0 \\ (\Delta V_L)_{\max} = (V_L)_{\max} - V_L^0 \\ (\Delta T_L)_{\max} = (T_L)_{\max} - T_L^0 \\ (\Delta Q_G)_{\max} = (Q_G)_{\max} - Q_G^0 \end{cases} \quad (5.3-5)$$

Le problème d'optimisation est résolu par application de la méthode de programmation quadratique.

Cette stratégie de contrôle a été appliquée au réseau d'IEEE de 30 noeuds et au réseau nordique en tant que méthode préventive d'effondrement de tension avec des résultats très intéressants.

5.4 MÉTHODE CORRECTIVE PAR LE DÉLESTAGE DE CHARGES

En cas de perturbations «légères», les méthodes préventives suffisent pour éviter l'effondrement de tension. Cependant, en cas d'incidents très graves les actions préventives ne peuvent que retarder l'effondrement de tension de quelques minutes. Dans ces situations, une méthode corrective doit être appliquée afin d'éliminer le risque d'effondrement de tension. Parmi les méthodes correctives, nous nous intéressons à la méthode de délestage de charge par les relais à basse tension (undervoltage load shedding - UVLS).

Les objectifs principaux de ces méthodes sont concentrés sur trois aspects :

- 1) Réduire au minimum la quantité de charge à délester
- 2) Déterminer l'endroit où la charge doit être délestée
- 3) Synchroniser le délestage le plus rapidement tout en en réduisant le risque d'oscillations.

Dans cette partie, nous proposons une règle pour l'UVLS qui pourrait être employée pour éviter l'effondrement de tension. Le réseau nordique est simulé sous PSS/E (Références : [57, 116, 127-131]).

5.4.1 Simulation Dynamique de l'UVLS

Le schéma d'UVLS a l'avantage de permettre la gestion directe des charges. L'activation de l'UVLS se fait 120 secondes (considéré l'influence du ULTCs et OELs) après un défaut. Les règles de délestage proposées se basent sur les seuils de tension :

- 5% de charge à délester si la tension est inférieure à 0.9pu avec un délai de 3.5 s.
- 5% de charge à délester si la tension est inférieure à 0.92pu avec un délai de 5 s
- 5% de charge à délester si la tension est inférieure à 0.93pu avec un délai de 8 s.

La validation des règles proposées est effectuée par la simulation dynamique du réseau nordique avec des résultats très satisfaisants. Plusieurs scénarios ont été étudiés. Pour le scénario 1, une ligne de transport dans la région du Nord entre les nœuds 4011-4021 est déclenchée à l'instant $t=5s$, et un générateur de 600 MW au nœud 4012 est mis hors service 0.1s après.

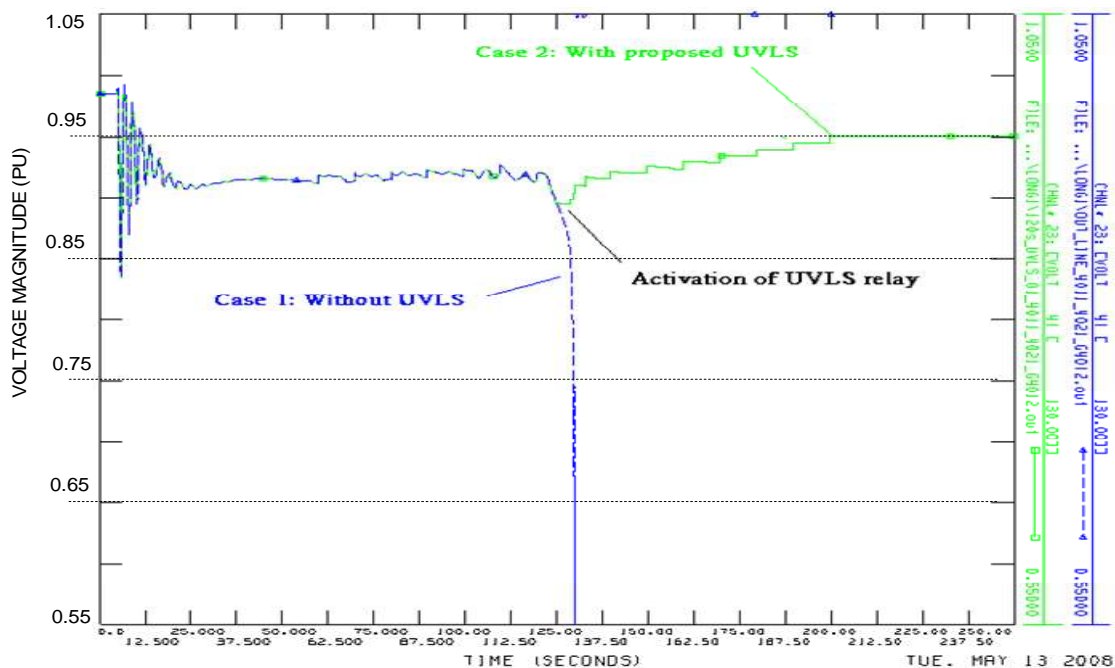


Figure 5-1: Scénario 1- tension au noeud 41 sans et avec UVLS

La figure 5-1 présente le profil de tension au noeud 41 pour deux cas : avec et sans UVLS. La ligne bleue est le profil de tension au nœud 41 sans UVLS. L'effondrement se produit environ 120 secondes après les perturbations. La ligne verte est le profil de tension au noeud 41 avec UVLS. Le réseau reste stable et les tensions sont maintenues à 0.95 pu.

CHAPITRE 6 : CONCLUSIONS ET PERSPECTIVES

6.1 CONCLUSIONS

Ce travail propose quelques contributions pour analyser les blackouts électriques récents des réseaux électriques. A partir des leçons tirées des blackouts électriques passés, quelques contributions pour éviter ces blackouts ont été apportées. Tout d'abord, des suggestions importantes pour prévenir les pannes ont été récapitulées à partir d'une analyse de l'expérience internationale. Puis, des contributions pour améliorer la stabilité angulaire et la stabilité de tension ont été présentées dans cette thèse. Quelques conclusions spécifiques sont tirées dont on trouve un résumé ci-dessous :

6.1.1 Suggestions majeures pour prévenir les blackouts

Les pannes sur les réseaux électriques sont principalement liées à de grandes perturbations. Les causes des pannes ne sont généralement pas uniques. Elles sont le résultat final d'une séquence d'événements. L'effondrement en cascade a souvent résulté d'un ou plusieurs incidents critiques, de dysfonctionnement des équipements ou de mauvaise coordination. Par conséquent, quelques suggestions pour la gestion du réseau ont été listées afin de prévenir les blackouts :

L'amélioration des systèmes existants et la rénovation des équipements, l'entretien, et le remplacement des composants critiques, l'investissement dans de nouveaux équipements du réseau (nouvelles lignes de transmission, ou nouvelle centrale) sont des éléments essentiels pour la prévention des événements en cascade.

Les études normales de planification ne peuvent pas prendre en compte tous les scénarios possibles qui peuvent mener à des pannes électriques, en raison du grand nombre d'incertitudes et de situations possibles de fonctionnement. Dans la phase de planification, le critère N-m ($m \geq 2$) devrait être considéré pour identifier des situations de pannes critiques. L'expérience acquise à partir des erreurs passées doit être incorporée à de nouvelles procédures de conception pour aider à développer des technologies nouvelles pour la conduite et la surveillance des réseaux.

Le perfectionnement des systèmes de protection peut être tout à fait efficace pour empêcher les pannes en cascade. L'application des régulateurs automatiques de tension avec les stabilisateurs devrait être obligatoires pour des générateurs.

Il est nécessaire d'assurer la redondance et la fiabilité des dispositifs de télécommande et de télécommunication. Ceci joue un rôle particulièrement important dans la coordination entre les centres de conduite et les implémentations des actions préventives et correctives.

La restauration rapide de système est extrêmement importante afin de réduire au minimum l'impact d'une panne sur notre société, les opérateurs du réseau doivent bénéficier de stages d'entraînement réguliers avec des exercices sur la restauration du réseau pour s'assurer qu'ils maîtrisent les meilleures procédures de restauration de réseaux.

6.1.2 Contribution à l'amélioration de la stabilité en présence de petites perturbations

Dans cette thèse, nous avons proposé une nouvelle méthode pour le choix optimal de configurations contrôleurs/capteurs en utilisant la notion de grammiens de commandabilité et d'observabilité. C'est une méthode préventive très efficace pour améliorer la stabilité en présence de petites perturbations.

Cette méthode a été testée sur divers scénarios. Les résultats obtenus présentent l'avantage d'une certaine robustesse pour améliorer la stabilité en présence de petites perturbations (amortissement rapide des oscillations de puissance). En appliquant la méthode proposée, le problème du placement optimal de quelques contrôleurs, par exemple le choix de placement d'un PSS, pourrait être fait sans avoir besoin de méthodes d'optimisation.

6.1.3 Contribution à l'amélioration de la stabilité transitoire des angles rotoriques

Dans cette thèse, quelques facteurs importants de la stabilité transitoire des réseaux électriques tels que le temps d'élimination de défaut, la localisation des défauts, ou le niveau de charge et de production ont été étudiés en détail. Pour le plan de défense, nous avons proposé une nouvelle stratégie préventive pour la stabilité transitoire. La méthode est une approche heuristique qui permet de redistribuer les puissances des générateurs afin d'augmenter le temps critique d'élimination de défaut. Dans cette thèse, le temps critique de d'élimination de défaut est considéré comme une mesure de l'action préventive pour la stabilité transitoire. Le rapport linéaire entre TECs et la puissance de générateur a été utilisé. La quantité de puissance à changer pour chaque générateur est calculée par le coefficient déterminé à partir du grammien de commandabilité.

La méthode préventive proposée a été testée sur quelques réseaux avec des résultats très satisfaisants.

6.1.4 Contribution à l'amélioration de la stabilité de tension

Les principaux facteurs de l'effondrement de tension ont été étudiés. En particulier, le comportement des charges, le transformateur réglable en charge, et les limiteurs de sur-excitation ont été étudiés en détail.

Pour les actions préventives, un indicateur statique d'effondrement de tension L a été employé pour l'évaluation d'effondrement de tension. Le but est de répondre à la question : quelle est la distance du réseau au point d'effondrement de tension? Les avantages principaux de la stratégie proposée sont non seulement une grande facilité de mise en oeuvre pratique mais également la possibilité de prendre une décision de conduite rapidement en utilisant seulement un calcul de répartition.

Pour les actions correctives, une stratégie de délestage de charge a été proposée en utilisant les relais de délestage à basse tension. Cette stratégie a été testée sur le réseau nordique avec des résultats très satisfaisants. Cette solution est très efficace en cas d'urgence afin de préserver le réseau d'un risque d'écroulement total de tension.

6.2 PERSPECTIVES

A partir des résultats obtenus, quelques perspectives et directions de recherches peuvent être envisagées :

Afin de proposer effectivement des méthodes préventives pour éviter les blackouts, il est nécessaire d'étudier soigneusement les mécanismes et les causes de ces phénomènes. Des leçons des blackouts sur les réseaux doivent être tirées à partir des simulations de ces blackouts. Les modèles exacts des générateurs, des charges, des contrôleurs et des dispositifs de protection doivent être pris en compte dans les simulations ou dans les outils de simulation ou d'aide à la décision.

L'utilisation des diagrammes de commandabilité ouvre de grandes perspectives pour des applications aux grands réseaux électriques. Par exemple, cette méthode peut être employée pour déterminer le placement optimal des dispositifs FACTS ou déterminer les consignes de puissance des générateurs afin d'améliorer la stabilité et la performance des réseaux. Pour les stratégies de réglage secondaire de tension afin d'améliorer la stabilité du réseau, cette méthode peut être appliquée pour déterminer les consignes des tensions terminales des générateurs, les bonnes valeurs des rapports de transformation des transformateurs, des valeurs raisonnables des bancs de capacités ...

Dans la pratique, on peut utiliser de nouveaux composants pour la conduite des réseaux, tels que les unités de mesures de phase (PMU : Phasor Measurement Unit). Le problème du placement optimal de PMU dans un grand réseau peut être résolu effectivement en utilisant la notion de diagramme d'observabilité.

Afin d'améliorer la stabilité angulaire, les chercheurs et les opérateurs recherchent toujours des méthodes efficaces. Il est évident que l'implantation des méthodes correctives est toujours plus difficile car la durée des phénomènes est très courte. L'utilisation du diagramme de commandabilité est utile pour identifier les générateurs critiques et pour redistribuer la puissance afin d'améliorer la stabilité du réseau. C'est une nouvelle direction pour améliorer la stabilité transitoire et il est encore nécessaire d'approfondir la question.

Pour les problèmes d'effondrement de tension, le réglage secondaire de tension est le plus efficace pour éviter ce phénomène. L'application de dispositifs de FACTS est une solution efficace. Lorsque les situations deviennent trop critiques, le délestage est nécessaire pour sauver le réseau. Le délestage a besoin de simulations dynamiques pour déterminer les bonnes décisions à prendre et la bonne localisation des relais de délestage de sous-tension pour un réseau donné. Le délestage dynamique est un problème d'optimisation en variables mixtes et entières qui reste difficile compte tenu des méthodes de résolution aujourd'hui disponibles.

Les blackouts sur les réseaux électriques constituent l'un des problèmes les plus difficiles à étudier. Ce type de catastrophes implique beaucoup d'actions à entreprendre à toutes les étapes de planification, de conception et d'exploitation en présence de facteurs souvent imprévus. Les blackouts provoquent une perte économique très importante. C'est pourquoi il est nécessaire de conduire plus de recherches sur ce sujet afin de proposer des méthodes préventives et correctives efficaces pour éviter les blackouts dans le futur.

CHAPTER 1

INTRODUCTION

1.1 MOTIVATION OF THE DISSERTATION

Power systems play an important role as the major economical infrastructure of any country. Traditionally, a power system is divided into three main parts: generation, transmission and distribution. In order to ensure normal operating conditions, the power systems have to meet some criteria of security, reliability, quality and economy.

However, power systems are facing with some critical problems. The first problem is highly increase in load demand while the rapid exhaustion of the natural resources causing increasingly high price in coal, gas and petrol. Furthermore, the potentially hydraulic energy has been almost surveyed and exploited, while nuclear energy is facing the problems of safety, environmental issues and high technology requirements in operation and management. These difficulties are the causes of highly pressure on the electrical industry, particularly on the output price of electrical energy.

The second problem is the presence of distributed generation. In order to introduce clean and renewable energy, many wind farms, photovoltaic stations and biomass power plants are now built and installed in the distribution side closed to customers. On the first hand, this could reduce power loss, make use of the renewable energy such as solar and wind energy, but on the other hand, this is changing the context of traditional distribution systems and making power systems more complicated and larger-scale in terms of control, monitoring and management.

The third problem concerns the environmental issues. For example, the fear of air pollution has prevented the expansion and use of coal fired power plant. Limited land and health concern also limit the expansion of transmission lines.

Another critical challenge is many electrical utilities are changing forward to power system deregulation, with many bilateral, multilateral contracts, independent power producers, and international connections between power systems. Generation, transmission, and distribution are separated and deregulated. Competition is present in both generation and consumption sides, whereas the transmission of power is integrated to provide open and equal access to all market participants to ensure fair competition. The problem of voltage and power flow control is more complicated in terms of management and operation than those in vertically integrated utilities, especially when dealing with critical situations. Even, some countries or electrical utilities have been trying to delay large amount of money investing in new power system facilities such as power plants and transmission systems.

All these difficulties make a power system more complex, large-scale, and operating closely to its security limit and vulnerable to any disturbance. Some serious power system blackouts with severe consequences occurred in the US and European countries are evident for these statements.

Although power system blackouts rarely occur and none is the same as the others but its consequences are enormous from both economic and energy security point of views. For example, the blackout occurred in the USA, in August 2003, had enormous consequences: 65 GW of load was cut off and it took nearly 30 hours to totally restore the system. The blackout happened in Italy, in September 2003, causing 27 GW of load was tripped off and the economic cost was estimated about 50 billions dollars. The most complicated disturbance in European countries in 2006 has affected 15 millions households.

Power system blackouts always have multiple causes. They are normally the final result of a chain of complicated dynamic phenomena. The causes may initiate from planning and designing stage, maintenance duty, operating mission. There are also some many unforeseen causes. The mechanisms of power system blackouts are always different from each other as well, with different types of power system stability.

Even, researchers and power system operators have been interested in the better understanding of these phenomena, main causes, and mechanisms as well as preventive and corrective method in order to avoid power system blackout for a long time. Nevertheless, with new challenges and recent power system blackouts mentioned above, this issue still needs for more attention. Therefore, this dissertation is also devoted to provide some contributions to power system blackouts preventions.

The specific objectives of dissertation are listed as following:

1.2 OBJECTIVES OF THE DISSERTATION

1.2.1 Contribution to Investigation of Major Power System Blackouts

Evidently, power system blackout is the most serious problem for any power system. The consequences are normally very huge in term of economy and energy security point of views. Therefore, this problem has become major concern for decades. A power system blackout is normally the final result of some complicated dynamic phenomena that could otherwise be manageable if they would happen alone.

Therefore, the dissertation is firstly devoted to investigate the major power system blackouts happened around the world in recent years. Some main causes and explanations for major mechanism leading to power system blackouts are then given next. Finally, the main proposed solutions to study and prevent power system blackout are summarized. These comprehensions could be not only useful for investigate previous blackouts but also essential for building preventive and corrective control strategies in the future.

1.2.2 Contribution to Improving Small Signal Stability

Small signal instability has been recognized as one cause leading to power system blackouts. In small signal stability analysis, there are many factors those are influenced on power system oscillations such as generator models, excitation system models, system loads, power system structures, and types of disturbances. However, disturbances are considered as small enough that the power system dynamic equations could be modeled by linearized equations.

From the preventive point of view, in order to prevent power system from blackout due to small signal instability, we have to improve the control system structure by adding damping controllers (for example: power system stabilizers-PSS- at generators and/or Flexible AC Transmission Systems-FACTS) and sensor (for example: Phasor measurement unit-PMU) in order to improve the overall power system performance. Practically, power systems are normally large-scale, and largely interconnected transmission systems while the number of controllers and sensors are always limited in terms of quantity and expensive in term of investing cost. Therefore, one of the most difficult issues is how to select optimal placement controllers and sensors (or equivalent to select optimal control inputs and outputs)

In this dissertation, a novel energy approach based on the use of controllability and observability gramians is proposed and applied to some systems. The results could be applied to large-scale power systems in order to build a new control structure with robustness properties.

1.2.3 Contribution to Improving Transient Stability

Transient stability is an especially difficult issue due to its complex and nonlinear characteristics, which are governed by highly non-linear integro-differential equations, which are generally bulky and with very fast time evolution. As a major concern, transient stability has been studied since the early time of electrical industry. Transient stability is often the initial cause of other types of power system stability such as small signal stability, and voltage stability those may lead to power system blackout. In practice, transient instability can be avoided by applying correctly preventive or corrective actions. Corrective control attempts to stabilize an unstable power system, by directing the system trajectory onto a new stable equilibrium point shortly after a severe contingency. The application of corrective actions is always difficult because we have to solve a set of nonlinear equations those may not be solvable. Sometimes, this problem occurs in a very short time period. On the other hand, preventive control is carried out before instability actually occurs. In fact, preventive controls are more desirable in power system operations. It is necessary to shift the operating system to stable side in advance by preventive control, so that the system can be stable even if some severe fault occurs.

In this dissertation, a new preventive method based on energy approach is introduced. The method employs a heuristic method based on controllability gramians for choosing generators used for redispatching generation output in order to improve transient stability by increasing critical clearing time (CCT). The results could be applied to real power systems in term of preventive transient stability.

1.2.4 Contribution to Improving Voltage Stability and Voltage Collapse

Prevention

Voltage instabilities and/or collapses have been recognized as one of the major causes of power system blackouts in the past. They are still the most anxious concern and one of the major causes for power system blackouts in the future. In accordance to the presence of power system deregulation, environmental constraints restrict the expansion of transmission networks; the management of power system, especially reactive management becomes more

difficult than before. These reasons are causing in high risk of voltage instability and/or voltage collapse. By analyzing the past blackouts, voltage collapses are normally related to a long-term time frame phenomenon. That is the final consequence of a chain of dynamic events involving many factors. In practice, voltage collapse can be avoided by correctly applying some preventive or corrective actions.

In this dissertation, major factors influenced on voltage collapse have been taken into account through long-term dynamic simulation. One preventive control strategy based on optimal power flow is proposed. In term of corrective point of view, some major discussions of under-voltage load shedding based on the assumption of intelligent and directly controlled load are given and tested with the “Nordic power system”.

1.3 ORGANIZATION OF THE DISSERTATION

The dissertation is organized as follows:

Motivations of the dissertation and general introductions are given in chapter 1.

Chapter 2 presents some general analyses of power system blackouts happened around the world in recent years. Major mechanisms as well as main causes of a power system blackout are also discussed in this chapter. General definitions of power system stability problems related to angle stability and voltage stability are then discussed briefly. Solutions for studying and preventing power system from blackouts are summarized in the late part of this chapter.

Chapter 3 presents a novel energy approach to optimal selection of controllers and sensors in order to improve small signal angle stability.

Transient stability problems are discussed in chapter 4. A heuristic preventive method for transient stability improvement is also proposed and discussed in this chapter.

Chapter 5 is devoted to studying voltage collapse problem. Long-term dynamic simulation method is firstly used for investigating factors influence on voltage collapse. A preventive method with the goal of maintaining voltage profile is proposed next. Under-voltage load shedding considered as corrective method is discussed in the late part of this chapter.

Major conclusions and perspectives are presented in chapter 6 of the dissertation.

1.4 LIMITATIONS AND SCOPE OF THE DISSERTATION

The power system blackouts are mainly related to power system stability problems. As defined by IEEE/CIGRE, there are three categories of power system stability. They are angle stability, frequency stability, and voltage stability. In this dissertation, the only two types of power system stability which are investigated are angle stability and voltage stability.

In term of voltage stability investigation, only long-term dynamic simulation of voltage collapse is taken into account.

For case studies, only power systems suggested by IEEE/CIGRE are used for illustration purposes.

CHAPTER 2

POWER SYSTEM BLACKOUTS: PHENOMENA, MECHANISMS, CAUSES AND SOLUTIONS

2.1 INTRODUCTION

Power systems are facing with many challenges. First of all, the load demand is rapidly increases, particularly for developing countries. Secondly, the exhaustion of primary energy, economic and environment pressure lead to the more and more appearance of power system deregulation and distributed generation. It is believed that these new trends could improve the security and performance of power system. However, the excessively economic tension is pushing power systems operating more closely to their stability and security limits than in previous decades. The existence of many power system operators makes the system more difficult than before in term of operation, monitoring, control, especially, when there are some disturbances. Power systems become more vulnerable to any disturbance. Recent blackouts in the USA or in Europe with serious consequences have demonstrated clearly these situations.

Therefore, better understanding of these phenomena, mechanisms, causes and solutions in order to prevent such the most serious problem have drawn the interest of researchers and operators for a long time. This chapter is devoted to investigations and analyses of major power system blackouts in recent years. From the analytical results, main causes as well as major mechanisms of power system blackouts are given and discussed. Finally, some methods to prevent power system blackouts in both preventive and corrective point of views are recalled briefly.

2.2 ANALYSIS OF POWER SYSTEM BLACKOUTS

2.2.1 Investigation of Recent Power System Blackouts

During over two decades, there were many serious blackouts with huge consequence had occurred in the recent years, even in well-developed countries. In this part, some typically past incidents of power system blackouts reported in references [1], [2], [3], [4], [5], [6], [7], [8], [9], [10], [11], [12], [13], [14], [15], [16], [17], and [18] are reviewed as below:

- France, December 19, 1978: France was importing electrical power from other countries. Load rise between hours from 7 am to 8 am was 4600 MW. The load increment was 1600 MW higher than the previous day. Voltage declined after 8 am and between hours 8:05 am and 8:10 am, some EHV/HV tap changers were locked. As a result, low voltages reduced some thermal production. At 8:20 am, voltages on the Eastern 400 kV transmission system were down in the range 342 kV to 374 kV. As a result, a major 400 kV line tripped due to over current protection. Tripping this

transmission line led to voltage collapse subsequently. During restoration process another collapse occurred. Amount of load interruption was about 29 GW and with a total energy loss of 100 GWh. The cost of outage was estimated about from \$200 to \$300 millions. The direct cause of blackout was long-term voltage instability after the period of 26 minutes [1], [2], [3].

- Belgium, August 4, 1982: The initial disturbance was the disconnection of a 700 MW unit during commission tests. After 45 seconds, over-excitation limiter actions reduced reactive power on two other units. Three to four minutes after the initial event, three units were tripped by “max MVAR protection”. At 3 minutes, 20 seconds, the voltage was down to 0.82 pu at a major generating station. At 4 minutes, 30 seconds, two additional generators tripped by impedance relays, resulting in power system collapse. The cause of the blackout was long-term voltage instability after the period of 4.5 minutes [1], [2], [3].
- Sweden, December 27, 1983: A disconnecter failure and fault at a substation in the west of Stockholm resulted in loss of the substation and two 400 kV transmission lines. Approximately 8 seconds later, a 220 kV line tripped off by overload current protection. Under load tap changer actions cause lower transmission line voltages and higher currents on remaining north to south lines. About 55 seconds after the fault, another 400 kV transmission line tripped off. Cascading and islanding of southern Sweden followed. Frequency and voltage collapse and under-frequency load shedding did not save the system. Nuclear units in the islanded system tripped by over-current or under-impedance protection resulting in a blackout. Load loss was about 11400 MW. The cause of blackout was long-term voltage collapse after experiencing a critical fault [1], [2], [3].
- Florida USA, May 17, 1985: A brush fire caused the tripping of three light-loaded 500 kV transmission lines and resulted in voltage collapse and blackout within a few seconds. Load loss was 4292 MW. The cause of the blackout was voltage collapsed by transient stability [2], [3].
- Tokyo Japan, July 23 1987, Tokyo suffered from very hot weather. After the lunch time, the load pick-up was about 1% per minute (or 400 MW/minute). Despite the fact that all the available shunt capacitors were switched on, the voltages started to decay on the 500 kV transmission system. After 20 minutes the voltage had fallen to about 0.75 p.u and the protective relays disconnected parts of the transmission network and by that action shed about 8000 MW of load. The cause of the blackout was long-term voltage collapse. Unfavorable characteristics of new type of air conditioners were considered as one of major causes of the blackout [1], [2], [3].
- Western France, January 12, 1987: Over a period of about fifty minutes, four units at the Cordemais thermal plant tripped. Voltage decayed and nine other thermal units tripped over the next seven minutes, eight-unit because of over-excitation protection, thus voltages stabilized at a very low level (from 0.5 pu to 0.8 pu). After about six minutes of voltage collapse, about 1500 MW of load was shed to recover the voltage [1], [2], [3].
- Finland August 1992, the power system was operated close to security limits, imported from Sweden was large, so that there were only three units directly connected to 400

kV system in southern Finland. The tripping of 735 MW generator unit, simultaneous maintenance work on 400 kV line and manual decrease of reactive power in another remaining generator unit, caused a disturbance where the lowest voltage at 400 kV network was 344 kV. The voltages were restored to normal level after 30 minutes by starting gas turbines, by some load shedding and by increasing reactive power production [3].

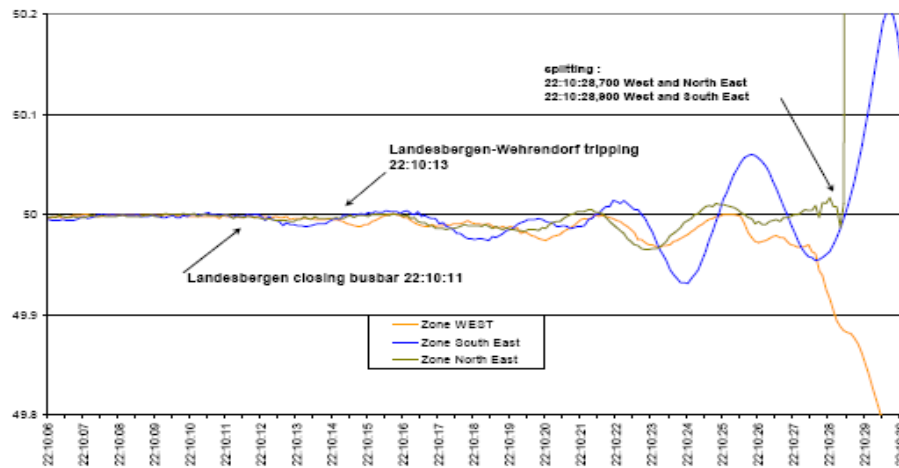
- Western Systems Coordination Council (WSCC) July 1996: A short circuit on a 345 kV transmission line started a chain of events leading to a break-up of the Western North America power system. The final reason for the break-up was rapid overload/voltage, collapse/angular instability. The event affected about 7.5 million customers and resulted in over 30,000 MW of load being interrupted and over 25,000 MW of generating capacity being dropped from the system. One of main causes was lack of power system damping of inter-area oscillations [1], [10].
- North American Electricity Reliability Council (NERC-USA) August 14, 2003. Based on NERC investigation, the system was being operated in highly loaded conditions. There were significant reactive power supply deficiencies in the Cleveland, Ohio area beginning in the early afternoon. The Midwest ISO (MISO) state estimator (SE) and real time contingency analysis (RTCA) software were not functioning properly due to software problems from 12:15 to 16:04. This prevented the MISO from performing proper “early warning” assessments of the system as the events were unfolding. At the First Energy (FE) control center, a number of computer software failures occurred on their Energy Management System (EMS) software starting at 14:14. These failures prevented FE from having adequate knowledge of the events taking place on its own system and contributed to inadequate situational awareness at FE. The first major event was the outage of FE Eastlake unit 5 generator at 13:31. Eastlake unit 5 and several other generators in FE northern Ohio service area were generating high levels of reactive power and the reactive power required from these generators continued to increase as the day progressed. The Eastlake unit 5 voltage regulator tripped manually because of over-excitation. As the operator attempted to restore automatic voltage control, the generator tripped. The Chamberlin-Harding 345 kV line tripped at 15:05 in FE system due to a tree fault even though the line was only loaded to 44% of its normal rating. The Hanna-Juniper 345 kV line, loaded to 88 % of its normal rating, tripped due to a tree fault at 15:32. The Star-Canton 345 kV line, loaded to 93% of its emergency rating, tripped due to a tree fault at 15:41. During this period, due to software problems at the FE and MISO control centers, no corrective actions were taken. A cascading loss of lines on the parallel 138 kV network continued over the next 15 minutes, but very little load reduction occurred. The critical event leading to uncontrolled, widespread cascading in Ohio and beyond was the tripping of the Sammis-Star 345 kV line at 16:05:57. At approximately 16:10:38, due to the cascading loss of major tie lines in Ohio and Michigan, the power transfer between the U.S. and Canada on the Michigan border shifted. At this point, the voltage around Detroit plummeted due to extremely heavy transmission line loadings and the system became transiently unstable, resulting in rapidly cascading outages of several hundred lines and generators and a blackout of a large area. It was estimated that about 65000 MW was cut off and it took nearly 30

hours to restore the system. Voltage collapse is one of causes of the blackout [5], [9], [10], [11], [12], [13], [14].

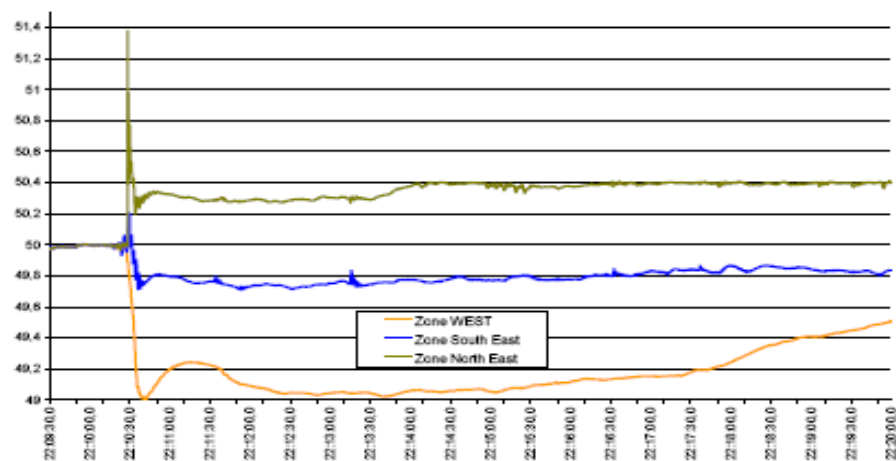
- Sweden/Denmark, September 23, 2003. Starting from 12:30, Oskarshamn nuclear plant tripped (due to technical problems), as a result, 1.1 GW lost; north-south flow on the west side increased. At 12:35 a switching device at Horred substation broke apart that caused Ringhals nuclear plant (1.8 GW) and two important north-south connections lost. From 12:35 to 12:37 the east side became overloaded leading to a voltage collapse; southern part of the grid (South Sweden and Eastern Denmark) becomes separated. At 12:37 insufficient generation capacity within the southern subsystem; frequency and voltage drop further, power stations tripped and the area blacks out. Total loss of supply: 6.3 GW and over six hours needed for restoration [9], [11], [15].
- Italy, September 28, 2003: at 3 am, the power system imported 6.9 GW, and 300 MW more than scheduled. At 03:01:42 am, a fault occurred on a highly loaded 380 kV transmission line from Mettlen -Lavorgo in Swiss power system that closed to border of Italy. The attempt to re-close automatically and manually the line were fails due to the large voltage phase angle across the breaker. This caused 110% overload the second 400 kV transmission line namely Sils - Soazza from Swiss to Italy. As these fluctuations did not induce any violation of the N-1 security conditions on the Italian grid. The Italian transmission system operators (GRTN) were not aware of the event happened in Switzerland and did not take any remedial action. At 03:11 am, the Swiss co-ordination centre of ETRANS asked GRTN to reduce import in order to help relieving the overloads in Switzerland and bring the system back to a safe state. Lacking of coordination between ETRANS and GRTN, and disputable actions of ETRANS caused the line Sils – Soazza tripped off at 03:25:21 am. Immediately after the tripping of the second line an internal 220 kV line Switzerland was highly overloaded and tripped off that interrupt a power flow to Italy (740 MW). After this event, others imported lines to Italy from Switzerland, France, Austria, Slovenia were excessively loaded. Operation of protection system disconnected these overloaded lines caused a cascade tripping. The Italian power system was fully blackout nearly half an hour later the first event. The causes of the blackout were somehow related to both voltage and frequency collapse. Total load loss was 27 GW and economic cost was estimated about tens of billions dollar. This blackout was recognized as the worst blackout in the Italian history [6], [7], [8], [9].
- Greece, July 12, 2004: Before 12:25, power system in the Athens area was heavy loaded (because of highly excessive use of air conditioning systems) and the unavailability of four 150 kV lines, a 125 MW and a 300 MW unit were further stresses the system. Until noon voltage declined to 90% of the nominal value. 12:30 to avoid voltage collapse 80 MW of load was manually disconnected. However, as the demand still rose, voltages dropped further; at 12:35 an additional load shedding of 200 MW was planned (but not executed anymore). 12:37, another generation unit tripped; consequently voltages were collapsing. At 12:39 the system was split by the line protection devices; the remaining generation in the separated southern part disconnects and the blackout spread in the area of Athens and the Peloponnes Island. Total load loss was about 9 GW [16]

- The system disturbance in European countries on November 4, 2006: This was one of the most complicated disturbances in which many power systems had been affected. The major causes and mechanism of this “large frequency deviation” are summarized in brief as follows [17], [18] (the technical report has been realized by CRE: Commission de Régulation de l’Energie and Prof. Jean-Luc Thomas-Professeur Titulaire de la Chaire d’Électrotechnique au Conservatoire National des Arts et Métiers -CNAM).
 - *The general power system conditions:* the European interconnected transmission system had been formed over 50 years in order to ensure the security of electrical energy supply in Europe. However, in the recent two decades, there have been fundamental changes of power system paradigm, for example, deregulation tendencies leading to higher cross-border energy exchanges, the presence of distributed generation (quite large capacity of wind power). Furthermore, due to the environmental pressure, the expansion of the transmission is restricted. All the new challenges were unfortunately considered in the regional system design
 - *The actual power system conditions before the disturbance:* the power system was operating under low load demand condition during the weekend as compared to the working day. Several transmission lines were tripped for scheduled maintenance. There were significant East-West power flows as a result of international power trade and the obligatory exchange of wind feed-in inside Germany (mainly from Germany to the Netherlands and Poland). Because of a request for a disconnection of the double circuit 380kV line between Conneforde and Diele for a cruise passing through. The Transmission System Operator in Germany - E.ON netz carried out an analysis of the influence of switching this line on the system security and found that the transmission system would be operated in heavy load condition but secure and there was no violation of N-1 criterion. However, another request for tripping the line was asked for one hour earlier. At this point, The transmission system operator in Germany - RWE Transportnetz Strom (RWE TSO) and The Transmission System Operator in Netherlands (TenneT) were not informed, and no security analysis was made. This late announcement made it impossible to reduce the exchange between Germany and Netherlands.
 - *Sequence of events:* At about 9.38 pm, the first circuit of 400 kV Conneforde-Diele transmission line was tripped off. The second circuit was tripped one minute later. From 9.38pm to 10.08 pm, the TSOs controlling power flows in northern Germany (RWE TSO and E.ON Netz) observed extremely heavy loads on the power network in the area, causing the usual safety limits to be reached and subsequently exceeded. At 10.10 pm, after carrying out an empirical estimate of the electricity flows on the network area, but without a digital simulation, without any further coordination with RWE TSO (because of necessary rush), E.ON Netz decided to modify the electrical operating topology at the Landesbergen substation by coupling two busbars. E.ON Netz believed that doing so would lead to a reduction in the load flows on the line connecting the Landesbergen and Wehrendorf. However, after the line

connecting the Landesbergen and Wehrendorf substations tripped, the load flows previously carried on it were instantaneously dispatched to the other remaining lines in northern Germany. (The post investigation shown that the action of coupling two busbar had the inverse effect as the E.ON's operators expected). Becoming saturated, those lines also automatically tripped as a cascade of trippings. A large number of lines in Germany, Austria, Hungary and Croatia automatically tripped one after the other in a "domino" effect, as their automated protection systems detected load flows over the safety limit. At 10.10 pm and 30 seconds, the European network was abruptly split into three unconnected areas: the western area (western Germany and Austria, Slovenia, Benelux, Switzerland, France, Spain, Italy, Portugal, part of Croatia); the north-eastern area (eastern Germany and Austria, Poland, Czech Republic, Slovakia, Hungary); the south-eastern area (Greece, Albania, Macedonia, Bulgaria, Serbia, Montenegro, Bosnia-Herzegovina, eastern Croatia and a small part of Hungary).



a. Frequency recording until the split



b. Frequency recording after the split

Figure 2-1: Frequency of the European power system before and after the split [17].

- A wide area power system blackout had been avoided by activating of the good performance of countermeasures of individual control areas. Especially, the effective underfrequency load shedding in France (with 6460 MW or 12% total load was shed) had provided considerable contributions to save the system. Even though, more than 15 million European households were affected.

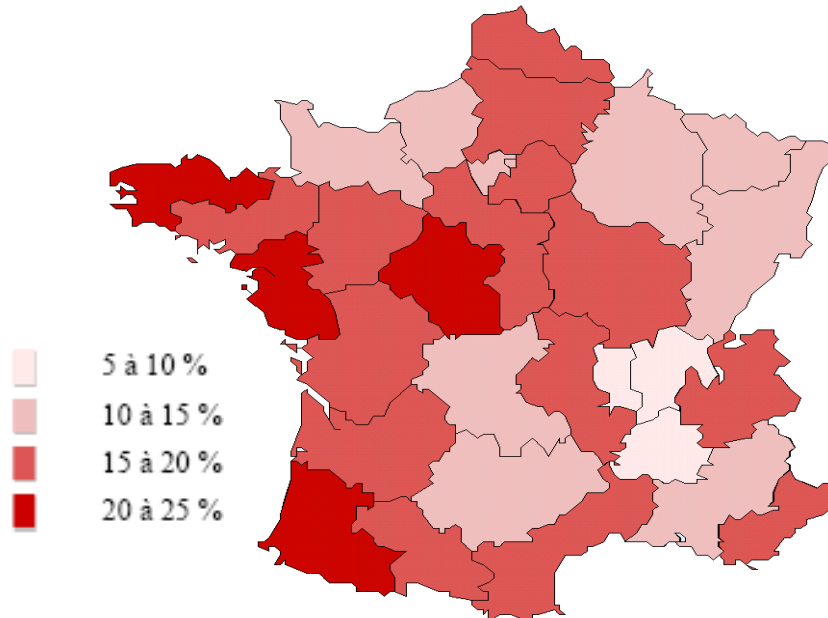


Figure 2-2: Map of under-frequency load shedding in the French power system [18].

- *Major causes:* Power system was not met the N-1 security criterion. The careless planning tripping and human errors are some examples: the lack of coordination between control centers were also the major cause of the disturbance. Another cause is related to the presence of distributed generation which made the power flow direction more complicated in the critical situation than the dispatcher had thought. However, most the TSO did not have real-time data of these distributed generators in distribution network. The lack of training courses for jointing control system operators was one of the main causes.
- When comparing to the blackout in USA 2003 and Italy 2003, the mechanism of the disturbance was related to the problem of large frequency deviation. Even, the system was split into three part because of large frequency deviation, but it was not a real power system blackout.
- There were also other blackouts that their direct causes have been investigating such as blackouts in: London (August 08, 2003), Helsinki (August 09, 2003), Shanghai (August 27, 2003), Athens (October 06, 2003), Georgia (September 23, 2003), Bahrain (August 08, 2004), Australia (August 14, 2004), Kuwait (November 1, 2004), Malaysia (January 13, 2005), Moscow (May 25, 2005), Swiss railways system (June 2005), Dubai (June 9, 2005) [19].

The clear analyses above have convinced that power system blackouts still need more attentions as the worst catastrophe of any power system. Even there have had considerable improvements in planning and designing stage, installing new equipments, intensive training

operators, but the power systems seem more vulnerable to disturbances, especially when they are operating very close to their limit. Therefore, it is essential to understand the main causes and mechanisms of such serious power system blackout in order to prevent future occurrences.

2.2.2 Causes of Power System Blackouts

Generally, a power system blackout is a very complicated phenomenon which has multiple causes. A blackout is normally a final result of progressively sequence events. The causes may come from many diversity sources. In this dissertation, some main causes are summarized as following:

The causes may be initiated at the time of planning and designing stage. For example, bad load forecasting that leads to the lack of electrical energy support for load demand (the blackout in Greece in 2004 was an example). Another important issue in this stage is the security criterion. Since securing the system against all possible contingencies is clearly impossible, it is typically assumed that the probability of two or more independent faults or failures taking place simultaneously is too low to be considered credible. Most security rules therefore request the system to be able to withstand the loss of any single component. When a power system satisfies this criterion, it is said to be “N-1 secure” because it could lose any one of its N components and continue operating. Similarly, in a system that is “N-2 secure”, no consumer would be disconnected even if two components were suddenly out. However, some wrong and/or poor power system designs in planning stage did not meet requirements of N-1 and/or N-2 security criteria were caused of power system blackouts (the power system blackout in southern Sweden and eastern Denmark in 2003 was an example). Wrong design and setting for protection system also considered as one cause of power system blackout (the different setting values between two ends of a transmission in the UCTE system- European disturbance in 2006). The changing in system structure and philosophy at this stage also plays very important role for system designers.

There are many critical causes for a power system blackout coming from the operating mission. In deregulation environment, there are many sub-systems operators which compete and control the interconnected transmission system (the so-called TSOs). The presence of quite large volume of distributed generation also makes the power systems more complicated in term of management and control. Therefore, the power systems operators may not fully understand the operating system, especially, when there are many contracts, complicated load-flow, and complex contingencies occurred in a very large system. As the result, the poor coordination and lack of urgent and exact cooperation prevention/correction actions between controlled centers were direct and critical reasons leading to power system blackouts (power system blackout in the Italy in 2003, and European disturbance in 2006 were some examples).

In the maintenance work, there are also some risks. For example, the failures of too old equipments, or unplanned maintenance work, even unplanned tree cutting, lack of training for system operators and jointed training between control centers have considered for some power system blackouts (the blackouts in London in 2003, Moscow in 2005, and European disturbance in 2006 were some examples).

Many other causes those are unpredictable, for example, malfunction of protection devices, or technical problems such as failures in energy system management (ESM), state estimator

(SE) and real time contingency analysis (RTCA) prevented power system operators from monitoring and accessing power system operating conditions in order to perform urgent preventive and corrective actions (power system blackout in the United States-in August, 2003 was an example). Critical weather conditions such as unusually high or low temperature that caused considerable unforeseen increases in load demand were considered as an initial reason. Severe natural disasters are also direct causes of some initial failures in power system. The general causes of power system blackouts can be summarized as the figure below.

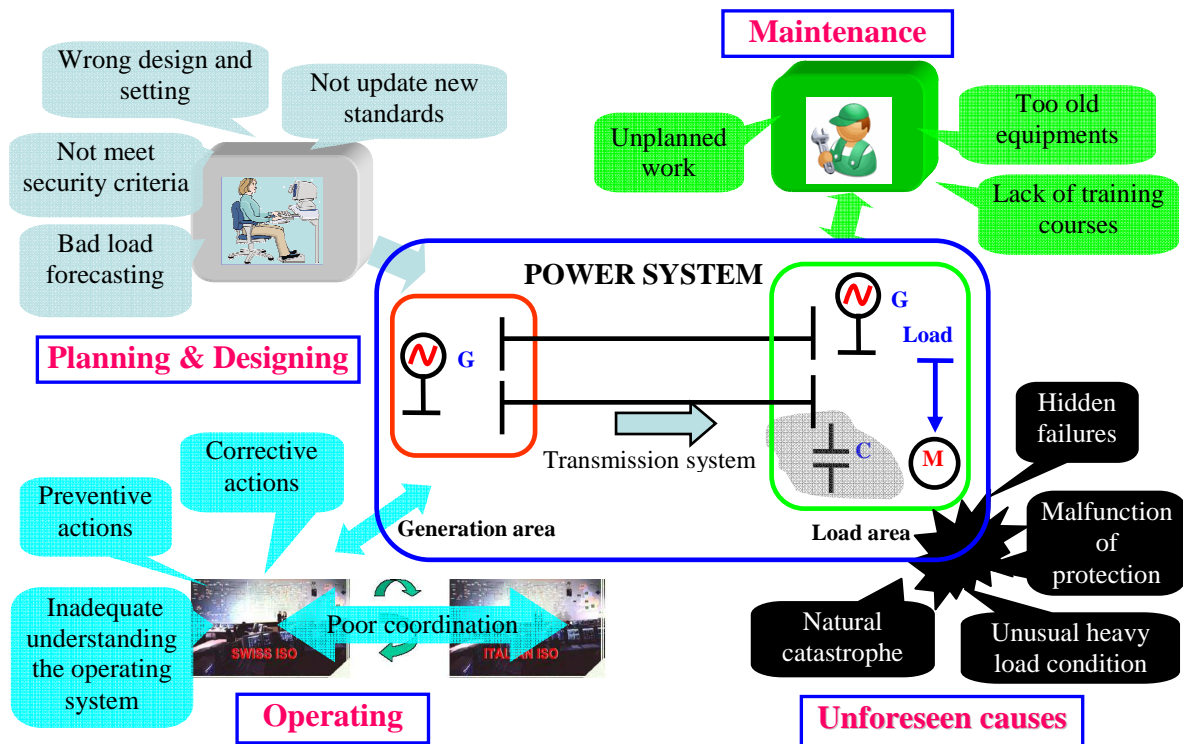


Figure 2-3: General causes of power system blackouts.

2.2.3 Mechanisms of Power System Blackouts

In the previous section, we have reviewed many power system blackouts happened in recent decades but the mechanisms of blackouts were different from each other, from single system to interconnected system, from integrated system to new structure system. However, all of them have a common process that power systems go from the normal operating steady state that may be closer to the security limit to instability and break up state eventually. The mechanisms of all power system blackouts are directly related to the problems of power system instability. Specifically, they are angle instability, frequency instability and voltage collapse. The typical mechanism for all blackouts could be generally summarized as follows:

- Power systems are initially operated at unfavorable and vulnerable conditions those may be very close to their stability limits. For example, the power system loses some generating units and/or transmission lines because of normal maintenance work or faults, while customer load demand may exceed the capacity of the power systems in both active and reactive power. Furthermore, load center areas may be too far from

power generating areas causing increasing in transmission loss. Such a heavily loaded condition may be too close to limitation of transmission lines or capacity of generating units. These inconvenient situations cause low voltage at some buses in the power system. Bad weather conditions (unusually too high or too low temperature causing unforeseen increase in load demand) may worsen the current situation.

- These severe conditions may face some fatal contingencies. Triggering with one or some more incidents (N-1 or N-m contingencies ($m \geq 2$)) such as tripping off very important transmission lines or important generating units will contribute to increase of active/reactive power loss in the whole power system. Some power system components may experience overloaded operating condition. Voltage at some buses may be out of desired range. Moreover, unbalance between load and generation may cause power system oscillation or synchronization that follows some angle/frequency instability problems.
- The lack of urgent prevention/correction actions between control centers, human errors or malfunction of some protection and/or control devices may cause further failures in power system. Especially, hidden failures in monitoring system (the failure of ESM is an example) may prevent power system operators from performing proper “early warning” assessments of the system. Voltage of power system may gradually reduce. Local and/or interarea power oscillations are increased and angle/frequency may become unstable.
- Activations of transformers with ULTCs try to recover voltage at load buses that require more reactive power from generators/shunt capacitors to support for the load. Limit protection of reactive power output of generating units or compensation devices may worsen overall power system security. These phenomena lower gradually the voltage of the power system until rapid cascade of voltage occurs. Consequently, power system voltage collapses in part or entirely. Therefore voltage collapse is one of the major causes of power system blackout.
- The lack of damping power oscillations and/or angle/frequency instability result in loss of some generator synchronism. Protection systems against loss of synchronism are active to trip off these generators, causing more unbalance between generation and load. Cascade tripping of other generators or overload transmission lines will follow angle and frequency instability. Therefore angle and frequency instability are major causes of power system blackout.

We can summarize the typical mechanism of power system blackout and divide it into some major steps as in the figure below:

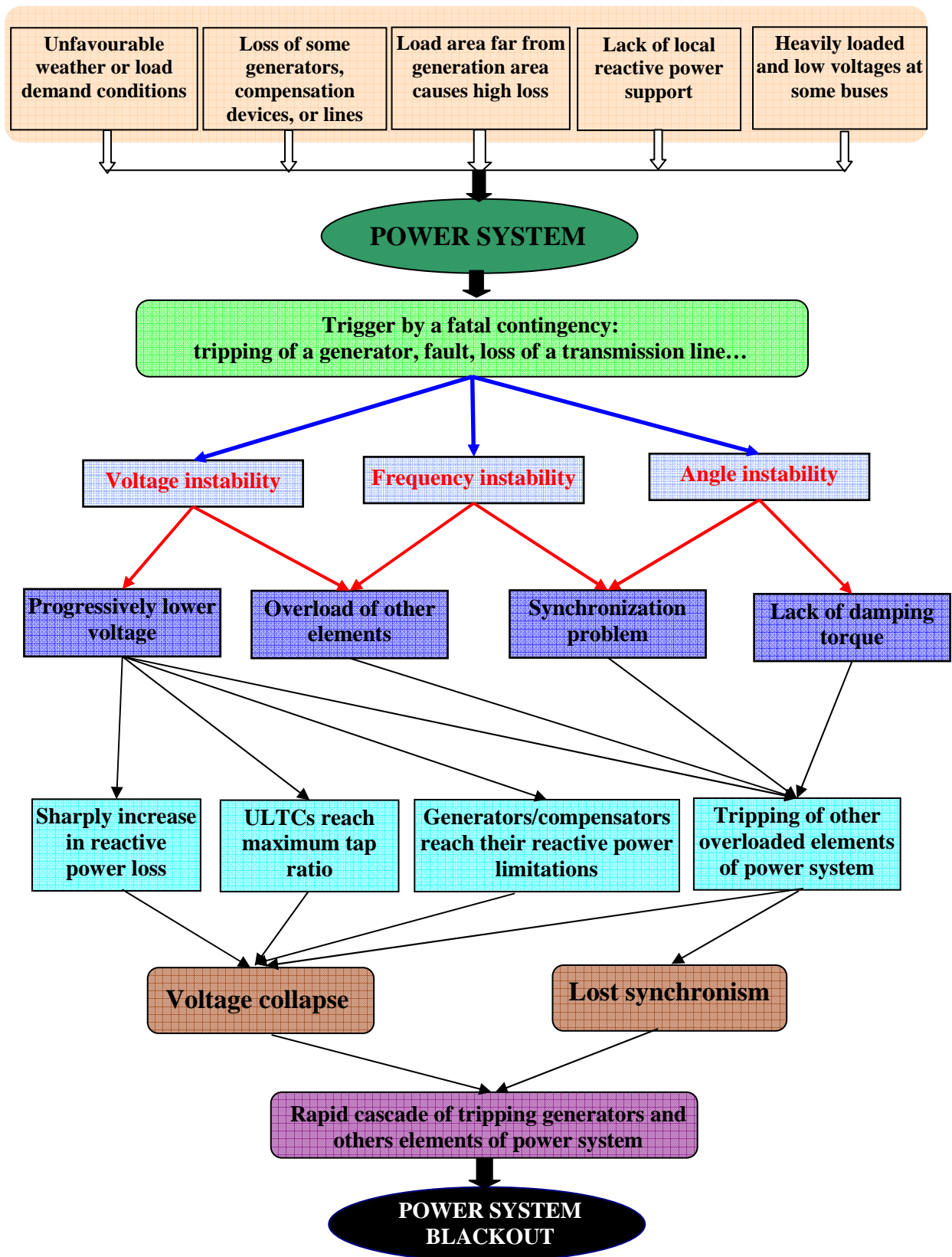


Figure 2-4: Typical mechanisms of power system blackout.

2.2.4 Power System Stability

As discussed in the previous part, there are many the causes for power system blackouts. They come from planning and designing stage, operating missions, maintenance duty or unforeseen causes. The direct cause of power system blackout is always related to the problem of power system stability. In power system stability analysis, the severity of and many types of small and large disturbances also have significant influence on power system blackouts.

When dealing with small disturbances such as minor load changing or slight faults, the system must be able to adjust to these changing conditions and operate satisfactorily security criteria. It must also be able to survive after experiencing one severe disturbance such as a loss of a transmission line or loss of a large generator. A large disturbance usually leads to structural changes due to the isolation of the faulty elements. If the power system is stable after occurrence of a disturbance, it will reach a new equilibrium state with the system integrity preserved. Some generators and loads may be disconnected by the isolation of faulty elements or intentional tripping to preserve the continuity of operation of bulk of the system. Interconnected systems, for certain severe disturbances, may also be intentionally split into two or more “islands” to preserve as much of the generation and load as possible. The actions of automatic controls and possibly human operators will eventually restore the system to normal state. On the other hand, if the system is unstable, it will result in a run-away or run-down situation; for example, a progressive increase in angular separation of generator rotors, or a progressive decrease in bus voltages. An unstable system condition could lead to cascading outages and a shutdown of a major portion of the power system.

A classification power system stability by IEEE and CIGRE is shown in the figure below [1], [20].

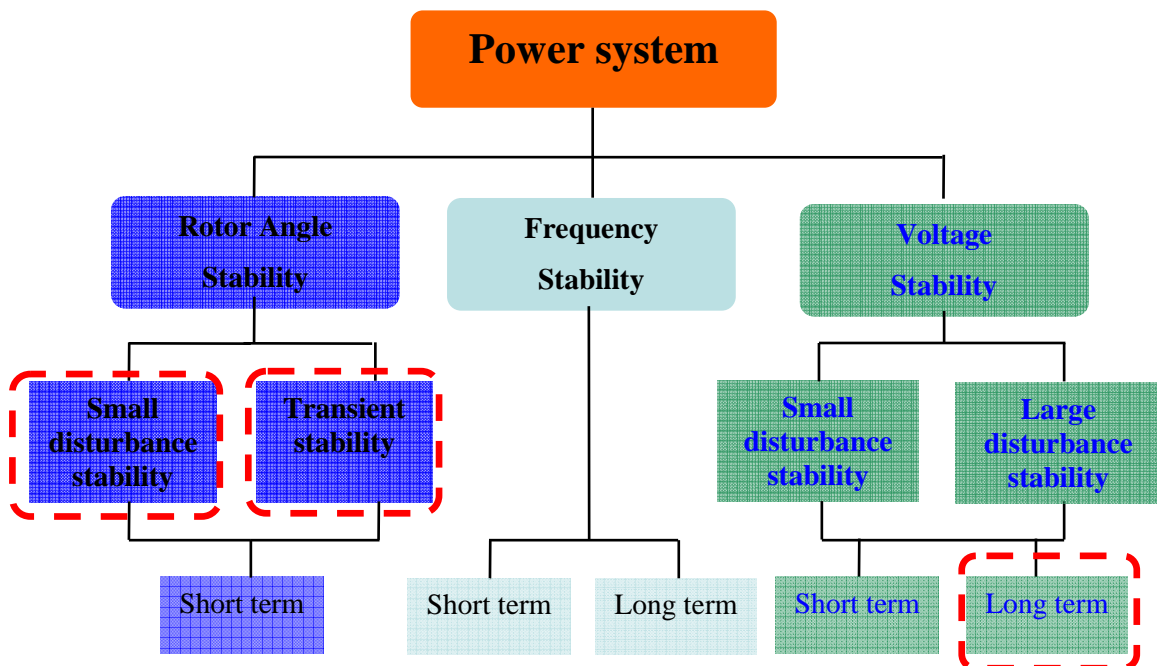


Figure 2-5: Classification of power system stability.

From Figure 2-5, the direct causes those lead to power system blackout could be considered as causes of angle instability, frequency instability or voltage collapse. The context of frequency instability is traditionally the imbalance between generation and load. Almost power systems around the world have been equipped with an effective frequency protection. However, the problem of frequency stability for very large interconnected system, where there are distribution generation and many transmission system operators (TSOs), is still a new issue and needs careful investigations. Therefore, we limit ourselves to study the problem of angle instability and long-term voltage collapse (as shown in Figure 2-5) which were dominant as major causes of power system blackouts in the past and future. Details causes as well as influenced factors for each type of interested instability problems will be investigated in next sections.

2.3 ANGLE STABILITY

2.3.1 Angle Stability Definitions

Some definitions of angle stability proposed by IEEE/CIGRE [20] are recalled in this part.

Rotor angle stability refers to the ability of synchronous machines of an interconnected power system to remain in synchronism after being subjected to a disturbance. It depends on the ability to maintain/restore equilibrium between electromagnetic torque and mechanical torque of each synchronous machine in the system. Instability that may result occurs in the form of increasing angular swings of some generators leading to their loss of synchronism with other generators. Angle stability could be classified into two categories:

Small-disturbance rotor angle stability (or small-signal rotor angle stability or small-signal stability-SSS) is concerned with the ability of the power system to maintain synchronism under small disturbances. The disturbances are considered to be sufficiently small that linearization of system equations is permissible for purposes of analysis. Small disturbance stability depends on the initial operating state of the system. Instability that may result can be of two forms:

- Increase in rotor angle through a non-oscillatory or aperiodic mode due to lack of synchronizing torque,
- Rotor oscillations of increasing amplitude due to lack of sufficient damping torque.

Figure 2-6 shows an example of the small signal instability during WSCC (USA) blackout, in August 1996. The figure shows the power swings on total California-Oregon Interconnection during the blackout.

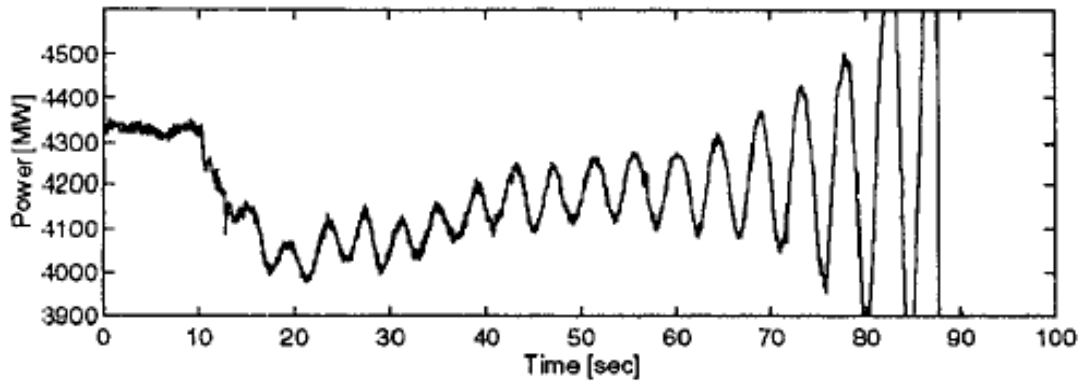


Figure 2-6: Total Power of California-Oregon Interconnection observed in the blackout in USA, August 10, 1996 [21].

Large-disturbance rotor angle stability or transient stability is concerned with the ability of the power system to maintain synchronism when subjected to a severe disturbance, such as a short circuit on a transmission line. The resulting system response involves large excursions of generator rotor angles and is influenced by the nonlinear power-angle relationship. Transient stability depends on both the initial operating state of the system and the severity of the disturbance. Instability is usually in the form of aperiodic angular separation due to insufficient synchronizing torque, manifesting as first swing instability.

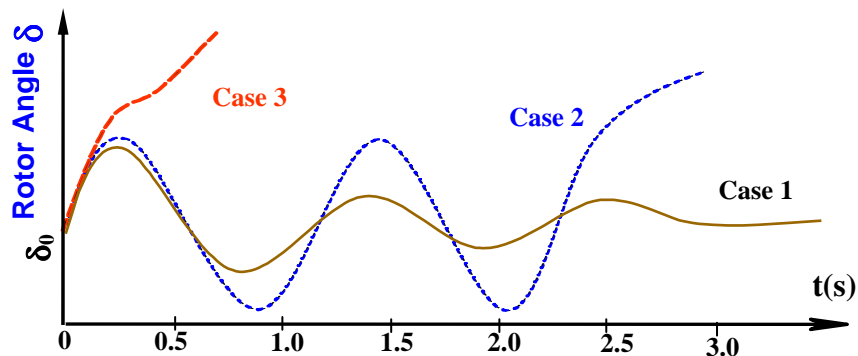


Figure 2-7: Rotor angle responses to a transient disturbance [1].

The Figure 2-7 illustrates the rotor angle responses to a disturbance. In the stable case, (case 1), the rotor angle reaches its maximum value and oscillates with decreasing amplitude until it reaches its stable value. In case 2, the rotor angle increases steadily until synchronism is lost. This form refers to first-swing instability. In case 3, the rotor angle is stable at the two first cycles but oscillates and becomes unstable after two circles as the result of growing amplitude oscillation as the end state is approached [1].

2.3.2 Methods for Angle Stability Analysis

2.3.2.1 Small Disturbance Rotor Angle Stability

When dealing with small disturbance rotor angle stability problems, the disturbances are normally considered to be sufficiently small such that linearization of power system equations

is applicable for study and analyze purposes. The traditional methods are based on the analyses of eigenvalues and related component such as eigenvectors and participation factor.

A dynamic power system can be described by a system of non-linear differential equations as follows [1], [22], [23]:

$$\begin{aligned}\dot{x} &= f(x, u) \\ y &= g(x, u)\end{aligned}\tag{2.3-1}$$

If the disturbance is small, equation (2.3-1) can be linearized around an operating point $x=x_0$, and the linearized form of the dynamic system can be written as:

$$\begin{aligned}\Delta \dot{x} &= A.\Delta x + B.\Delta u \\ \Delta y &= C.\Delta x + D.\Delta u\end{aligned}\tag{2.3-2}$$

where:

Δx is the state vector of dimension $n \times 1$

Δy is the output vector of dimension $m \times 1$

Δu is the input vector of dimension $r \times 1$

A is the state matrix of dimension $n \times n$

B is the control matrix of dimension $n \times r$

C is the output matrix of dimension $m \times n$

D is the matrix which defines the proportion of inputs which appear directly in the output, dimension $m \times r$

a. Eigenvalues

By taking Laplace transform of the equation (2.3-2) we get

$$\begin{aligned}s.\Delta x(s) - \Delta x(0) &= A.\Delta x(s) + B.\Delta u(s) \\ \Delta y(s) &= C.\Delta x(s) + D.\Delta u(s)\end{aligned}\tag{2.3-3}$$

Rearranging equation (2.3-3), we get

$$\begin{aligned}(sI - A).\Delta x(s) &= \Delta x(0) + B.\Delta u(s) \\ \Delta x(s) &= \frac{adj(sI - A)}{\det(sI - A)}[\Delta x(0) + B.\Delta u(s)]\end{aligned}\tag{2.3-4}$$

The poles of the dynamic system are the roots of the equation

$$\det(sI - A) = 0\tag{2.3-5}$$

The values s , which satisfy the above are known as eigenvalues of matrix A , and the equation (2.3-5) is called the characteristic equation of matrix A . The eigenvalues provide meaningful senses in term of small disturbance stability analysis.

Following Lyapunov first method for evaluating small disturbance stability properties [1] the eigenvalues (or modes) determine the system stability characteristics. A real positive (negative) eigenvalue determines an exponentially increasing (decreasing) behavior. A complex eigenvalue of positive (negative) real part results in increasing (decreasing)

oscillatory behavior. The systems response is the combination of the system response to each of n modes.

b. Eigenvectors and modal matrices

We assume that $\lambda = \lambda_1, \lambda_2, \dots, \lambda_n$ are the eigenvalues of matrix A. For each eigenvalue λ_i , the associated right eigenvectors Φ_i and left eigenvectors Ψ_i are defined according to:

$$\begin{aligned} A \cdot \Phi_i &= \lambda_i \cdot \Phi_i \\ \Psi_i^T \cdot A &= \lambda_i \cdot \Psi_i^T \end{aligned} \quad (2.3-6)$$

The left and right eigenvector corresponding to different eigenvalues are orthogonal. In practice, it is common to normalize these vectors, so that $\psi_i \phi_i = 1$ and $\psi_j \phi_i = 0$ if λ_i is not equal to λ_j . In order to express the eigenproperties of matrix A, some matrices are introduced under modal form.

$$\begin{aligned} A \cdot \Phi &= \Phi \Lambda \\ \Psi \cdot \Phi &= I \\ \Psi_i &= \Phi_i^{-1} \\ \Phi^{-1} A \cdot \Phi &= \Lambda \end{aligned} \quad (2.3-7)$$

where: $\Phi = [\Phi_1, \Phi_2, \dots, \Phi_n]$, $\Psi = [\Psi_1^T, \Psi_2^T, \dots, \Psi_n^T]^T$ the right and left eigenvectors and Λ is a diagonal matrix with eigenvalues $\lambda_1, \lambda_2, \dots, \lambda_n$.

Power system response to a disturbance is the combination of system to each of n mode shapes. The right eigenvector matrix Φ is known as the mode shape matrix, that is, eigenvector Φ_i is known as the i^{th} mode shape corresponding the eigenvalue λ_i . The right eigenvector defines the physical mode shape of natural response (for example: the grouping, phases, and magnitudes of generators' frequency swings experienced in an electromechanical mode). It measures the activity of state variables participating in a certain oscillation mode. The corresponding left-eigenvector measures the control effect on this mode.

c. Participation factors

One problem in using right and left eigenvectors individually for identifying the relationship between the state variables and the modes is the elements of the eigenvectors are dependent on units and scaling associated with the state variables. Solution for this problem is a matrix called *the participation matrix (P)* which combines the right and left eigenvectors as a measure of the association between the state variables and modes.

$$P = [p_1 \ p_2 \ \dots \ p_n] \quad (2.3-8)$$

with

$$p_i = \begin{bmatrix} p_{1i} \\ p_{2i} \\ \vdots \\ p_{ni} \end{bmatrix} = \begin{bmatrix} \Phi_{1i} \Psi_{i1} \\ \Phi_{2i} \Psi_{i2} \\ \vdots \\ \Phi_{ni} \Psi_{in} \end{bmatrix} \quad (2.3-9)$$

where:

Φ_{ki} : the element on the k^{th} row and i^{th} column of the modal matrix Φ , or k^{th} entry of the right eigenvector.

Ψ_{ik} : the element on the i^{th} row and k^{th} column of the modal matrix Ψ , or k^{th} entry of the right eigenvector.

The element $p_{ki} = \Phi_{ki} \Psi_{ik}$ is called the *participation factor*. A participation factor is a dimensionless magnitude. It is a measure of the influence of the k^{th} state variable in the i^{th} mode. Therefore, the participation factor can be used to determine whether a power system stabilizer (PSS) is needed to damp system oscillations. If the participation factor of a generator in an area is large, then a PSS placed at that generator would damp the oscillations of the system.

d. Methods for eigenvalues analysis of large-scale power systems

The eigenstructure of the state matrix of the linear model of a power system provides a great deal of quantitative information to analyze and control power system oscillation. However, full eigenvalue analysis (computation of all eigenvalues, and associated eigenvectors as well as participation factors of all modes) is impracticable to large-scale power systems because of computational requirement, for instance, with a practically large power system that includes hundreds of generators, the number of state variables may reach to thousands; therefore, a procedure of full eigenvalue analysis will involve the calculation of some very large matrices with very large dimensions (over than 10000). This procedure will be costly from the computational point of view and needs huge storage capacity.

An alternative to full eigenvalue analysis of power systems is to use some order reduction techniques consisting of a small fraction of all system modes. Several successful methods have been reported in some literature [1], [24], [25], [26] such as Selective Modal Analysis (SMA), Modifier Arnoldi Method, Dominant Pole Spectrum Eigensolver and AESOPS algorithm developed by EPRI. All of them build a reduced matrix of much smaller dimension that contains the eigenvalues of interest. They use different approaches to build that reduced matrix. Selective Modal Analysis (SMA) is based on an assumption that the modes of interest are associated to a subset of relevant state variables, which have much influence on the dynamic behavior of the power system in question. The Modified Arnoldi Method is a mathematical approach that has been adapted to compute a small number of eigenvalues around a selected point of the complex plane using a reduction technique in which the matrix A is reduced to an upper Hessenberg matrix. The Dominant Pole Spectrum Eigensolver makes use of the Bi-Iteration eigenanalysis algorithm and concentrates on the dominant modes of a selected function. AESOPS method calculates eigenvalues that associated only with rotor angle models, one complex conjugate pair of eigenvalues at a time.

Each of the methods described above has some special features by itself, which makes it attractive for a particular type of application. However, none of them could satisfy all the requirements of small signal stability analysis of power systems. Therefore, the best solution is to use several techniques in a complementary manner.

2.3.2.2 Large Disturbance Rotor Angle Stability or Transient Stability

a. Equal-Area Criterion

In this section, the fundamental concepts and principles of transient stability corresponding to large disturbance will be analyzed by using very simple models. Consider a Single-machine and infinite bus system (SMIB) [1], [27] as shown in the Figure 2-8. The equivalent circuit with classical generator model is shown in the Figure 2-9.

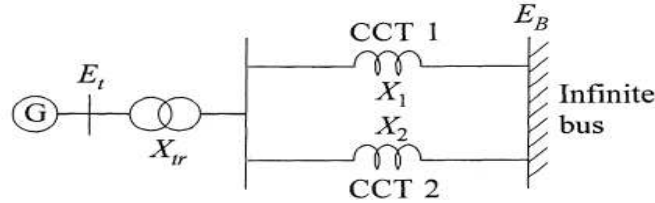
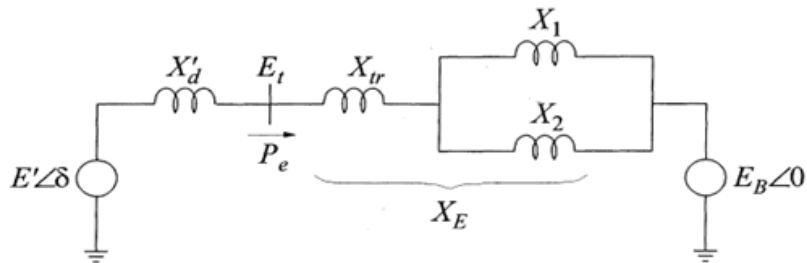
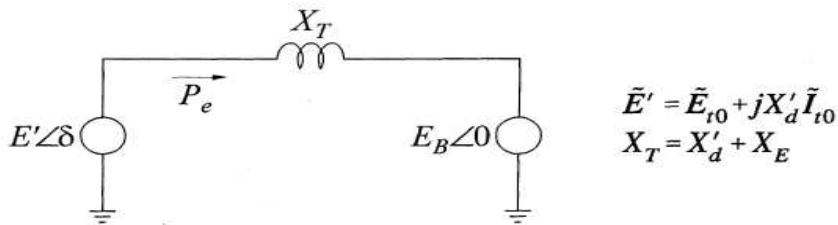


Figure 2-8: Single machine infinite bus (SMIB).



a, Equivalent circuit



b, Reduced equivalent circuit

Figure 2-9: System representation with generator represented by classical model.

The voltage behind the transient reactance (X'_d) is denoted by E' . The rotor angle δ represents the angle by which E' leads E_B .

The electrical power output is calculated as:

$$P_e = \frac{E' E_B}{X_T} \sin \delta = P_{\max} \sin \delta \quad (2.3-10)$$

where: $P_{\max} = \frac{E' E_B}{X_T}$.

The *equation of motion* or *swing equation* is now written as:

$$\frac{2H}{\omega_0} \frac{d^2\delta}{dt^2} = P_m - P_{\max} \sin \delta \quad (2.3-11)$$

where:

H is inertia constant (MW.s/MVA)

P_m is mechanical power input (pu)

P_{\max} is maximum electrical power output (pu)

δ is the rotor angle (elec.rad)

t is time (s)

ω_0 is rated angle velocity (rad/s)

In this simple case, it is not necessary to formally solve the swing equation in order to determine whether the rotor angle increases indefinitely or oscillates about an equilibrium position. The factor influence on transient stability could be investigated graphically by using power-angle diagram as shown in Figure 2-10

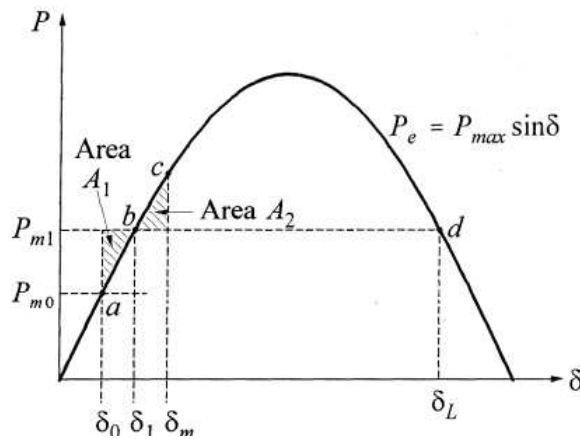


Figure 2-10: Power-angle varies to a step change in mechanical power input.

The relationship between the rotor angle and the accelerating power is calculated as:

$$\frac{d^2\delta}{dt^2} = \frac{\omega_0}{2H} (P_m - P_e) \quad (2.3-12)$$

Since P_e is a nonlinear function of δ , and therefore the above equation cannot be solve directly. Multiply both side by $2d\delta/dt$, then we have

$$2 \frac{d\delta}{dt} \frac{d^2\delta}{dt^2} = \frac{\omega_0}{H} (P_m - P_e) \frac{d\delta}{dt}$$

or

$$\frac{d}{dt} \left[\frac{d\delta}{dt} \right]^2 = \frac{\omega_0 (P_m - P_e)}{H} \frac{d\delta}{dt} \quad (2.3-13)$$

Integrating both sides, we get:

$$\left[\frac{d\delta}{dt} \right]^2 = \int \frac{\omega_0 (P_m - P_e)}{H} d\delta \quad (2.3-14)$$

The speed deviation $d\delta/dt$ is initially zero, it will change as a result of the disturbance.

For stable operation

The deviation of angle δ must be bounded. It reaches a maximum value (point c as in the Figure 2-12) and changes direction. Therefore, a criterion for stability is written as follows:

$$\int_{\delta_0}^{\delta_m} \frac{\omega_0 (P_m - P_e)}{H} d\delta = 0 \quad (2.3-15)$$

where δ_0 is the initial rotor angle and δ_m is maximum rotor angle as in Figure 2-10. Thus, the area under the function $(P_m - P_e)$ plotted against δ must be zero if the system stable. This satisfies condition accelerated area A1 is equal to decelerated area A2. Kinetic energy gained by the rotor during acceleration when δ changes from δ_0 to δ_1 is calculated as:

$$E_1 = \text{area A1} = \int_{\delta_0}^{\delta_1} \frac{(P_m - P_e)}{H} d\delta \quad (2.3-16)$$

The energy lost during deceleration when δ changes from δ_1 to δ_m is:

$$E_2 = \text{area A2} = \int_{\delta_1}^{\delta_m} \frac{(P_m - P_e)}{H} d\delta \quad (2.3-17)$$

For stable case, the area A1 must be equal to the area A2. This forms of the basic for the equal area criterion. It enables us to determine the maximum swing of δ and hence the stability of system without computing the time response through formal solution of the swing equation. The criterion can be readily used to determine the maximum permissible increase in P_m for the system. The stability is maintained only if an area A2 at least equal to A1 can be located above P_{m1} . If A1 is greater than A2 then $\delta_m > \delta_L$ (limit angle) and stability will be lost.

Response to a fault

Assume that there is a three phase fault occurred at point F on one of two parallel lines as in the Figure 2-11 and the fault is cleared by tripping this line. The clearing time depends on the delay of protection system. The most critical case is when the fault occurs near the HT bus. During the fault time, active power of generator, P_e , that corresponding to electrical torque T_e has a value of zero, and only reactive power output is transmitted. If the fault occurs far enough from the HT bus as in Figure 2-11, a portion of active power could be transported to the infinite bus during the fault.

Figure 2-12 shows the curves of P_e and δ for three operating conditions of the power system with constant mechanical power P_m .

1. Prefault condition: two transmission lines are on service
2. During the fault condition:
3. Postfault condition: faulted transmission line is tripped.

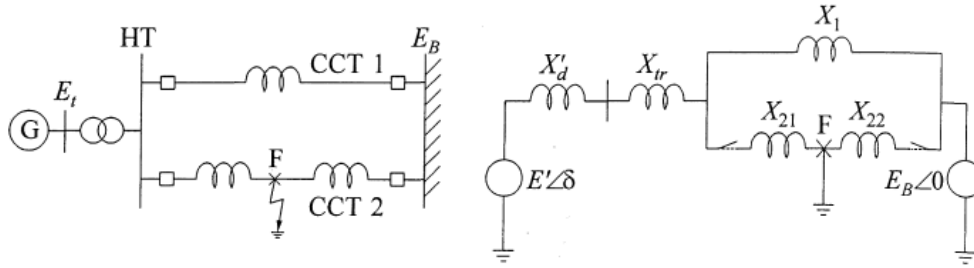


Figure 2-11: Single machine infinite bus (SMIB) and equivalent circuit.

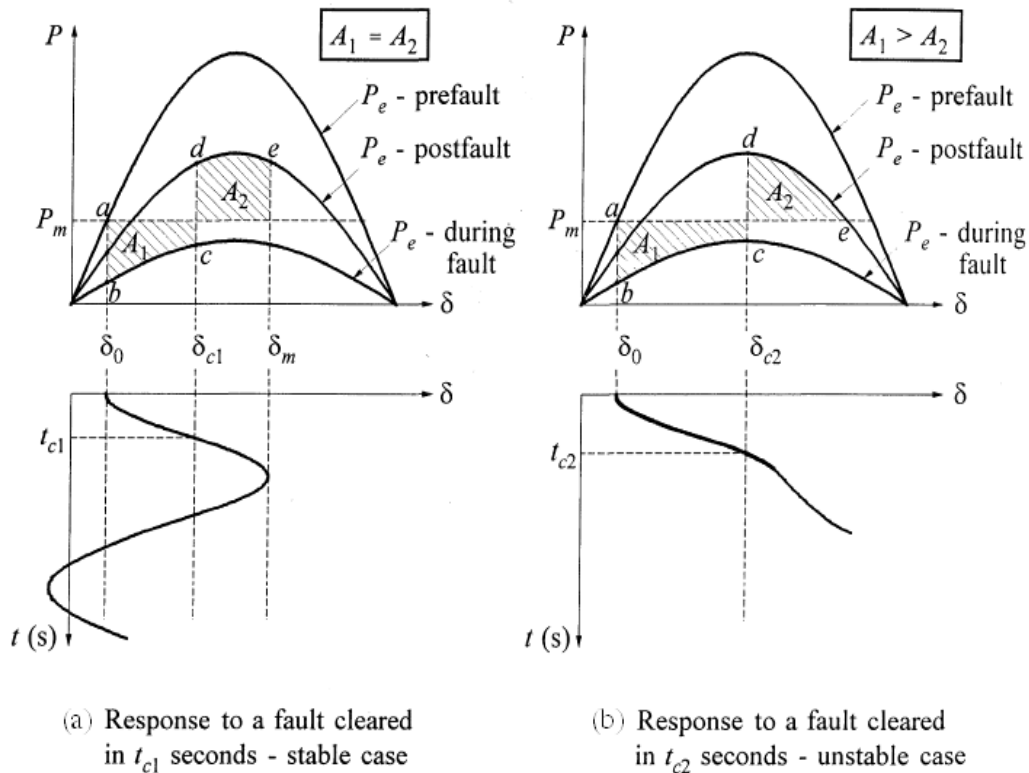


Figure 2-12: System response to a fault: stable case and unstable case.

For the stable case as in Figure 2-12 (a), with clearing time t_{c1} : The system is initially operating with both circuits such that $P_e = P_m$ and $\delta = \delta_0$. When the fault occurs, operating point suddenly moves from a to b. Due to inertia and angle δ cannot change instantly. Since P_m is now greater than P_e , the rotor accelerates until the operating point reaches c. When fault is cleared by tripping the faulted transmission line, the operating point then suddenly shifts to d. Now P_e is greater than P_m , causing deceleration of the rotor. Since the rotor speed is greater than the synchronous speed ω_0 , angle δ continues to increase until the kinetic energy gained during the period of acceleration (represented by accelerating area A_1) is expended by transferring the energy to the system. The operating point moves from d to e, such that decelerating area A_2 is equal to A_1 . At point e, the speed is equal to ω_0 and δ has reached its maximum value δ_m . Since P_e is still greater than P_m , the rotor continues to retard, with the speed dropping below ω_0 . The rotor angle δ decreases, and the operating point retraces the path from e to d and follows the P_e - δ curve for the postfault system further than down. The

minimum value of δ such that it satisfies the equal-area criterion for the postfault condition. In the absence of any source of damping, rotor continues to oscillate with constant amplitude.

For the unstable case as in Figure 2-12 (b) with clearing time t_{c2} is longer than t_{c1} . The area A2 is less than A1. When the operating point reaches, the kinetic energy gained during the accelerating period has not yet been completely expended. Consequently, the speed is still greater than ω_0 and δ continues to increase. Beyond point e, P_e is less than P_m , and the rotor begins to accelerate again. The rotor speed and angle continue to increase, leading to the loss of synchronism.

In case of large-scale power system, considerable research has been concentrated on studying transient stability that could be classified into some categories [1]:

b. Time domain simulation by numerical integration methods

P. Kundur [1] summarized different numerical methods that are used to solve a typical differential equation of power system when power system experiencing a fault.

$$\frac{dx}{dt} = f(x, t) \quad (2.3-18)$$

where x is the state vector of n independent variable and t is the time.

Explicit methods include modified Euler, original and modified Runge-Kutta methods which try to solve x as a function of t , with initial value of x and t equal to x_0 and t_0 respectively. These methods are easy to implement for the solution of a complex set of system state equations. These methods are also called the explicit integration methods.

The significant limitation of explicit integration methods is that they are not numerically A-stable [1], as a consequence, the length of the integration time step is restricted by the small time constant of the system. In order to overcome these limitations, some implicit methods that use the *trapezoidal rule* are employed. These methods are normally employed in simulation software in order to investigate the system response with respect to time of fault, duration of fault or fault location. The effect of controller devices such as PSS, excitation system, load models are also investigated by using these methods. The major drawback of this method is the stability region of the power system is unpredictable.

c. Direct methods using an energy function

The direct methods determine stability without explicitly solving the system differential equations [1], [27]. The energy-based methods are a special case of more general Lyapunov second method or the direct method. (The Lyapunov second method attempts to determine stability directly by using suitable functions which are defined in the state space. The sign of the Lyapunov function and the sign of its time derivative with respect to the system state equations are considered:

The equilibrium of equation (2.3-4) is *stable* if there exists a positive definite function $V(x_1, x_2, \dots, x_n)$ such that its total derivative \dot{V} with respect to equation (2.3-4) is not positive. The equilibrium of equation (2.3-4) is *asymptotically stable* if there exists a positive definite function $V(x_1, x_2, \dots, x_n)$ such that its total derivative \dot{V} with respect to equation (2.3-4) is negative definite. The system is *stable* in that region in which \dot{V} is negative semi-definite and asymptotically stable if \dot{V} is negative definite [1])

The context of rolling ball is used to explain the application of this method. The method is summarized for multiple machines cases as follows [1]:

The generator transient reactances and load admittances included in the node admittance matrix are described as:

$$I_G = Y_R E_G \quad (2.3-19)$$

where Y_R is the reduced admittance matrix with all nodes other than the generator internal nodes eliminated, E_G is the generator internal source voltage vector and I_G is generator current vector.

Let the internal voltage of the i^{th} generator in phasor notation be given by

$$\dot{E} = E_i \angle \delta_i \quad (2.3-20)$$

and

$$y_{ij} = G_{ij} + j.B_{ij} \quad (2.3-21)$$

For a system with n machines, the active power output of the i^{th} generator is given by:

$$\begin{aligned} P_i &= \text{Re}(\dot{E}_i \dot{I}_i^*) = \text{Re} \dot{E}_i \left(\sum_{j=1}^n \dot{y}_{ij}^* \cdot \dot{E}_j^* \right) \\ &= E^2 G_{ii} + \sum_{\substack{j=1 \\ j \neq i}}^n E_i \cdot E_j \left[B_{ij} \sin(\delta_i - \delta_j) + G_{ij} \cos(\delta_i - \delta_j) \right] \end{aligned} \quad (2.3-22)$$

For the application of the Transient Energy Function (TEF) method, it is necessary to describe the transient behavior of the system with the generator rotor angles expressed regarding to the inertial centre of all the generators. The position of the Centre of Inertia (COI) is defined as:

$$\delta_{COI} \square \frac{1}{H_T} \sum_{i=1}^n H_i \delta_i \quad (2.3-23)$$

where: H_T is the sum of the inertia constants of all n generators in the system. The motion of the COI is determined as

$$2H_T p(\Delta\omega_{COI}) = P_{COI} = \sum_{i=1}^n (P'_{mi} - P_{ei}) \quad (2.3-24)$$

where:

$$\begin{aligned} P'_{mi} &= P_m - E_i^2 G_{ii} \\ P_{ei} &= \sum_{\substack{j=i+1 \\ j \neq i}}^n \left[C_{ij} \sin(\delta_i - \delta_j) + D_{ij} (\delta_i - \delta_j) \right] \\ C_{ij} &= E_i E_j B_{ij} \\ D_{ij} &= E_i E_j G_{ij} \end{aligned} \quad (2.3-25)$$

P_{mi} is mechanical input power of the i^{th} machine

ω_0 is synchronous speed in elec.rad/s

$\Delta\omega_{COI}$ is per unit speed deviation of Central of Inertia (COI) from synchronous speed.

H is inertia constant

δ is rotor angle, in elec.rad

The motion of generators with respect to the COI can be expressed by defining

$$\theta_i = \delta_i - \delta_{COI} \quad \text{rad} \quad (2.3-26)$$

and

$$\omega_i = \frac{\dot{\theta}_i}{\omega_0} = \left(\frac{\dot{\delta}_i}{\omega_0} - \Delta\omega_{COI} \right) \quad \text{pu} \quad (2.3-27)$$

The energy function V describing the total system transient energy for total system transient energy for the post-disturbance system is defined as:

$$V = \frac{1}{2} \sum_{i=1}^n J_i \omega_i^2 - \sum_{i=1}^n P'_{mi} (\theta_i - \theta_i^s) - \sum_{i=1}^{n-1} \sum_{j=i+1}^n \left[C_{ij} (\cos \theta_{ij} - \cos \theta_{ij}^s) - \int_{\theta_i^s + \theta_j^s}^{\theta_i + \theta_j} D_{ij} \cos \theta_{ij} d(\theta_i + \theta_j) \right] \quad (2.3-28)$$

θ_i^s is angle of bus i at the post-disturbance Stable Equilibrium Point (SEP)

$J_i = 2H_i \omega_0$ is per unit moment of inertia of the i^{th} generator.

The transient energy function is composed of four terms:

1. $\frac{1}{2} \sum_{i=1}^n J_i \omega_i^2$: is the change in rotor kinetic energy of all generators in the COI reference frame. This term is also called the kinetic energy (V_{ke}) and is a function of only generator speed
2. $\sum_{i=1}^n P'_{mi} (\theta_i - \theta_i^s)$: is the change in rotor potential energy of all generator relative to COI
3. $\sum \sum C_{ij} (\cos \theta_{ij} - \cos \theta_{ij}^s)$: is the change in stored magnetic energy of all branches.
4. $\sum \sum \int D_{ij} \cos \theta_{ij} d(\theta_i + \theta_j)$: is the change in dissipated energy of all branches.

The sum of terms (2), (3), and (4) is called Potential Energy (V_{pe}) and is a function of generator angles.

The transient stability assessment involves the following steps.

1. Calculation of the critical energy V_{cr} (the boundary of the region of stability)
2. Calculation of the total system energy at the instant of fault-clearing V_{cl} .
3. Calculation of stability index $V_{cr} - V_{cl}$. The system is stable if the stability index is positive.

Time-domain simulation is run up to the instant of fault clearing to obtain the angles and speeds of all the generators. These are used to calculate the total energy (V_{cl}) at fault clearing. However, calculation of the boundary of the region of stability V_{cr} is the most difficult step in applying the transient energy function (TEF) method. Three different methods are normally applied to calculate the critical energy as follows [1]:

1. The closest Unstable Equilibrium Point (UEP) approach [28].
2. The controlling UEP approach.
3. The boundary of stability-region-based controlling UEP (BCU) method [29].

d. The SIME method

D. Ruiz-Vega and M. Pavella [30] proposed the Single Machine Equivalent (SIME) method that is a combination between the time-domain method and the equal area criterion.

The method could be summarized briefly as follows:

1. From a given power system. Using time-domain method for the purposes of contingencies analyses.
2. For each contingency, the angles of generators are plotted in the same axis system. Based on the increase of angle variation, generators are classified into two groups: stable and unstable group.
3. All generators in the same group will be described equivalently as one machine. From these two machines, an equivalent machine is formed the so called OMIB (one machine infinite bus).
4. Using the equal area criterion to assess the stability region of one machine OMIB with an infinite bus.

The parameters and dynamic equations of the OMIB are determined as follows:

The parameters of the OMIB angle, speed, inertia coefficient, mechanical power, electrical power and accelerating power are identified respectively by δ , ω , M , P_m , P_e , P_a . At any given moment, these parameters are calculated on the basis of the system machine parameters.

Angle of OMIB:

$$\delta(t) = \delta_C(t) - \delta_N(t) \quad (2.3-29)$$

where: index C is related to critical machines and index N to non-critical machines,

Inertia of OMIB

$$M_C = \sum_{k \in C} M_k, M_N = \sum_{j \in N} M_j, \quad (2.3-30)$$

$$M = \frac{M_C \cdot M_N}{M_C + M_N}$$

Speed of OMIB:

$$\omega(t) = \omega_C(t) - \omega_N(t) \quad (2.3-31)$$

Mechanical power of OMIB:

$$P(t) = M \left(M_C^{-1} \sum_{k \in C} P_{mk}(t) - M_C^{-1} \sum_{j \in N} P_{mj}(t) \right) \quad (2.3-32)$$

Accelerating power of OMIB

$$P_a(t) = P_m(t) - P_e(t) \quad (2.3-33)$$

Finally, the swing equation of OMIB

$$M \frac{d^2 \delta}{dt^2} = P_m(t) - P_e(t) \quad (2.3-34)$$

Once the swing equation of OMIB is formulated, the equal area criterion is applied to stability analysis purpose.

2.3.3 Preventive Methods for Angle Stability Improvement

2.3.3.1 Preventive Method for Small Signal Stability Improvement

The main cause of small signal stability (SSS) is directly related to the insufficient damping torque that leads to power system oscillations. Therefore, in order to prevent small signal instability, we have to add some damping torque devices.

Power system stabilizes (PSS) has been considered as the main and the most-cost effective devices used to add supplement damping in order to prevent power system oscillations. The main function of a PSS is to add an additional stabilizing control signal at the input of exciter. Considerable research concentrated on the optimal placement and design power system stabilizers has been discussed in references [1], [31], [32], [33], [34], [35] and [36]. These approaches are some algebraic methods based on the sensitivity analysis of eigenvalues and related components such as eigenvectors, participation factors, the so-called “eigenvalues-based method”. The optimal selection of PSS is classically determined by using participation factors of some critical modes.

Flexible AC Transmission System (FACTS devices), or High Voltage Direct Current (HVDC) are also considered as an alternative way used to add damping torque in order to prevent power system oscillations [1], [37], [38], [39]. For example, the uses of Static Var Compensator-SVC and HVDC with supplementary control signals have been used for damping power system oscillations. The problem of sub-synchronous resonance has been effectively mitigated by using Thyristor Controlled Series Compensator (TCSC) [40].

2.3.3.2 Preventive Method for Transient Stability Improvement

Methods used to improve transient stability of the power system could be classified into some categories as follows [1]:

- Reduction in the disturbing influence by minimizing the fault severity and duration: The amount of kinetic energy gained by the generators during a fault is directly proportional to the fault duration; therefore, the quicker fault is cleared, the less it causes severity. Selective and fast protection system, ultra-fast breaker are normally applied to shortening time of fault. Independent pole operation or single pole switching

breaker are used to clear selectively single phase fault. Auto-reclosing system or is an alternative for fast clearing fault in case of flashed-over faults.

- Increase of the restoring synchronizing forces: This method could be implemented by applying high-speed excitation system to increase rapidly temporary terminal voltage generator stator. Facts devices or compensation capacitor are also used to reduce transmission line reactance during disturbances that increase restoring synchronizing forces.
- Reduction of the accelerating torque through control of prime-mover mechanical power. Steam Turbine Fast-valving is a technique applicable to thermal units to assist in maintaining power system transient stability. It involves rapid closing and opening of steam valves in a prescribed manner to reduce the generator accelerating power following the recognition of a severe transmission system fault.
- Reduction of accelerating torque or applying artificial load. Rescheduling power generation is a way of reduce accelerating torque. Another alternative is fast load shedding.

2.4 VOLTAGE STABILITY

2.4.1 Voltage Stability Definitions

Some definitions of angle stability proposed by P. Kundur [1], C. W. Taylor [2], I.Dobson [41], and IEEE/CIGRE [20] are recalled in this part.

2.4.1.1 Voltage Stability

Voltage stability refers to the ability of a power system to remain steady voltage at all buses in the system after being subjected to a disturbance from a given initial operating condition.

Voltage stability problem can be further divided into sub-problems, which are large-disturbance voltage stability and small-disturbance voltage stability respectively.

- **Large-disturbance voltage stability** refers to the system ability to maintain steady voltages following large disturbances such as system faults, loss of generation, or circuit contingencies. Determination of large-disturbance voltage stability requires the examination of the nonlinear response of the power system over a period of time sufficient to capture the performance and interactions of such devices as motors, under load transformer tap changer (ULTC), and generator field-current limiters (or overexcitation limiters-OELs).
- **Small-disturbance voltage stability** refers to the system ability to maintain steady voltages when subjected to small perturbations such as incremental changes in system load. This form of stability is influenced by the characteristics of loads, continuous controls, and discrete controls at a given instant of time. This concept is useful in determining, at any instant, how the system voltages will respond to small system changes. With appropriate assumptions, system equations can be linearized for analysis

thereby allowing computation of valuable sensitivity information useful in identifying factors influencing stability. This linearization, however, cannot account for nonlinear effects such as tap changer controls (dead-bands, discrete tap steps, and time delays). Therefore, a combination of linear and nonlinear analyses is used in a complementary manner.

The time frame of interest for voltage stability problem may vary from few seconds to tens of minutes. Therefore, voltage stability may be either *short-term* or *long-term* phenomenon.

- **Short-term voltage stability** involves dynamic of fast acting load components such as induction motors, electronically controlled loads and HVDC converters. The study period of interest is the order of several seconds and techniques and analysis requires solution of appropriate system differential equations.
- **Long-term voltage stability** involves slower acting equipment such as ULTCs, thermostatically controlled loads, and OELs. The study period of interest may extend to several or many minutes, and long-term simulations are required for analysis of system dynamic performance. Stability is usually determined by the resulting outage of equipment, rather than the severity of the initial disturbance. Instability is due to the loss of long-term equilibrium (for example: when loads try to restore their power beyond the capability of the transmission network and connected generation).

2.4.1.2 Voltage Instability and Voltage Collapse

Voltage instability stems from the attempt of load dynamics to restore power consumption beyond the capability of the combination of transmissions and generation systems [20].

The term **voltage collapse** is the process by which the sequence of events accompanying voltage instability leads to a blackout or abnormally low voltages in a significant part of the power system.

Figure 2-13 shows an example of voltage collapse during USA blackout in August, 2003.

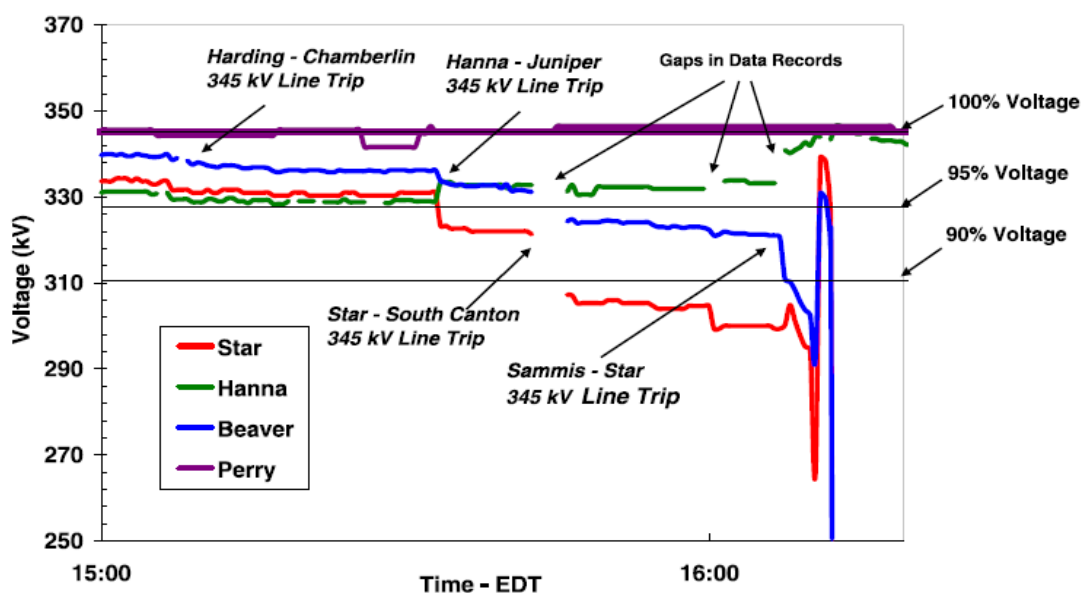


Figure 2-13: Voltage collapse during the blackout in USA, August 14, 2003 [14].

2.4.1.3 Voltage Security

The term *voltage security* means the ability of a power system, not only to operate in a stable manner but also to remain stable after credible contingencies or load increases [1], [2], [20], [41].

2.4.2 Voltage Collapse Scenarios

2.4.2.1 Scenario 1: Loads Build up (Long-term Voltage Collapse)

In this scenario, the main factors contributing to voltage collapse are:

- The stiffness of the load characteristics are continuing to demand high values of active and reactive power despite voltage dips in the load area.
- The control of ULTCs in distribution and sub-transmission networks tries to maintain constant voltage, and therefore high reactive power demand is needed, when the supply voltage decreases.
- Due to field and armature current limits, a high reactive power demand by the system loads may cause the generators to lose their ability to act as a control voltage source. The generator then behaves like a voltage source behind the synchronous reactance and its terminal voltage reduces.
- A voltage collapse due to load build up may be caused by some or all of the above factors. The dynamics of the various voltage control devices (generators, compensators, and transformers) may interact in such a way that the actual voltage collapse is different to the predicted by static consideration.
- Blackouts occurred in France in 1978 and Japan in 1987 are some examples.

2.4.2.2 Scenario 2: Network Outages (Transient Voltage Collapse)

Obviously, the network parameters play a crucial role in determining the maximum power that can be delivered to load areas. Tripping one of the lines in the transmission system increases the equivalent reactance between the equivalent voltage source and the load, reduces the critical power and increases the probability of voltage collapse. Generator tripping has a similar effect in that it not only increases the equivalent reactance but also reduces the system capability to generate real and reactive power. Blackouts that occurred in Belgium 1982, Sweden 1983, USA 1985 or Sweden/Denmark 2003 are some examples.

2.4.2.3 Scenario 3: Phenomenon Inside the Composite Load

The dynamic response of the composite load may result in the dynamic and static load characteristics being different. This difference is mainly attributed to induction motors and may result in a reduction in the system stability ultimately leading to voltage collapse. For instant, a rapid, severe, voltage dip, such as that which occurs during a slowly-clear short circuit, can cause a reduction in the motor torque and consequent motor stalling. The stalling of motor demands reactive power further reducing the voltage stability conditions. In this scenario, the voltage continues to fall until the protection equipment trip the motors from the

system thereby reducing the reactive power demand. The voltage will then starts to recover but an uncontrolled restoration of the composite load by heavy induction motor self-starts can again reduce the voltage and lead to a total voltage collapse.

2.4.2.4 Scenario 4: Voltage Collapse and Asynchronous Operation

Voltage collapse at one or a few network buses may cause the voltage to dip at neighboring buses leading to voltage collapse at these buses. The voltage then dips at other buses and then this phenomenon propagates though out the network and affects the synchronous generators. Consequently, some generators may lose synchronism and be tripped out because of asynchronous protection. This worsens the current situation and lead to whole voltage collapse eventually.

2.4.3 Methods for Voltage Stability Analysis

The problem of voltage stability has been studied for decades. However, with the occurrence of serious power system blackouts related to voltage collapse phenomena in recent years, this problem is still an issue for researchers and power system utilities. Considerable researches have been conducted on many aspects of the voltage stability problem [1], [2], [41], [42], [43], [44]. Particularly, some aspects have been considered:

- **Tools and techniques:** choosing some appropriate tools and techniques those can be used to understand the mechanism of the voltage stability problem and make operations and planning decisions based on more reliable simulations. Power flow analysis, quasi-steady-state analysis and transient stability analysis are the major tools which can be selected to do static and dynamic analysis of the power system.
- **Modeling issues:** Selecting suitable models and scenarios or contingencies for the simulation that is associated with voltage collapse is very important. The interaction of system load and equipment such as generator protection devices, OEL, ULTC, shunt compensation and load shedding plays an important role in this process.
- **Indices:** Indices could be used to help operators to determine whether the system state is secure or dangerous. Additionally, they could be considered as the criteria for the system security assessment.
- **Control strategy:** Finally, a comprehensive preventive and corrective methodology is needed to mitigate voltage collapse. In cases for which voltage stability criterion is not satisfied, remedial control measures have to be designed to enhance the system to meet the criteria.

Many methods for voltage stability analysis have been listed in references [41], [42], [43], and [44]. These methods could be classified into two main categories as static methods and dynamic methods as summarized on Figure 2-14

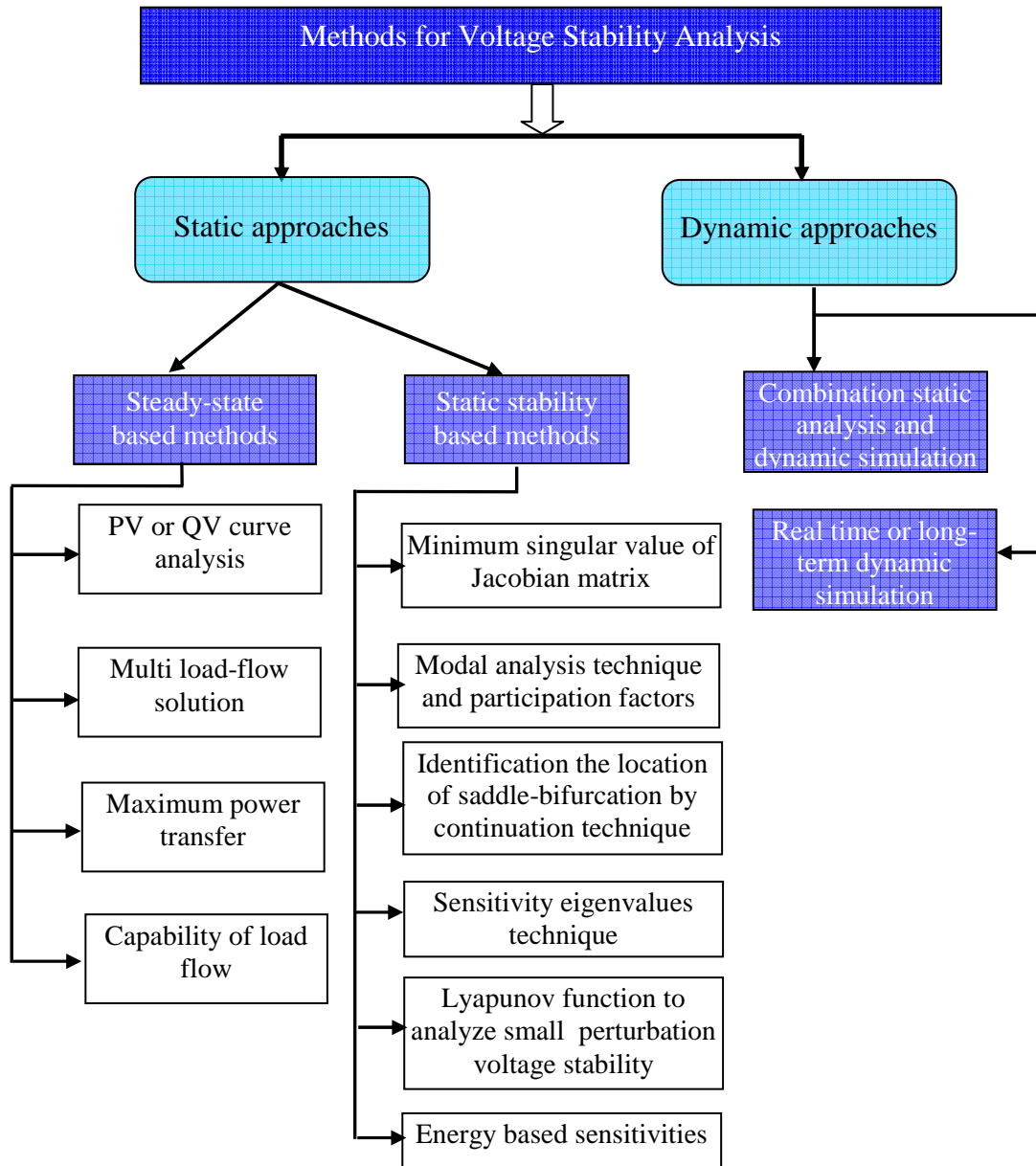


Figure 2-14: Main methods for voltage stability analysis.

2.4.3.1 Steady-state Based Methods

The use of P-V and/or Q-V curve is widely used for investigating voltage stability problems with slower forms of voltage instability as steady-state problems [1], [2]. Power flow simulation is the primary method and only conventional load flow programs are needed for approximation analysis. The method determines steady-state loadability limits which are related to voltage stability. This approach is not only useful for conceptual analysis of voltage stability and study of radial system but also applicable for large meshed network. The Q-V curve is currently used not only in many electrical utilities for voltage stability assessment but also for evaluating some other voltage stability assessment approaches. For example, Thomas J. Overbye and Ian Dobson [45] used the Q-V curve for evaluating the use of energy function based voltage security measure, or authors in [46] compared the V-Q simulation versus

dynamic simulation in the voltage stability analysis. By estimating the amount of reactive power needed to remain the desired voltage magnitude at buses with respect to a contingency, the operators could determine the margin of voltage stability. Main drawbacks of these methods are load flow calculation diverging near the maximum power point on the curve and generation must be realistically rescheduled as the area load is increased.

The authors in [47] discussed the relationship between voltage instability and multiple load flow problem which tends to occur in heavily loaded conditions. That may be related to the voltage instability. A closely-located multiple solution pair is worthy of attention in the multiple solutions from the standpoint of practical power system operations, because both of them seem to be operable for their close location. They seem to be related to the voltage instability for the next reasons; Jacobian rank of the load flow calculations using the Newton-Raphson method reduces and load flow sensitivity for a multiple load flow solution pair becomes opposite each other.

K. P. Basu [48] investigated the maximum power transfer of transmission lines as considering voltage stability problem. The authors in [49] presented an application of optimization techniques to voltage collapse studies. The authors firstly determined an index of the voltage collapse proximity indicator that was the ratio between Thevenin impedance seen by the load bus in question and impedance of that load bus. Then, the original OPF objective function is secondly introduced as the voltage stability criterion.

2.4.3.2 Static Stability Based Methods

The authors in [50] proposed a method based on the minimum singular value of Jacobian matrix as a voltage stability index that indicates the distance between the studied operating point and the steady state voltage stability limit. A load flow Newton-Raphson equation is derived. From the theory of singular value decomposition of the load flow Jacobian matrix, the authors stated that: The minimum singular value is an indicator of the proximity to the steady state stability limit. The right singular vector is corresponding to the minimum singular value that indicates sensitivity voltage and the left singular vector corresponding to minimum singular value that indicates the most sensitive direction for changes of active and reactive power injection.

The authors in [51] proposed a method to analysis the voltage stability of large-scale power system by using a modal analysis technique by computing a specified number of the smallest eigenvalues and the associated eigenvectors of a reduced Jacobian matrix. The eigenvectors were used to describe the mode shape and to provide information about the network elements and generators, which participate in each mode. Buses, branches, and generators were considered by participation factors.

The authors in [52] used the tangent vectors to define a clustering method for the identification the location of saddle-bifurcation in power system as the critical area at the point of collapse. A voltage stability index was defined based on the identification of this critical area. A predictor-corrector methodology based on this index was proposed for computation of voltage collapse points.

A. Teshome and E. Esiyok [53] proposed a method that determines the distance to voltage collapse corresponding to the maximum reactive power limit by using second-order

eigenvalue sensitivity technique. Sensitivities to changes in load bus voltage and the level of voltage that was most sensitive to load changes could be determined by this method. The technique permitted the determination of a minimum voltage level that could be estimated to track the status of the system as to how close and where the voltage collapse might occur.

The authors in [54] presented a method to analyze small perturbation voltage stability for power system with varying load by mean of quadratic Lyapunov function. By using Lyapunov stability theory, such a dynamic phenomenon like the voltage stability is analyzed algebraically.

The authors in [55] and [56] proposed a method using an energy function approach to assess the vulnerability of an electrical power system to voltage collapse which is based on Lyapunov direct method. The voltage stability of a particular portion of the system was measured by using a defined energy function that included voltage dependent reactive loads, reactive power limits on generators and transmission line losses. The difference between the system normal operating point and one unstable equilibrium point of the system measured by the energy function was then evaluated.

2.4.3.3 Methods Based Dynamic Approaches

Dynamic voltage simulation is widely used to investigation the dynamic behavior of power system during dynamic phenomena such as voltage collapse [1], [2], [57], [58]. Especially, the method of combining static-dynamic simulation is widely used to study and investigate voltage stability problem [59], [60]. This approach combines both advantages of static and dynamics simulation method by providing more precise results in presence of dynamic models of controller devices such as generator, excitation, over-excitation limiter, ULTC...

2.4.4 Preventive and Corrective Methods to Prevent Voltage Collapse

The problem of voltage collapse evidently emerges as important concerns for planners and operators of power systems. To deal with this problem, most of electrical utilities have given their reasonable control strategies and strict guidelines that operators must conform to urgent situations. The controls are the physically controllable devices or quantities for which the preventive and corrective control will give the optimal setting values. There are many different remedial measures that can be applied to enhance system voltage stability however, the practicability and availability of each option depend on the particularly system. Some of the possible control strategies that can be automatically adjusted include:

1. Implementation of secondary voltage control: This strategy may include generator secondary voltage control as increment of reactive power, or inclusion of additional shunt capacitor, and adjustment of transformer taps equipped with ULTC.
2. Rescheduling of active power generation.
3. Emergency ULTC control such as careful tap blocking, tap reversing, tap locking.
4. Shedding of load.

Traditionally, preventive and corrective control can be formulated as a nonlinear optimization problem. The three major components of this problem are objective function, control measures and system constraints. It can generally be expressed as follows:

$$\begin{aligned}
& \text{Min} && f(x, y, u) \\
& \text{s.t.} && g(x, y, u) = 0 \\
& && h(x, y, u) \leq 0
\end{aligned} \tag{2.4-1}$$

where

x : the vector of state variables;

y : the vector of algebraic variables;

u : the vector of all controllable variables;

$f(x, y, u)$: the objective function;

$g(x, y, u)$: system equality constraints including load-flow balance equations;

$h(x, y, u)$: system inequality constraints including the limits for state variables and control variables;

In general, the objective function can be one of the following:

- To minimize the number of control equipment
- To minimize load shedding
- To minimize control costs

In this part provides a brief review of preventive and corrective control methods that are proposed based on the above model.

2.4.4.1 Implementation of Secondary Voltage Control

M. M. Begovic et al [61] used the sensitivity analysis of total generated reactive power to get useful information about vulnerability of the parts of the power system with respect to voltage instability. For a class of voltage instabilities corresponding to static bifurcations of load flow equations, minimum singular values of Jacobian matrix and total generated reactive power were calculated as indicators of stability margin. Then sensitivity methods were used for reactive support allocation. An algorithm was presented to determine the sensitivities of total generated reactive power with respect to loads at various locations in the system. Allocation and amount of shunt compensation have strong effects on voltage stability margin.

J. V. Hecke et al [59] presented a coordinated voltage control experience in Belgium. The objective function is based on the global import-export balance of reactive power from the neighboring system tends to zero. A "Tertiary Voltage Control" procedure was proposed as follows: a) Starting load flow based on "State Estimator" results, b) Objective function set-up, c) A first optimization with all control variables treated as "continuous", d) capacitor bank scheduling, d) A second optimization with fixed capacitor bank scheduling, the other control variables treated as "continuous", e) Choices of transformer tap positions, f) A third and last optimization with generator reactive output as only remaining control variables, g) Computation of the commands. This procedure is calculated for a period of every 15 minute.

Costas Vournas and Michael Karystianos in [62] firstly reviewed the role of automatic and non-automatic ULTCs for emergency and preventive voltage stability control. They discussed how tap-blocking and tap-reversing of bulk power delivery transformers ULTCs can prevent

an approaching voltage collapse, as well as the problems and limitations of these countermeasures and the advantages gained by tap-reversing. It was also shown that ULTCs at higher voltage levels (including those of generator step-up transformers, if available) can help maximizing the load-ability margin either by automatic control, or by selection of tap adjustments using offline optimization. An algorithm based on gradient projection was proposed in order to maximize the load-ability margin. The authors also pointed out that capacitor switching has some advantages over ULTC in term of voltage control.

2.4.4.2 Rescheduling of Active Power Generation

T. T. Quoc et al [63] proposed a method based on rescheduling active and reactive power generation for improvement of voltage stability. The authors firstly discussed different static indices that used for determine how the system voltages are dangerous and then a $L_{\text{indicator}}$ based on voltage drop was chosen as a reference that varies between 0 (at no load) and 1 (stability limit). From this index, countermeasures for voltage collapse on the Vietnam power system were proposed such as optimization of the amount and localization of Var compensating devices, rescheduling of active power and reactive power generations, lower factor generators, and load shedding. An objective function was proposed to minimize the indicator. The major goal is to achieve a better voltage profile after rescheduling active and reactive power conjunction with eigenvalues sensitivity analysis.

T. V. Menezes et al [64] proposed a methodology to be added into the power system dispatch problem in order to evaluate and improve voltage stability margin by optimizing generators and synchronous condensers reactive injection. Through the load flow linearized equations, the reduced active and reactive matrices can be obtained by considering the decoupled effects of active and reactive power variations on system voltage stability. Two proposed indices: APF_{PV} is the active participation factor for PV buses and APF_{PQ} is the active participation factor for load (PQ) buses. APF_{PQ} can be used to design a reactive power re-scheduling process since it provides a participation factor for each generator, while APF_{PV} gives participation factors just for PQ buses. Generators with large APF should inject more active power to improve the Voltage stability margin and generators with small APF should inject less. The main idea is to add the above information to an OPF program, so that the final solution leads to an optimized reactive power injection for each generator and synchronous condensers, from a perspective of improving voltage stability margin.

Y. Su et al [65] used a pseudo-gradient evolutionary programming (PGEP) to search the optimization problem of reactive power generation rescheduling to improve voltage stability margin (VSM). The modal analysis technique was used to guide the searching direction. The main objective of the optimization is to increase the reactive power reserves as well as to decrease the active power loss by rescheduling the reactive power injection of the generator units.

T. V. Cutsem [58] calculated sensitivities of the reactive power generation with respect to demand which are used to determine the generators to be rescheduled. The potentially dangerous contingencies are identified by using the eigenvalues of the linearized matrix that includes ULTCs on the voltage stability of the system. Then control actions are taken to improve the voltage stability margin.

The authors in [66] considered the corrective and preventive actions against voltage instability as an optimal problem where a control cost function was taken as the objective function to be minimized. In this paper, preventive/corrective control could be formulated as a static nonlinear optimization problem as a one kind of optimal power flow (OPF)

Z. Feng et al [67] proposed a comprehensive approach for preventive and corrective control to mitigate voltage collapse. For the cases with insufficient voltage stability margin, the margin sensitivity is first computed to identify the most effective preventive controls, and then a linear optimization with the objective of minimizing the control cost is performed to coordinate the control actions. For the cases when no steady-state equilibrium point exists, that mostly result from severe contingencies, a parameterized control strategy is first utilized to restore the system solvability. Then, the continuation method is applied to compute the corresponding minimum corrective control actions. The control actions consist of rescheduling real power generations, implementing generator secondary voltage controls, switching on shunt capacitors and shedding loads.

2.4.4.3 Emergency ULTC Control

Several emergency ULTC control measures are in use or have been proposed in the literature for containing voltage instability [68], [69], [70]

- Tap blocking is the simplest countermeasure involving emergency ULTC control. It simply deactivates the control mechanism that is normally restoring the secondary voltage (normally the distribution side) of the power delivery transformer. By this way, load restoration is cancelled, or, in the worst case, delayed in some minutes. However, Pal in [69] pointed out that tap blocking should be implemented in careful manner. Because, incautious tap blocking actions could not prevent voltage, even this may aggravate the situation.
- Tap reversing consists in changing the control logic, so that the ULTC is controlling the transmission side voltage instead of the distribution side.
- Tap locking is the action of assigning a specific tap position, where the ULTC will move and then lock.

The above actions are able to efficiently stop the system degradation, especially if ULTC control is the only source of load power restoration. However, ULTCs are relatively slow devices, unable to quickly correct a situation with severe voltage drops caused by an initial disturbance. Hence, they can be used to counteract disturbances with moderate impact or in conjunction with other countermeasures.

2.4.4.4 Shedding of Load

C. W. Taylor [57] proposed a concepts of under-voltage load shedding based on the least cost solution to avoid voltage instability. The load-shedding scheme was of a predefined type where the amount of load to be shed, corresponding to specific percentage of decay voltage at load buses, was fixed a priori. Based on these concepts, Puget Sound area utilities have been using this under-voltage load shedding algorithm. This method has some advantages such as its simplicity of implementation. The effect of avoiding voltage collapse is obviously

observed through dynamic simulation. This method could be applicable for dynamic simulation in the presence of different types of dynamic loads and ULTCs.

T. Tran-Quoc et al [71], [72] proposed a load shedding algorithm that is based on the indicator of risk of voltage stability. The goal of the method is to achieve an indicator profile lower than a threshold value through load-shedding to ensure that the power system remains in a state far from voltage instability point.

R. Balanathan et al [73] presented an under-voltage load shedding criterion that using dynamic load model in which the parameters of the dynamic load model were estimated online using a nonlinear least squares technique, namely the Gauss-Newton method. The method could be used to calculate the minimum amount of load to be shed at any time to avoid a voltage collapse. The major advantage of this approach is that the effect of dynamic loads can be easily investigated and suitable for practically calculating the shedding necessary to ensure the power system voltage stability following a disturbance.

C. Moors et al [74] proposed a methodology for the design of automatic load shedding against long-term voltage instability on Hydro-Quebec power system. This methodology includes two steps. In the first step, a set of training scenarios is set up, corresponding to various operating conditions and disturbances. Each scenario is analyzed to determine the minimal load shedding which stabilizes the system, with due consideration for the shedding location and delay. In the second step, the parameters of a closed-loop under-voltage load shedding scheme are determined so as to:

- Approach as closely as possible the optimal shedding computed in the first step, over the whole set of scenarios.
- Stabilize the system for all the unstable scenarios and shed no load for the stable ones. The corresponding optimization problem is solved using a (micro-) Genetic Algorithm.

2.5 MAJOR SUGGESTIONS FOR PREVENTIONS OF POWER SYSTEM BLACKOUTS

Power system blackouts often come from a sequence of interrelated events that would otherwise be manageable if they appeared alone. The causes may derive from planning and design stages to current operating conditions. In order to prevent future power system blackouts, some international recommendations including many aspects were made as follows [13], [75], [76]:

1. Planning and designing stages:
 - a. In this stage, load forecasting should be investigated and studied carefully in order to anticipate the increasing load tendency, and maximum loaded conditions. This will help to install on time power system facilities such as building new transmission lines, or new power plants.
 - b. Despite the fact that performing analyses of all the contingencies that could occur in power system are impossible, attention should be paid to high probabilistic contingencies. Precise models of power system components should be used to analyze the contingencies and phenomena in power system.

- c. Normal planning studies cannot capture all of the possible scenarios that may lead to a blackout condition, due to the vast number of possible uncertainties and operating actions. In some past power system blackouts, the security criterion “N-1” was clearly insufficient to save power system. Therefore, new security criterion based on N-m ($m \geq 2$ or 3) should be applied in order to ensure that the power system should be withstood the loss of several component.
 - d. The application of automatic controls such as automatic voltage regulators, and where applicable power system stabilizers, should be mandatory for generators.
 - e. The lessons learned from past mistakes must be incorporated into new procedures as well as using such lessons learned to help develop new and improved technologies for system control and monitoring.
2. Maintenance work:
- a. The improvement of existing substations and other equipment through refurbishing and replacement of critical components is vital for the prevention of cascading events. Tree cutting should be done regularly along the transmission line corridor.
 - b. Control and monitoring devices should be maintained and tested regularly in order to discover early the failures.
 - c. It is greatly significant to enforce and constantly encourage training programs for system operators and their supporting staff. The operators should be qualified enough they should be able to grasp all critical situations in order to give out correct and timely actions.
3. Operating issues:
- a. Ensure the redundancy and reliability of remote control and telecommunication devices.
 - b. Improve the calibration of recording instruments, especially in establishing time synchronization.
 - c. Establish pre-defined data reporting requirements and standardized data formats.
 - d. Power system operators and control centers should have highly sense of responsibility and cooperation in order to have urgent and correct decisions.
4. Disturbance Monitoring [76]: To facilitate better insights into the cause of blackouts and enable detailed postmortem, both adequate analysis and appropriate disturbance monitoring are required. This has been achieved to some extent in the development of wide area measurement systems (WAMS)
- a. Refine the process for integration, analysis, and reporting of WAMS data. This must also include the development and support of staff and resources.
 - b. Establish a WAMS Website to allow the free exchange of WAMS data, documents, and software and thus promote its development.

- c. Extend the collection of benchmark events and dynamic signatures to determine the range of normal system behavior.
- d. Perform related studies to assist proper interpretation of observed system behavior.
- e. Fully utilize the capabilities often available in modern HVDC and/or FACTS equipment to directly examine system response to test inputs.
- f. Automate the means of disturbance reporting.

Rapid system restoration is extremely important in order to minimize the impact of a blackout on society. Thus, means should be put into place to measure and reduce restoration times. System operators should be given regular refresher training and live drills on system restoration to ensure that they remain familiar with restoration procedures and best practices.

2.6 CONCLUSIONS

In this chapter, major analyses of recent power system blackouts around the world were investigated briefly. The phenomena of power system blackouts are related to complicated dynamic events and none is the same as the others. The consequences of power system blackouts are always very huge from both power system security and economy point of view.

There are many causes leading to power system blackouts. The causes may come from planning and designing stage, operation missions, maintenance duty, or from many unforeseen diversity reasons.

Major mechanisms of power system blackouts were discussed in detail. Blackout occurrences are the result of a chain of events such as: starting with unfavorable loading conditions, lack of both active and reactive power reserve, triggered by a fatal contingency causing power system in dangerous state. Lack of preventive action, coordination between control centers, and activation of automatic controller may worsen situation. Human errors sometimes amplified the severity. Lack of corrective actions and/or urgent control actions are final stage that leading blackout occurrence.

In this dissertation, we will concentrate on the problem of angle stability and voltage collapse. Some general definitions related to these two types of power system stability, as well as main methods used for analysis and prevention of angle instability and voltage collapse were discussed in this chapter.

CHAPTER 3

AN ENERGY APPROACH TO OPTIMAL PLACEMENT OF CONTROLLERS/SENSORS FOR IMPROVEMENT OF ANGLE STABILITY

3.1 INTRODUCTION

As mentioned in the previous chapter, many power systems are facing the problem of power system oscillations due to the lack of damping torque at generators rotors [12], [33]. Lacking of damping torque may cause some critical power system blackouts, for example, the power system disturbance in WSCC-USA (August 10, 1996) [77] and the blackout in Sweden/Denmark (September 23, 2003) [15]. Frequency responses of power system oscillations are usually in the range from 0.1Hz to 2Hz and depend on the number of generators involved. Local oscillations are in the upper part of the frequency range and consist of the oscillations of a single or a group of generators against the rest of power system. Interarea oscillations are in the lower part of the range and correspond to the oscillations among groups of generators. Some technical incidents (lines or generating units tripping ...) but also adverse weather conditions (storms, snow, unusual high/low temperature...) may strongly amplify the power system oscillations, especially when control systems are not adequate. Sometimes, human errors together with monitoring problems represent some additional sources of failure.

One big challenge is now to develop some strategies in order to prevent critical situations. Obviously, both corrective and preventive actions need to be considered. From the preventive point of view, beside the equipment improvements, some significant improvements of control system structures are needed to deal with critical situations such as local and interarea oscillations. In fact, it is now well established that “remote” controllers/sensors those are based on measurements coming from different areas (often far) of the overall power system are suitable for network stability improvement [78].

Controllers (power system stabilizer – PSS or FACTS devices) are commonly used not only to damp power system oscillations but also to increase the damping swing modes in power systems or in others words to improve the performance of power systems. For example, a PSS is the most effective device which is installed at generators in order to add damping torque. The main function of a PSS is to add an additional stabilizing control signal at the input of exciter. There are many types of PSS for example: PSS based on shaft speed signal (delta-omega), PSS based on delta-P-omega, Frequency-based PSS, and digital PSS. The Figure 3-1 shows an example of a thyristor excitation with PSS-speed signal type [1].

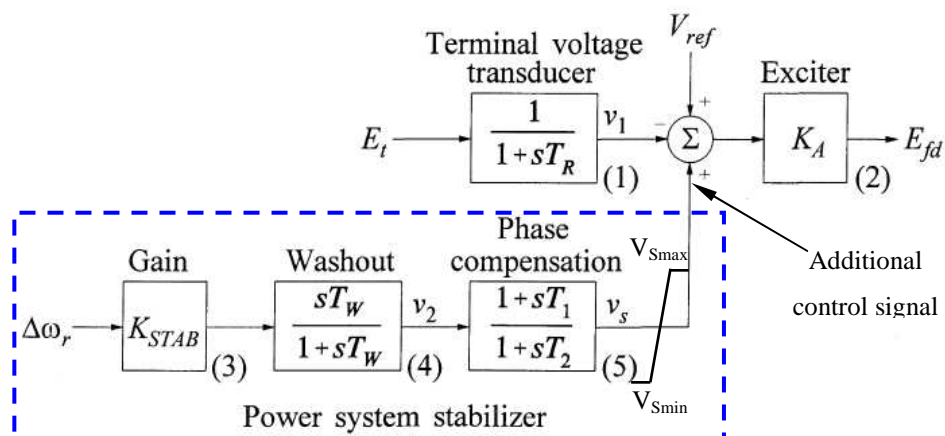


Figure 3-1: Thyristor excitation system with PSS [1].

Where

- **The stabilizer gain K_{STAB}** has an important effect on damping of rotor oscillations. The value of the gain is chosen by examining the effect for a wide range of values. The stabilizer gain is normally set to a value that results in as high a damping of the critical system modes as practical without compromising the stability of other system modes or causing excessive amplification of signal noise
- **The stabilizing signal washout** is a high-pass filter that prevents steady changes in modifying the field voltage. The value of the washout time constant T_W should be high enough to allow signals associated with oscillations in rotor speed to pass unchanged.
- **The phase-lead compensation** produces a component of electrical torque in phase with rotor speed deviation. The phase-lead circuits are used to compensate for the lag between the exciter input and the resulting electrical torque. The phase characteristic to be compensated varies to extent with system conditions. Therefore, a characteristic acceptable for different system conditions is selected. Generally, slight undercompensation is preferable to overcompensation so that the PSS does not contribute to the negative synchronizing torque component.
- **The stabilizer limits** is used in order to restrict the level of generator terminal voltage fluctuation during transient conditions.

Sensors are installed in power system to measure desired signals that are useful for monitoring, protection and control the power system. For example, Phasor Measurement Unit (PMU) based state estimation that used in wide area protection and control (WAPC) offers many advantages such as linear estimator, true simultaneous measurements and dynamic monitoring [78], [79]. The power systems would become more controllable with fewer measurements. The Figure 3-2 shows an example of WAPC with PMUs. The PMUs measures the voltage and current phasors of generators or voltage and current phasors of transmission system. These measured signals are synchronized and transmitted to the control centers by the Global Positioning System (GPS) system. These signals are used for monitoring, controlling and making control decisions of operators or as input control signals of controller (for example: multiple input control signal power system stabilizer).

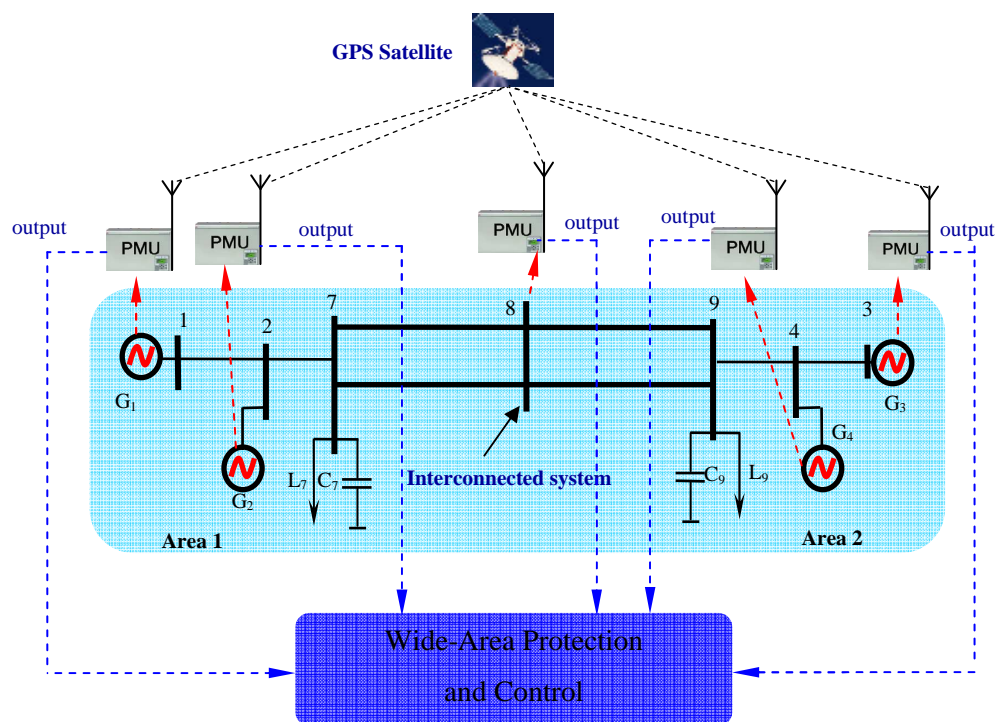


Figure 3-2: Wide-Area Protection and Control with PMUs [19], [80].

However, these devices are normally very expensive in term of investing cost and limited in term of available quantity, therefore, these devices must be installed at suitable positions (at suitable generators, buses or transmission lines) in order to have maximum effect (for example, maximum damping effect). For that reason, the problem of choosing optimal placement of these devices has arisen for many years.

The problem of choosing optimal placement of controllers (for example: PSS, or FACTS) as well as sensors (for instance: PMU) has been studied for a long time [22], [31], [32], [33], [81] and [82]. Most of the existing approaches are algebraic methods based on the sensitivity analysis of eigenvalues and related components such as eigenvectors, participation factors, the so-called “eigenvalues-based method”. The optimal selection of controllers/sensors is classically determined by using participation factors of some critical modes. These methods have several drawbacks: Firstly, the determination of critical modes may be problematic in case of large-scale systems because the critical mode may not be unique. Furthermore, the definition of critical modes also depends on different types of oscillation: local or interarea modes. Secondly, the participation factor approach only deals with the state variables and neglects the input and output behaviors. This approach cannot effectively identify a controller site and an optimal feedback signal in the absence of information on the input and output, which is more important when output feedback is employed.

When dealing with small signal stability analysis, the disturbance is considered small enough, the analysis is performed on the basis of a linearized model, valid at a vicinity of a particular operational configuration. Since power systems are highly nonlinear dynamical systems, linear modes are sensitive to the operation point changes such as load level changes. As a consequence, optimal selection of controllers/sensors may strongly depend on the current operating point. In order to overcome these drawbacks, in this chapter, an energy approach is proposed for the optimal selection of both controllers/sensors based on the use of

controllability and observability gramians and combined with balancing realization reduction. To take into account the effect of changes in power system, we propose a stochastic approach based on scenarios that also include the occurrence of faulty situations, such as transmission lines tripping, loads changes to introduce some robustness properties. This approach relies on the maximization of an index that defined as the trace of the controllability and observability gramians for each scenario.

The main idea is to select the controllers (equivalent to control inputs) corresponding to the minimum energy needed to control the most significant modes of the system and to select the placement of sensors (equivalent to outputs) corresponding to maximum energy output in order to improve small signal stability of power system. This approach may be regarded as part of a structural optimization procedure aiming at defining some new control systems in the context of power system security improvement (for instance: to choose optimal selection of PSSs to improve angle stability).

3.2 CONTROLLABILITY AND OBSERVABILITY GRAMIANS

3.2.1 Gramians Definitions

Consider a system described in state-space form by:

$$\begin{aligned} \dot{x}(t) &= A.x(t) + B.u(t) \\ y &= C.x(t) \end{aligned} \quad (3.2-1)$$

where: $A \in \mathbb{R}^{n \times n}$, $B \in \mathbb{R}^{n \times m}$, $C \in \mathbb{R}^{r \times n}$ and $x \in \mathbb{R}^n$. We assume that the system in equations (3.2-1) is controllable and observable. The transient controllability and observability functions of a continuous-time linear system are defined as respectively.

$$\begin{aligned} L_c(X, T) &= \min_{u, x(0)=X} \frac{1}{2} \int_{-T}^0 \|u(\tau)\|^2 d\tau, x(-T) = 0 \\ L_o(X, T) &= \frac{1}{2} \int_0^T \|y(\tau)\|^2 d\tau, x(0) = X, u \equiv 0 \end{aligned} \quad (3.2-2)$$

We recall the following well-known result (see [83], [84]).

Theorem 1: The transient controllability and observability functions are given by:

$$\begin{aligned} L_c(X, T) &= \frac{1}{2} X^T W_c^{-1}(T) X \\ L_o(X, T) &= \frac{1}{2} X^T W_o(T) X \end{aligned} \quad (3.2-3)$$

where: $W_c(T) = \int_{-T}^0 e^{At} B B^T e^{A^T t} dt$, $W_o(T) = \int_0^T e^{A^T t} C^T C e^{At} dt$ are the transient controllability

and observability gramians on horizon T respectively. $W_c(T)$ and $W_o(T)$ are the positive definite solutions, obtained at time $t = T$, of the following differential Lyapunov equations:

$$\begin{aligned}
-\dot{W}_C(t) + AW_C(t) + W_C(t)A^T &= -BB^T, W_C(0) = 0 \\
-\dot{W}_O(t) + A^TW_O(t) + W_O(t)A &= -C^TC, W_O(0) = 0
\end{aligned}
\tag{3.2-4}$$

If the system in equations (3.2-1) is asymptotically stable around the origin, the controllability function \bar{L}_C and observability function \bar{L}_O are definite and given by:

$$\begin{aligned}
\bar{L}_C &= \min_{u, x(0)=X} \frac{1}{2} \int_{-\infty}^0 \|u(\tau)\|^2 d\tau, x(-\infty) = 0 \\
\bar{L}_O &= \frac{1}{2} \int_0^{\infty} \|y(\tau)\|^2 d\tau, x(0) = X, u \equiv 0
\end{aligned}
\tag{3.2-5}$$

When $T \rightarrow \infty$: $\lim_{T \rightarrow \infty} W_C(T) = \bar{W}_C$ and $\lim_{T \rightarrow \infty} W_O(T) = \bar{W}_O$. Then \bar{W}_C and \bar{W}_O are obtained as the unique positive definite solutions of the following Lyapunov equations:

$$\begin{aligned}
AW_C + W_C A^T + BB^T &= 0 \\
A^T W_O + W_O A + C^T C &= 0
\end{aligned}
\tag{3.2-6}$$

Since the controllability matrix W_C depends on the control input matrix B , the control energy can be affected by properly choosing this control input matrix while the observability matrix W_O depends on the output signal matrix C , the energy output of sensors can be affected by properly choosing this signal outputs matrix. Furthermore, when the system is only stabilizable and detectable (there exist some non-controllable and non-observable, but stable state variables), the gramians given by (3.2-4) will be only some non-negative matrices since the singular values corresponding to the non-controllable or non-observable states will be equal to zero.

From equations (3.2-1) and (3.2-2), it is suggested that in order to minimize the control input energy, we have to minimize $(W_C)^{-1}$ or equivalently to maximize W_C in the sense of a given matrix norm. In order to maximize energy output of sensors, we have to maximize W_O according to some measures (for example, $\text{trace}(W_C)$ could be use as a norm in order to calculate the energy).

3.2.2 Balanced Realization for Model Reduction of Linearized Power System

One of the most difficult problems when dealing with large-scale linearized power systems is the number of state variables. For instance, a practical power system that may contain from tens to hundreds of generators and the numbers of state variables may reach number of thousands. The computation of full eigenvalues and related eigenvectors of such large matrices is time consuming, even with modern computer systems. Furthermore, we only take into account the numbers of important state variables that play the important role in small signal stability analysis. These numbers of state variables are normally smaller than the numbers of state variables of the original system. Therefore, this problem can be generally solved by model order reduction.

B. C. Moore [85] explained how to use controllability and observability gramians for the goal of model reduction using balanced realization. The main idea is that the singular values of the controllability gramian correspond to the amount of energy that has to be injected into

the system in order to control state variables. For the observability gramian, its singular values refer to the output energy that is generated by the system state variables. Thus, the Hankel singular values provide a measure for the importance of the system states. For model reduction, the state variables that contribute very few to the input–output behavior can be eliminated, and the reduced system retains the best possible approximation to the full-order system.

J. Hahn and Th. F. Edgar in [86], [87], [88] reviewed different techniques of model reduction for linear system. After comparing the balancing realization technique to truncation and residualization that is based upon modal reduction, the authors concluded that balanced reduction methods are more suitable than others and are well suited for controller design since they preserve the input–output behaviors.

The authors in [89] applied a technique for order reduction of linearized power systems in the studying of interarea oscillations that are based on the computation of the controllability and observability Gramians. The technique is actually based on the truncation technique and is used to reduce order of power system in term of generating a smaller system that is suitable for control design.

In this section, we recall the balancing realization technique for order reduction of linear systems that is applied to analyze oscillations of large-scale power systems. The procedure is summed up as below:

A system whose controllability and observability gramians are equal and have the following form [86]:

$$\bar{W}_C = \bar{W}_O = \Sigma = \begin{bmatrix} \sigma_1 & 0 & 0 & \dots & 0 \\ 0 & \sigma_2 & 0 & \dots & 0 \\ 0 & 0 & \sigma_3 & \dots & 0 \\ \dots & \dots & \dots & \dots & \dots \\ 0 & 0 & 0 & \dots & \sigma_n \end{bmatrix} \quad (3.2-7)$$

where $\sigma_1 \geq \sigma_2 \geq \sigma_3 \geq \dots \geq \sigma_n \geq 0$ is called a balanced system. The σ_i 's are the Hankel singular values.

Consider a linear system given by (3.2-1), which is assumed to be asymptotic stable, both stabilizable and detectable. It can be shown that there exists a regular transformation P defined in [85].

$$\bar{x} = P.x \quad (3.2-8)$$

such that the transformed system, given by the equivalent representation:

$$\begin{aligned} \bar{x} &= PAP^{-1}\bar{x} + PBu = \bar{A}\bar{x} + \bar{B}u \\ y &= CP^{-1}\bar{x} = \bar{C}\bar{x} \end{aligned} \quad (3.2-9)$$

is in balanced form.

P may be obtained from the following procedure:

1. Perform a Cholesky decomposition of W_C : $W_C = R^T.R$

2. Perform a singular value decomposition of $R^T W_O R$:

$$R W_O R^T = U \Sigma^2 U^T \text{ to get } \Sigma^2 = \text{dig}(\sigma_1^2, \dots, \sigma_n^2)$$

3. Balanced gramians are given by:

$$\begin{aligned} \bar{W}_C &= P W_C P^T = \Sigma \\ \bar{W}_O &= (P^{-1})^T W_O (P^{-1}) = \Sigma \end{aligned}$$

The new system given by equations (3.2-9) is then called a balanced realization. We can perform system reduction by eliminating all state variables corresponding to the Hankel singular values that are less than a small value given threshold (say smaller than 10^{-5}).

3.3 PROCEDURE FOR OPTIMAL SELECTION OF CONTROLLERS AND SENSORS IN POWER SYSTEM

The use of controllability and observability gramians method for optimal placement of controllers/sensors has been already proposed in various literature [90], [91], [92], [93], [94], [95].

M. A. Wicks et al [90] formulated an energy approach for the control of linear system. They proposed the sum of singular values of the controllability gramian as a measure of minimum energy needed to drive any controllable states to the origin of the state space.

D. Georges [91] proposed a method for optimal location of sensors and actuators for both linear and nonlinear dynamic system. In the linear case, an observability and controllability gramians method was proposed. A general procedure for computing the optimal design parameters that are based on both integer programming and a Branch and Bound method suitable for large-scale systems was proposed.

S. Leleu et al [92] addressed different energetic approaches for actuators and sensors positioning in linear dynamic model. In the case of a transient disturbance, it must impose a final state variable at final time while minimizing the input energy. This is equivalent to maximizing a norm of the controllability gramian matrix (W_C). The second point of view corresponds to maximizing the total energy transmitted from the actuators to the structure for a given input, this equivalent to maximizing the trace of W_C . The third approach is a geometrical interpretation of gramian matrix. If the system is controllable, W_C is a symmetric positive definite matrix that associated with quadratic form, i.e. to ellipsoids whose axis directions are given by eigenvector of W_C and lengths proportional to eigenvalues. The biggest the ellipsoid is, the more controllable the system is, and this is equivalent to maximize the gramian eigenvalues.

However, none of these authors proposed a specific algorithm for optimal placement of controllers/sensors for power system. In this section, an energetic approach using controllability and observability gramians is proposed for the optimal selection of controllers/sensors in power systems (see also in [96]). The approach consists in selecting controllers that provides additional input control signal with the goal of increasing robustness with respect to disturbances. It also takes into account the influence of all existing controllers in the whole power system. The problem is then to determine a set of M control inputs among m possible inputs related to generators of the power system in order to maximize the overall controllability of the system. While the problem of optimal placement of sensors is to

determine a set of P sensors for the measurement of P network states among n measurable states.

In order to take into account the nonlinear behavior of power system dynamics, we propose a stochastic approach based on scenarios, which have to be properly chosen to explore the nonlinear dynamics of the system and to introduce some robustness with respect to some fault occurrences. Because of duality of controllability and observability gramians and using balanced realization, a measure is proposed, which is used to optimal placement both controllers and sensors .

We propose the following algorithm:

1. Generating a set of N independent scenarios ω_i with occurrence probability $p(\omega_i)$, $i=1,\dots,N$ (large enough) corresponding to N stable equilibrium. These scenarios could be chosen based on typical operation situations of power system in question. Unstable equilibrium cases are eliminated by checking stable conditions of characteristic matrix A .
2. For each scenario ω_i , $i=1,\dots,N$, perform linearization around the corresponding equilibrium state of the power system dynamics to get state space as in (3.2-1). For each scenario ω_i and each configuration of control inputs α_i and measurements β_i , we perform balanced realization to get reduced system as follows:

$$\begin{aligned} \dot{x}^{\omega_i} &= A^{\alpha\beta}(\omega_i)x^{\omega_i} + \sum_{j=1}^m \alpha_j B_j^{\beta}(\omega_i)u_j = A^{\alpha\beta}(\omega_i)x^{\omega_i} + B^{\alpha\beta}(\omega_i)u \\ y^{\beta} &= C^{\beta}(\omega_i)x^{\omega_i} \end{aligned} \quad (3.3-1)$$

3. The system in equations (3.3-1) has their controllability and observability gramians which satisfy $W_C = W_O = \Sigma^{\alpha\beta}$. Where α_i 's are equal to 1 when control input u_i is selected otherwise equal to 0, β is a vector of sensor configuration: β_i is equal to 1 when the "physical" state $x_i(\omega_i)$ is measured, otherwise equal to 0. α and β satisfy conditions: $\sum_{i=1}^m \alpha_i = M$ and $\sum_{i \in I} \beta_i = P$.
4. For each scenario ω_i , calculate the controllability and observability gramians of the balanced system: $\Sigma^{\alpha,\beta}(\omega_i)$ which satisfies one of these two Lyapunov equations:

$$\begin{aligned} (A^{\alpha\beta}(\omega_i)) \cdot (\Sigma^{\alpha\beta}(\omega_i)) + (\Sigma^{\alpha\beta}(\omega_i)) \cdot (A^{\alpha\beta}(\omega_i))^T + (B^{\alpha\beta}(\omega_i)) \cdot (B^{\alpha\beta}(\omega_i))^T &= 0 \\ \text{or} & \\ (A^{\alpha\beta}(\omega_i))^T \cdot (\Sigma^{\alpha\beta}(\omega_i)) + (\Sigma^{\alpha\beta}(\omega_i)) \cdot (A^{\alpha\beta}(\omega_i)) + (C^{\beta}(\omega_i))^T \cdot (C^{\beta}(\omega_i)) &= 0 \end{aligned} \quad (3.3-2)$$

5. For each scenario ω_i , calculate the individual energy by a norm corresponding to the control inputs and signal outputs as follows:

$$E(\omega_i) = \text{trace}(\Sigma^{\alpha\beta}(\omega_i)) \quad (3.3-3)$$

6. The optimal selection of controllers/sensors is chosen base on the total maximum energy over all scenarios that is calculated by

$$\max_{\substack{\alpha_i \in \{0,1\}, i=1, \dots, m \\ \beta_j \in \{0,1\}, j \in I}} \left(E_{\omega}(X) = \frac{1}{N} \sum_{i=1}^N p(\omega_i) E(\omega_i) \right) \quad (3.3-4)$$

where $E_{\omega}(X) = \frac{1}{N} \sum_{i=1}^N p(\omega_i) X(\omega_i)$ is the average expectation of over all scenarios ω_i . (For simple cases, $p(\omega_i)$ could be considered equal to 1 that means all the scenarios have the same probability of occurrence).

Notice that this approach may also be extended to the case of scenarios leading to unstable realizations. In this case, the function (3.3-2) may be reformulated by using the transient controllability and observability gramians obtained by solving (3.2-4) with a horizon T properly chosen according to the transient behavior of the system. We should also emphasize that this approach can be successfully applied even in the case when the system has stable non controllable or non observable modes: in practice, this is often the case for the kind of applications we consider in power systems.

When the scenarios and number of controllers/sensors are relatively small (say, $n < 20$), an optimal solution can be found by enumerating of the solutions. However, when dealing with large-scale system, the optimal location of controllers/sensors is usually a highly combinational optimization problem. To overcome the curse of dimensionality due to the combinatorial burden, some efficient suboptimal solutions could be obtained from using heuristic methods such as simulated annealing [95] or a Branch and Bound approach [91] (see the appendix A).

3.4 TWO APPLICATIONS

The use of this method is applied to choose optimal placement of controllers/sensors (or equivalent to optimal selection of control inputs/outputs) for generator in order to improve power system oscillations for two systems-namely “Two Area Power System” and “39 Bus New England”. In this section, the Program Power System Simulation Engineering (PSS/E) [97] is employed for load-flow calculation and perform linearization of power system corresponding to each scenario. Because dynamic models of power system devices play a very important role in studying dynamic phenomena such as local oscillation and inter-oscillation, therefore all dynamic models are taken from PSS/E dynamic model library. Specifically, generators, excitation systems are modeled by the detail models. Transmission systems and load are modeled by models that are used in load flow calculation. The Matlab software is used to perform order reduction and calculate reduced gramian matrix $\Sigma^{\alpha\beta}$ in equation (3.3-2). In these examples, we limit ourselves on some small scenarios; therefore the optimal problem in (3.3-4) can be solved by using enumeration solutions.

3.4.1 A Two-Area Power System

The “Two-area power system” is widely used for fundamental studies of power system oscillations that is taken from the book of P. Kundur [1]. For power system models, all generators are identical and modeled by using Round Rotor Generator Model (Six Orders Exponential Saturation generator model) - GENROE, all excitation system are identical, and modeled by using IEEE Type ST1 Excitation System - EXST1 [98]. The load flow data and

dynamic parameters are taken from [1], [33] and listed in detail in the Appendix B. The system diagram is shown in Figure 3-3

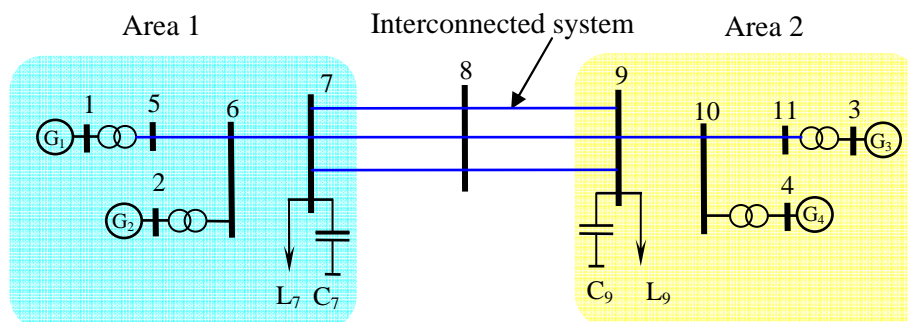


Figure 3-3: The “Two area power system” [1] .

In order to illustrate easily the approach, we consider only a very small number of (equi-probabilistic) scenarios. Some scenarios have been generated and are listed in Table 3-1.

The problem is to select some controllers/sensors locations (or control inputs/outputs) to install in the power system with the goal of improving its performance and security. A typical application is choosing optimally placement of a local power system stabilizer to damp out power system oscillation. In order to illustrate the effectiveness of the proposed approach, a comparison between the used of participation factor and the energy approach is investigated.

Table 3-1: Some generated scenarios for “Two area power system”.

Scenario	Power from Area 1 to Area 2 (MW)	No of tie line	Generation/Load (MW)	
			Area 1	Area 2
1	0	1	1400/1367	1400/1367
2	100	1	1400/1267	1400/1467
3	200	1	1400/1167	1400/1567
4	400	1	1422/967	1428/1767
5	0	2	1400/1367	1400/1367
6	300	2	1400/1067	1400/1667
7	400	2	1400/967	1400/1767
8	600	2	1400/767	1400/1967
9	400	2	1600/1157	1570/1917
10	600	2	1605/947	1533/2067

3.4.1.1 Choosing Optimal PSS Location by Participation Factor Method

The use of maximum participation factor for choosing optimal placement of local PSS is firstly investigated in this part. We consider here two cases of optimal selection PSS in order to improve small signal stability.

The procedure is summed up as follows:

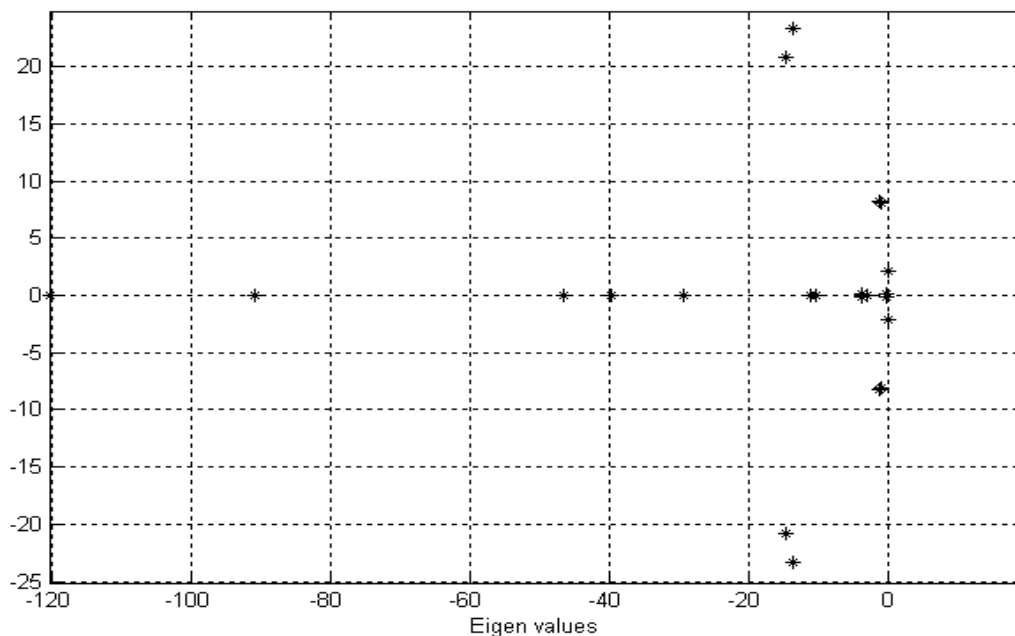
- Form a linearized state system as in (3.2-1)
- Calculate the critical eigenvalues that corresponding to poor damping modes.
- Calculate participation factors for the critical eigenvalues calculated above
- Based on maximum participation factors to choose the generator where PSS is placed

Two cases are investigated in details as below:

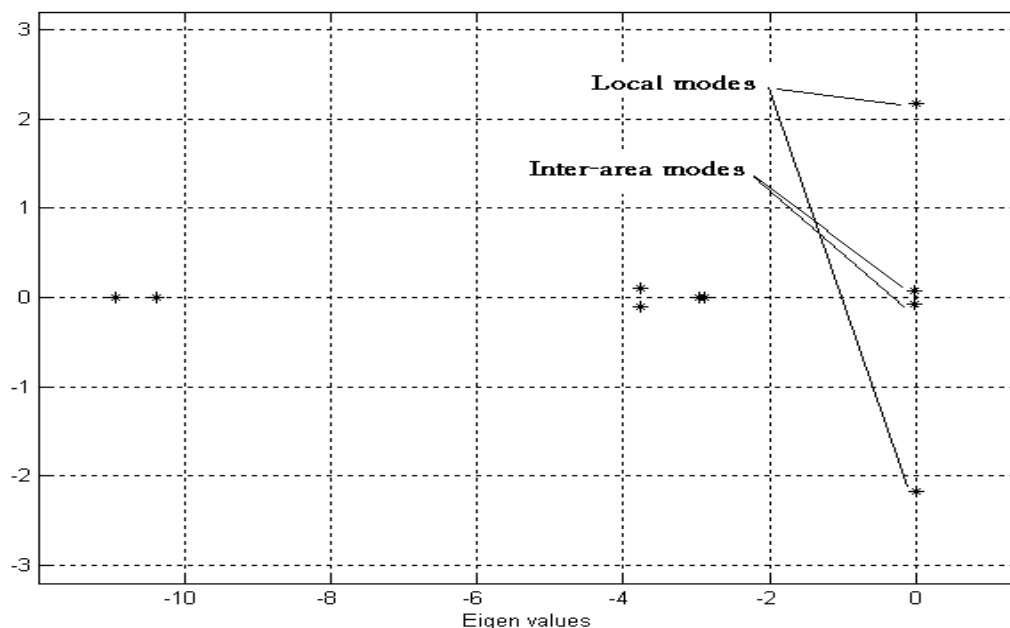
Case 1: Choose location of one PSS among four generators

The software PSS/E is used to form linearized system as in (3.2-1). The eigenvalues, eigenvectors and participation factors are calculated as in chapter 2 and shown in Table 3-2.

Figure 3-4 shows the full eigenvalues and critical eigenvalues of the “two area power system” (plotted for scenario 4 on complex plan).



a. Full eigenvalues of the “two-area power system”.



b. Critical eigenvalues of the “Two-area power system”.

Figure 3-4: Full eigenvalues and critical eigenvalues of “Two-area power system”.

Table 3-2 shows a full detail result of eigenvalues analyses for each scenario of “two area power system”. From Figure 3-4 and Table 3-2, we could observe that the method based on eigenvalues analyses provides full understandings about the stability properties of the power system. However, for each scenario, there are two pairs of the most critical eigenvalues and two maximum normalized participation factors corresponding to local and interarea oscillation modes. Because the participation factor measures only the influence of a state variable with respect to a specific mode therefore, the choosing a PSS based on maximum normalized participation factor has only maximum damping effect for a chosen particular mode, not for all other modes. As looking at the Table 3-2, scenario 1 for example, there are two pairs of critical modes corresponding to local and interarea modes. For each critical local mode, the state variable: speed of G3 has maximum influence on the critical local mode when comparing to other state variables. While, for each critical interarea mode, the state variable: angle of G2 has the maximum influence on these critical modes. Furthermore, the use of participation factors in choosing PSS location only deals with state variables and it neglects the input/output behavior.

If only one PSS is available, we have to choose between two available placements: G3 with damping local modes or G2 with damping interarea modes. The decision could be based on specific goal of the system in order to damping out local or interarea modes. For example, in scenario 1, placement of one PSS at G3 has only maximum damping effect for local modes: $-0.50080e-01 \pm j3.4548$, whereas, placement of one PSS at G2 has only maximum damping effect for interarea modes: $-0.27621e-01 \pm j0.68143e-01$.

Table 3-2: Critical eigenvalues, damping coefficient, oscillation frequency and the maximum normalized participation factor for each scenario of “Two area power system”.

Scenario	Critical eigenvalues	Damping ratio	Oscillation Frequency	Normalized Participation Factor
1	-0.50080e-01 ±j 3.4548 -0.27621e-01 ±j 0.68143e-01	0.14494e-01 0.37565	0.54985 0.10845e-01	Speed of G3 Angle of G2
2	-0.53640e-01 ±j 3.4090 -0.27200e-01 ±j 0.70285e-01	0.15733e-01 0.36091	0.54256 0.11186e-01	Speed of G3 Angle of G2
3	-0.51224e-01 ±j 3.2783 -0.27326e-01 ±j 0.87857e-01	0.15623e-01 0.29699	0.52176 0.13983e-01	Speed of G3 Angle of G2
4	-0.66371e-02 ±j 2.1782 -0.26680e-01 ±j 0.91936e-01	0.30471e-02 0.27871	0.34666 0.14632e-01	Angle of G4 Angle of G2
5	-0.78109e-01 ±j 4.4231 -0.27056e-01 ±j 0.62067e-01	0.17656e-01 0.39961	0.70396 0.98782e-02	Speed of G3 Angle of G2
6	-0.83954e-01 ±j 4.2976 -0.27257e-01 ±j 0.85218e-01	0.19531e-01 0.30465	0.68399 0.13563e-01	Speed of G3 Angle of G2
7	-0.77388e-01 ±j 4.1954 -0.27528e-01 ±j 0.98216e-01	0.18443e-01 0.26988	0.66771 0.15631e-01	Speed of G3 Angle of G2
8	-0.42242e-01 ±j 3.7644 -0.28115e-01 ±j 0.12927	0.11221e-01 0.21253	0.59913 0.20574e-01	Speed of G3 Angle of G2
9	-0.63879e-02 ±j 4.2255 -0.31228e-01 ±j 0.10687	0.15118e-02 0.28046	0.67251 0.17010e-01	Angle of G3 Angle of G2
10	-0.15939e-02 ±j 3.7725 -0.30638e-01 ±j 0.11911	0.42252e-03 0.24910	0.60041 0.18958e-01	Angle of G3 Angle of G2

Although the principles of a PSS design for damping local and interarea modes are similar, but the mechanisms by which a PSS contributes to the damping of the two types of oscillation are different. A PSS adds damping to an interarea mode largely by modulating system loads, whereas the performance of the PSS with regard to a local mode is only slightly affected by load characteristics [33].

Case 2: Choose locations of two PSSs among four generators

The critical eigenvalues and four maximum normalized participation factors are shown in Table 3-3. The critical eigenvalues, damping ratios and oscillation frequencies are the same as in Table 3-2.

There are four maximum normalized participation factors for each local and interarea oscillation modes. Because the participation factor measures only the influence of a state

variable with respect to a specific mode therefore, the choosing a PSS based on maximum normalized participation factor has only maximum damping effect for a chosen particular mode, not for all other modes.

Table 3-3: Critical eigenvalues and four maximum normalized participation factors for each scenario of “Two area power system”.

Scenario	Critical eigenvalues	Four Maximum Normalized Participation factor corresponding to critical modes
1	-0.50080e-01 ±j 3.4548 -0.27621e-01 ±j 0.68143e-01	Speed and angle of G3, Speed and angle of G1 Angle and Speed of G2, Angle and Speed of G1
2	-0.53640e-01 ±j 3.4090 -0.27200e-01 ±j 0.70285e-01	Speed and angle of G3, Speed and angle of G1 Angle and Speed of G2, Angle and Speed of G1
3	-0.51224e-01 ±j 3.2783 -0.27326e-01 ±j 0.87857e-01	Speed and angle of G3, Speed and angle of G1 Angle and Speed of G2, Angle and Speed of G1
4	-0.66371e-02 ±j 2.1782 -0.26680e-01 ±j 0.91936e-01	Angle and speed of G4, Angle and speed of G3 Angle and Speed of G2, Angle and Speed of G1
5	-0.78109e-01 ±j 4.4231 -0.27056e-01 ±j 0.62067e-01	Speed and angle of G3, Speed and angle of G1 Angle and Speed of G2, Angle and Speed of G1
6	-0.83954e-01 ±j 4.2976 -0.27257e-01 ±j 0.85218e-01	Speed and angle of G3, Speed and angle of G1 Angle and Speed of G2, Angle and Speed of G1
7	-0.77388e-01 ±j 4.1954 -0.27528e-01 ±j 0.98216e-01	Speed and angle of G3, Speed and angle of G1 Angle and Speed of G2, Angle and Speed of G1
8	-0.42242e-01 ±j 3.7644 -0.28115e-01 ±j 0.12927	Speed and angle of G3, Speed and angle of G4 Angle and Speed of G2, Angle and Speed of G1
9	-0.63879e-02 ±j 4.2255 -0.31228e-01 ±j 0.10687	Angle and Speed of G3, Angle and Speed of G4 Angle and Speed of G2, Angle and Speed of G1
10	-0.15939e-02 ±j 3.7725 -0.30638e-01 ±j 0.11911	Angle and Speed of G3, Angle and Speed of G1 Angle and Speed of G2, Angle and Speed of G1

As looking at the Table 3-3, scenario 1 for example, there are two pairs of critical modes corresponding to local and interarea modes. For each critical local mode, two state variables of G3, which are speed and angle state variable have maximum influence on this mode when comparing to other state variables. And two state variables of G1 which are speed and angle state variables have the next maximum influence on this mode. So if we need to choose optimal location for two PSSs in order to damping out local modes, they should be placed at G3 and G1. For each critical interarea mode, two state variables of G2, which are angle and speed state variables, have the maximum influence on this mode when comparing to other state variables. And two state variables of G1 which are angle and speed state variables have the next maximum influence on this mode. So if we need to choose optimal location for two PSSs in order to damping out interarea modes, they should be placed at G2 and G1. In order to damp over all oscillation, it is difficult to decide where we should place two PSSs, at (G1

and G2), (G1 and G3) or (G2 and G3). This is one of drawbacks of the participation factor method when dealing with the problem of choosing several PSSs in the large-scale power system.

For example, in scenario 1, placement of two PSSs at G1, and at G3 has only maximum damping effect for local modes: $-0.50080e-01 \pm j 3.4548$, whereas, placement of two PSSs at G2, and at G1 has only maximum damping effect for interarea modes: $-0.27621e-01 \pm j0.68143e-01$. Therefore, with two PSSs are available, we could not damp out both local and interarea oscillation modes. Even the placement of two PSSs at G2 and G3 does not ensure the maximum damping effect to both local and interarea oscillations.

To overcome the drawbacks that are discussed above, the energy approach proposed in section 3.3 will be investigated in order to choose controllers and sensors in power systems. The new approach is not only considering the input/out behavior of the state space system but also taking into account the total response all state variables in power system when adding one or more controllers/sensors.

3.4.1.2 Choosing Optimal Controller/Sensor Location by the Proposed Method

For this small power system, we consider two cases. In the first case, the problem is to choose the optimal location of one set of local controller/sensor at one generator among four generators. In the second case, the problem is to choose the optimal location of two set of local controller/sensor at two generators among four generators of the system.

For each scenario in Table 3-1, we consider *two* input control signals; the mechanical power set-point and the voltage set-point (ΔP_{mec} and ΔV_{ref}), and *three* outputs quantities that can be measured by meters; active power output (P), reactive power output (Q) and terminal voltage (E_{ter}) that correspond to each generator respectively. Voltage at bus 8 (V_{bus_8}) is taken as one *remove* measured signal. The original dynamic system includes 40 state variables.

Case 1: Selecting the optimal location of local controller/sensor for one generator

Figure 3-5 shows the Hankel singular values of reduced “two-area power system”. Only, 21 maximum Hankel singular values have been finally retained. Singular values that are smaller than $1e-5$ have been eliminated after using balanced realization reduction.

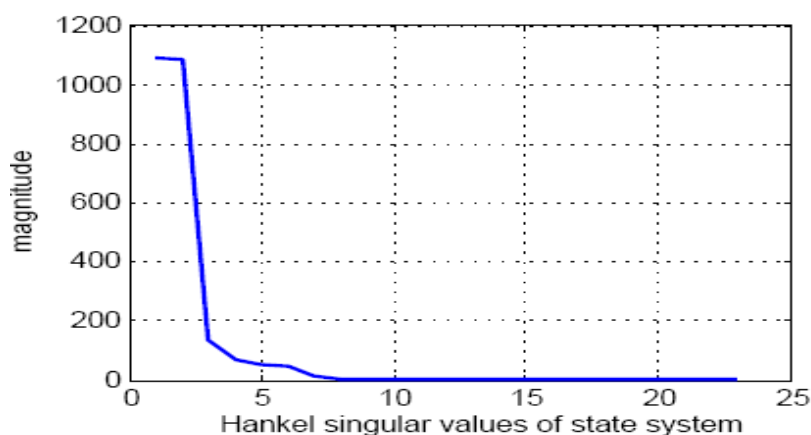


Figure 3-5: Distribution of Hankel singular values of reduced “Two-area power system”.

Figure 3-6 plots frequency responses of both original and reduced “two-area power system” that include two inputs ΔV_{ref} and speed reference of each generator. There is no difference between two control signals in the practical bandwidth from $10^{-\infty}$ to 10^4 . We can conclude that two systems are equivalent in term input-output behavior. From the bandwidth 10^4 to 10^{∞} the frequency response of the reduced system is flat because the order of reduced system is smaller than the original order. Therefore the two the systems are equivalent in term of robustness.

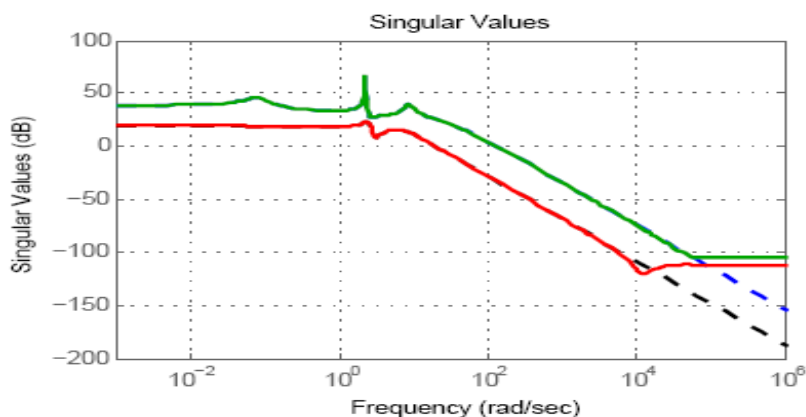


Figure 3-6: Frequency response of original and reduced of “Two-area power system”.

For the first case, the value of $E(\omega_i)$ for each scenario i (with $T = \infty$) are given in Table 3-4 Figure 3-7. In this case, an enumerative solution may be obtained without the need of using an integer programming method. We can see that with the selection of inputs/outputs of **G2** leads to the maximum values of the index $E(X)$. This means that if we need to add one set of controllers/sensors into one of generators of the power system in order to improve the over all performance, the optimal place is at **G2**.

Table 3-4: Index values according generator selection.

Scenarios	E(ω_i) corresponding to control inputs and outputs at				Corresponding number of Controllable/observable state variables			
	G1	G2	G3	G4	G1	G2	G3	G4
1	295	402	305	426	18	18	18	18
2	306	471	291	387	18	18	18	18
3	322	512	279	363	18	18	18	18
4	868	4070	710	2488	16	18	18	16
5	301	420	318	453	18	18	18	18
6	320	451	277	347	18	18	18	18
7	315	461	275	321	18	18	18	18
8	1802	2753	1591	1518	18	18	18	18
9	381	758	303	396	18	18	18	18
10	4945	13121	4062	6304	18	18	18	18
Eω	986	2342	841	1300				

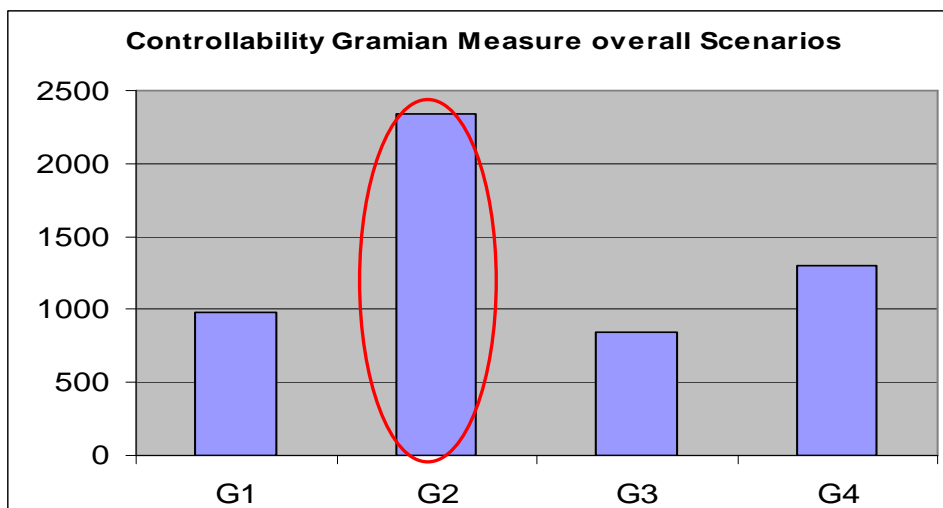


Figure 3-7: Expected controllability gramian overall scenarios.

Case 2: Selecting the controllers/sensors location for two generators

The values of $E(\omega_i)$ for each scenario when the transient horizon is equal to $T = \infty$ are given in Table 3-5 and Figure 3-8. The results show that when we choose generators G2 and G4, we get the maximum value of the index. This means that if we need to add two set of controllers/sensors into two generators of the power system to improve the performance, the optimal places are at G2 and G4.

Table 3-5: Index values according to generators selection.

Scenario	$E(\omega_i)$ corresponding with inputs and outputs at					
	G1,G2	G1,G3	G1,G4	G2,G3	G2,G4	G3,G4
1	708	602	727	713	831	744
2	786	599	712	764	872	696
3	844	606	715	793	901	655
4	5093	1590	3556	4936	6621	3356
5	731	622	760	743	878	784
6	780	603	689	734	824	636
7	786	595	663	742	819	611
8	4582	3396	3352	4364	4353	3132
9	1151	691	850	1074	1243	731
10	18224	9015	11418	17315	19587	10457
Eω	3369	1832	2344	3218	3693	2180

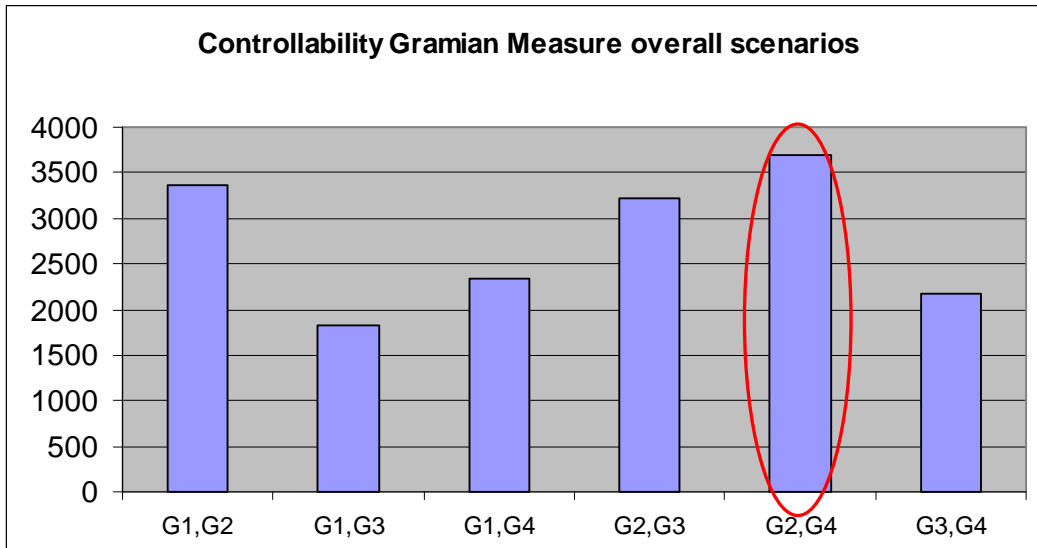


Figure 3-8: Expected controllability gramian overall scenarios.

3.4.1.3 Validation by Dynamic Simulation

In order to illustrate the effectiveness of this method, we consider the implementation of a standard power system stabilizer (PSS)-The basic function of a PSS is to add damping to the generator rotor oscillations by controlling its excitation using auxiliary stabilizing signals. The effectiveness of PSS is not only damping oscillation but also increasing angle stability. The typical PSS used in this simulation is the speed sense type and modeled by using the STAB1 model the dynamic device library of PSS/E and parameters are taken from [1], [33] (see the appendix B1 and Figure 3-9).

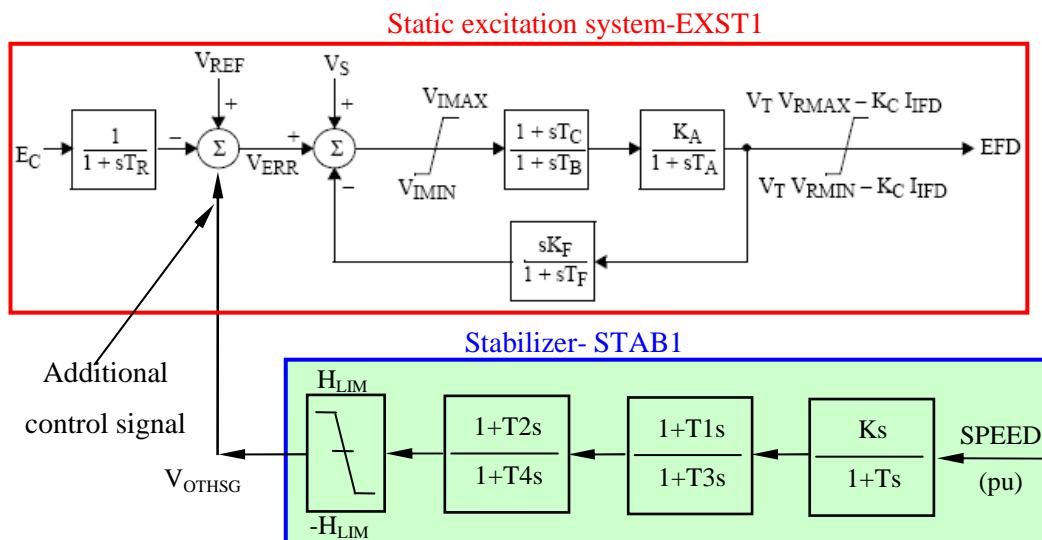


Figure 3-9: Static excitation system with a standard PSS.

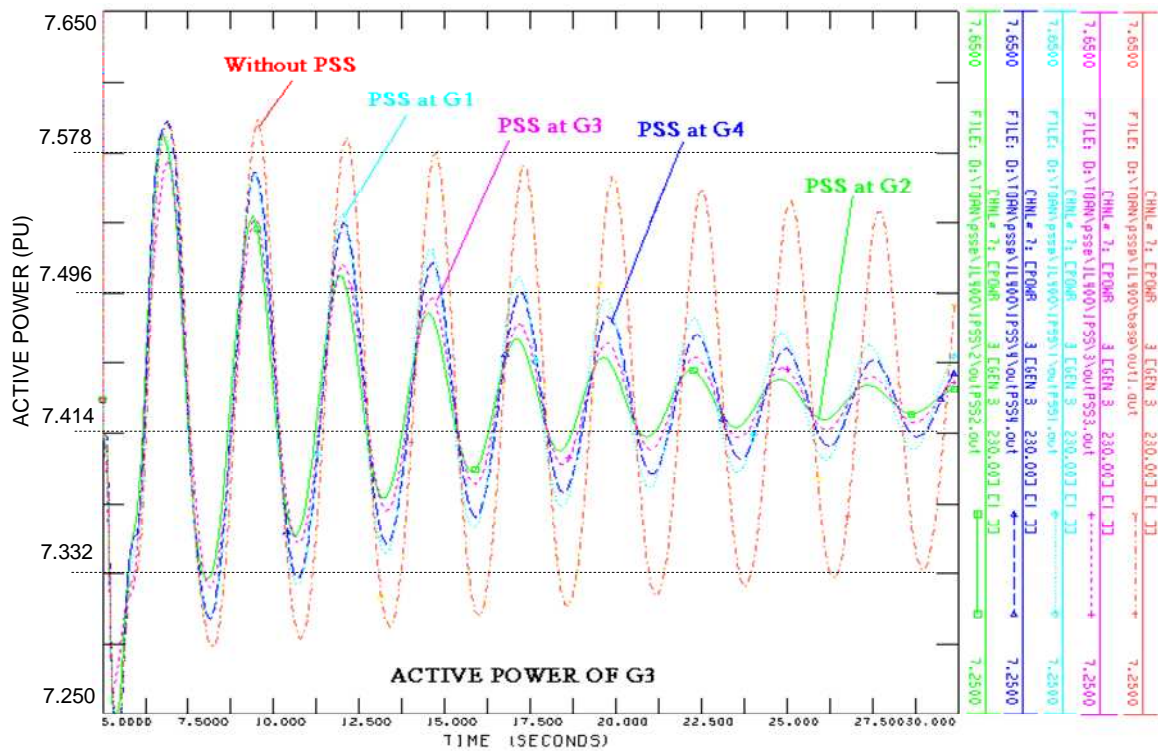


Figure 3-10: Power output of G3 with different placements of a PSS.

Figure 3-10 shows a comparison of power oscillation damping corresponding to the three possible placements of a PSS at G1, G2, G3). This simulation was done for the scenario 4 when applying a three-phase fault with duration 5 ms at bus 7, time period for simulation is 30 seconds. The figure is plotted for active power output of G3 corresponding to the fault. From the figure, placement of a PSS at **G2** (the green line) gives better results in term of damping effect comparing to the others cases.

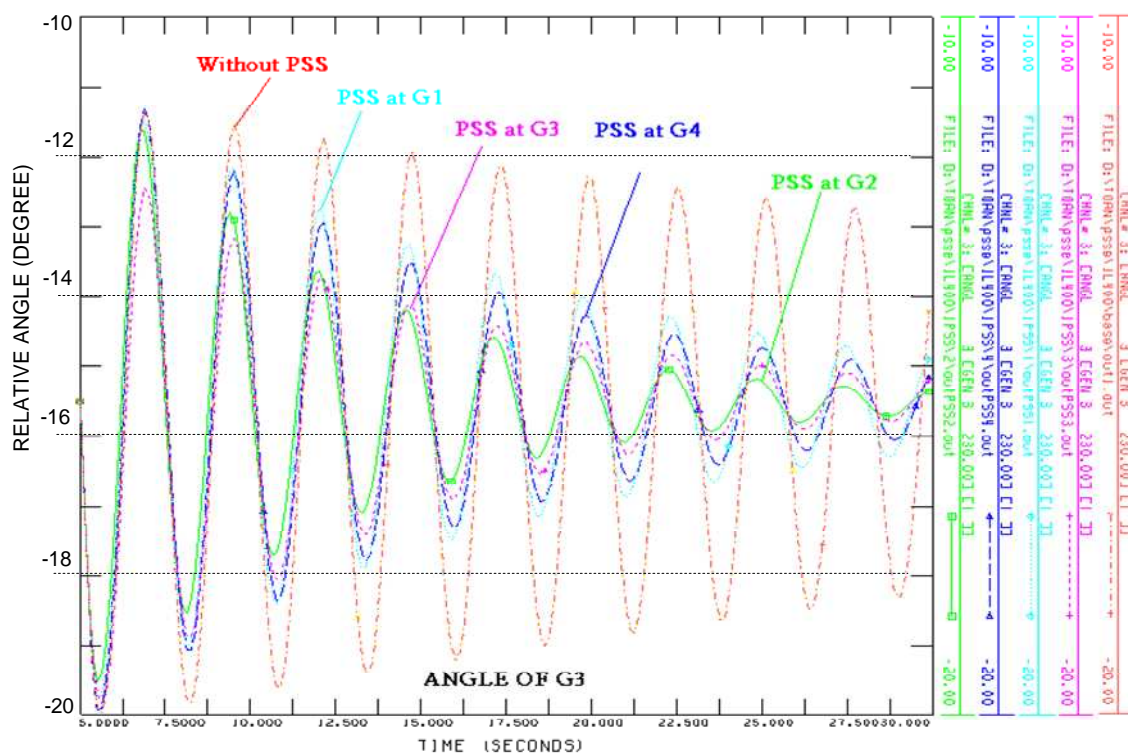


Figure 3-11: Angle of G3 with different placements of a PSS.

Figure 3-11 plots angle of G3 with different placement of one PSS. When placing a PSS at G2 (the green line), increment of angle is the smallest that gives the best effect in term of improvement angle stability comparing others placements.

Figure 3-12 shows a comparison of oscillation damping corresponding to the three possible placements of two PSSs at (G1, G2), (G3, G4) and (G2, G4). This simulation is done for the scenario 4 when applying a three-phase fault with duration 5ms at bus 7. From the figure, placement of two PSSs at (**G2, G4**) gives better results in term of damping effect.

Figure 3-13 plots angle of G3 with different placement of two PSSs. When placing two PSSs at G2 and G4, increment of angle is the smallest that gives the best effect in term of improvement angle stability comparing others placements

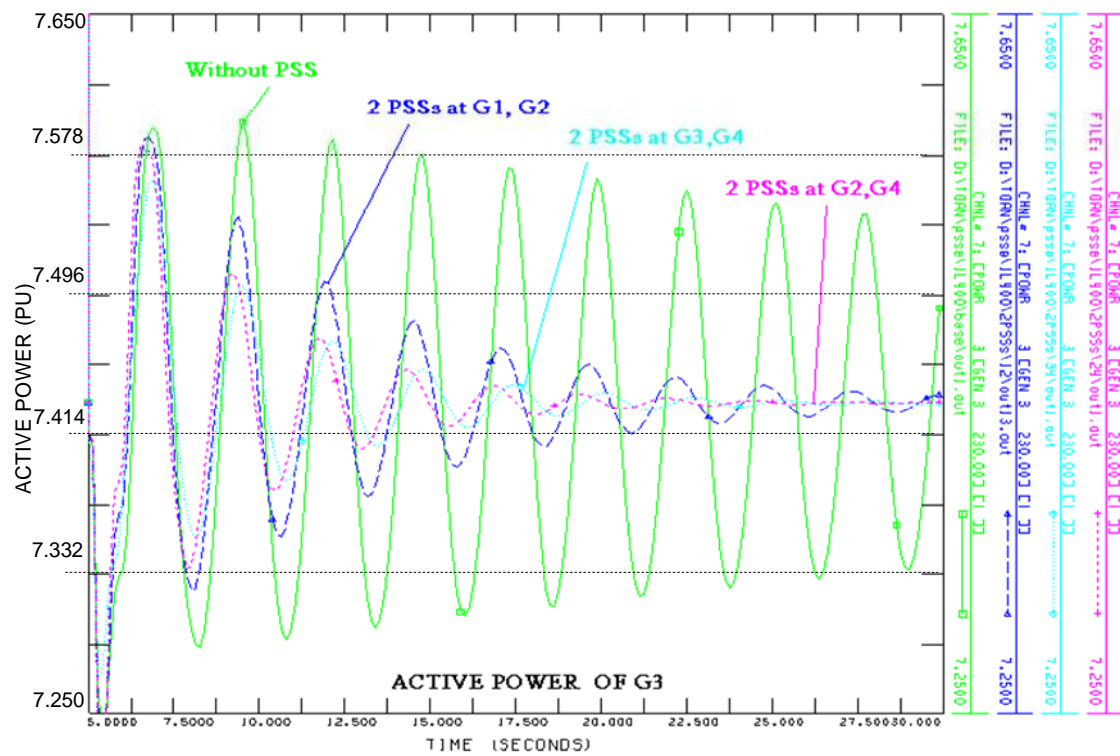


Figure 3-12: Power output of G3 with different placements of two PSSs.

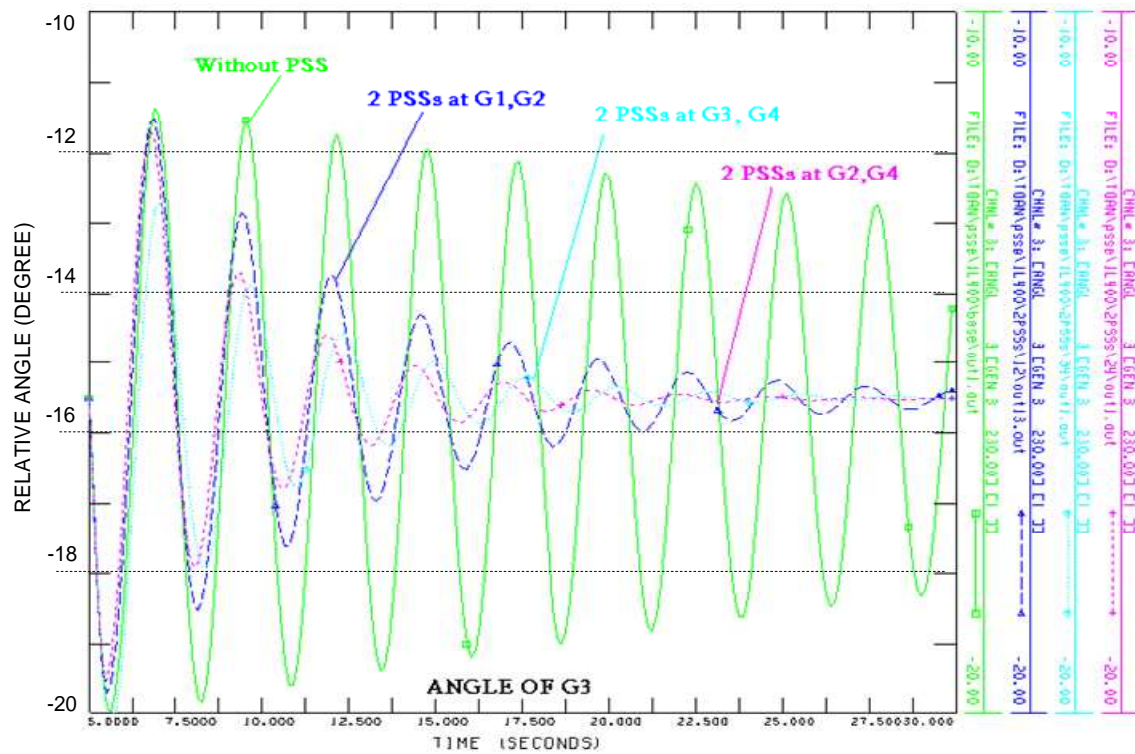


Figure 3-13: Angle of G3 with different placements of two PSSs.

3.4.2 A “39 Bus New England Power System”

A “39 bus New England” [27] is considered as a larger tested power system. All generators are identical and modeled by using Round Rotor Generator Model (quadratic saturation) – GENROU, all excitation systems are identical, and modeled by using IEEE Static Excitation System- EXST1. The load flow data and dynamic parameters are taken from and listed in detail in the Appendix B2. The system diagram is shown in Figure 3-14

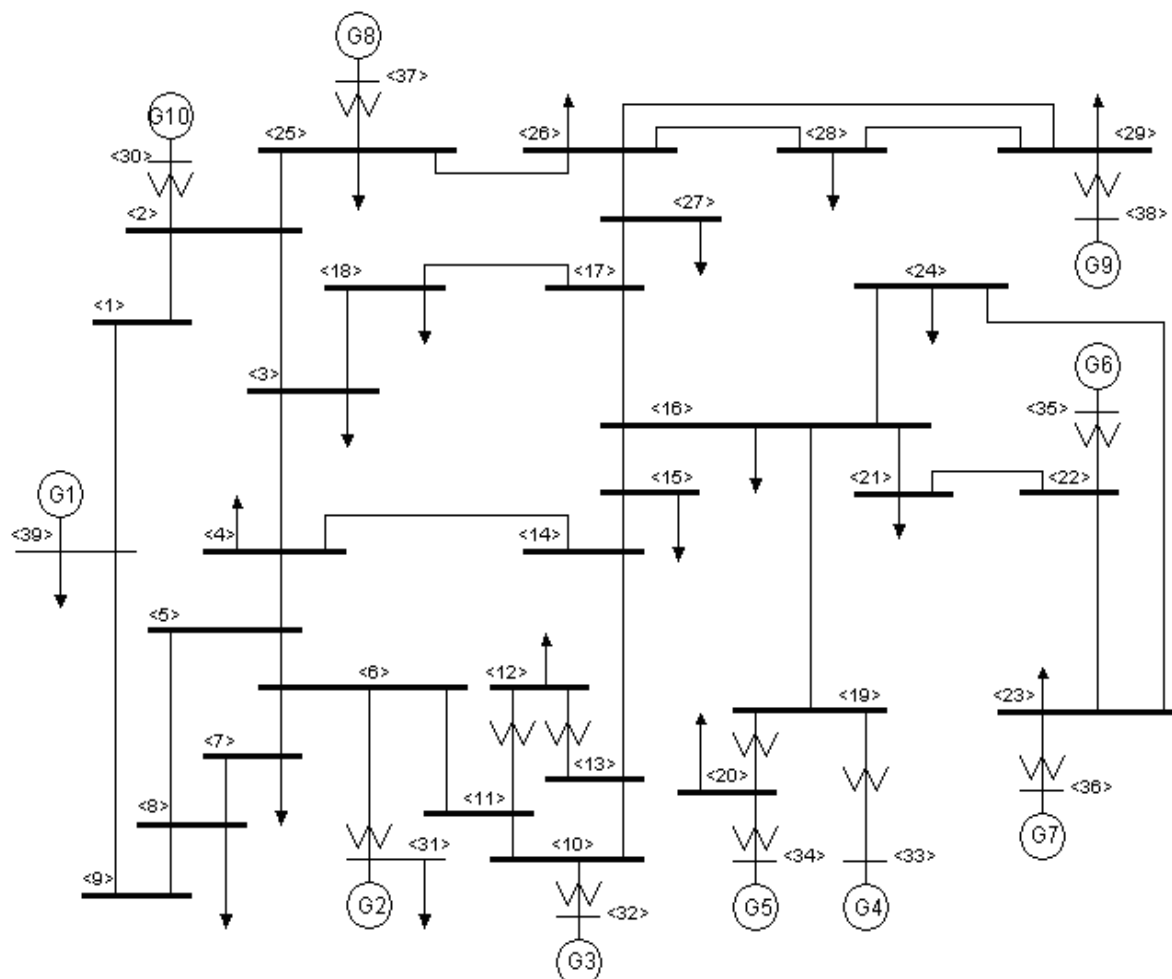


Figure 3-14: The “39 Bus New England power system”.

In order to illustrate the approach, we consider very small number of (equi-probabilistic) scenarios that were chosen as typical operating states. The scenarios are listed in Table 3-6.

For each scenario, we consider *two* input control signals; the mechanical power set-point and the voltage set-point (ΔP_{mec} and ΔV_{ref}), and *three* outputs quantities that can be measured by meters; angle, active power output (P), reactive power output (Q) that correspond to each generator respectively. The original dynamic system includes 96 state variables.

Table 3-6: Some generated scenarios for “39 bus New England system”.

Scenario	Description of scenarios
1	Base case 1
2	Trip tie line 4-14
3	Trip tie line 17-18
4	Trip tie line 25-26
5	Trip tie line 27-26
6	Trip tie line 39-9
7	Base case 2
8	Trip tie line 4-14
9	Trip tie line 17-18
10	Trip tie line 25-26
11	Trip tie line 27-26
12	Trip tie line 39-9
13	Trip tie line 39-9,25-26
14	Trip tie line 39-9,17-18
15	Trip tie line 3-4
16	Trip Gen 10
17	Base case 3

3.4.2.1 Selecting the Optimal Location of Local Controller/Sensor for one Generator

Figure 3-15 shows the Hankel singular values of reduced “39 bus New England”. Only, 31 maximum Hankel singular values have been finally retained. Singular values that are smaller than $1e-5$ have been eliminated after using balanced realization reduction. Therefore, the reduced system now includes 31 state variables that have much influence to input/output behavior of power system.

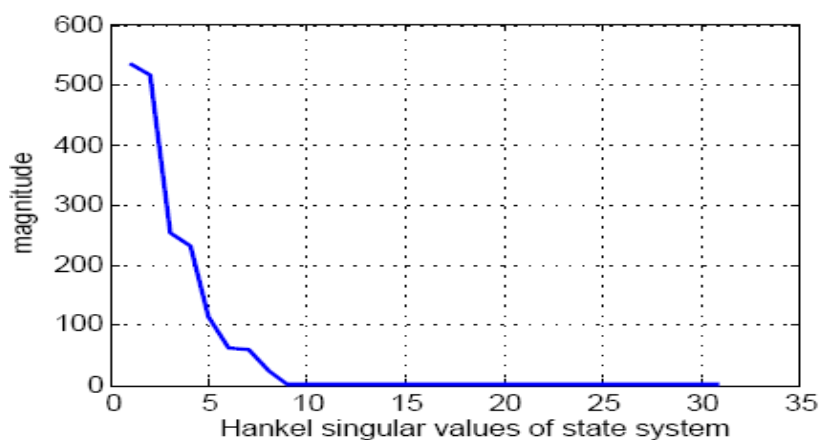


Figure 3-15: Distribution of Hankel singular values of reduced “39 bus New England power system”.

Figure 3-16 plots the frequency responses of both original and reduced systems that include two inputs ΔV_{ref} and speed reference of each generator. There is no difference between two control signals in the practical bandwidth from $10^{-\infty}$ to 10^4 . We can conclude that two systems are equivalent in term input-output behavior. Therefore the two the systems are equivalent in term of robustness. (From the bandwidth 10^4 to 10^{∞} the frequency response of the reduced system is flat because the order of reduced system is smaller than the original order).

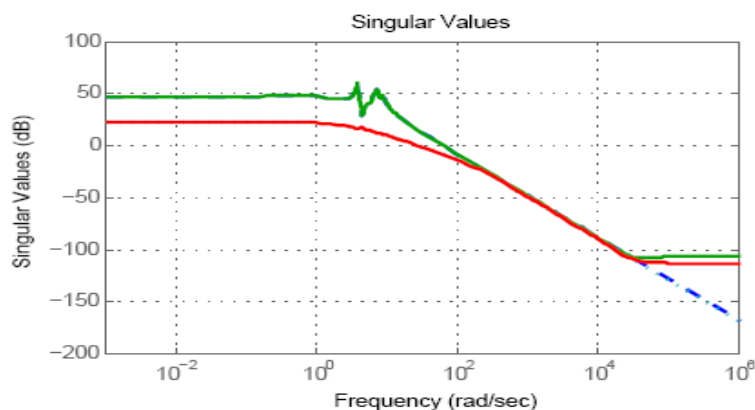


Figure 3-16: Frequency response of original and reduced of “39 bus New England power system”.

Table 3-7: Index values according to generator selection.

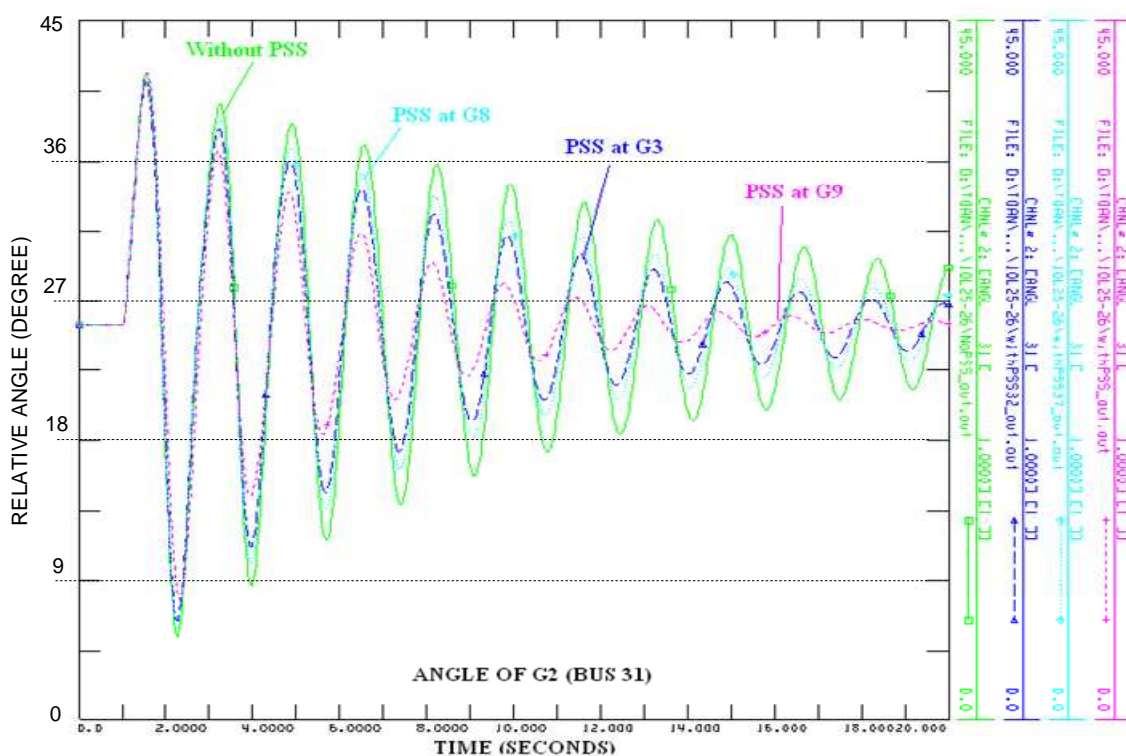
Scenario	$E(\omega)(\times 10^3)$ corresponding with inputs and outputs at								
	G10	G2	G3	G4	G5	G6	G7	G8	G9
1	1.4716	1.6597	1.9230	3.0629	3.3224	2.9712	3.1885	1.7909	3.1377
2	1.8389	2.0810	2.5446	4.0705	4.3957	3.9666	4.2337	2.2136	3.9344
3	2.4965	2.9423	3.5082	7.2692	7.7870	7.1506	7.5393	3.0803	6.3102
4	1.7119	2.1298	2.4924	4.3741	4.6876	4.2954	4.5518	1.9255	6.2099
5	1.4475	1.6175	1.8742	3.0731	3.3474	2.9804	3.2029	1.7763	3.5814
6	3.2953	5.5326	5.6529	6.1744	6.4373	6.1570	6.2509	3.6298	5.9327
7	0.7518	0.9087	1.0372	1.4423	1.5706	1.3761	1.5049	0.9696	1.6578
8	0.8266	0.9820	1.1671	1.6301	1.7703	1.5639	1.7010	1.0478	1.8007
9	0.7990	0.9681	1.1191	1.8607	2.0089	1.7986	1.9317	1.0326	1.8911
10	0.7502	0.9141	1.0520	1.5776	1.6988	1.5262	1.6548	0.9158	2.5978
11	0.8152	0.9311	1.0645	1.5593	1.7143	1.4897	1.6330	1.0689	2.3019
12	0.8175	1.3372	1.3828	1.4053	1.4892	1.3591	1.4324	0.9976	1.6437
13	0.7729	1.3037	1.3502	1.4617	1.5394	1.4182	1.4815	0.9215	2.4444
14	0.8489	1.3988	1.4523	1.6662	1.7628	1.6159	1.6787	1.0348	1.7965
15	0.8689	0.9776	1.1056	1.5057	1.6255	1.4472	1.5756	1.0759	1.8013
16		2.5231	2.9398	5.0022	5.4516	4.7849	5.1108	2.6950	4.8363
17	0.7518	0.9087	1.0372	1.4423	1.5706	1.3761	1.5049	0.9696	1.6578
Eω	1.269	1.713	1.924	2.858	3.069	2.781	2.952	1.597	3.149

The value of $E(\omega_i)$ for each scenario (at $T = \infty$) are given in Table 3-7. In this case, an enumerative solution may be obtained without the need of using an integer programming method. We can see that with the selection of inputs/outputs of **G9** (bus 38) leads to the maximum values of the index. This means that if we need to add one set of controllers/sensors into one of generators of the power system to improve the overall performance of the system. Therefore, the optimal placement is at **G9** (bus 38).

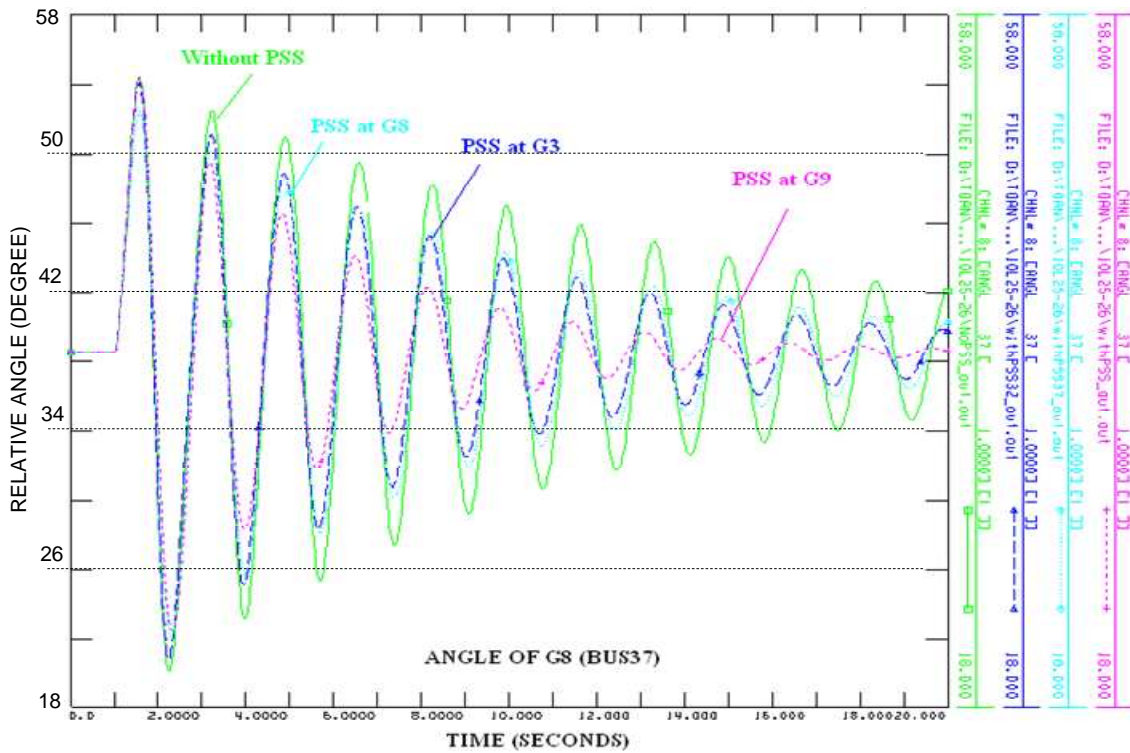
3.4.2.2 Validation by Dynamic Simulation

In order to illustrate the effectiveness of this method, we consider here the implementation of a standard power system stabilizer (PSS) that the input control is mechanical power of turbine of generator. The PSS is modeled by using model STAB1 in PSS/E dynamic library and parameters are typical data.

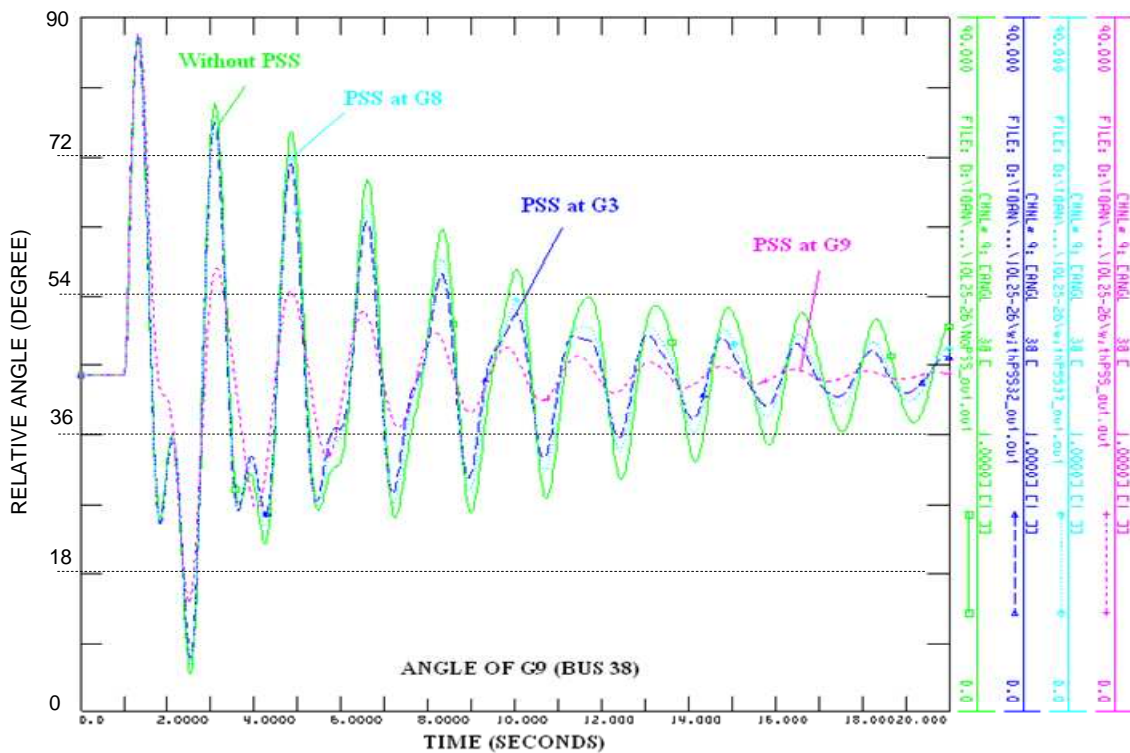
The first simulation was done for the scenario 10 (that could be chosen arbitrarily) when applying a three-phase fault at the transmission line 25-26, the line was tripped off after duration of 100(ms), time of simulation is 20 seconds. Figure 3-17 shows comparisons of oscillation damping corresponding to the three possible placements of a PSS at G3, G8, G9. Evidently through two figures, when placing a PSS at G39 had the best effect in term of oscillation damping comparing to other placements.



a) Angle of G2



b) Angle of G8

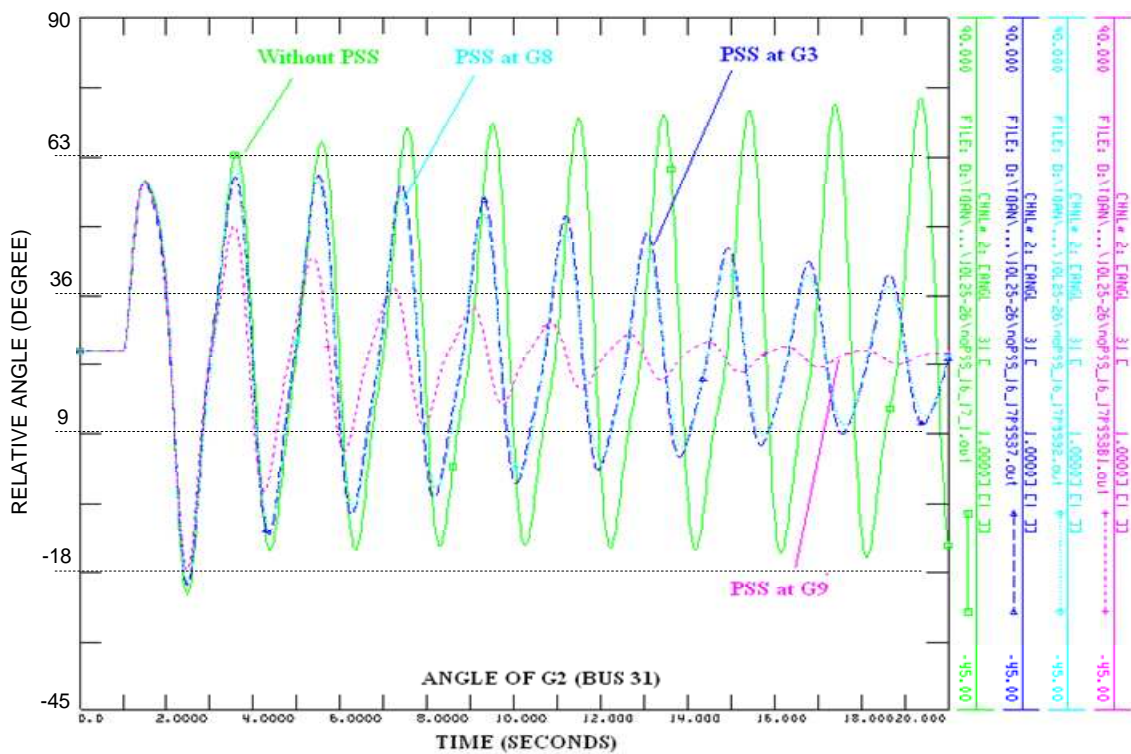


c) Angle of G9

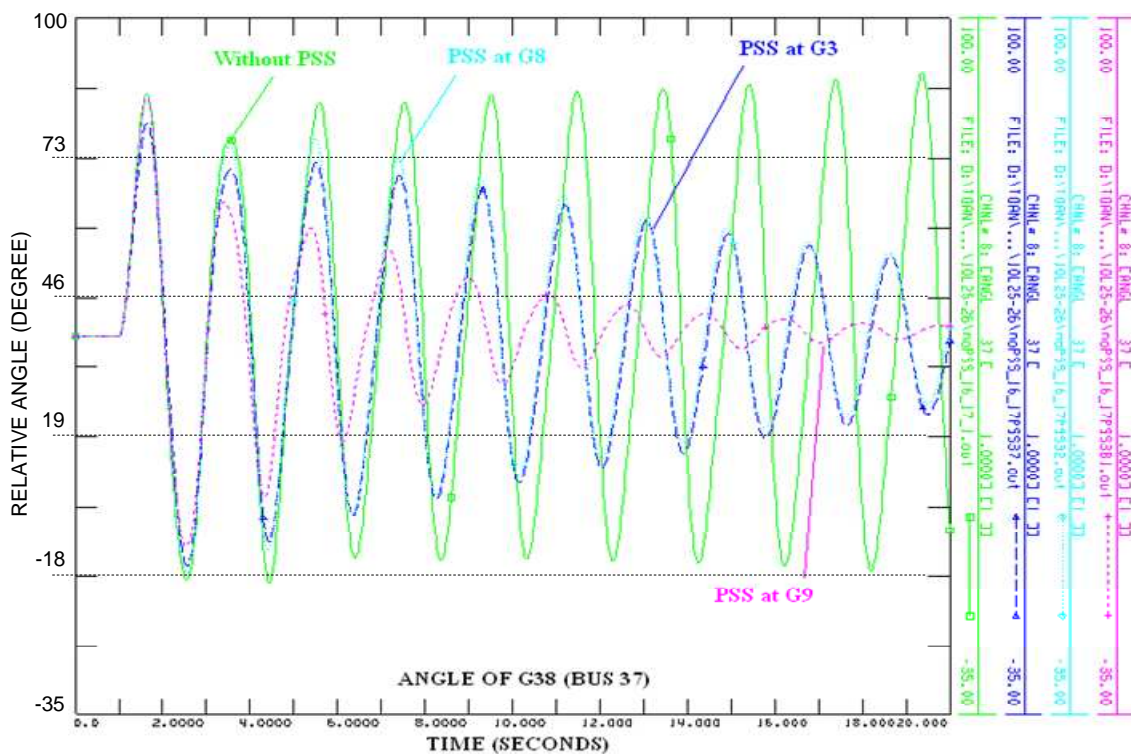
Figure 3-17: Relative angles of G2, G8, and G9 respectively in case of fault at the line 25-26.

The second simulation was done for the scenario 10 when applying a three-phase fault on line 15-16, the line was tripped off after duration of 150ms, time simulation is 20 seconds. Figure 3-18 showed comparisons of oscillation damping corresponding to the three possible

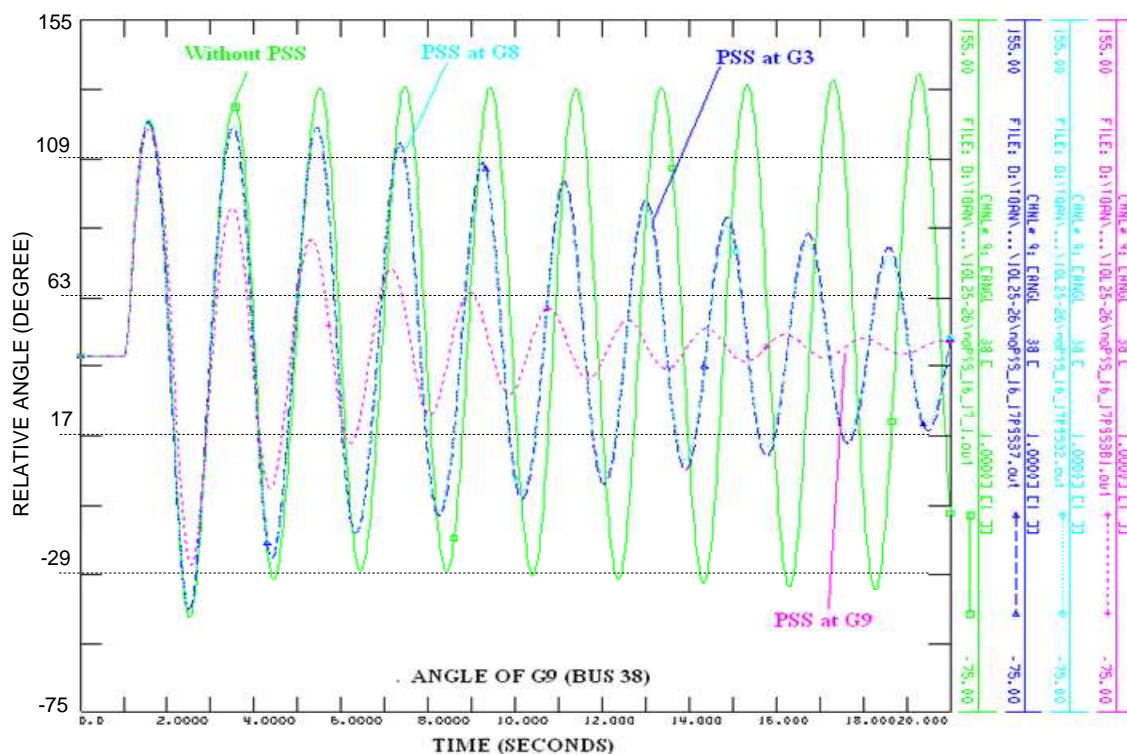
placements of a PSS at G3, G8, and G9. The placement of a PSS at G39 had the best effect in term of oscillation damping when compared to other placements.



a) Angle of G2.



b) Angle of G8.



c) Angle of G9.

Figure 3-18: Relative angles of G2, G8, and G9 respectively in case of fault at the line 16-17.

In this section, we restricted ourselves to a limited number of scenarios in order to easily illustrate the approach. Effectiveness of the method relies strongly on the availability of a large number of independent scenarios. However, for illustrating purpose, these typical scenarios were chosen limitedly with assumption that the scenarios are mainly and practically operating states of investigated power system.

3.5 CONCLUSIONS

In this chapter, a method for the optimal selection of controllers/sensors (equivalent to selection control inputs/outputs) with the goal of improving both controllability and observability have been proposed as one of preventive method to improve small signal angle stability. Since the computation of controllability and observability gramians can be very time-consuming in the case of very large-scale power system, the model reduction has been also introduced in this chapter.

This method is based on various scenarios reflecting different set-points or failure situations. This important characteristic introduces some robustness in decision making with respect to system nonlinearities and failure scenarios of power system. This is not provided by any of the existing methods used for optimal location of controllers/sensors.

Furthermore, application of eigenvalues sensitivity methods relies on a complex modal analysis, which may be problematic for large-scale systems (curse of dimensionality, dependency of the eigenvalues with respect to the set-points, etc). In our cases, no explicit model analysis is needed.

Optimal placement of standard Power System Stabilizers in order to improve small signal stability to a “two-area system” and a “39 bus New England system” have demonstrated very promising results that can apply for real and large-scale power systems.

Further studies will be devoted to the use of multi-criteria optimization for controller design purposes. One possible approach is to combine controllability and observability objectives with robustness objectives and optimal control system design (optimal design a power system stabilizer with multiple inputs is an example).

In practice for large-scale power systems, computation complexity renders crucial the use of both model reduction and adequate integer programming techniques.

CHAPTER 4

TRANSIENT STABILITY AND PREVENTION CONTROL

4.1 INTRODUCTION

As mentioned in chapter 2, both environmental and economical pressures are pushing power systems operating closer to their security limit. Power systems are not only more complicated but also more vulnerable to any disturbances. Some serious power system blackouts with severe consequences that occurred in the US and European countries are some examples of these situations. Causes of blackouts are always multiple and one of them is directly related to transient stability problem. Transient stability analyses are especially difficult because the power systems response to faults that have highly nonlinear characteristics and fast time evolution. As a major concern, transient stability has been studied for a long time. However, transient stability is still an issue as the initial causes of other types of power system stability such as small signal stability, and voltage stability. We still need to fully understanding and analyses the transient stability mechanisms and to find effectively and economically justified solutions for this problem.

In practice, transient stability can be avoided by correctly applying some preventive or corrective actions. The corrective control is the attempt to stabilize an unstable power system, directing the system trajectory onto a new stable equilibrium point shortly after a severe contingency. The application of corrective actions is always difficult because we have to solve a set of nonlinear equations that may not be solvability or sometimes this problem occurs in very rapidly short period. On the contrary, the preventive control is carried out before the instability actually occurs, or may sometimes be performed in the operating planning stage (for example: one day or one week ahead operating planning that is based on the practical daily load curves). Therefore, preventive control will be not only easier in term of implementation but also more desired in the power system operations.

From the traditional transient stability preventive control point of view, researchers have developed some control methods, which could be applied with the goal of identification zone of stability, critical clearing time, and stability margin in order to be applicable in real power system operation. The equal-area criterion gives some clear comprehensions about critical clearing time, margin of stability, and concept of preventive and corrective method of transient stability. However, this method is only applied to a simple system the so-called Single Machine Infinite Bus (SMIB) [1] and only suitable for illustration purposes of transient stability.

The time-domain methods [1] could identify critical clearing time (CCT) for a specific contingency; but they could not identify zone of stability and/or margin of stability.

Some researchers have developed a direct approach that is based on the so-called transient energy function [27]. The function was called Transient Energy Function (TEF). In this method, the critical transient energy, which is associated with the relevant unstable equilibrium points of the post fault network encountered by the disturbed system trajectory, is

identified. If system transient energy at the end of fault, (i.e., at clearing) is less than this critical energy, the system is stable; otherwise, it is unstable. This leads to a very fast assessment of transient stability as compared to the conventional methods. There has been a great deal of progress achieved in developing a direct method for analyzing first swing transient stability of multi-machine power system. However, one of the most difficult problems is the identification of the disturbed system trajectory.

As the transient stability monitoring, a method based on the single machine equivalent (SIME) was proposed [30]. This method is actually a combination between time-domain methods and the equal area criterion. From a given power system, a time-domain method is used for the purposes of contingencies analyses. For each contingency, the angles of generators are plotted in the same axes system. Based on the increase of angle variation, generators are classified into two groups: stable and unstable group. All generators in the same group will be described equivalent as one machine, from these two machines, an equivalent machine is formed the so-called OMIB (one machine infinite bus). The equal area criterion is used to assess the stability region of one machine OMIB with an infinite bus.

Several methods have been tested using actual power systems and put into actual practice [99]. Some methods that based on none-linear optimization and post contingency information were proposed in [100], [101], [102]

Beside theoretical methods mentioned above, there are some methods to prevent power system transient stability based on the heuristic approaches but could be applicable in the real power system with less calculation and complexity. One of them is the redispatching power output with the goal of improving CCT bigger than a threshold. The idea of this method is that it is necessary to shift the system to the stable side beforehand by a preventive control, so that the system can be stable even if some severe fault occurs. The method to redispatch generation output while considering critical clearing time (CCT) in order to prevent transient stability have been proposed in some literature.

Y. Kato and authors in [103], [104], [105], concentrated on one of the most important transient stability indices- the so-called CCT and proposed a new transient stability preventive control method using linear relationships between CCTs and generator rotor angles. At first, CCT calculations, as contingency screenings, were carried out to find contingencies that had smaller CCTs than predefined target values. The target values were taken as larger values than the actual circuit breaker operating times in the power system. A preventive control to achieve a more stable power system operating point was carried out by generator output rescheduling and generator terminal voltage control, which were determined using the relationships between CCTs and generator rotor angles. Y. Katoh [103] used a coherency index (PI) proposed in [106] to rank contingencies identifies the worst contingencies and the most critical machines for each severe contingency. Then kinetic stored during fault was used to calculate power output for rescheduling procedure. Authors in [107] used CCT as the index for transient stability assessment. And the concept of generation margin was used to calculate the amount of generation output for unstable generators.

Based on the literature, in this chapter, we introduce a new preventive method that is based on a transient energy point of view. The method employs a heuristic method combination with controllability gramian as a measure to choose generators that are used to redispatch power generation output in order to improve transient stability by increasing CCT. This

method is not only easy to perform for any power system by employing a set of linearized equations, but it also offers reliable results in term of transient stability prevention [108].

4.2 TRANSIENT STABILITY TIME-DOMAIN SIMULATION

In the transient stability prevention point of view, transient stability characteristics of a power system should be investigated in detail with respect to severity of disturbances such as fault clearing time (FCT) and fault location. With a given dynamic parameters of generators, levels of active power output is also a major factor that influence on transient stability. In this part of the chapter, some factors affecting transient stability are firstly investigated through a time domain simulation.

A “39 bus New England system” shown in Figure 4-1 is considered as a test case. All generators are identical and modeled by using Round Rotor Generator Model (quadratic saturation) – GENROU, all excitation systems are identical, and modeled by using IEEE Static Excitation System- EXST1 (generator 1 is considered as infinite bus).

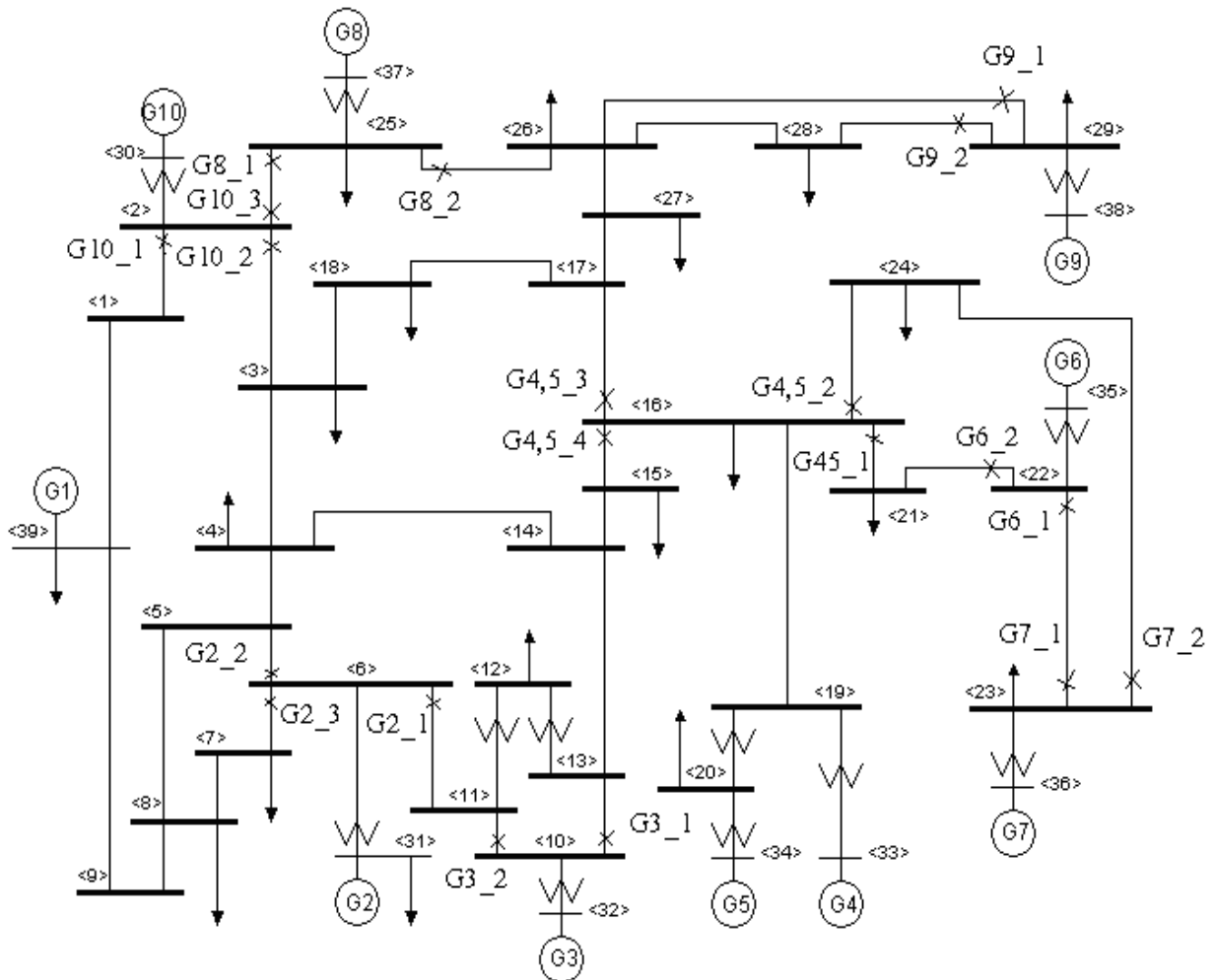


Figure 4-1: Different contingencies of “39 bus New England system”.

4.2.1 Active Power Output of Generator near a Fault

As discussed in [1], the pre-contingency output of the generator plays an important role in studying transient stability. Therefore, in this part, the influence of active power output of generator near a fault is investigated in details.

Transient stability properties of G9 are investigated with different active power output. We consider some scenarios with different levels of active power output as shown in Table 4-1 below.

Table 4-1: Active power output of G9.

Generator	G9	G9	G9	G9
Active power output (MW)	830	810	780	700
Fault clearing time (s)	0.100	0.100	0.100	0.100
Fault location	G9_2	G9_2	G9_2	G9_2

Figure 4-2 shows a comparison of internal angle of G9 with different active power outputs. The simulation is done for the same scenario with a three-phase line ground fault on transmission line 29-28 at $t = 1$ second, the fault is cleared 100 ms latter by tripping this transmission line (scenario G9_2). Time of simulation is extended to 10 seconds, and the angle axis varies from 0 to 180°.

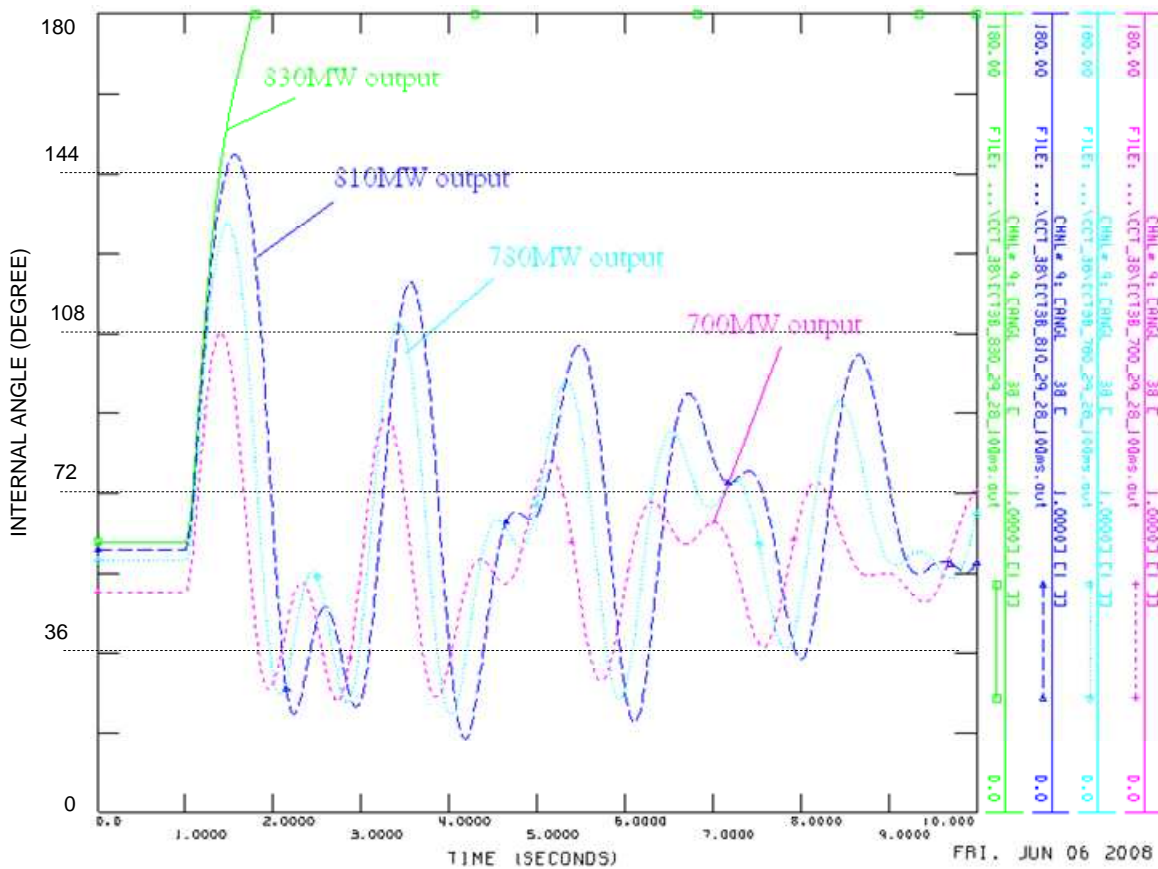


Figure 4-2: Internal angle of G9 with different active power output.

From the illustration of the equal area criterion with SMIB case study as in [1], when active power output of the generator gets bigger value, then the accelerate area becomes greater than the decelerate area with the same contingency and fault clearing time (FCT). As a result, the instability tendency is increased. Therefore, when dealing with a specific contingency, the more active power output is, the more transient instability is. From Figure 4-2, by time domain simulation for larger power system, the above conclusion is consistently verified and validated. When considering the same fault location and fault clearing time, the generator G9 loses angle stability because the angle is increased bigger than 180^0 at the first swing that is corresponding to the case of active power output equals 830 (MW). In other cases, the generator G9 is oscillating with the decreased magnitude and having stable tendency. Therefore, the increment of internal angle is proportional to the active power output.

In term of preventive point of view, reduction of the pre-contingency output of the plant is considered as a measure to improve transient stability.

4.2.2 Fault Locations

It is clear that, when a fault is “close” to the generator, the severity of fault is increased, and the risk of instability is increased as well. In this part, the influence of fault locations on transient stability is investigated through time domain simulation.

Transient stability properties of G9 are investigated with different fault locations. Consider some scenarios as shown in Table 4-1.

Table 4-2: Different locations of fault.

Generator	G9	G9	G9	G9
Active power output (MW)	810	810	810	810
Fault clearing time (s)	0.100	0.100	0.100	0.100
Fault location	G9_2	G8_2	G7_2	G4,5_3

Figure 4-3 shows a comparison of internal angle of G9 with respect to different fault locations. The simulation is done for the same scenario with a three-phase line ground fault on a transmission line at $t=1$ second, the fault is cleared 100 ms latter by tripping the faulted transmission line. Time of simulation is extended to 10 seconds, and the angle axis varies from 0 to 180^0 . As discussed in [1], the transient stability severity depends very much on the duration and the post-fault conditions. This characterizes by fault locations to the generator in question. From Figure 4-3, by time domain simulation, with the same power output and fault clearing time, when the fault location gets closer to a generator, the severity is greater, and the risk of instability is greater. Therefore, a fault near a generator is considered as the most critical contingency.

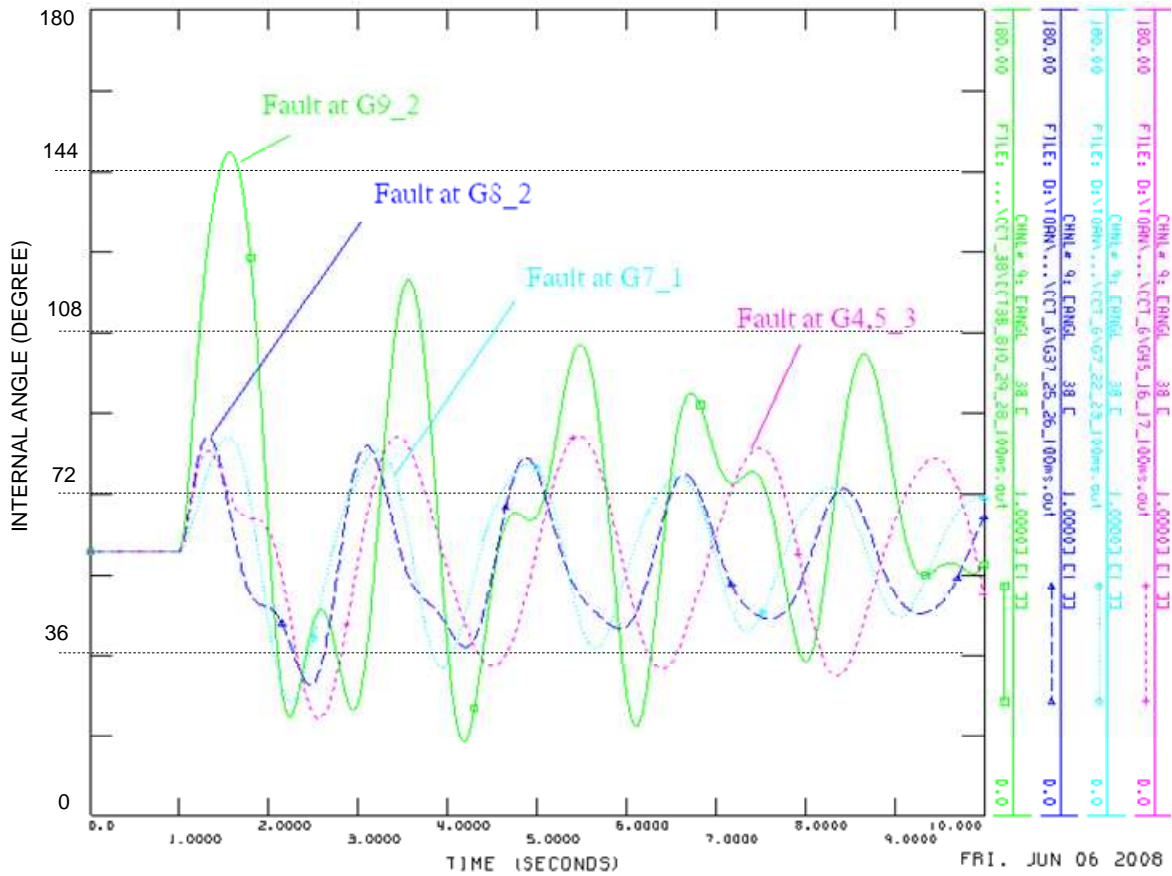


Figure 4-3: Internal angle of G9 with different fault locations.

4.2.3 Fault Clearing Time

Fault clearing time (FCT) is one of major factor influenced on transient stability. As mention and illustration in the equal area criterion, the greater FCT is, the less power system remaining in stability is. In this part of the chapter, the influence of FCT on transient stability of G9 is investigated through time domain simulation. The Table 4-3 shows a scenario with different fault clearing time.

Table 4-3: Different fault clearing time.

Generator	G9	G9	G9	G9
Active power output (MW)	810	810	810	810
Fault clearing time (s)	0.050	0.100	0.120	0.130
Fault location	G9_2	G9_2	G9_2	G9_2

Figure 4-4 shows a comparison of internal angle of G9 with respect to different FCT. The simulation is done for the same scenario with a three-phase line ground fault on a transmission line at $t = 1$ second, the fault is cleared FCT (s) latter by tripping the faulted transmission line. Time of simulation is extended to 10 seconds, and the angle axis varies from -100° to 250° .

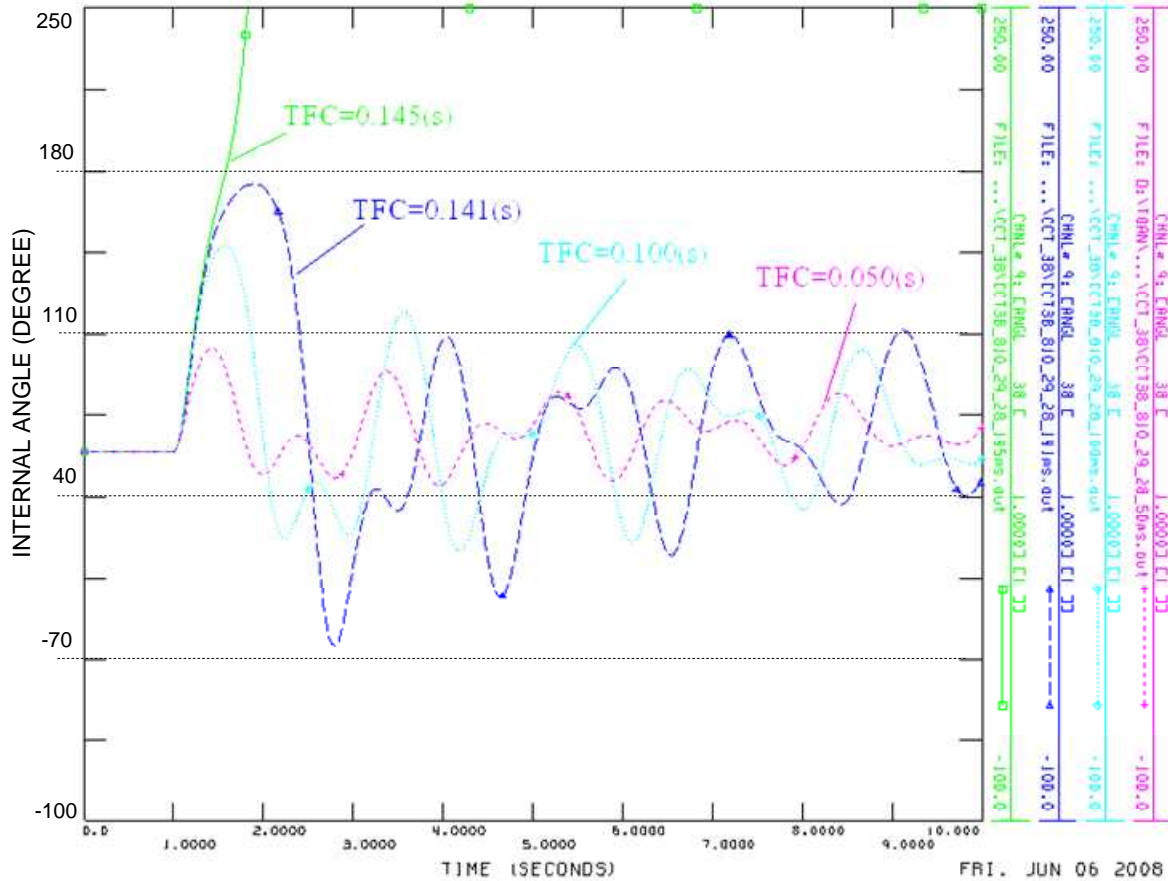


Figure 4-4: Internal angle of G9 with different fault clearing time (FCT).

From Figure 4-4, we can observe that with the same scenario of fault and active power output, the risk of instability increases proportional to FCT. As mentioned in [1], the amount of kinetic energy gained by the generators during a fault is directly proportional to the fault duration. In practice, the maximum value of FCT for which the system remains the stabilized properties after experiencing a contingency is called as the critical clearing time (CCT). Therefore, maximize CCT is also considered as a preventive action in order to improve transient stability.

From these above investigations, in order to prevent transient stability, one possibility is to redispatch active power output of generator in order to increase CCT greater than a desired threshold. In this chapter, a heuristic method based on controllability gramian is introduced as follows.

4.3 NEW PREVENTION METHOD FOR TRANSIENT STABILITY

4.3.1 Some Recalls on Controllability and observability gramians

Refer to the section 3.2 in chapter 3, the problem of redispatching power output of generators in order to improve CCT as a transient stability preventive method is equivalent to the use of control inputs (for example: delta mechanical power) to adjust power output of generators in question (dispatching generators: reduced and increased power output

generators). Because the preventive context is considered before the contingency actually occurs, then the stable characteristic of power system is maintained. A linearized state space system could be employed as follows:

Refer to the section 3.2: Since the controllability matrix W_C depends on the control input matrix B , the transient controllability energy can be affected by properly choosing the control input matrix. On the other hand, since the observability matrix W_O depends on the output signals matrix C , the energy output of sensors can be affected by properly choosing this signal outputs matrix. Two remarks are made as below:

- *From a control point of view:* In order to stabilize a system after experiencing a disturbance, we need a **transient energy** to bring state variable back to original. To minimize the control input energy, we have to minimize W_C^{-1} transient energy or equivalently to maximize W_C in the sense of a given matrix norm. In order to maximize energy output of sensors, we have to maximize W_O according to some measures.
- *From a preventive point of view:* The transient energy depends on the current operating of power system, especially, depends on active power output of generators. Generators those have big transient energy will be less sensible to disturbance. Therefore, we have to shift power output of some critical generators to other generators which have maximum transient energy, equivalent to maximum controllability gramian W_C^{-1} (or equivalently to minimize W_C) in the sense of a given matrix norm. A weighted factor based on the transient energy is built for partition shifted power in order to improve transient stability.

For large-scale power system, controllability/observability gramians could be used for the purpose of reduction order of state space system (see also in references: [85], [86], [87], [88], [109], [110], [111]).

4.3.2 Redispatch Generation Output to Improve Critical Clearing Time

The method to redispatch generation output while increasing the critical clearing time (CCT) in order to improve transient stability have been proposed in some literature [103], [104], [105], [106], [107]. In practice, power systems are very large-scale and complicated systems. The number of contingencies that we should estimate becomes very huge, and it usually takes a long time to analyze all contingencies in details. When dealing with transient stability, only angle of generators are taken into account. Therefore, in this part, response of rotor angle to the most critical contingency that is a three-phase line ground fault occurred at bus near a generator is investigated. In addition, as discussed above, FCT is a major factor influence on transient stability. In practice, we desire the value of CCT as much as possible and it must be greater than the activation time of protection system (included acting time of relay and circuit breaker). In this chapter, a prevention method by redispatch active power output of generators that is based on controllability gramian is proposed in the sense of improving CCT larger than a predefined threshold while considering the most critical contingency.

The contingency is considered here is a three phase bold fault at a bus near a generator, and is cleared by tripping one circuit of a double circuit line at the CCT. The concept of preventive transient stability by reschedule power generation is illustrated in Figure 4-5.

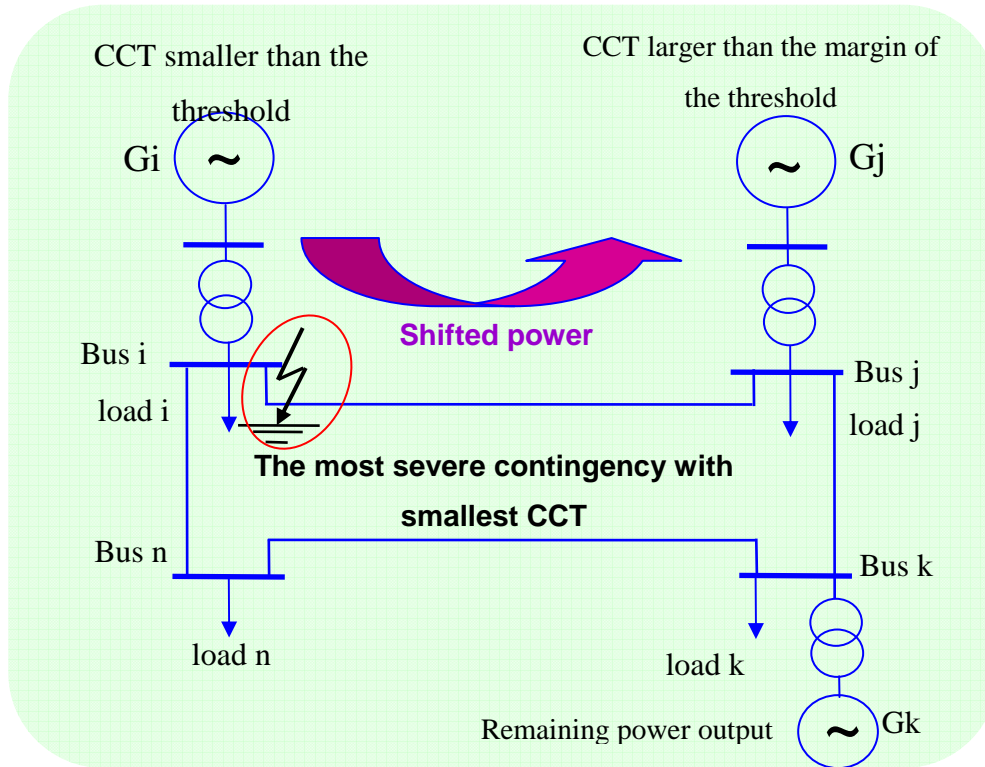


Figure 4-5: Rescheduling power generation with the smallest CCT.

The preventive procedure is summarized as follows.

To find the dispatching generators:

1. For a given power system, run a faulty contingencies analysis by applying a three phase bold fault at a bus near generator, and then, calculate the CCT for the nearest generator
2. According to contingencies analysis, the result of a CCT ranking is made. Defined a threshold of CCT. The threshold value is taken as larger value than the actual circuit breaker operating times in the power system. In preventive control point of view; we need to improve transient stability by increasing the value of CCT.
3. Once the threshold of CCT is set, generators are classified into three groups
 - a. The generators that have CCTs smaller than the threshold will be chosen as candidates for reducing their output power (the so-called shifted power output generators).
 - b. The generators that have CCTs greater than the threshold but smaller than the margin (said 130%) comparing to the threshold will remain the active power output during redispatching process.
 - c. The generators that have CCTs greater than the threshold and have a large enough margin (said 130%) comparing to the threshold will be chosen as candidates for taking over shifted power output (the so-called candidate generators).

To find individual shifted power output and total shifted power output:

4. The amount of reduced power output for each shifted power generator is calculated through quasi-linear relationship between CCT and active power output [103], [104].

$$\operatorname{tg} \alpha_{-i} = \frac{CCT_{i2} - CCT_{i1}}{P_{i1} - P_{i2}} = \frac{(CCT_{i\text{-desired}} - CCT_{i1})}{P_{i1} - P_{i\text{-desired}}} \quad (4.3-1)$$

$$P_{i\text{-desired}} = P_{i1} - \frac{(CCT_{i\text{-desired}} - CCT_{i1})}{\operatorname{tg} \alpha_i} \quad (4.3-2)$$

$$\text{Total shifted power output: } P_{\text{shifted}} = \sum_{i=1}^N (P_{i1} - P_{i\text{-desired}}) \quad (4.3-3)$$

where:

P_{i1} , P_{i2} , CCT_{i1} , CCT_{i2} , are calculated through training simulations in order to build a quasi-linear relationship between CCT and active power output (the quasi-linear relationship could be estimated by two or three training simulations), P_{i1} is initial power output. $CCT_{i\text{-desired}}$, is the desired threshold, N is the number of shifted power output generators. Figure 4-6 illustrates the calculation procedure for shifted power output

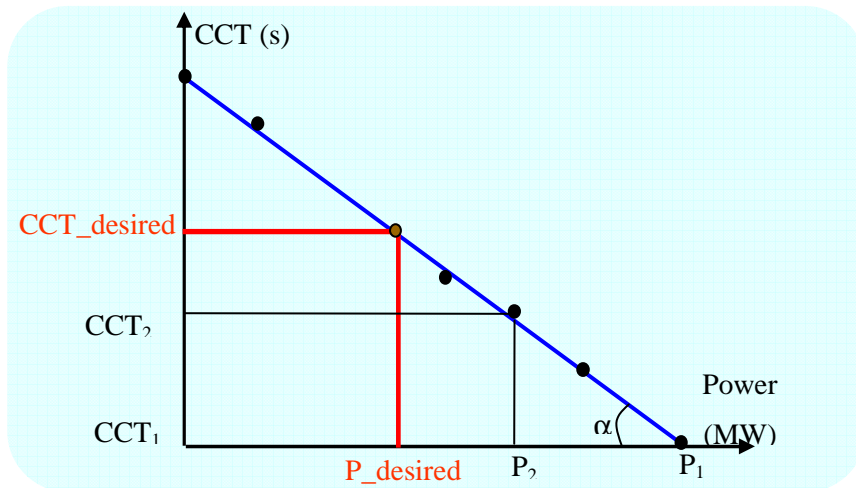


Figure 4-6: Quasi-linear relationship between CCT and active power output.

To partition the total shifted power to candidate generators:

5. In order to keep the balance between power output and power demand, one or more candidate generators are needed to take over amount of shifted power output. Consider the candidate generators above, which have the maximum transient energy (or minimum trace(W_c)) are chosen for taking over shifted power. A weighted factor based on controllability gramian is proposed to choose amount of load for the candidate generators.

$$W_i = \frac{1/W_{c-i}}{\sum_{i=1}^n 1/W_{c-i}} \quad (4.3-4)$$

Where n is number of candidate generators for taking over total shifted power.

6. Verify power generation limits of candidate generators and validate by dynamic simulation when there is a critical fault with duration equal to threshold of CCT.

4.4 APPLICATION

A modified of “39 bus New England power system” is chosen as test case in order to illustrate this approach.

Step 1: Some contingencies are shown in Figure 4-1. Remark that bus 39 is considered as infinite bus. Initial power generation condition is summarized in the Table 4-4. The result of screening contingencies is shown in the Table 4-5

Table 4-4: Initial conditions of power output.

Generator	Power output/ rated value (MW)	Generator	Power output/ rated value (MW)
G2	541/700	G7	560/700
G3	650/750	G8	540/700
G4	632/750	G9	830/900
G5	508/700	G10	250/350
G6	650/750		

Table 4-5: CCT for contingencies.

Contingency	Faulted point	Branch Tripped off		CCT (s)
1	G2_1	6	11	0.190
2	G2_2	6	5	0.180
3	G2_3	6	7	0.190
4	G3_1	10	11	0.190
5	G3_2	10	13	0.170
6	G4,5_1	16	21	0.140
7	G4,5_2	16	24	0.150
8	G4,5_3	16	15	0.140
9	G4,5_4	16	17	0.130
10	G6_1	22	23	0.180
11	G6_2	22	21	0.110
12	G7_1	23	22	0.180
13	G7_2	22	24	0.180
14	G8_1	25	2	0.200
15	G8_2	25	26	0.210
16	G9_1	29	26	0.100
17	G9_2	29	28	0.088
18	G10_1	2	1	0.250
19	G10_2	2	3	0.220
20	G10_3	2	25	0.200

Step 2: From the Table 4-5, we can see that, contingencies 11th, 16th, 17th have the smallest CCTs corresponding to generators G6 and G9. In order to improve transient stability of these generators by mean of increasing CCT, a value of 0.130(s) is chosen as the desired threshold of CCT.

Step 3: Compare to the threshold, there are two generators G6 and G9 that have CCTs less than the threshold, therefore these generators are chosen to reduce their power output. Power output of generators G3, G4, G5, and G7 with the margin of CCT smaller than 30% will be kept as constant values. Generators G2, G8, and G10 which have both the greatest CCTs and margins (said 30%) greater than the threshold are then chosen as candidate generators.

Step 4: From the quasi-linear relationship between power output and CCT of G6, and G9 as in Figure 4-7and Figure 4-8, new power output of shifted power generators are shown in the Table 4-6.

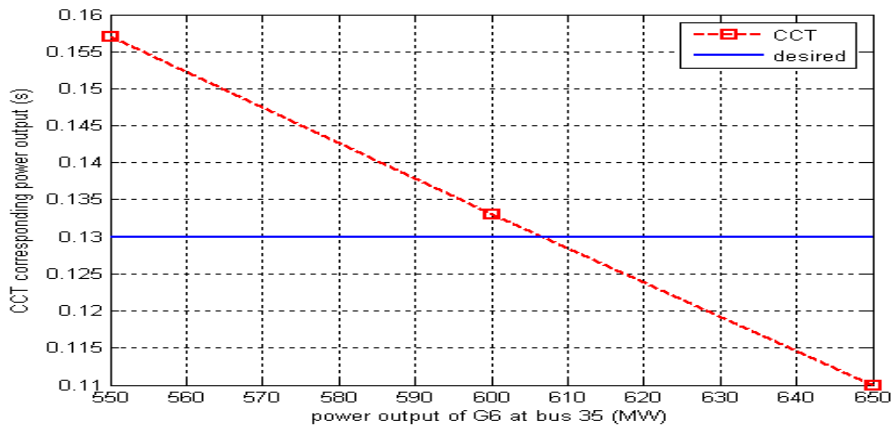


Figure 4-7: CCT with respect to power output of G6.

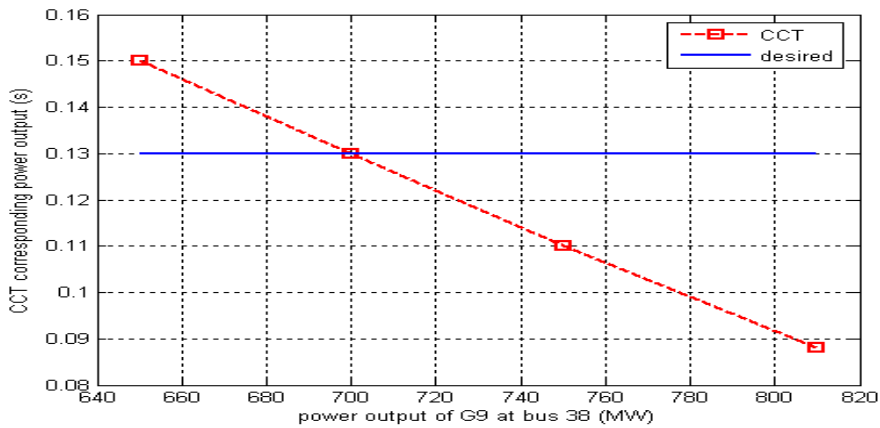


Figure 4-8: CCT with respect to power output of G9.

Table 4-6: New power output and total amount of shifted power.

Generator	New power output (MW)	Shifted power (MW)	Total power shifted (MW)
G6	607	43	156
G9	697	113	

Step 5: The problem of redispatching power generation is equivalent to input a mechanical power control signal into the candidate generators of the system to get a new stabilized system. Therefore, generator has the maximum transient energy (or minimum controllability gramian trace(W_C)) will be chosen for taking over the amount of shifted power. Build a linearized system as (3.2-1). The controllability gramian based on a matrix norm with one control signal input ΔP_{mec} is given in the Table 4-7 below:

Table 4-7: Controllability gramian of generators.

Generator	Trace of (W_C) $\times 10^3$	Generator	Trace of (W_C) $\times 10^3$
G2	0.4390	G7	0.6317
G3	0.5051	G8	0.4620
G4	0.5820	G9	1.0841
G5	0.6466	G10	0.2047
G6	0.5715		

Consider the CCTs from Table 4-5 and controllability gramians in Table 4-7, three generators G2, G8, and G10, which have the greatest CCTs and smallest controllability gramian are chosen as candidate generators. The weighted factor based on trace(W_C) is calculated as in Table 4-8

Table 4-8: Weighted factor and corresponding new power output of candidate generators.

Generator	W_i	Shared shifted power (MW)	New active power output (MW)
G2	0.244	38.1	579.5889
G8	0.236	36.2	576.2003
G10	0.520	81.7	331.7027

Step 6: Check the power generation limits and perform a dynamic simulation, with FCT equal to the threshold value, for generators before and after redispatching.

In order to observe angle output of generators before and after redispatching, time domain simulation with time of clearing equal to the threshold of CCT=0.130s is done for critical fault contingencies: 11,16, 17. Angles of both G6 and G9 are shown in Figure 4-9 and Figure 4-10. From these figures, the transient stability has been increased thanks to increasing CCT.

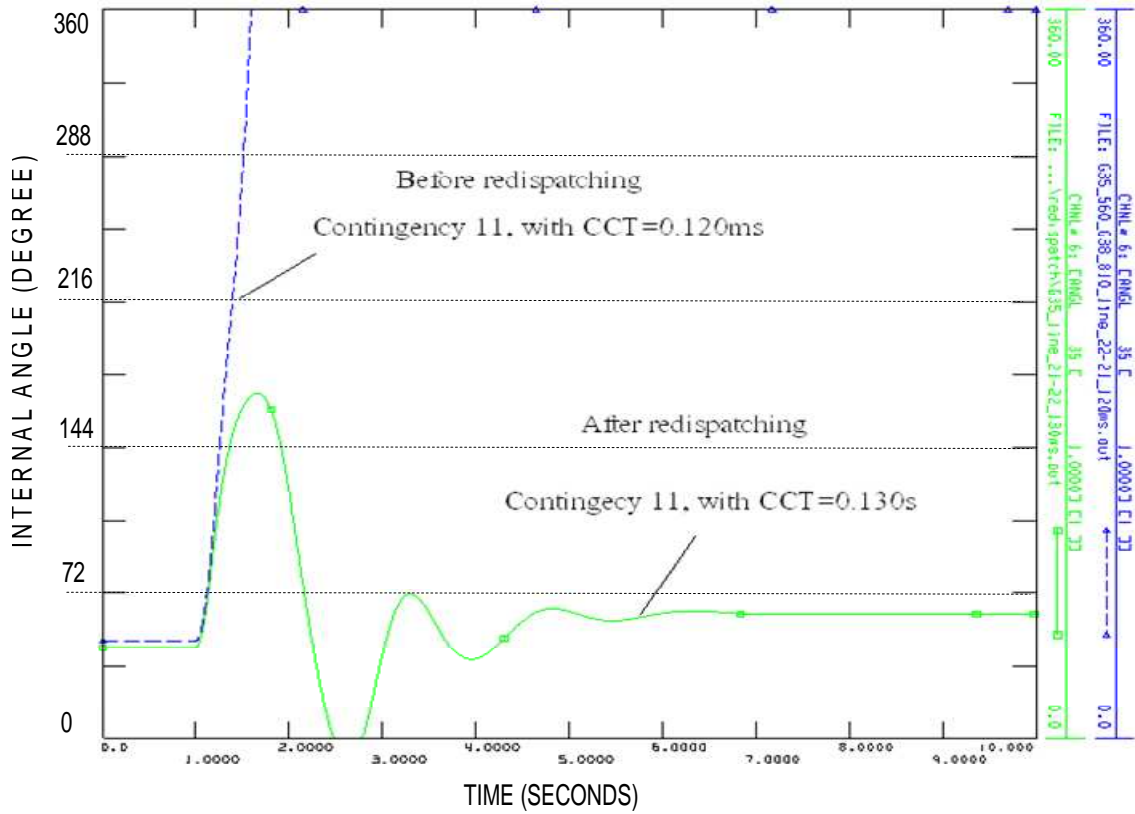


Figure 4-9: Angle of G6 before and after redispaching with FCT equal to the threshold.

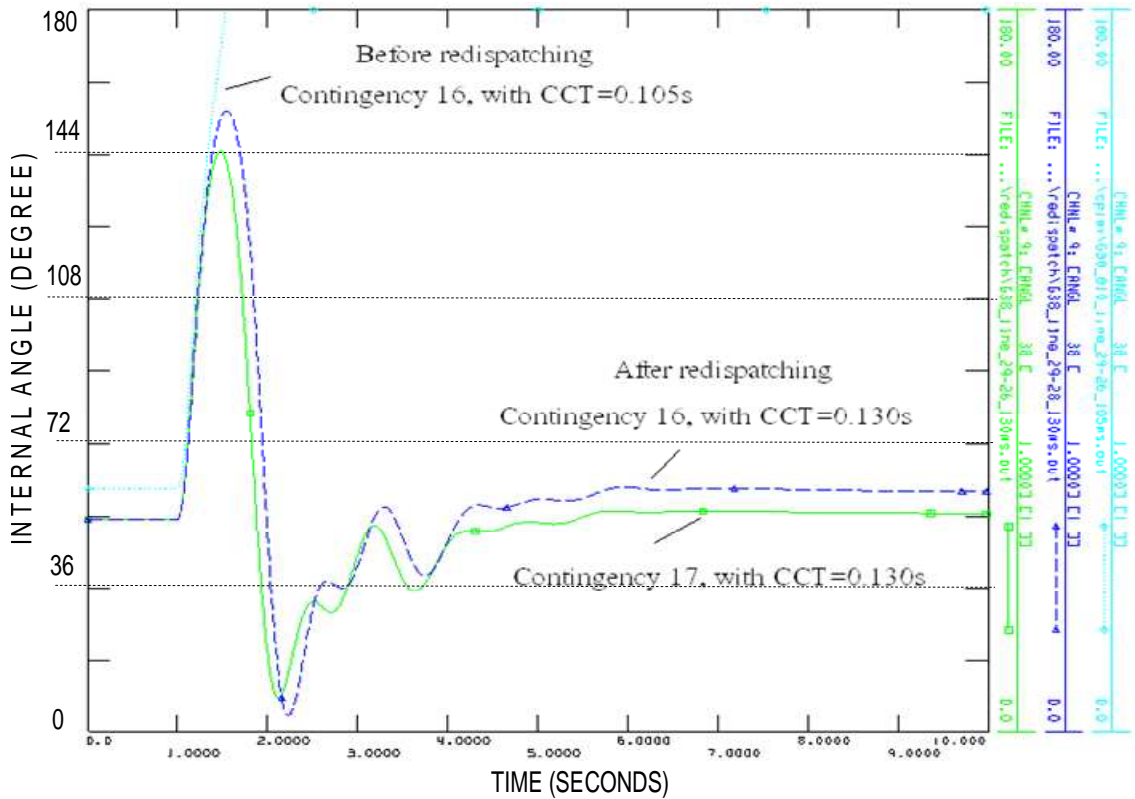


Figure 4-10: Angle of G9 before and after redispaching with FCT equal to the threshold.

Angles of candidate generators G2, G8, and G10 after redispatching are plotted in Figure 4-11, Figure 4-12 and Figure 4-13 with fault clearing time equals threshold 130(ms) for verifying the stability limits.

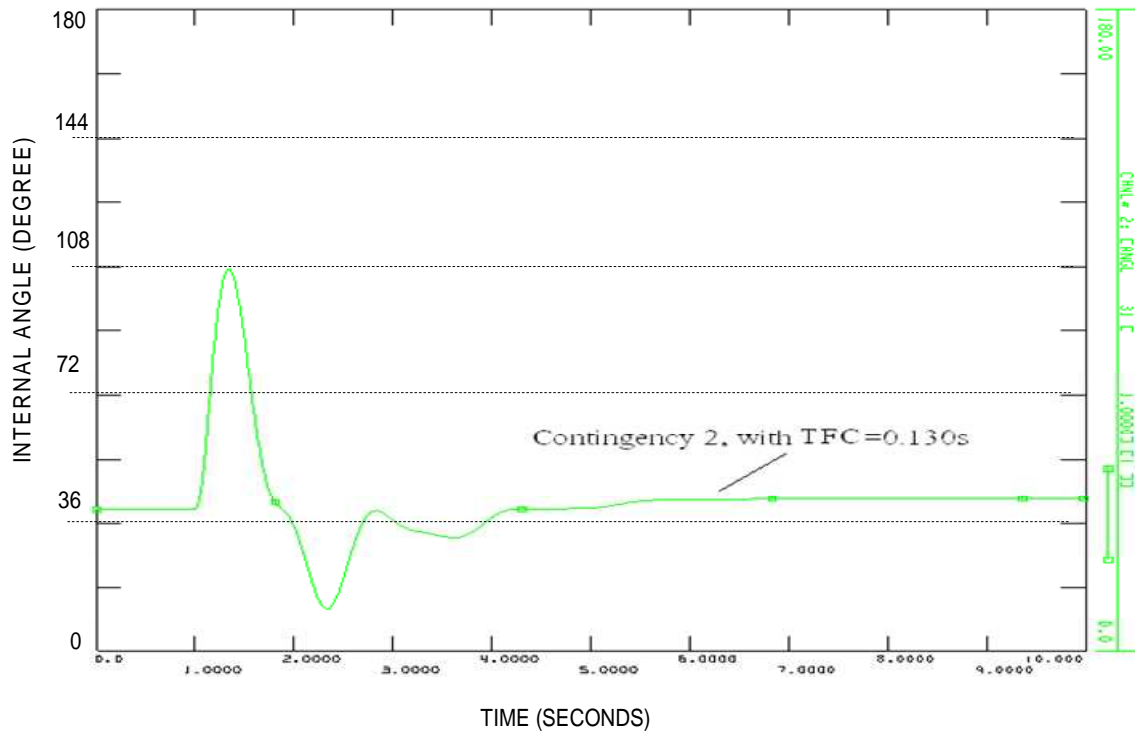


Figure 4-11: Angle of G2 after redispatching with FCT equal to the threshold.

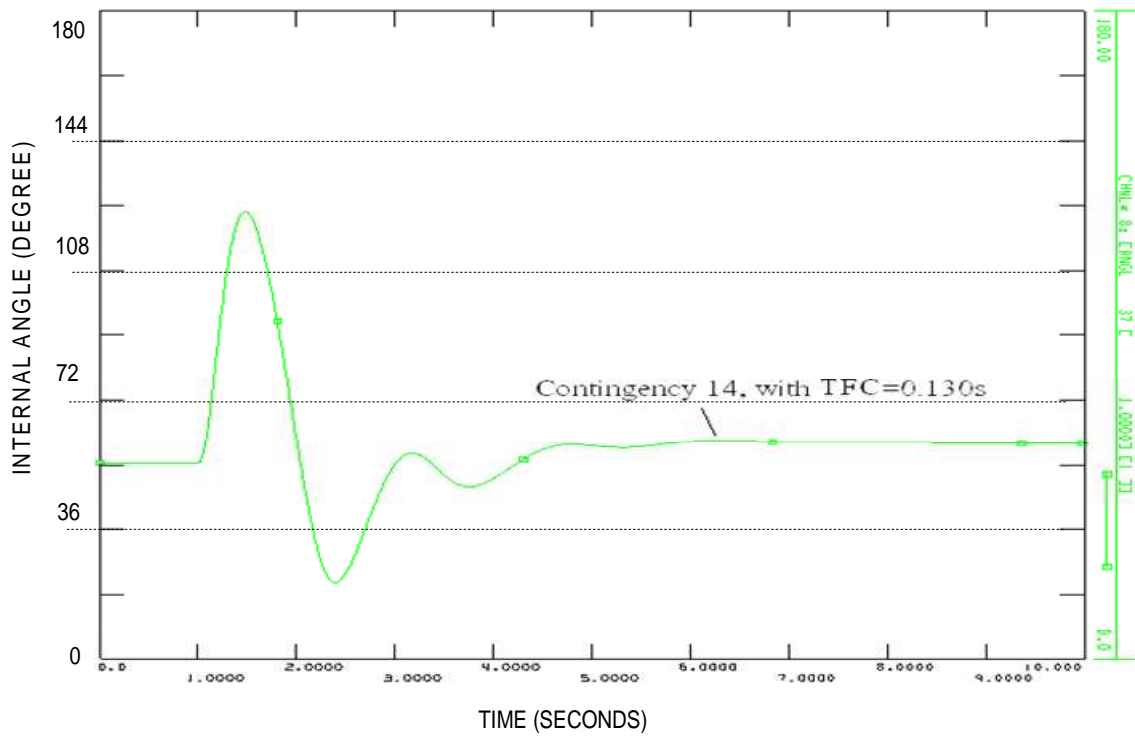


Figure 4-12: Angle of G8 after redispatching with FCT equal to the threshold.

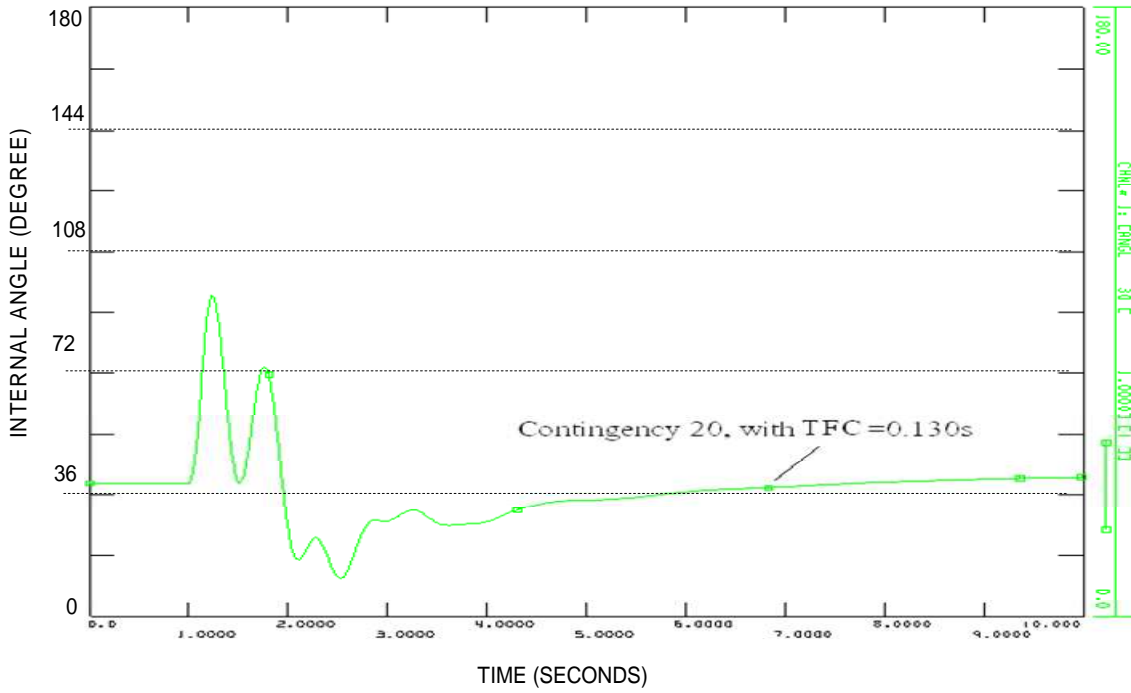


Figure 4-13: Angle of G10 after redispatching with FCT equal to the threshold.

In order to investigate the influence of redispatching procedure on the critical clearing time of generators that remained current power output during the procedure, angles of these generators are plotted in Figure 4-14, Figure 4-15 and Figure 4-16 with FCTs equals to the threshold.

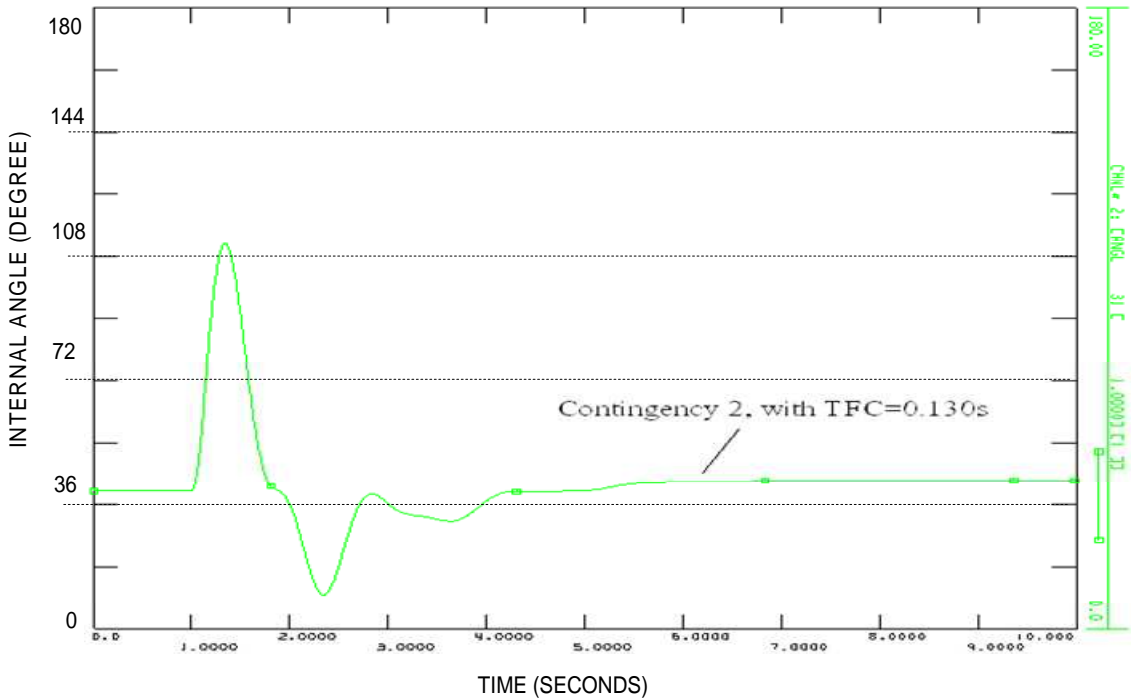


Figure 4-14: Angle of G3 after redispatching with FCT equal to the threshold.

4.5 CONCLUSIONS

In this chapter, major factors influenced on transient stability were investigated firstly. For a given power system, some factors such as active power output, fault clearing time, and fault location were investigated in details by using time-domain simulation. We reconfirmed that the instable tendency of a power system is directly related to the level of active power output. Both the severity of the fault and the risk of instability are directly proportional to the fault clearing time. The locations of fault also have a great impact on the stability. With the same active power output and fault clearing time, the closer to generator of the fault is, the more instability risk increases when the fault occurs at the vicinity of the generator.

Based on the analyses of major factors influencing on transient stability, a transient stability preventive strategy was proposed. The method is a heuristic approach that is used to redispatch power generation output in order to increase the critical clearing time greater than a predefined threshold. By comparing the CCTs of generator to the threshold, generators are firstly divided into three groups: The first group includes generators that have CCTs smaller than the threshold. The active power output of these generators are reduced and called the shifted power generators. The quasi-linear relationship between CCTs and active power output has been utilized to calculate the total amount of shifted power output. The second group includes generators that have CCTs greater than the threshold but smaller than the margin. The active power output of these generators will be constant during the preventive procedure. The third group includes generators that have CCTs greater than the threshold and the margin. The active power output of these generators will be changed in order to take over the total shifted power output. These generators are called the candidate generators. The weighted factors that are based on the controllability gramian are used to partition the total shifted power to the candidate generators. The validity of the proposed method has been applied to the “39 bus New England system”. Dynamic simulation results have shown the improvement in transient stability.

In this chapter, the notion of transient energy is first proposed and discussed in term of transient stability preventive point of view. We believe that the transient stability preventive strategy proposed in this chapter will be useful for power system operations in the future. The major advantages of the method are that we use only linear power system models, which are easily tractable with classical algebra. The preventive effect is gained by simple calculation without solving any differential equation. This method is especially effective in the case of daily or weekly operating planning. One of the limitations of this method is that the linearized models are valid only at the vicinity of the current operating point, but we can imagine introducing a stochastic approach similar to the one proposed in chapter 3.

CHAPTER 5

DYNAMIC SIMULATION, PREVENTIVE AND CORRECTIVE METHODS TO PREVENT VOLTAGE COLLAPSE

5.1 INTRODUCTION

Voltage collapse has been considered as one of the major causes of recent power system blackouts. Therefore, full understandings of voltage collapse mechanism as well as factors that have direct influences on voltage collapse are essential requirements for operators and researchers. Voltage collapse phenomenon is mostly related to dynamic and complicated phenomena that compound of the influences of system dynamic elements in power system such as generator, automatic device actions, load models ...etc. Therefore, for better understanding of these phenomena as well as factors that influenced on voltage collapse, the dynamic simulation should be employed. The major advantages of the dynamic simulation are to offer more precise results and to provide more information about the dynamic behavior of power system devices during voltage stability analysis. Especially, we could observe not only variation of voltage profile at buses but also sequence of activation of automatic voltage control devices over the time of simulation. As discussed and observed from practical power system blackouts, voltage collapse phenomena are normally related to long-term in term of period of time (say longer than a half minute). The authors in [1], [2], [68] also stated that the long-term simulation is necessary because of many factors as follows: the time coordination of equipments, clarification of phenomena, confirmation of less computationally intensive static analysis, demonstration and presentation of power system performance by easy understand the voltage stability phenomena with respect to progression of time. Whereas, simulation of fast dynamics is only associated with the final phases of a collapse. Therefore, in this part, we limit our study only to the dynamic phenomena in the long-term of the voltage stability by using the software PSS/E. The dynamic behaviors of power system devices such as: generators, OEL, ULTC, different types of load ... are investigated by using standard models in the library of PSS/E. We will analyze factors having influence on voltage collapse by long-term simulation of two typical power systems: the BPA and Nordic power systems that are widely used for the purposes of voltage collapse investigation. Two systems have been modified in order to present and investigate the typical scenario of voltage collapse.

After having full understandings of mechanism as well as factors influenced on such complicated phenomenon as voltage collapse, it is necessary to find a rational control plan against voltage collapse with preventive and corrective actions.

From the preventive point of view, the preventive actions are implemented before the voltage collapse has actually occurred in order to estimate the stability margin with respect to foreseeable and credible contingencies. Therefore, power system is actually operating at an equilibrium point. For a given power system, if parameters, for example: topology of system, power generation and load are known, load flow equations are solved as to provide the state of power system (angles and voltage magnitudes). In normal operating condition, load flow

relationships could be described by decouples equations. That indicate reactive powers injected are sensible to variation of voltage. When reactive power is injected on a load bus, voltage magnitude of this bus is increased. When a bus of power system has abnormal value, (out of the desired range), power system operators must adjust control elements to restore voltage into the desired range by: switching shunt capacitors, changing tap positions of transformer, or changing terminal voltage of generators. In power systems, the voltages of buses are always variable by diverse reasons such as: load fluctuations, reactive power changing, changing tap positions, system topology changing...etc. Therefore, a preventive control strategy must be constructed to ensure voltage magnitudes of buses in the desired range whenever having contingencies in power system. The control strategy must be calculated easily to eliminate rapidly voltage fluctuations of load buses by control variables. In this chapter, a secondary voltage control strategy is proposed that is based on the use of optimal power flow in order to prevent risk of voltage collapse. Changing control variables such as terminal voltage of generators, tap changer of transformer, switching capacitors could repartition reactive power in power system, especially reactive output of generators. Therefore, a relationship between variation of control variables and reactive power output of generators must be formulated first. All these relationship constitutes a sensitivity matrix [112], [113]. From this matrix, we could construct a cost function that could be solved by employing quadratic programming [112], [114], [115].

From the corrective actions point of view, there are many way of implementing corrective methods to avoid voltage collapse that were mentioned in chapter 2. However, in order to maintain voltage magnitude of buses in power system after some severe contingencies, a rapid and easy corrective method must be implemented. In this chapter, a new scheme of under voltage load shedding (UVLS) based on the rules of C. W. Taylor [57] and D. Lefebvre [116] is used as a corrective method.

5.2 DYNAMIC SIMULATION OF VOLTAGE COLLAPSE

5.2.1 Factors Influencing on Voltage Collapse of “BPA Power System”

5.2.1.1 Descriptions of “BPA Power System”

The power system presented in Figure 5-1 suggested by the company of electricity of Bonneville Power Administration (BPA) is taken from [117]. The system includes two areas: a generation area and a load area that are linked though five 500 kV transmission lines.

The parameters of both load flow and dynamic data of this network are presented in the Appendix C. Specifically, all dynamic devices of the system are modeled by using models in the library of PSS/E. Specifically, G1 is modeled by using Constant Internal Voltage Generator Model (GENCLS), G2 and G3 are modeled by using Round Rotor Generator Model (GENROU). Simplified excitation system models (SEXSSs) are used to model excitation system of G2, and G3. For overexcitation limiter, the model of MAXEX2 is used, and for modeling under load tap changer transformer, the model OLTC1 is employed.

Summary of voltages and reactive power output of generators before the contingency is shown in Table 5-1. The result indicates there are some buses with very low voltage

magnitude, and in the reactive power reserve point of view, there are two machines G2 and G3 that have reached their reactive power output limits.

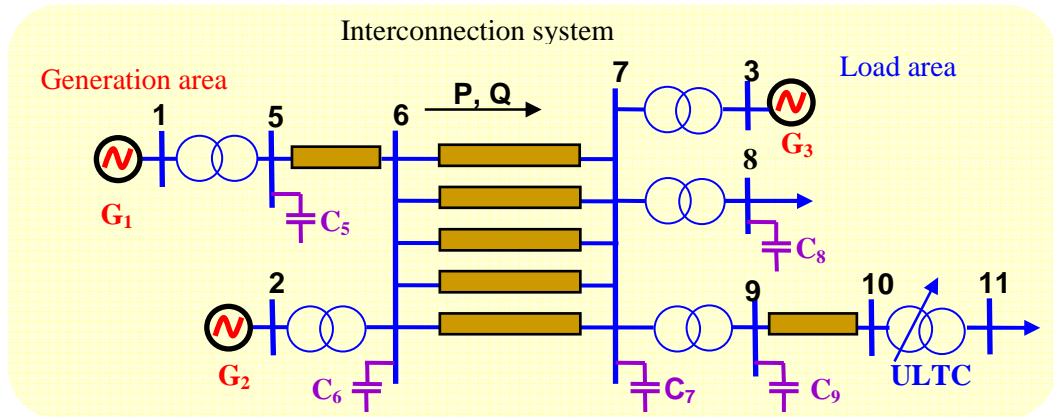


Figure 5-1: The “BPA power system”.

Table 5-1: Voltage and reactive power output of initial condition.

Bus	1	2	3	5	6	7	8	9	10	11
V(pu)	0.980	0.964	0.955	1.087	1.061	1.019	0.936	0.933	0.884	0.906
Q _G (MVar)	1208.8	725.0	700	0	0	0	0	0	0	0
Q _{Sh} (MVar)	0	0	0	118.2	112.6	999.8	612.7	348.1	0	82.2

Table 5-2: Cases study and typical scenario.

Case	Load		OEL			ULTC(T6)
	Bus 8	Bus 11	G1	G2	G3	
A	Const Z	Const Z	Infinite	No	No	No
B	Const I	Const Z	Infinite	No	No	No
C	Const P	Const Z	Infinite	No	No	No
D	Const P	Const Z	Infinite	No	No	Yes
E	Const P	Const Z	Infinite	Not	Yes	Yes
F	Const P	Const Z	Infinite	Yes	Yes	Yes
G	Motor load	Const Z	Infinite	Yes	Yes	Yes
Scenario	Trip off one transmission line between bus 6 and bus 7					

In this part, we consider the same scenario that is the tripping one 500 kV transmission line between bus 6 and 7 for some cases of voltage collapse investigation. This scenario presents the increase active and reactive power loss on the transmission system after tripping off one

transmission line. The power system responses with different involvements of automatic voltage regulation devices will investigate in detail in the next section of this chapter. The Table 5-2 lists all cases and the typical scenario.

5.2.1.2 Influence of Different Types of Load

A major factor in the initiation of a voltage collapse is the reaction of the system load to the decrease of the voltage magnitude in the load area. Therefore, the modeling of loads is essential in voltage stability analysis. The modeling of load is always complicated because there are large number of devices such as fluorescent, incandescent lamp, refrigerators, heated, compressors, motors, furnaces, ... etc. Therefore, load representation in voltage collapse studies is based on the typical load models that have been justified by some simplification. The modeling of voltage dependence loads requires proper considerations of voltage control devices such as ULTCs, thermostatically controller... In addition, the dynamic models for electrical motors should be used when the power system includes a significant amount of motor load. Load modeling is generally divided into two categories: Static modeling and dynamic modeling.

a. Static load modeling

Static load models are generally used that associated with the study of voltage stability in the short-term post-transient to long-term timeframe (for example: short-term transients and dynamics are ignored). The load drawn by a customer or load drawn in aggregate at a substation is dependent upon the bus voltage and frequency as follows [1], [2], [118], [119]:

$$\begin{aligned} P &= P_0 \left[p_1 V^2 + p_2 V + p_3 \right] \left[1 + k_p f \Delta f \right] \\ Q &= Q_0 \left[q_1 V^2 + q_2 V + q_3 \right] \left[1 + k_q f \Delta f \right] \end{aligned} \quad (5.2-1)$$

or

$$\begin{aligned} P &= P_0 \left[Z_p (V/V_0)^2 + I_p (V/V_0) + P_p \right] \\ Q &= Q_0 \left[Z_q (V/V_0)^2 + I_q (V/V_0) + Q_q \right] \end{aligned} \quad (5.2-2)$$

where:

P, Q: are the active and reactive power at the particular bus,

P₀, Q₀: are the active and reactive power at that bus at the initial system state,

p₁, p₂, p₃ and q₁, q₂, q₃: are fractional portions of active and reactive power representing constant impedance, constant current and constant power respectively with their sum equaling 1.0.

k_pfΔf, k_qfΔf terms represent frequency effects on the load.

The first terms in equations (5.2-1), represent the portion of load that changes directly with the square of the voltage magnitude and is commonly referred to as the constant impedance type load (const Z). Therefore, we can assign these term as Z_p and Z_q respectively. The second terms represent the portion of load that changes in direct proportion to the voltage magnitude and is referred to as the constant current type load (const I). These terms have notation as I_p

and I_q respectively. The last terms represent the portion of load that does not change with variations in voltage and is commonly known as constant power (const P) type load that assigned as P_p, Q_q .

Static models of load sometimes can be formed as [2]

$$P = P_0 \left[\frac{V}{V_0} \right]^{P_v} \left[\frac{f}{f_0} \right]^{P_f} \quad \text{and} \quad Q = Q_0 \left[\frac{V}{V_0} \right]^{Q_v} \left[\frac{f}{f_0} \right]^{Q_f} \quad (5.2-3)$$

Where: P_0, Q_0 are the active and reactive power at $V=1.0(\text{pu})$, P_v, Q_v are the voltage sensitivity exponent of active and reactive power respectively. When $P_v = 2, Q_v = 2$, the load becomes a constant impedance type.

Typical values for P_v and Q_v for different load components are presented in table below.

Table 5-3: Typical values for exponents of load model [2].

Load type	P_v	Q_v
Electrical heating	2.0	($Q=0$)
Television	2.0 5.2	5.2
Refrigerator/freezer	0.8-2.11	1.89-2.5
Fluorescent lighting	0.95-2.07	0.31-3.21
Frequency drives	1.47-2.12	1.34-1.98
Small industrial motors	0.1	0.6
Large industrial motors	0.05	0.5

b. Dynamic load modeling

The responds of most composite loads to voltage and frequency changes is fast, and the steady-state of the response is reached very quickly. Therefore, the use of static models described above is justified in such cases. However, there are many cases where it is necessary to account for the dynamic of load components. Studies of interarea oscillations, especially voltage stability and long-term stability often require load dynamics to be modeled. Typically, motors consume 60 to 70% of the total energy supplied by a power system. Therefore, the dynamic attributably to motors are usually the most significant aspect of dynamic characteristics of the system load. The dynamic model and equations describing some induction motors are given in references [1], [2], [118], [119], [120]. In PSS/E, CIM5 series are used to model dynamic induction motor.

Other types of load such as small motors, fluorescence and incandescent lighting, heating, air-conditioning ...etc are attributed also as dynamic loads. Modeling such complicated devices is always difficult tasks. However, when the detail models of dynamic loads are unavailable or inaccessible, the complex dynamic load model could be applied to dynamic load investigation. In PSS/E, the model CLOAD is used as non-motor dynamic complex loads as shown in the figure below.

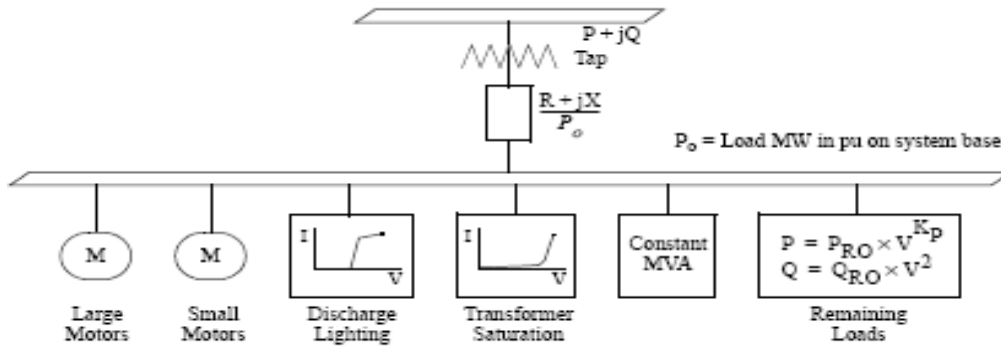


Figure 5-2: Dynamic complex load model (CLOAD type).

In this section, we investigate the sensitivity of voltage with respect to static load. The static load model is considered as constant impedance (const Z), constant current (const I) and constant power (constant P). The influence of dynamic load will be discussed in the next section. We will take into account the changing voltage profile of the system with respect to static load by investigating two cases A, B and C that are described in the Table 5-2

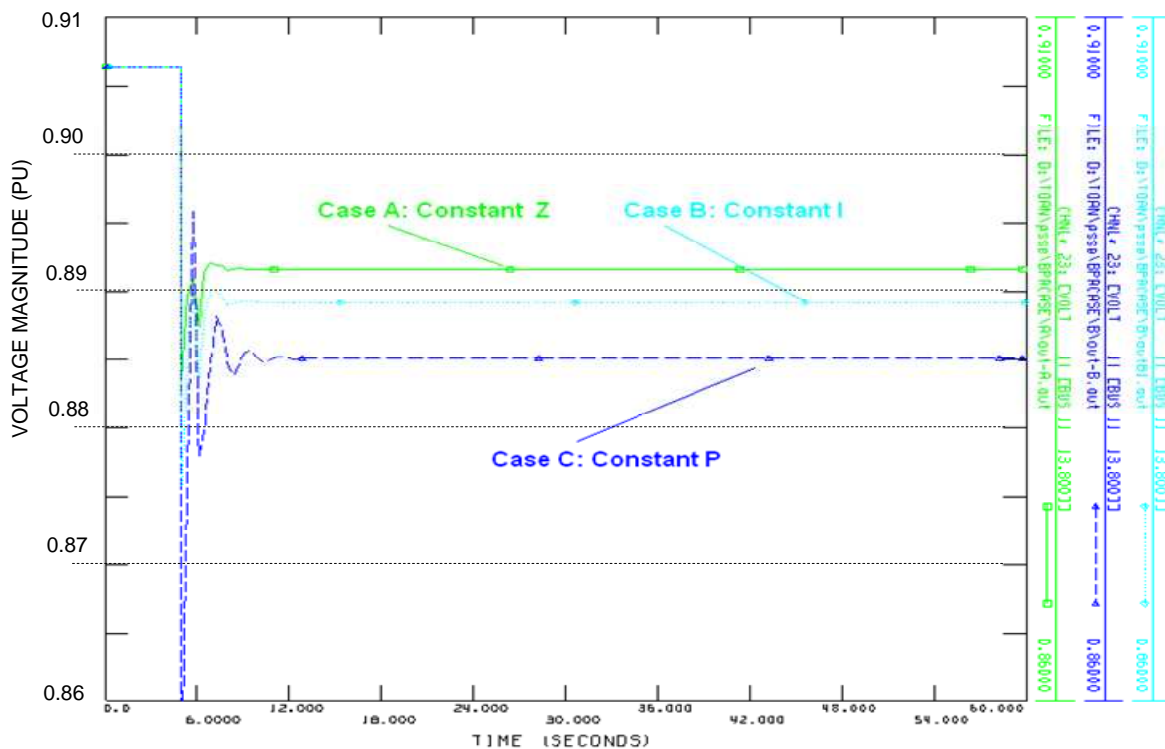


Figure 5-3: Voltage profile at bus 11 for cases A, B and C.

The voltage profile of bus 11 before and after contingency for cases A, B and C are plotted in Figure 5-3 where the duration of time simulation is 60 seconds. For all cases, the power systems are completely stabilized after transient period at lower value because reactive power loss increased when a line between buses 6 and 7 is tripped off. The cases B and C are more dangerous than case A in term of voltage stability because of the voltage dependence that is exponential. The case C corresponding to constant power has the lowest voltage magnitude because the load with constant power does not depend on the voltage. Therefore, when

voltage decays, constant power load tries to recover the load to the initial value as before contingency that causes voltage decrease further. Voltage magnitude at bus 11 before contingency is 0.9065(pu). The final values after contingencies for three cases A, B, and C are 0.8916(pu), 0.8891(pu) and 0.885(pu) respectively.

5.2.1.3 Influence of Under Load Tap Changer (ULTC) on Voltage Collapse

The automatic voltage control of power transformers is equipped with ULTC. The action of ULTC affects the voltage dependence loads seen from the transmission network [2], [118]. Typically, a transformer equipped with an ULTC feeds the distribution network. The main function of ULTC in distribution system in normal operation conditions is to adjust the voltage of controlled bus toward its original value when load changing. When voltage in the distribution system decreases, the load also decreases. The tap changer operates after time delay if voltage error is large enough restoring the load. The stepping down of the tap changer increases the voltage in a distribution network, thus reactive power transfer increases from the transmission network to the distribution network

However, the action of an ULTC might be dangerous for a power system under disturbance. Especially, in highly loaded conditions or some reactive resources reached their limit, when voltages at some buses are quite low, changing tap position of ULTCs actually is to get more reactive power from power system to support for their load. Therefore, ULTCs may have a reverse effect in term of voltage stability. In this section, the influence of ULTC to voltage collapse is taken into account by dynamic simulation.

The typical ULTC model [2], [118] with three major elements is presented in Figure 5-4

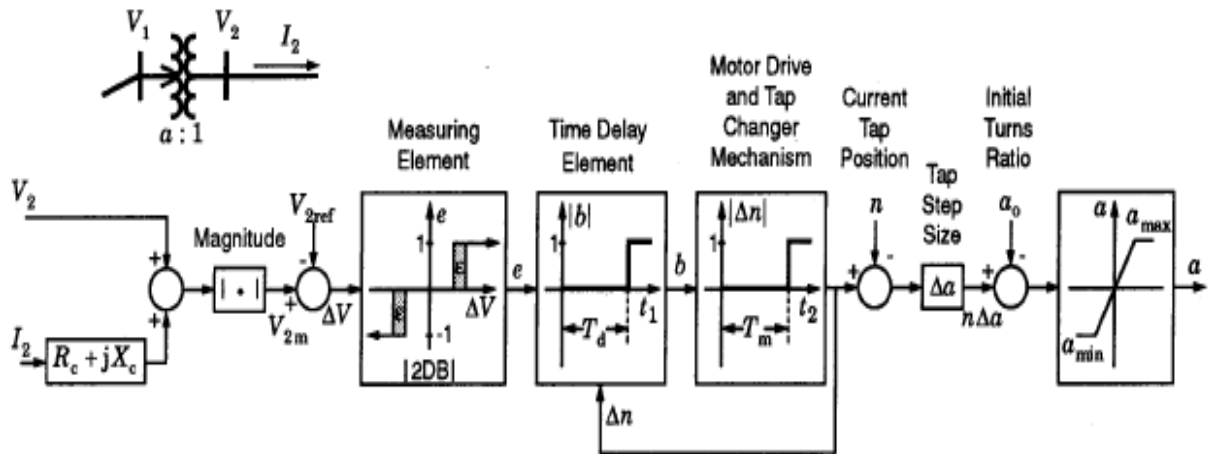


Figure 5-4: Model for load tap changer transformer regulating secondary voltage.

where:

$$\text{Measuring element:} = \begin{cases} 0 & \text{for } -DB \leq \Delta V \leq +DB \\ 0 & \text{for } DB < \Delta V \leq +DB+\epsilon, \text{ previous } e \leq 0 \\ 0 & \text{for } -DB-\epsilon \leq \Delta V < -DB, \text{ previous } e \geq 0 \\ +1 & \text{for } \Delta V > DB+\epsilon \\ +1 & \text{for } DB < \Delta V \leq +DB+\epsilon, \text{ previous } e=1 \\ -1 & \text{for } \Delta V < -DB-\epsilon \\ 11 & \text{for } -DB-\epsilon \leq \Delta V \leq -DB, \text{ previous } e=-1 \end{cases}$$

$$t_1 = 0 \text{ for } e=0 \text{ or } \Delta n \neq 0$$

$$t_1 = t_1 + \Delta t \text{ otherwise}$$

$$\text{Time delay element: } T_d = T_{d0} \text{ for the first step}$$

$$T_d = T_{d1} \text{ for subsequent taps}$$

$$b = \begin{cases} 0 & \text{for } t_1 \leq T_d, e = \text{arbitrary} \\ 1 & \text{for } t_1 > T_d, e = 1 \\ -1 & \text{for } t_1 > T_d, e = -1 \end{cases}$$

$$t_2 = 0 \text{ for } b=0$$

$$\text{Motor drive Unit and Tap Changer Mechanism: } t_2 = t_2 + \Delta t \text{ for } b \neq 0$$

$$\Delta n = \begin{cases} 0 & \text{for } t_2 \leq T_m, b = \text{arbitrary} \\ 1 & \text{for } t_2 > T_m, b = 1 \\ -1 & \text{for } t_2 > T_m, b = -1 \end{cases}$$

A ULTC transformer modeled by the OLTC1 model in PSS/E has two components. The first component is the voltage sensor, which compares the input voltage to the pre-selected setting (voltage level) and a tolerance, or spread, in voltage level (bandwidth). If the voltage input to the sensor is out of the control band, the control will operate after the time delay has been exceeded. The second major component of ULTC is the time-delay circuit. The time delay enables the transformer to correct only those voltage variations, which exist for longer than a pre-set time.

In order to investigation of influence of ULTC on voltage collapse, We consider two cases C and D corresponding without and with the presence of ULTC that are listed in the Table 3-1. A comparison of voltage at bus 11 between case C and case D with time of simulation is about 200(s) is shown in Figure 5-5. In case C, because there is no ULTC and OEL so the voltage at bus 11 could not be able to recover its original value as before contingency. The voltage magnitude is stabilized at a value of 0.885(pu). In case D, by adjusting tap ratio of high voltage side of the transformer to keep voltage at the low voltage side as constant as before the contingency. Therefore the final voltage at bus 11 in case D is greater than in case C.

The sequences of ULTC actions are plotted in Figure 5-6. The power system responds by adjusting tap position of high voltage side -bus 10- to keep voltage at low voltage bus side as constant - bus 11 - however, the lower desired voltage limit has reached therefore, voltage at bus 11 get only a value of 0.90(pu) smaller than pre-faulted value 0.9065(pu).

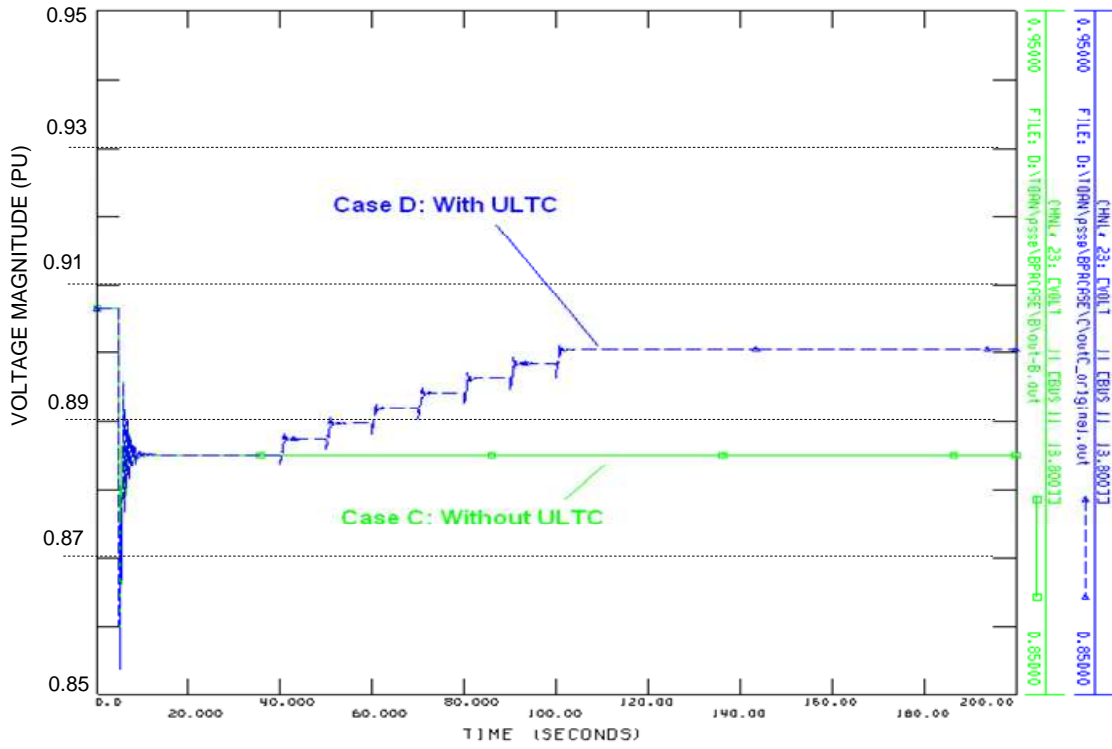


Figure 5-5: Voltage profile of bus 11 for both case C and D.

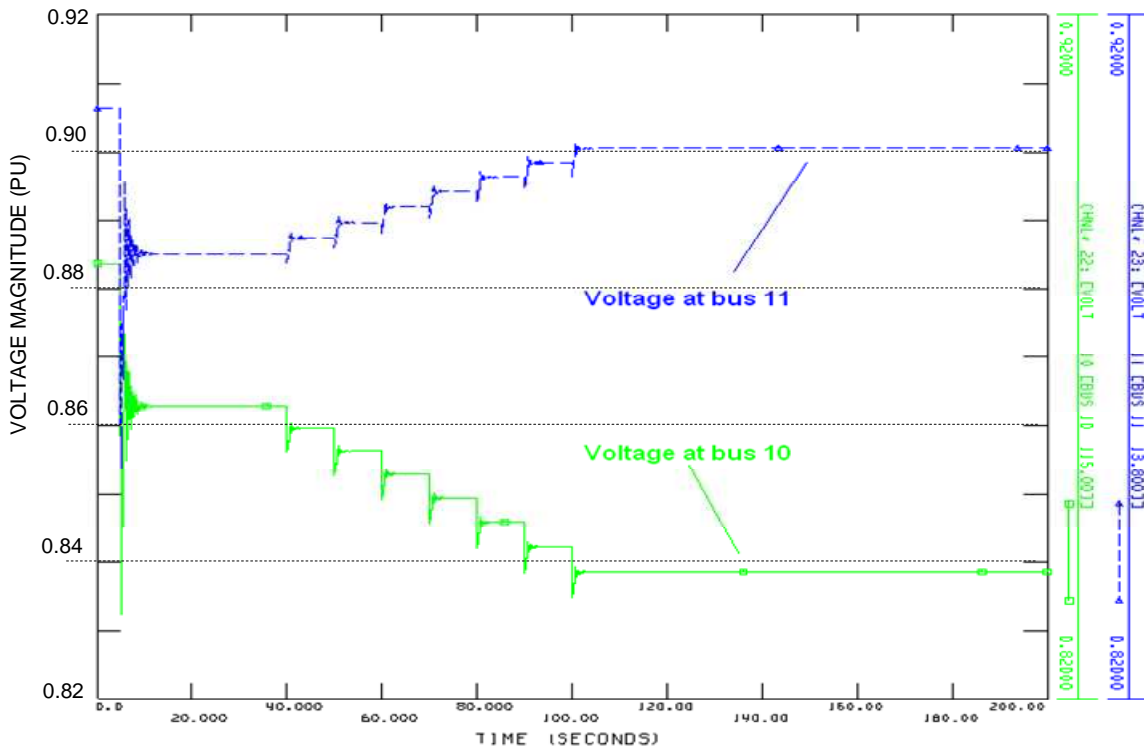


Figure 5-6: Voltage profile at bus 10 and bus 11 in case D.

Sequences of the simulation are observed as below:

- At t=5(s): the transmission is tripped off. The power system is stabilized after transient period.
- At t=35(s): ULTC is activated. First changing of tap position is completed at t=40(s). The time between two changing taps is 10 seconds.
- At t=100(s), ULTC reaches the lowest value of control range. Timer is set to zero.
- Voltage at bus 11 is stable at the value of 0.9(pu) at t=200(s)

5.2.1.4 Influence of OEL and ULTC on Voltage Collapse

Overexcitation limiters (OELs) play an important role in voltage collapse studying [1], [2], [68], [121]. The main function of an OEL is to protect synchronous machine field windings from overheating. It usually is disabled in the transient period to allow the excitation system to force several times the rated voltage across the rotor winding and more than rated continuous current, to help retain transient stability. After a few seconds, the limiter is activated with an inverse time function - the higher the rotor current, the sooner the limiter is activated. The limiter brings the continuous rotor current down to, or just below, rated level to ensure the rotor is not overheated by excessive current.

Although, the importance of OEL is clear however, standard models for OEL have not been developed yet [1]. Researchers have tried to develop their own models for a particular purpose of study and particular plant. In this part, we use a model of OEL namely MAXEX2 in the PSS/E dynamic model library. The block and time inversed characteristic are given in Figure 5-7. The model has three setting values corresponding to three inverse time functions as follows:

$$I_{FD1}(E_{FD1})/(\text{rated value}) = 1.5, \text{ with } t_{FD1} = 10(\text{s}).$$

$$I_{FD2}(E_{FD2})/(\text{rated value}) = 1.2, \text{ with } t_{FD1} = 60(\text{s}).$$

$$I_{FD1}(E_{FD1})/(\text{rated value}) = 1.05, \text{ with } t_{FD1} = 120(\text{s}).$$

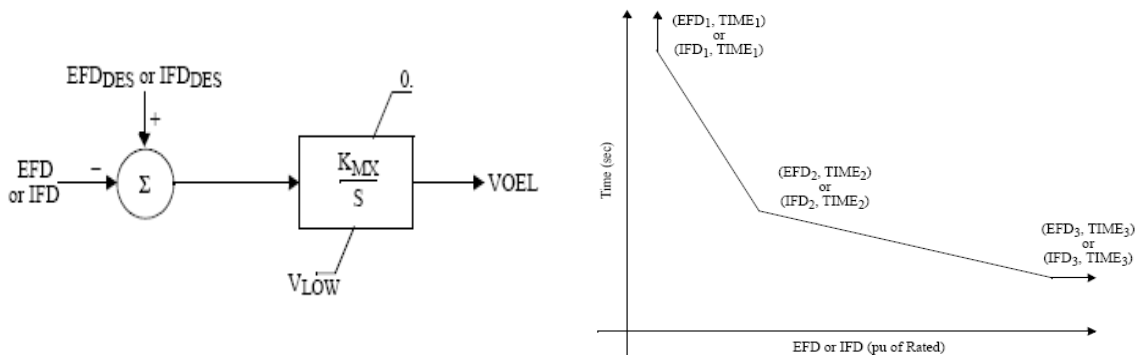


Figure 5-7: Block diagram and Inverse time characteristic of MAXEX2.

The influence of OEL and ULTC with respect to voltage collapse is investigated in case E with the presence of an OEL at G3. The scenario is described in case E in Table 3-1.

The evolution of reactive power output of generators G2, and G3 and voltage profile of bus 11 for both cases D and E are plotted in Figure 5-8 (a, b, c, d). This result is an influential combination of both ULTC and OEL.

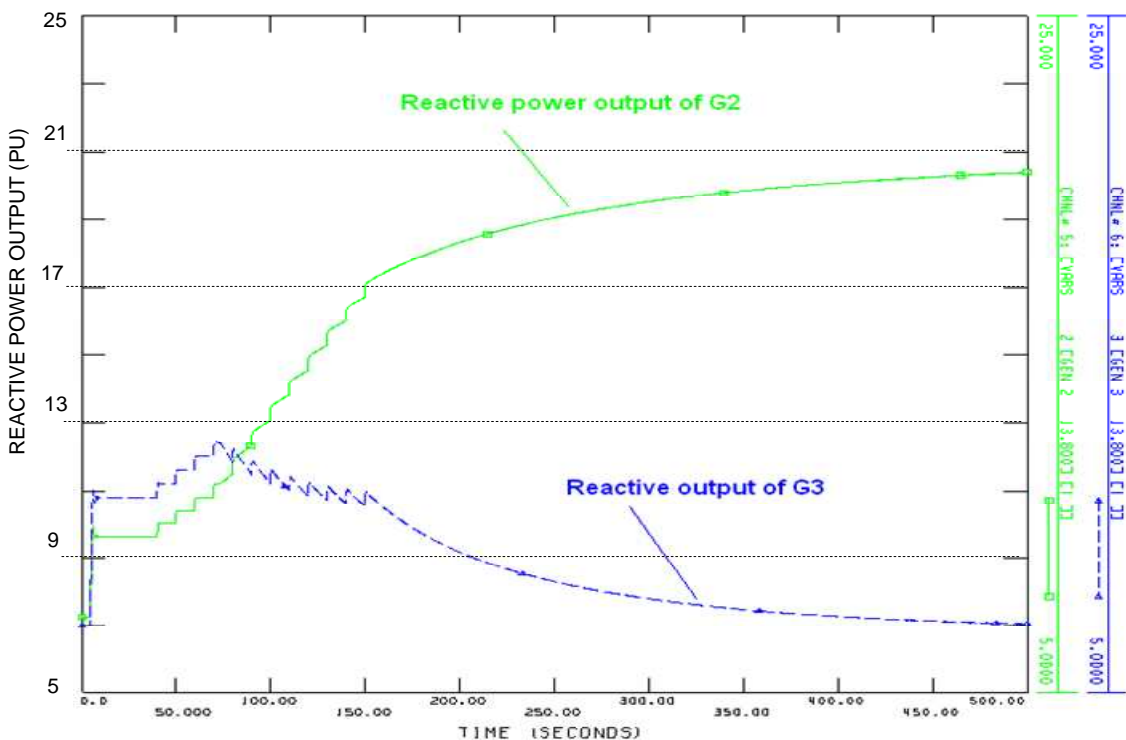
At $t=5(s)$, a line is tripped off. In the transient period, the effect of excitation system is to stabilize the power system by increasing excitation current sharply and the power system is stabilized after some seconds. As the transmission line loss increases, the active and reactive power loss is increased also and voltages of the system are reduced.

At $t=35(s)$, the voltage at bus 11 is lower than preset value and time is exceeded preset value of ULTC, then ULTC is activated. ULTC adjusts its tap ratio to maintain voltage at secondary bus as its original value that demands more reactive power support from generators. The excitation current is continuously increased to meet this demand of reactive power. This chain of such events is continuous until either the voltages at buses are recovered or the maximum tap of transformer reached.

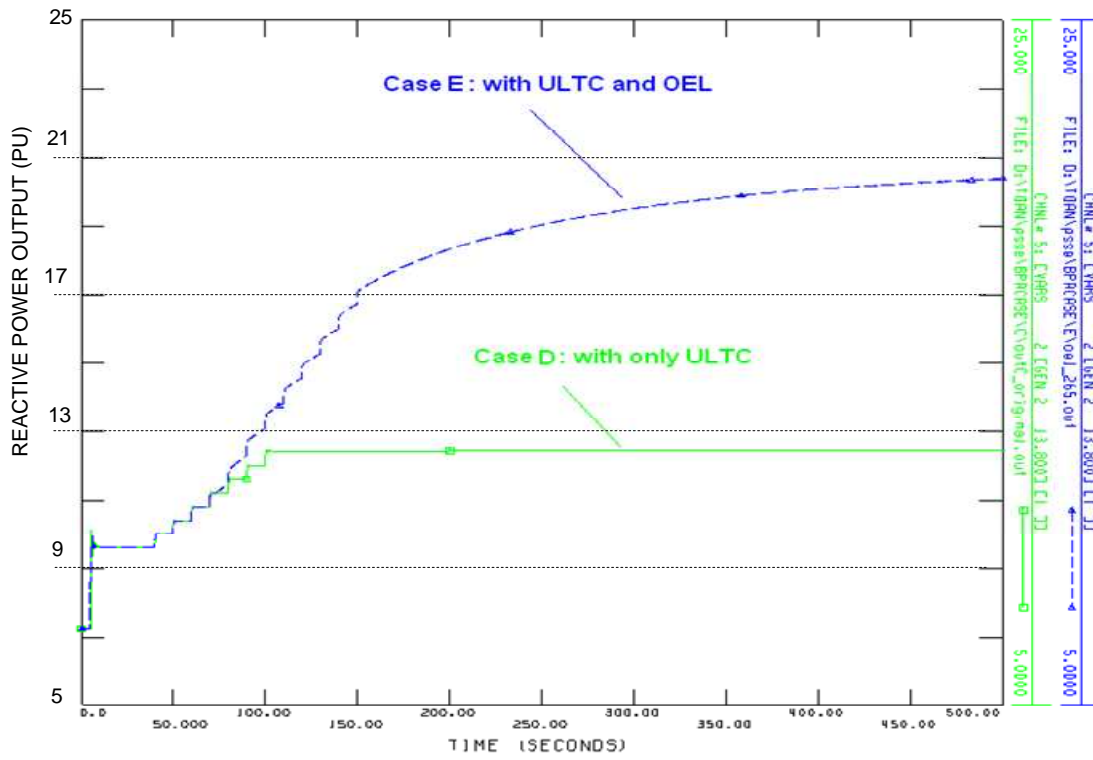
At $t=65(s)$, the excitation current and time is exceeded the preset value ($I_{FD2}=1.2$ and $t_{FD2}=60(s)$), OEL is activated to bring its value to the rated one. While reducing excitation current, the reactive power output of generator G3 is reduced; as a result, the voltages of the system are also reduced. The slope of the curve depends on the ratio of the excitation current and the rated value, if the value of the ratio is bigger, larger the slope is.

At $t=150(s)$, ULTC reaches its maximum tap position. Then timer is set to zero, while OEL still reduces its field current.

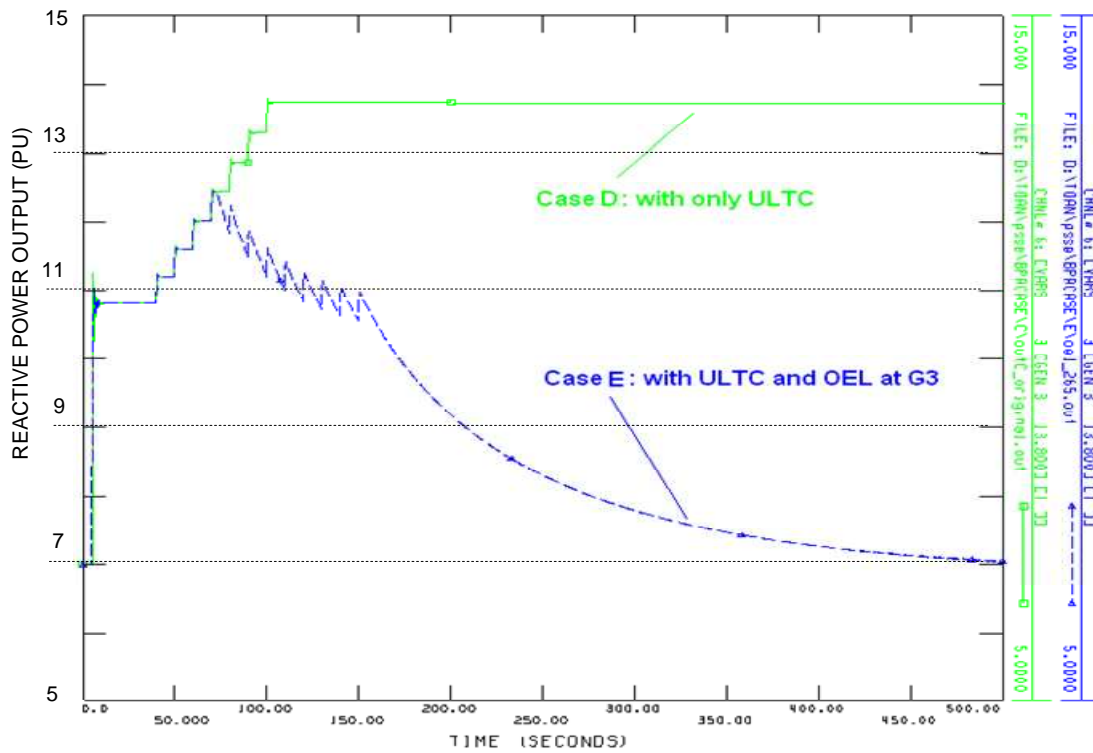
At $t=500(s)$, the field current is reduced to its rated value, reactive power output of G3 is kept at its limit (700 MVar). Voltage magnitude of bus 11 is about 0.8(pu) because there is no OEL at G2 and G1 is considered as an infinite bus.



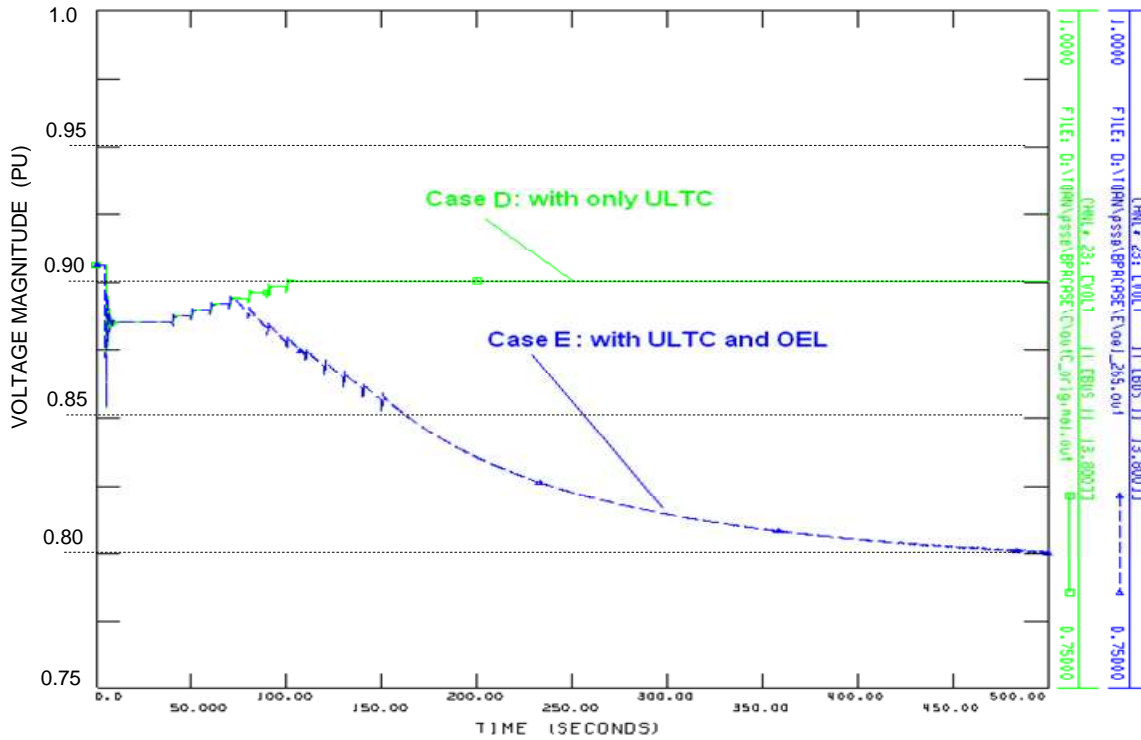
a, Reactive power output of G2 and G3 in case E.



b, Reactive power output of G2 in cases D and E.



c, Reactive power output of G3 in cases D and E.



d, Voltage magnitude of bus 11 in cases D and E.

Figure 5-8: Influence of ULTC and OEL with respect to voltage collapse

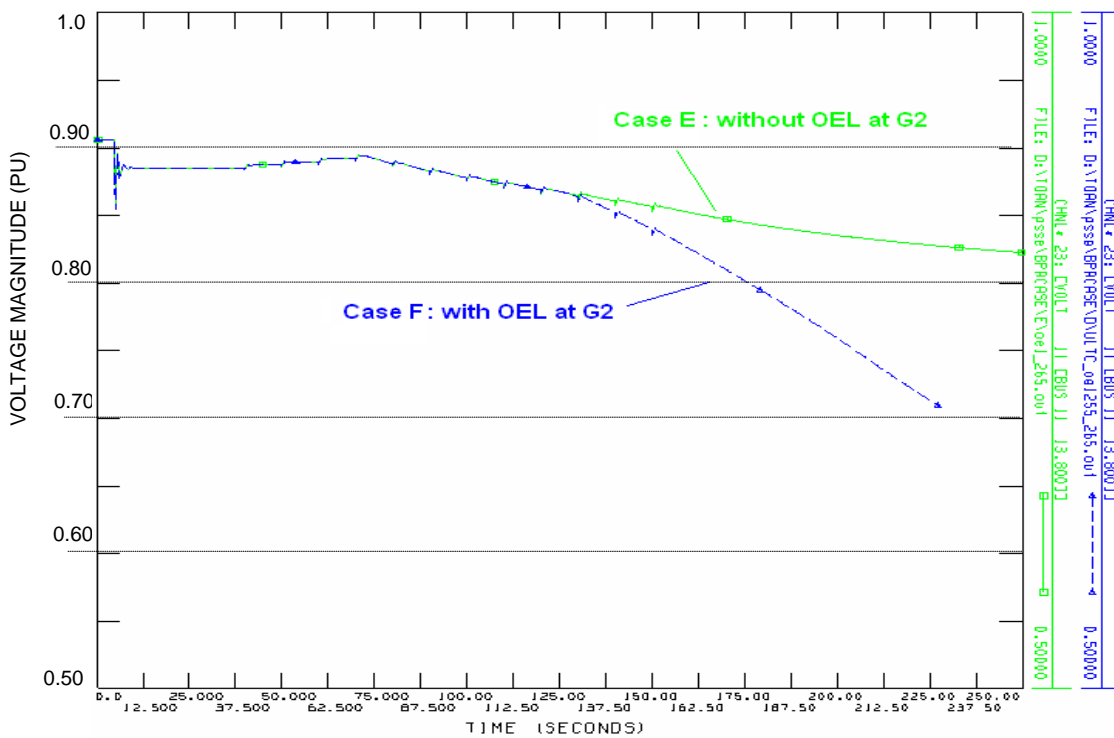


Figure 5-9: Voltage profiles of buses 11 for both cases E and F.

In case F, we consider influence of both OELs at G2 and G3. The power system responses are the same as previous case (case E), but voltages are collapse after some minutes because

both reactive power output of both G2 and G3 are limited (OEL at G2 is activated at $t=125$ seconds). Power system responds are plotted in Figure 5-9.

5.2.1.5 Influence of Dynamic Load

In this case, the influence of dynamic load modeling is investigated with the assumption that the load at bus 8 is modeled by using a motor model. Figure 5-10 (a, b) show the influence of motor load with respect to voltage collapse. Power system responds are summarized as follows:

At $t=5$ (s), a line is tripped off. In the transient period time, the effect of excitation system is to stabilize the power system by increasing excitation current sharply and the power system is stabilized after some seconds. The loss of a transmission line increase both active power and reactive power in the system. As G3 is reaching its limit, it is no longer possible to control its reactive power output.

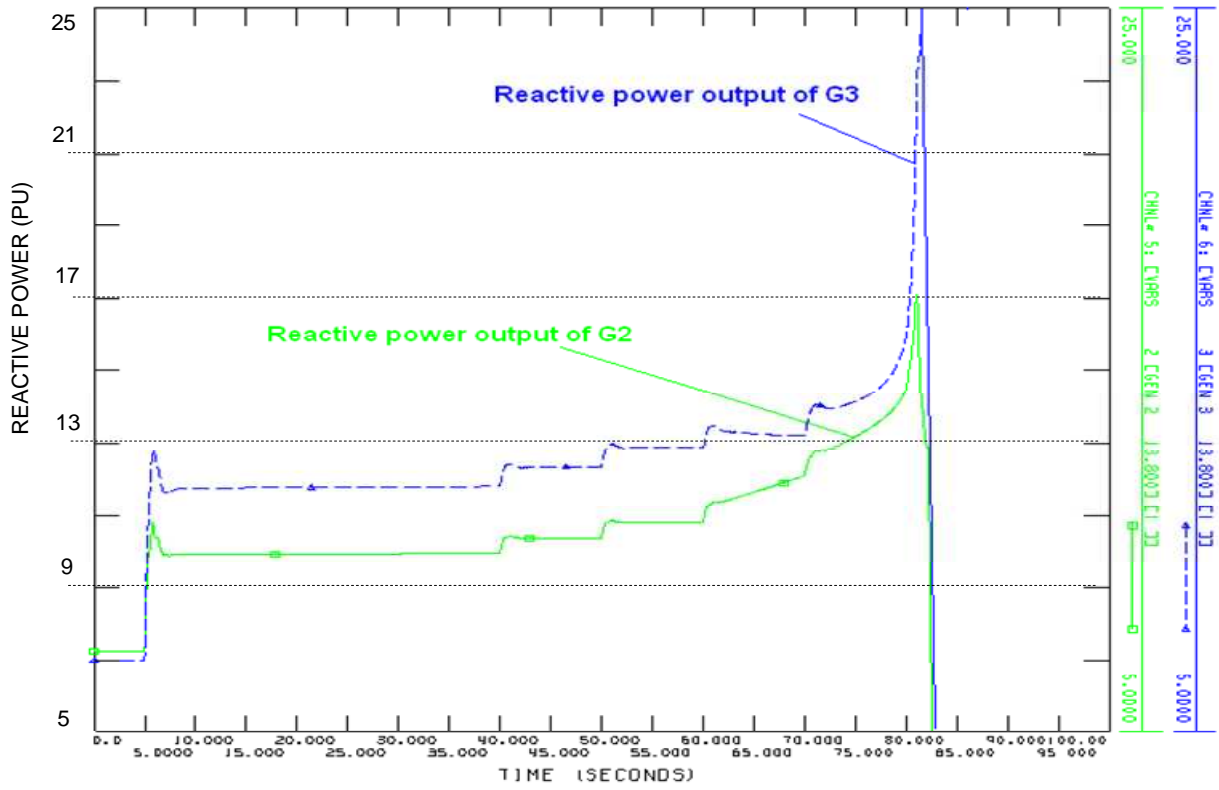
At $t=35$ (s), the voltage is lower than preset value and time is exceeding preset value of ULTC, then ULTC is activated. ULTC adjusts its tap ratio to maintain voltage at secondary bus as its original value that demands more reactive power support from generators. The excitation current is continuously increased to meet this demand of reactive power.

At $t=65$ (s), the excitation current and time is exceeded the preset value ($I_{FD2}=1.2$ and $t_{FD2}=60$ (s)), OEL at G3 is activated to bring its value to the rated one. While reducing excitation current, reactive power output of generator G3 is reduced; as a result, voltages of the system are also reduced.

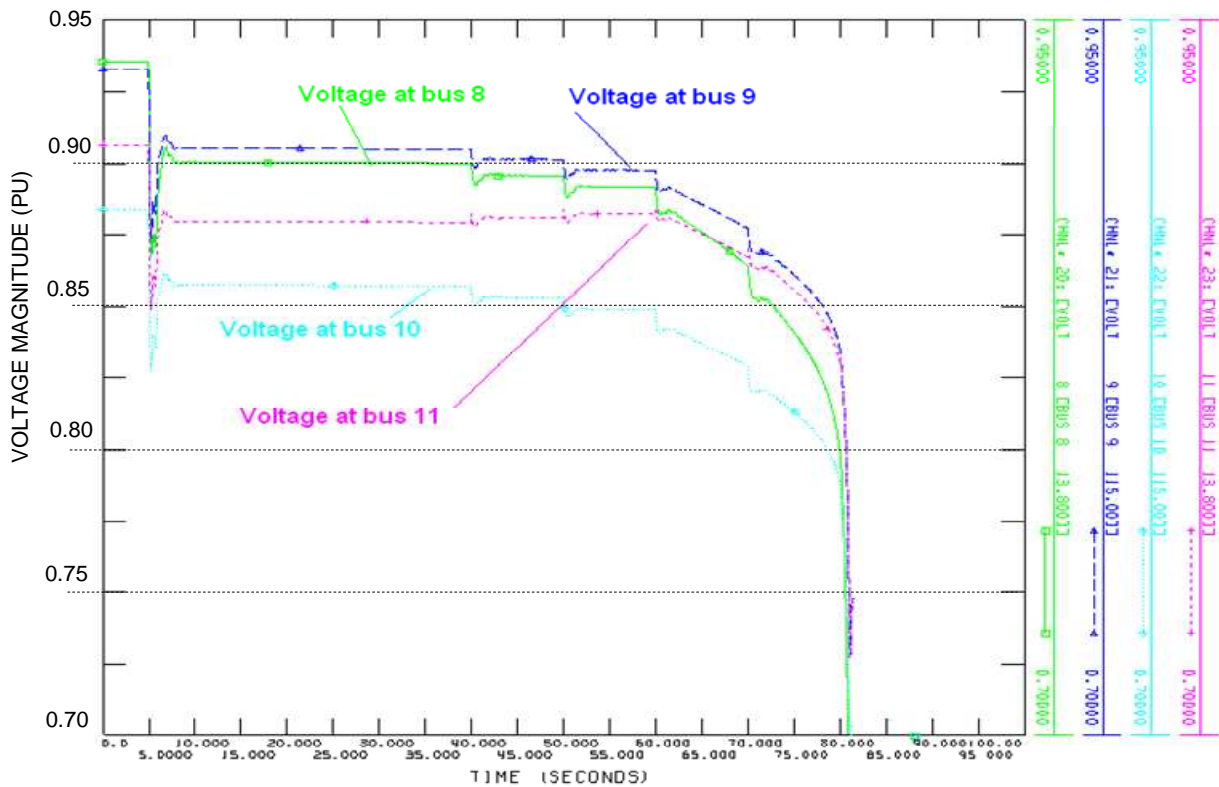
Voltage at bus 8 is reduced progressively that causes the motor torque is reduced proportionally to square of voltage magnitude. Then, the motor is stalled at about $t=80$ (s). This results in the voltage recovering. Then, the motor is self started. Consequently, the reactive power absorbed by motor is increased sharply. This causes the voltage of the power system collapse.

Figure 5-10 (a) plots the reactive power output of G2 and G3. When the motor is stalled at $t=80$ (s), the reactive power output of these generators are increased sharply in order to meet the highly demand reactive power absorbed by the motor.

Figure 5-10 (b) plots the voltage profile of buses 8, 9, 10 and 11 during the contingency. At $t=80$ (s), the voltages are totally collapsed.



(a) Reactive power out of G2 and G3 in case G.



(b) Voltage at bus 8,9,10, and 11 in case G.

Figure 5-10: Case G-Influence of Motor load with respect to voltage collapse.

5.2.2 Dynamic Simulation of Voltage Collapse for “Nordic Power System”

5.2.2.1 Descriptions of “Nordic Power System”

In this part, a dynamic voltage collapse simulation is implemented for a larger system: the “Nordic power system” taken from [122] as shown in Figure 5-11.

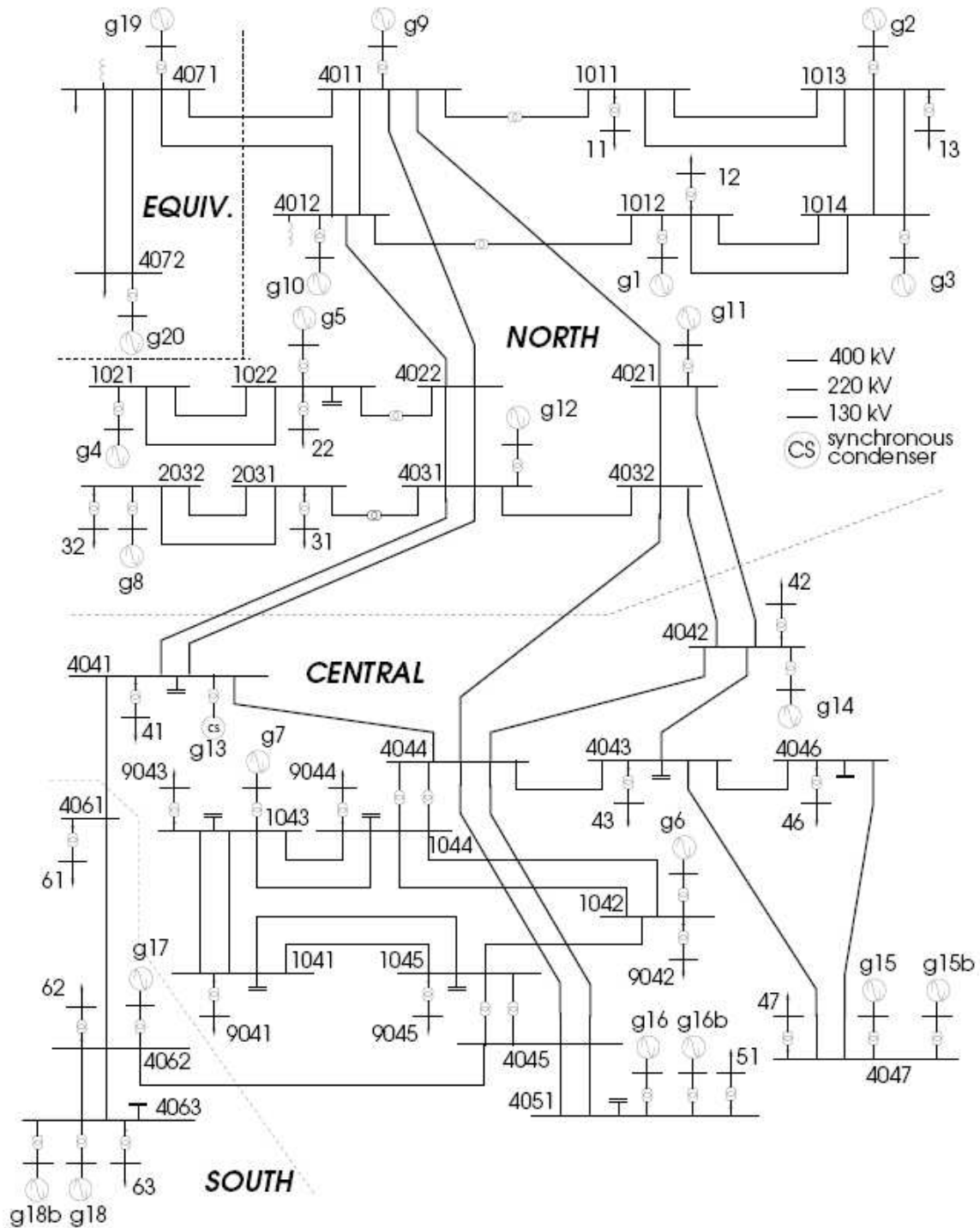


Figure 5-11: The “Nordic power system”.

The system includes some areas: Equivalent External area (buses 4071, 4072), North area, Central or Load area and South area (buses: 4061, 4062, and 4063). The system is long with large transfers from a hydro dominated part (North area) to a load area with a large amount of thermal power plants (centre area). The power transfer is limited by transient and voltage instability in case of certain contingencies. The system is suitable for several types of simulation such as transient stability, interarea oscillation and long-term voltage stability. Many voltage collapse scenarios have been investigated in the literature [122] and [123] but in this part, we only consider several dynamic simulations of voltage collapse.

Some system parameters are modified in order to investigate voltage collapse phenomenon. The system includes details and standardized dynamic models such as generators, governors, exciters, OEL, ULTC, step-up transformers are modeled internally. In this simulation, these devices are modeled by standard models in the library of PSS/E. The dynamic behaviors of the system include influence of all automatic devices during time frame of simulation. The generators in the hydro dominated region (North) are modeled by GENSAL model, with hydraulic governor model as: HYGOUV. The generators in the thermal dominated region (South) are modeled by GENGOU model. All the generators have a simplified excitation system model: SEXS, maximum excitation limiter model: MAXEX2 and power system stabilizer model STAB2. All transformers in southern region have ULTCs. The loads are modeled as follows: 100% constant current for active power and 100% constant impedance for reactive power.

At the initial operating condition, there are two generators that reach their reactive power limit as shown in Table 5-4, and all voltage magnitudes are in the normal range from 0.95 (pu) to 1.1 (pu).

Table 5-4: Generators with reactive power output limit.

Bus	Q_{actual} (MVar)	Q_{limit} (MVar)	V_{scheduled} (pu)	V_{actual} (pu)
1043	100.0	100.0	1.0000	0.9896
4021	-30.0	-30.0	1.0000	1.0083

In this part, four scenarios were proposed to investigate long-term dynamic of voltage collapse. The actions of the system to each scenario proposed are final results of power system topology, loading pattern and dynamic behaviors of different automatic voltage regulators such as OEL, and ULTC with different time setting.

5.2.2.2 Scenario 1

Scenario 1 is proposed as follows: a transmission line in the “North area”, between buses 4011-4021 is tripped at t=5(s) and generator at bus 4012 is tripped off 0.1(s) latter. As results, loss of 600 MW active power and 4.4 MVar reactive power.

For this scenario, two cases of simulation were performed which correspond to situations without and with the presence of ULCTs and OELs.

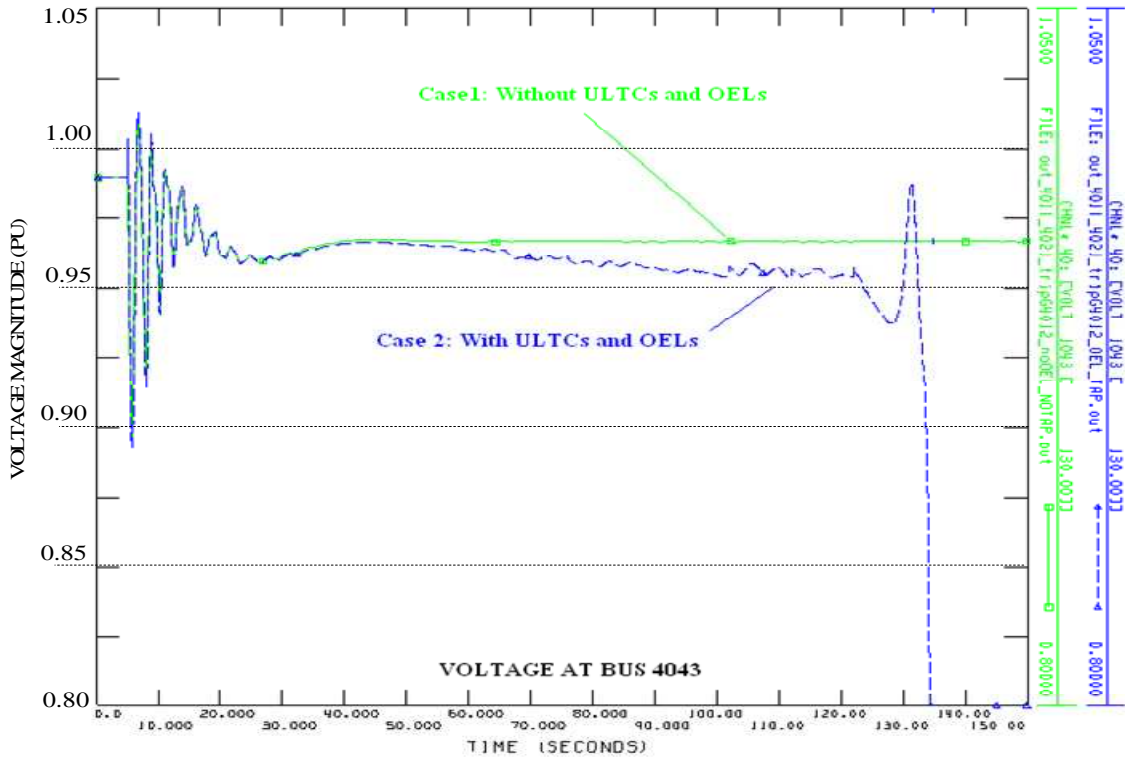


Figure 5-12: Scenario 1-Voltage profile of bus 4043 with respect to different cases.

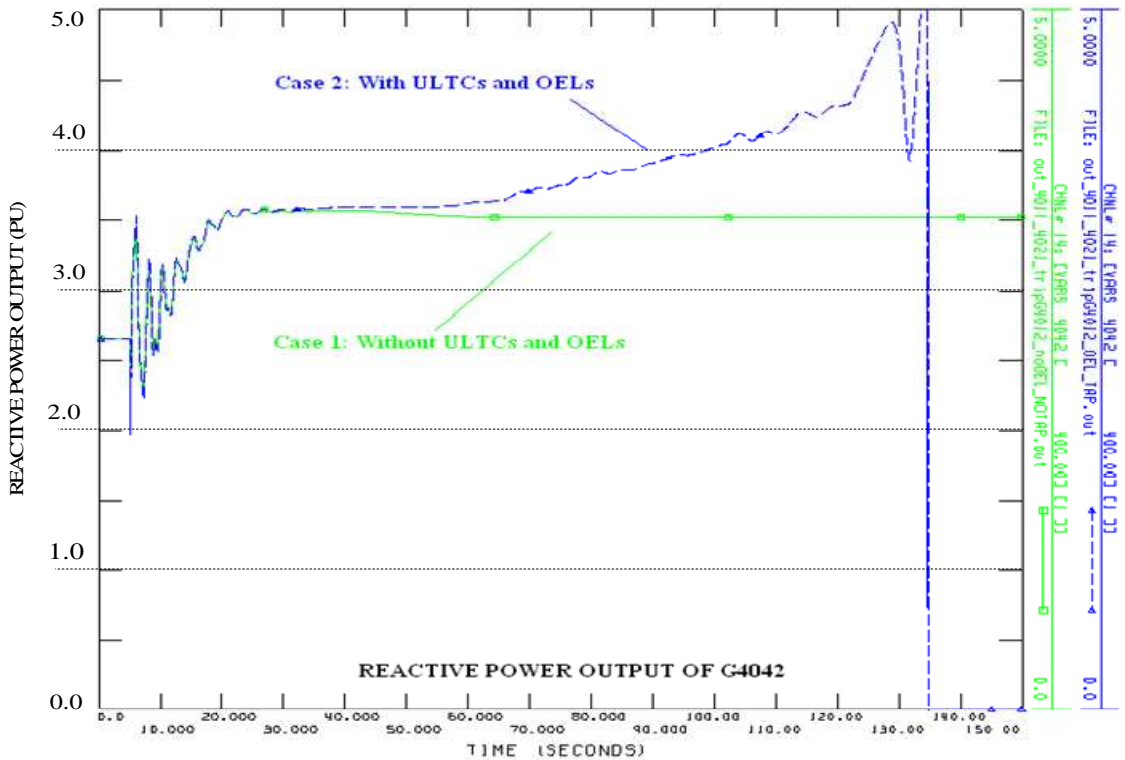


Figure 5-13: Scenario 1-Reactive power of generator at bus 4042 with respect to different cases.

The variation in voltage profile of bus 4043 and reactive power output of generator 4042 are shown in Figure 5-12 and Figure 5-13 with respect to different cases. ULTC and OEL models are not presented in case 1 (the green line), after the transient period, the voltage is

stable at about 0.965 (pu). In case 2 (the blue line), only ULTC models are presented, the voltage at bus 4003 is collapse at t=135(s) after experiencing two contingencies. The response of the power system is final results of actions of both ULTCs and OELs. The system voltages were totally collapsed after having the activation of OELs (normally after 120 seconds).

5.2.2.3 Scenario 2

Scenario 2 is proposed as follows: Trip off a generator at bus 4047 in “Central area” at t=5(s) that causes loss of a generator with 540 MW active power and 152 MVAR reactive power.

For this scenario, two cases of simulation were done corresponding to without and with the presence of ULTCs and OELs. The variation in voltage of bus 41 and reactive power output of G4042 are shown in Figure 5-14 and Figure 5-15 with respect to different cases. In case 1 (the green line), the ULTC and OEL models are not presented, the voltage is stable at about 0.93 (pu) after transient period. In case 2 (the blue line), both the ULTC and OEL models are presented. As the generator G4042 is lost, the voltages of the system are reduced. Activations of ULTCs try to recover the voltage by changing tap positions, as the result the voltages of the system are increased (as in Figure 5-14). At t=125 seconds, the activation of OELs to reduce the field current to the rated value, that reduces reactive power output (as in Figure 5-15). Combination of actions of both ULTCs and OELs lead the system going to oscillate at t=240(s) and is collapsed at about t =270(s).

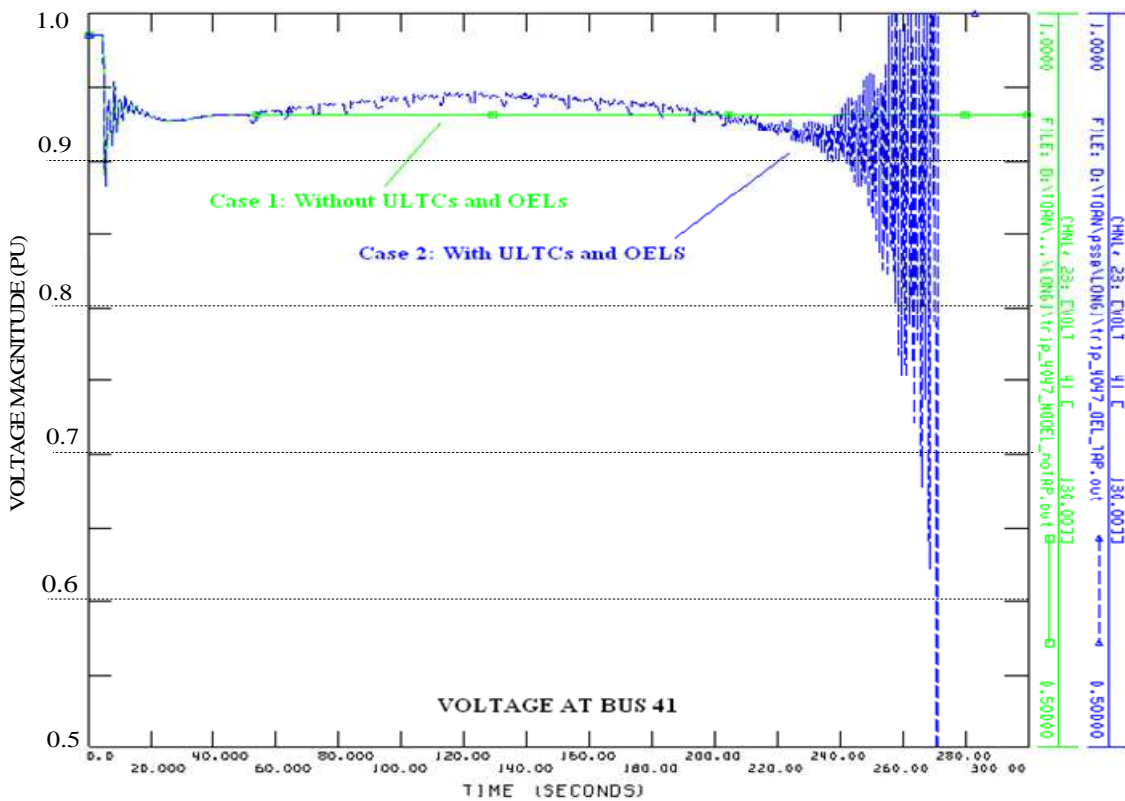


Figure 5-14: Scenario 2-Voltage profile of bus 41 with respect to different cases.

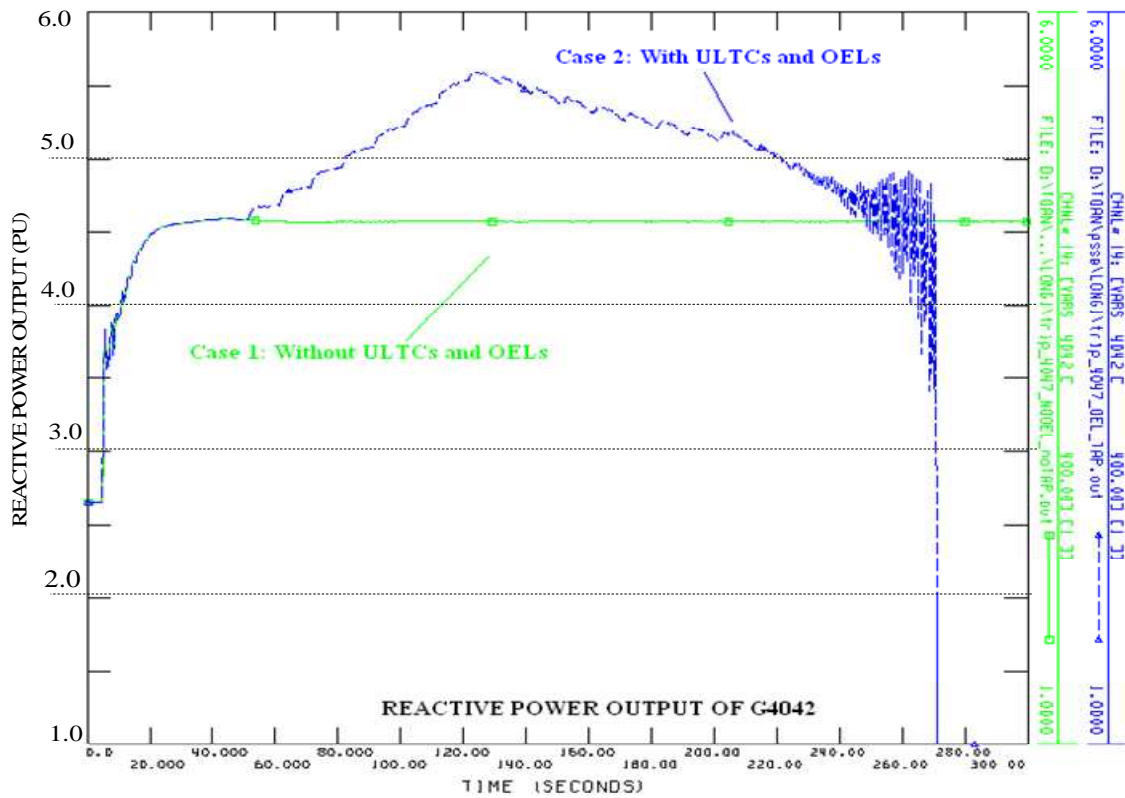


Figure 5-15: Scenario 2-Reactive power output of G4042 with respect to different cases.

5.2.2.4 Scenario 3

Scenario 3 is proposed as follows: a generator at bus 4042 in the “Central area” is tripped at $t=5(s)$ as loss of 630 MW active power and 265 MVar reactive power.

The variation in voltage at bus 46 is shown in Figure 5-16 with respect to different cases. In case 1 (the green line), the ULTC and OEL models are not presented, the voltage is stable at about 0.91(pu) after transient period. In case 2, when both the ULTC and OEL models are presented, the system response is similar as in scenario 2, and voltage is collapsed at $t=205(s)$.

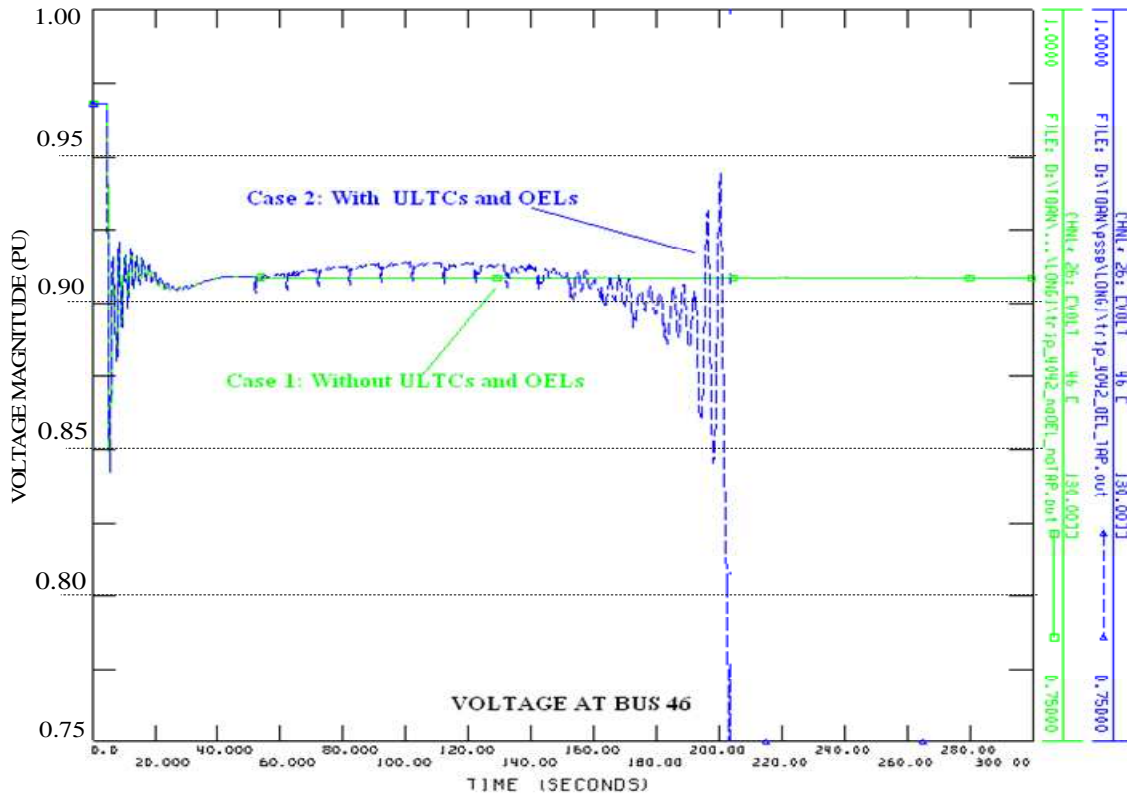


Figure 5-16: Scenario 3-Voltage profile of bus 46 with respect to different cases.

5.2.2.5 Scenario 4

Scenario 2 is proposed as follows: a generator at bus 1043 in the “Central area” is tripped at $t=5(s)$ as reducing 180 MW and 100 MVAR to create a low voltage operating condition. Power system is stabilized at $t=500(s)$, voltages at some buses are still bigger than 0.95(pu). From this time, the load is increased with a speed of 1% per minute.

The variation in voltage of buses 41, 42, 43, 46 and the reactive power output of generators in centre area are shown in Figure 5-17 and Figure 5-18. When the loads are increased, both active and reactive powers are required from generators to support for the changing. As a consequence, the voltages at some buses are below the desired values. ULTCs decide to change the tap position to keep voltages at controlled buses at the desired values. Simultaneously, the excitation systems also increase the reactive power output to meet the reactive power increment. At about 650(s), OELs active in order to protect the rotor windings, reactive power output of generators are reduced as OELs reduce their field currents. While voltages decay gradually, UTLCs changes their tap position to get more reactive power from generator to support for loads. At about $t=950(s)$, the power system is oscillating and voltage collapsed.

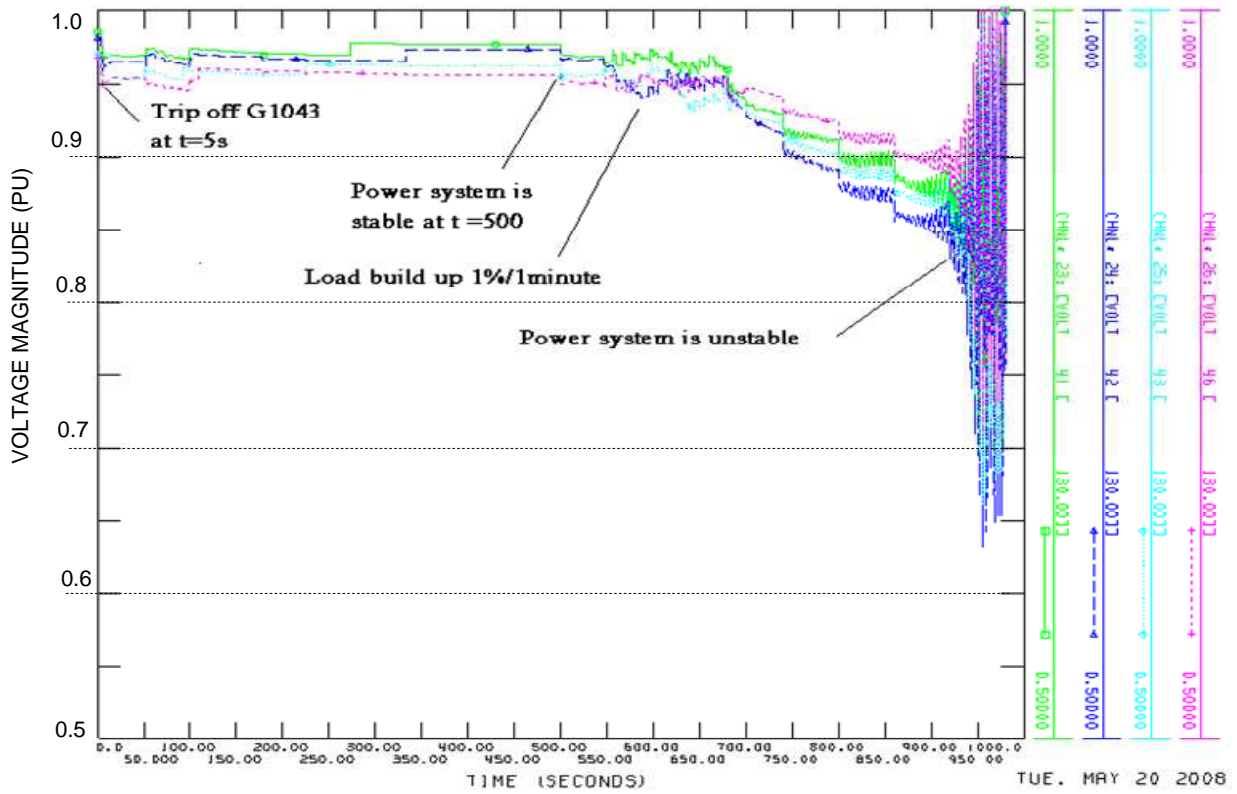


Figure 5-17: Scenario 4-Voltage profile of buses 41, 42, 43, and 46.

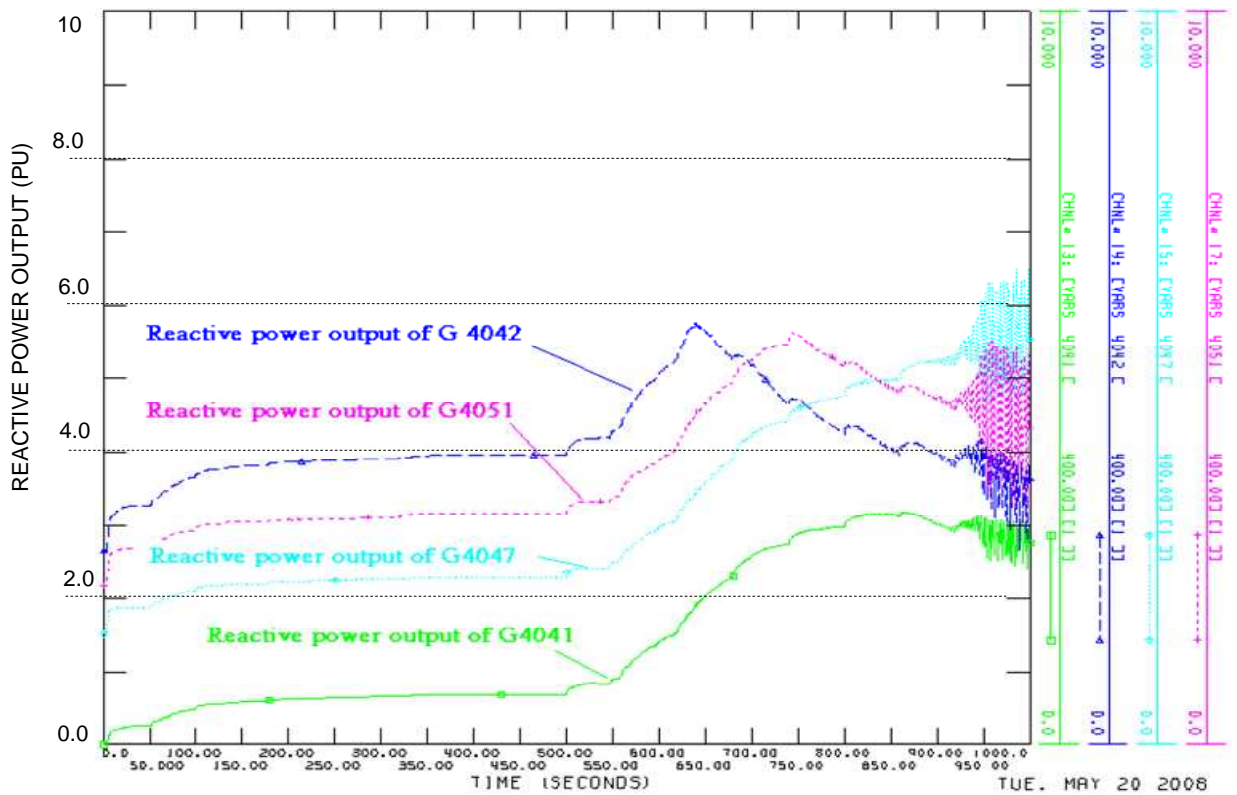


Figure 5-18: Scenario 4-Reactive power output of G4041, G4042, G4047, and G4051.

From the results of analyzing factors that influenced on voltage collapse for the BPA and Nordic power systems, we could observe, in agreements with the analyses of P. Kundur [1], C. W. Taylor [2], C. A. Aumuller and T. K. Saha [123] and the reference [117], [122] who have made similar studies, that the voltage collapse is due to a complex interaction of the following factors:

- The apparent impedance and consequently the voltage drop and losses across the lines of the transmission corridor increase when the line or a generator has been disconnected.
- The load recovery dynamics of the load at buses and the combined transformers equipped with ULTCs are unfavorable, since they aim to restore the load demand even at the reduced voltage.
- After the overexcitation limiters have been activated, the generators are unable to supply enough reactive power to compensate for the increased losses in the lines of the transmission corridor, and consequently they can no longer regulate their respective terminal voltages. As a result, voltage collapse is followed.

Other mechanisms can cause or play a significant role in voltage collapse phenomena include; line protection, the response of governor and automatic generation controls following generation outage, the control limits of FACTS devices and rapid load increase [1]. As illustrated above, voltage collapses are often cascades of events, with many contributing factors, that leads to the final breakup of the system.

5.3 PREVENTIVE METHOD FOR VOLTAGE COLLAPSE

5.3.1 Voltage Collapse Indicator

Voltage collapse is a dynamically complex phenomenon; therefore, to ensure secure states of operation, power system operators must know where the power system is and when it is going to a dangerous situation and which corresponding actions needed to prevent power system from collapsing. The context of voltage collapse indicator helps the operators know where the current state of the system is and how far the system is from collapse point. Many indicators are mentioned in chapter 2, however for prevention period, we introduce here the L indicator that was proposed by P. Kessel and H. Glavitsch [124]. Even this static index is based on only load-flow data, and considered as a static indicator; moreover it could not reflect dynamical behavior of the system, however this indicator is fast enough and good for power system state prediction. The procedure is summarized as follows:

Consider a multiple buses power system, the load flow equations can be described as

$$\begin{bmatrix} I_L \\ I_G \end{bmatrix} = \begin{bmatrix} Y_{LL} & Y_{LG} \\ Y_{GL} & Y_{GG} \end{bmatrix} \begin{bmatrix} V_L \\ V_G \end{bmatrix} \quad (5.3-1)$$

Where: I_G , I_L and V_G , V_L represent complex current and voltage vectors at the generator nodes and load nodes. The sub matrices $[Y_{GG}]$, $[Y_{GL}]$, $[Y_{LL}]$, and $[Y_{LG}]$ are the corresponding partitioned portions of the network Y-bus matrix.

Rearrange (5.3-1) we get

$$[V_L] = [Y_{LL}]^{-1} [I_L] - [Y_{LL}]^{-1} [Y_{LG}] [V_G] \quad (5.3-2)$$

Notation

$$[F] = -[Y_{LL}]^{-1} [Y_{LG}] \text{ and } [Z] = [Y_{LL}]^{-1} \quad (5.3-3)$$

We can re-write (5.3-2) in the form as follows

$$|V_j|^2 + \sum_{i \in \alpha_G} F_{ij} V_i V_j^* = \sum_{i \in \alpha_L} Z_{ji} I_i V_j^* = Z_{jj} S_j + \sum_{\substack{i \in \alpha_L \\ i \neq j}} Z_{ji} I_i V_j^* \quad (5.3-4)$$

or

$$|V_j|^2 + V_{0j} V_j^* = \frac{S_j + \sum_{\substack{i \in \alpha_L \\ i \neq j}} \frac{Z_{ji}}{Z_{jj}} I_i V_j^*}{Y_{jj}} = \frac{S_j^*}{Y_{jj}} \quad (5.3-5)$$

From this equation, authors in [124] proposed an indicator to measure the risk of voltage instability of load buses as follows:

$$L_j = \left| 1 + \frac{V_{0j}}{V_j} \right| = \left| 1 - \frac{\sum_{i \in \alpha_G} F_{ji} V_j^*}{V_j} \right| \quad (5.3-6)$$

The global indicator is determined by

$$L = \max\{L_j\}, j \in \alpha_L \text{ and } 0 < L < 1 \quad (5.3-7)$$

where: α_G is number of generator bus, α_L is number of load bus and F_{ij} is participation factor of load determined by (5.3-2)

By using this static indicator, the power system operators will know how the system is far from collapse point, and what the load power margin is. A multiple load-flow technique is employed to calculate load-flow in which, when a generator reaches its reactive output limit, this bus loses ability to control voltage and it is assigned as load bus and load-flow calculation procedure is repeated until getting new solution. Even through this procedure does not reflect all dynamic behaviors of power system during midterm or long term time of scale of voltage collapse phenomena but this is fast enough and simple to implement, time used is small.

In this part, the “39 bus New England system” is considered as a test case system that $L_{\text{indicator}}$ is used to measure the distance to voltage collapse.

Figure 5-19 shows variation of voltage magnitude of bus 11 and corresponding $L_{\text{indicator}}$ with respect to different level of reactive power injected at bus 11. From Figure 5-19, the reactive power margin at bus 11 is estimated about 1450 MVar and maximum $L_{\text{indicator}}$ is about 0.7. From this value, we could know the maximum reactive power of load that can be applied at a particular bus.

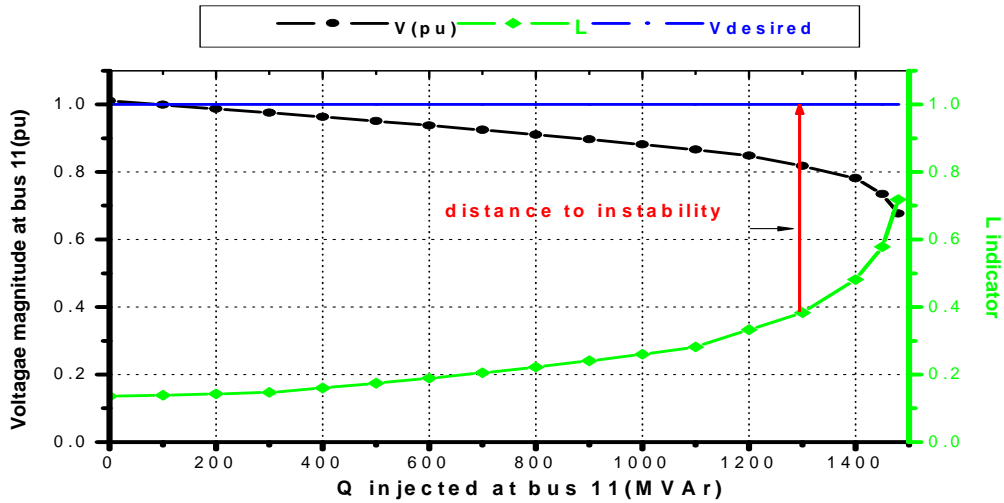


Figure 5-19: Voltage and L_indicator with different reactive power injected at bus 11 of “39 Bus New England power system”.

Figure 5-20 shows variation of minimum voltage magnitude and L_indicator with respect to different level of K_{load} . From Figure 5-20, the minimum voltage magnitude is 0.69(pu) and L_indicator is 0.52 corresponding with maximum K_{load} is 1.285 (or maximum load-ability of the system is about 128.5%).

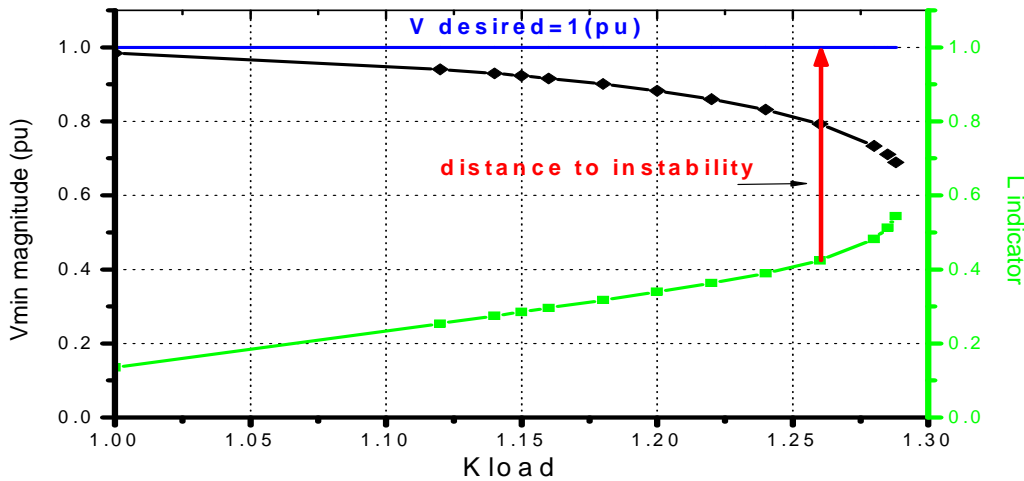


Figure 5-20: Voltage and L_indicator with respect to different K_{load} .

5.3.2 Secondary Voltage Control to Avoid Risk of Voltage Collapse

5.3.2.1 Formulating Sensitivity Equations

Consider a power system, the complex power at any bus i is calculated by formula:

$$P_i - jQ_i = V_i I_i^* = |V_i| \angle -\delta_i \sum_{j=1}^n |Y_{ij}| |V_j| \angle \theta_{ij} + \delta_j \quad (5.3-8)$$

Separating the real and the imaginary parts:

$$\begin{aligned} P_i &= \sum_{j=1}^n |V_i| |V_j| |Y_{ij}| \cos(\theta_{ij} - \delta_i + \delta_j) \\ Q_i &= -\sum_{j=1}^n |V_i| |V_j| |Y_{ij}| \sin(\theta_{ij} - \delta_i + \delta_j) \end{aligned} \quad (5.3-9)$$

Taking partial derivatives to form Jacobian matrix we get

$$\begin{aligned} \frac{\partial P_i}{\partial \delta_i} &= \sum_{j \neq i} |V_i| |V_j| |Y_{ij}| \sin(\theta_{ij} - \delta_i + \delta_j) \\ \frac{\partial P_i}{\partial \delta_j} &= |V_i| |V_j| |Y_{ij}| \sin(\theta_{ij} - \delta_i + \delta_j) \end{aligned} \quad (5.3-10)$$

$$\begin{aligned} \frac{\partial P_i}{\partial V_i} V_i &= 2.V_i^2 \cdot |Y_{ii}| \cos(\theta_{ii}) + \sum_{j \neq i} |V_i| |V_j| |Y_{ij}| \cos(\theta_{ij} - \delta_i + \delta_j) \\ \frac{\partial P_i}{\partial V_j} V_j &= |V_i| |V_j| |Y_{ij}| \cos(\theta_{ij} - \delta_i + \delta_j), \quad i \neq j \end{aligned} \quad (5.3-11)$$

$$\begin{aligned} \frac{\partial Q_i}{\partial \delta_i} &= \sum_{j \neq i} |V_i| |V_j| |Y_{ij}| \cos(\theta_{ij} - \delta_i + \delta_j) \\ \frac{\partial Q_i}{\partial \delta_j} &= -|V_i| |V_j| |Y_{ij}| \cos(\theta_{ij} - \delta_i + \delta_j), \quad i \neq j \end{aligned} \quad (5.3-12)$$

$$\begin{aligned} \frac{\partial Q_i}{\partial V_i} V_i &= -2.V_i^2 \cdot |Y_{ii}| \sin(\theta_{ii}) - \sum_{j \neq i} |V_i| |V_j| |Y_{ij}| \sin(\theta_{ij} - \delta_i + \delta_j) \\ \frac{\partial Q_i}{\partial V_j} V_j &= -|V_i| |V_j| |Y_{ij}| \sin(\theta_{ij} - \delta_i + \delta_j), \quad i \neq j \end{aligned} \quad (5.3-13)$$

Calculate sensitivity matrix from Jacobian matrix

$$\begin{bmatrix} \Delta P_G \\ \Delta P_L \\ \Delta Q_G \\ \Delta Q_L \end{bmatrix} = \begin{bmatrix} \frac{\partial F_G}{\partial \delta_G} & \frac{\partial F_G}{\partial \delta_L} & \frac{\partial F_G}{\partial V_G} & \frac{\partial F_G}{\partial V_L} \\ \frac{\partial F_L}{\partial \delta_G} & \frac{\partial F_L}{\partial \delta_G} & \frac{\partial F_L}{\partial V_G} & \frac{\partial F_L}{\partial V_L} \\ \frac{\partial G_G}{\partial \delta_G} & \frac{\partial G_G}{\partial \delta_G} & \frac{\partial G_G}{\partial V_G} & \frac{\partial G_G}{\partial \delta_L} \\ \frac{\partial G_L}{\partial \delta_G} & \frac{\partial G_L}{\partial \delta_G} & \frac{\partial G_L}{\partial V_G} & \frac{\partial G_L}{\partial V_L} \end{bmatrix} \begin{bmatrix} \Delta \delta_G \\ \Delta \delta_L \\ \frac{\Delta V_G}{V_G} \\ \frac{\Delta V_L}{V_L} \end{bmatrix} \quad (5.3-14)$$

or

$$\begin{bmatrix} \Delta P_G \\ \Delta P_L \\ \Delta Q_G \\ \Delta Q_L \end{bmatrix} = \begin{bmatrix} A_1 & B_1 & C_1 & D_1 \\ A_2 & B_2 & C_2 & D_2 \\ A_3 & B_3 & C_3 & D_3 \\ A_4 & B_4 & C_4 & D_4 \end{bmatrix} \begin{bmatrix} \Delta \delta_G \\ \Delta \delta_L \\ \frac{\Delta V_G}{V_G} \\ \frac{\Delta V_L}{V_L} \end{bmatrix} \quad (5.3-15)$$

Sensitivity matrix of variation of load bus reactive power output with respect to their voltage magnitudes is calculated as

$$[S_{Q_L V_L}] = [D_4] - [A_4 \quad B_4] \begin{bmatrix} A_1 & B_1 \\ A_2 & B_2 \end{bmatrix}^{-1} \begin{bmatrix} D_1 \\ D_2 \end{bmatrix} \quad (5.3-16)$$

Sensitivity matrix of load bus voltage magnitudes with respect to generator bus voltage magnitude is calculated as

$$[S_{V_L V_G}] = -[S_{Q_L V_L}]^{-1} \left\{ [C_4] - [A_4 \quad B_4] \begin{bmatrix} A_1 & B_1 \\ A_2 & B_2 \end{bmatrix}^{-1} \begin{bmatrix} C_1 \\ C_2 \end{bmatrix} \right\} \quad (5.3-17)$$

Sensitivity matrix of variation of generator bus reactive power output with respect to load bus reactive power demand is calculated as

$$[S_{Q_G Q_L}] = - \left\{ [D_3] - [A_3 \quad B_3] \begin{bmatrix} A_1 & B_1 \\ A_2 & B_2 \end{bmatrix}^{-1} \begin{bmatrix} D_1 \\ D_2 \end{bmatrix} \right\} [S_{Q_L V_L}]^{-1} \quad (5.3-18)$$

Sensitivity matrix of variation of generator bus reactive power output with respect to their voltage magnitudes is calculated as

$$[S_{Q_G V_G}] = [C_3] - [A_3 \quad B_3] \begin{bmatrix} A_1 & B_1 \\ A_2 & B_2 \end{bmatrix}^{-1} \begin{bmatrix} C_1 \\ C_2 \end{bmatrix} - [S_{Q_G Q_L}] [S_{Q_L V_L}] [S_{V_L V_G}] \quad (5.3-19)$$

Sensitivity matrix of variation of load bus voltage with respect to all bus active power

$$[S_{V_L P}] = -[S_{Q_L V_L}]^{-1} [A_4 \quad B_4] \begin{bmatrix} A_1 & B_1 \\ A_2 & B_2 \end{bmatrix}^{-1} \quad (5.3-20)$$

In transmission line systems, a decoupled model is normally employed. The Jacobian matrix now becomes:

$$\begin{bmatrix} \Delta P_G \\ \Delta P_L \\ \Delta Q_G \\ \Delta Q_L \end{bmatrix} = \begin{bmatrix} A_1 & B_1 & 0 & 0 \\ A_2 & B_2 & 0 & 0 \\ 0 & 0 & C_3 & D_3 \\ 0 & 0 & C_4 & D_4 \end{bmatrix} \begin{bmatrix} \Delta \delta_G \\ \Delta \delta_L \\ \frac{\Delta V_G}{V_G} \\ \frac{\Delta V_L}{V_L} \end{bmatrix} \quad (5.3-21)$$

Therefore, the sensitivity matrices are now calculated as

$$[S_{Q_L V_L}] = [D_4] - [A_4 \quad B_4] \begin{bmatrix} A_1 & B_1 \\ A_2 & B_2 \end{bmatrix}^{-1} \begin{bmatrix} D_1 \\ D_2 \end{bmatrix} = [D_4] \quad (5.3-22)$$

$$\begin{aligned} [S_{V_L V_G}] &= -[S_{Q_L V_L}]^{-1} \left\{ [C_4] - [A_4 \quad B_4] \begin{bmatrix} A_1 & B_1 \\ A_2 & B_2 \end{bmatrix}^{-1} \begin{bmatrix} C_1 \\ C_2 \end{bmatrix} \right\} \\ &= -[S_{Q_L V_L}]^{-1} [C_4] = -[D_4]^{-1} [C_4] \end{aligned} \quad (5.3-23)$$

$$\begin{aligned} [S_{Q_G Q_L}] &= - \left\{ [D_3] - [A_3 \quad B_3] \begin{bmatrix} A_1 & B_1 \\ A_2 & B_2 \end{bmatrix}^{-1} \begin{bmatrix} D_1 \\ D_2 \end{bmatrix} \right\} [S_{Q_L V_L}] \\ &= -[D_3] [S_{Q_L V_L}]^{-1} = -[D_3] [D_4]^{-1} \end{aligned} \quad (5.3-24)$$

$$\begin{aligned} [S_{Q_G V_G}] &= [C_3] - [A_3 \quad B_3] \begin{bmatrix} A_1 & B_1 \\ A_2 & B_2 \end{bmatrix}^{-1} \begin{bmatrix} C_1 \\ C_2 \end{bmatrix} - [S_{Q_G Q_L}] [S_{Q_L V_L}] [S_{V_L V_G}] \\ &= [C_3] - [S_{Q_G Q_L}] [S_{Q_L V_L}] [S_{V_L V_G}] \\ &= [C_3] - \{-[D_3] [D_4]^{-1}\} \{[D_4]\} \{-[D_4]^{-1} [C_4]\} \\ &= [C_3] - [D_3] [D_4]^{-1} [C_4] \end{aligned} \quad (5.3-25)$$

$$[S_{V_L P}] = -[D_4]^{-1} [A_4 \quad B_4] \begin{bmatrix} A_1 & B_1 \\ A_2 & B_2 \end{bmatrix}^{-1} \quad (5.3-26)$$

Moreover, in decoupled model, some assumptions are taken into account as:

$$\begin{aligned} \cos \theta_{ij} &\approx 1 \\ G_{ij} \sin \theta_{ij} &\ll B_{ij} \\ Q_i &\ll B_{ii} |V_i|^2 \end{aligned} \quad (5.3-27)$$

Therefore we can rewrite (5.3-14) under the following form

$$\begin{bmatrix} \frac{\Delta P}{V} \\ \frac{\Delta Q}{V} \end{bmatrix} = \begin{bmatrix} B' & 0 \\ 0 & B'' \end{bmatrix} \begin{bmatrix} \Delta \delta \\ \Delta V \end{bmatrix} \quad (5.3-28)$$

where

$$B'_{ij} = -\frac{1}{X_{ij}}, B''_{ii} = -\sum_{i \neq j} B'_{ij}, B''_{ij} = -B_{ij}, B'_{ii} = -B_{ii} \quad (5.3-29)$$

When calculating sensitivity matrix we can use the following equations

$$\begin{bmatrix} \frac{\Delta Q_L}{V_L} \\ \frac{\Delta Q_G}{V_G} \end{bmatrix} = \begin{bmatrix} D_4 & C_4 \\ D_3 & C_3 \end{bmatrix} \begin{bmatrix} \Delta V_L \\ \Delta V_G \end{bmatrix} = \begin{bmatrix} B'' & B_{LG} \\ B_{GL} & B_{GG} \end{bmatrix} \begin{bmatrix} \Delta V_L \\ \Delta V_G \end{bmatrix} \quad (5.3-30)$$

Sensitivity matrix of variation of load bus voltages with respect to variation of generator bus voltages is calculated as:

$$\left[S_{V_L V_G} \right] = -[D_4]^{-1} [C_4] = -[B'']^{-1} [B_{LG}] \quad (5.3-31)$$

Notation

$$\Delta V_L = [S_{V_L V_G}] \Delta V_G \quad (5.3-32)$$

Sensitivity matrix of variation of generator bus reactive power output with respect to variation of generator bus voltage is calculated as:

$$\left[S_{Q_G V_G} \right] = [C_3] - [D_3][D_4]^{-1}[C_4] = [B_{GG}] + [B_{GL}] \left[S_{V_L V_G} \right] \quad (5.3-33)$$

Notation

$$\frac{\Delta Q_G}{V_G} = [S_{Q_G V_G}] \Delta V_G \quad (5.3-34)$$

Sensitivity matrix of variation of load bus voltage with respect to variation of load bus reactive power demand is calculated as:

$$\left[S_{V_L Q_L} \right] = [D_4]^{-1} = [B'']^{-1} \quad (5.3-35)$$

Notation

$$\Delta V_L = \left[S_{V_L Q_L} \right] \frac{\Delta Q_L}{V_L} \quad (5.3-36)$$

Sensitivity matrix of variation of generator bus reactive power output with respect to variation of load bus voltage is calculated as:

$$\left[S_{Q_G Q_L} \right] = -[D_3] * [D_4]^{-1} = [B_{GL}] \left[S_{V_L Q_L} \right] \quad (5.3-37)$$

Notation

$$\frac{\Delta Q_G}{V_G} = \left[S_{Q_G Q_L} \right] \frac{\Delta Q_L}{V_L} \quad (5.3-38)$$

In case of adding a shunt capacitor at load buses, we could have $S_{Q_G Q_C}$ and $S_{V_L Q_C}$ that are taken from the corresponding columns of matrices $S_{Q_G Q_L}$ and $S_{V_L Q_L}$.

Sensitivity matrix of variation of load bus voltage with respect to variation of tap position at transformer:

$$\Delta V_L = [B^{-1}] \begin{bmatrix} \vdots \\ (-2V_j^0 + V_k^0 \cos \theta_{jk}^0) b_{jk} \\ \vdots \\ V_j^0 b_{jk} \cos \theta_{kj}^0 \end{bmatrix} \Delta T_{jk} = [S_{V_L T_L}] \Delta T_{jk} \quad (5.3-39)$$

with T_{jk} is tap position

Notation

$$\Delta V_L = [S_{V_L T_L}] \Delta T \quad (5.3-40)$$

Sensitivity matrix of variation of generator bus reactive power output with respect to variation of tap position at transformer:

$$[S_{Q_G T_L}] = [B_{GL}] [S_{V_L T_L}] \quad (5.3-41)$$

Notation

$$\frac{\Delta Q_G}{V_G} = [S_{Q_G T_L}] \Delta T \quad (5.3-42)$$

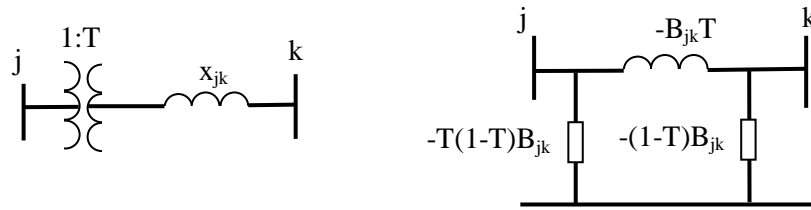


Figure 5-21: Tap modeling for load-flow calculation.

Finally, we get sensitivity matrix:

$$\begin{bmatrix} S_{V_L V_G} & S_{V_L Q_G} & S_{V_L T_L} \\ S_{Q_G V_G} & S_{Q_G Q_G} & S_{Q_G T_L} \end{bmatrix} \quad (5.3-43)$$

5.3.2.2 Minimizing Control Variations to Avoid Risk of Violated Voltage

In a heavily loaded situation or after experiencing a disturbance, some bus voltages of power system may be violated their limits, if suitably control strategies are not implemented timely, the power system may face with some risk of voltage instability or even voltage collapse eventually. Therefore, a controlled voltage strategy is needed to maintain quickly the bus voltages at the normal limits. For a steady-state power system, there are some ways to control voltage magnitude at buses in power system: by changing tap positions of transformers, switching capacitor banks, or terminal voltage of generator. These are also called control variables in term of voltage control. Hereafter, we present a control strategy for optimizing controlled variables in order to avoid risk of voltage collapse.

Assume that a power system is operating in heavy load conditions or experiencing some outages, voltages at some buses are violated, and we need adjust the control variable in order to maintain the voltage profile in a desirable range:

The cost function is to minimize the control variations:

$$\text{Min}_{\Delta V_G, \Delta Q_L, \Delta T_L} \left\{ (C_1 \Delta V_G)^2 + (C_2 \Delta Q_C)^2 + (C_3 \Delta T_L)^2 \right\} \quad (5.3-44)$$

Where: C1, C2, C3 are weight factor when changing controlled bus voltage, load bus reactive power and tap position of transformer.

That satisfied constraints:

$$\left\{ \begin{array}{l} \left[\begin{array}{l} (\Delta V_L)_{\min} \\ \left(\frac{\Delta Q_G}{V_G} \right)_{\min} \end{array} \right] \leq \left[\begin{array}{ccc} S_{V_L V_G} & S_{V_L Q_C} & S_{V_L T_L} \\ S_{Q_G V_G} & S_{Q_G Q_C} & S_{Q_G T_L} \end{array} \right] \left[\begin{array}{l} \Delta V_G \\ \Delta Q_C \\ \Delta T_L \end{array} \right] \leq \left[\begin{array}{l} (\Delta V_L)_{\max} \\ \left(\frac{\Delta Q_G}{V_G} \right)_{\max} \end{array} \right] \\ (\Delta V_G)_{\min} \leq \Delta V_G \leq (\Delta V_G)_{\max} \\ (Q_C)_{\min} \leq Q_C \leq (Q_C)_{\max} \\ (\Delta T_L)_{\min} \leq \Delta T_L \leq (\Delta T_L)_{\max} \end{array} \right. \quad (5.3-45)$$

where:

$$\left\{ \begin{array}{l} (\Delta V_G)_{\min} = (V_G)_{\min} - V_G^0 \\ (\Delta V_L)_{\min} = (V_L)_{\min} - V_L^0 \\ (\Delta T_L)_{\min} = (T_L)_{\min} - T_L^0 \\ (\Delta Q_G)_{\min} = (Q_G)_{\min} - Q_G^0 \end{array} \right. \text{ and } \left\{ \begin{array}{l} (\Delta V_G)_{\max} = (V_G)_{\max} - V_G^0 \\ (\Delta V_L)_{\max} = (V_L)_{\max} - V_L^0 \\ (\Delta T_L)_{\max} = (T_L)_{\max} - T_L^0 \\ (\Delta Q_G)_{\max} = (Q_G)_{\max} - Q_G^0 \end{array} \right. \quad (5.3-46)$$

Assumption that C_i are all positive and cost of increasing and decreasing control variables are identical for each type of controlled variables, the cost function could be form as

$$\text{Min}_{\Delta V_G, \Delta Q_L, \Delta T_L} \left\{ C_1 (\Delta V_G)^2 + C_2 (\Delta Q_C)^2 + C_3 (\Delta T_L)^2 \right\} \quad (5.3-47)$$

The optimization problem is solved by application of quadratic programming method. The L_{indicator} is used to verify the effectiveness of proposed method. By using this criterion, the controller could quickly correct the violated voltage buses with least changing in control variables in order to prevent voltage collapse. The procedure could be illustrated by the figure as below

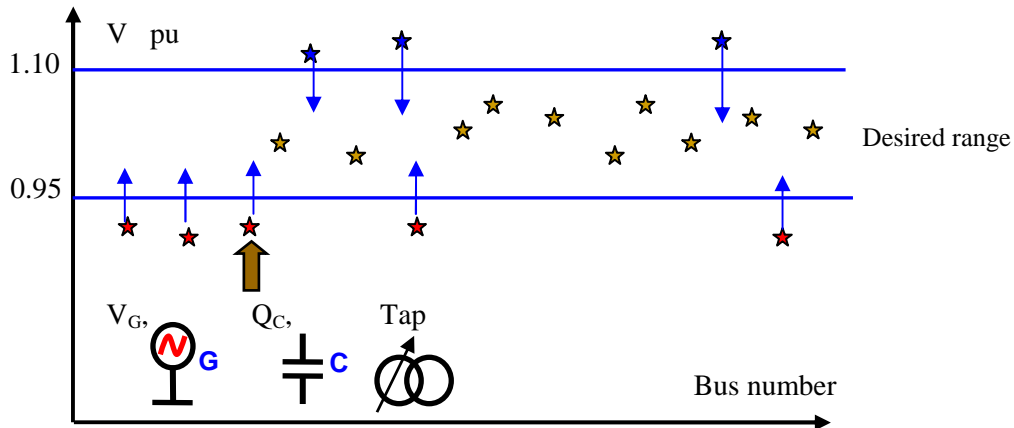


Figure 5-22: Principle of method to maintain voltage profile.

5.3.2.3 Application for “30 Bus IEEE Power System”

The system [125] is shown in Figure 5-23, with assumption that operated in heavily loaded. The problem is to minimize changes of controlled variables in order to boost up the violated bus voltages by changing generators’ terminal voltages, adding a shunt capacitor at bus 21 and changing tap positions of transformers. In this case, we set all $C_i = 1$.

At initial operating condition, there are 22 buses that their voltage magnitudes are slower than the preset low limit 0.95(pu). The initial conditions of controlled variables are listed in Table 5-5

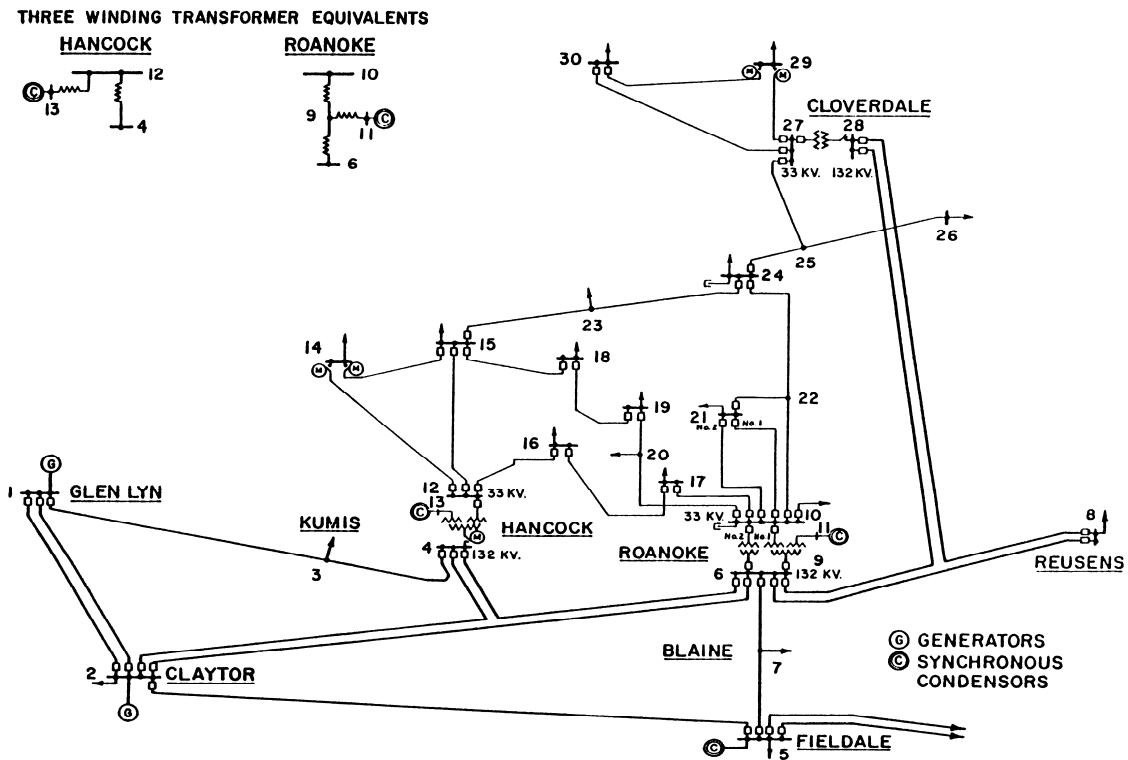


Figure 5-23: The 30 bus IEEE power system.

Table 5-5: Controlled variables before and after adjustment for the “30 bus IEEE power system”.

Bus	V (pu)		Q _G		Tap		Added Shunt (MVar)
	Initial	Final	Initial	Final	Final	Initial	
1	1.06	1.098	91.755	97.643			
2	0.993	1.030	37.304	41.692			
5	0.92	0.954	39.528	34.668			
8	0.92	0.954	34.901	37.725			
11	1.01	1.038	23.178	23.321			
13	1.00	1.000	24.000	7.1611			
4-12					0.932	0.9326	
6-9					0.978	0.9814	
6-10					0.969	0.9645	
28-27					0.968	0.9000	
21							14.3

Case 1: No line tripped off

Figure 5-24 shows the voltage profile of “30 bus IEEE power system” before and after readjusting the control variables. The blue line corresponds to the original voltage profile, and the red line is the final voltage profile after readjusting control variables. From the figure, we could see that the system voltages are improved and lain into the desired range from 0.95(pu) to 1.1(pu). There are four buses that have voltage magnitude slightly smaller than 0.95(pu). They are buses 7, 18, 19, 26 with 0.9496(pu), 0.9485(pu), 0.945(pu) and 0.9486(pu) respectively. The voltage profile is clearly improved as shown in Figure 5-24

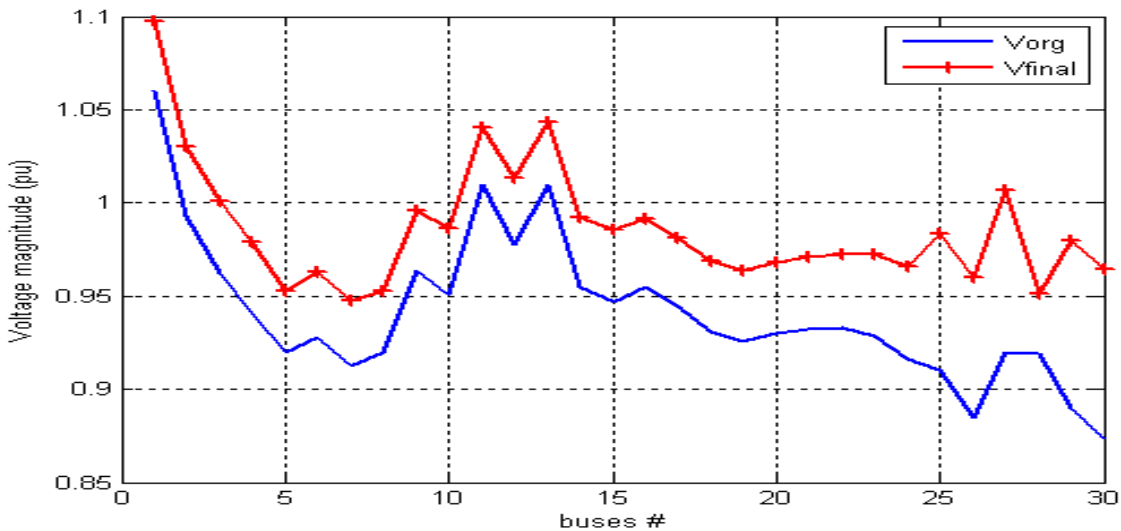


Figure 5-24: Voltages of the “30 bus IEEE power system” before and after re-adjustment.

By using this control strategy, the risk of voltage instability or voltage collapse also is reduced. The L_indicator of both cases before and after adjustment controlled variables are

plotted in Figure 5-25 we could see that the L_indicator (0.1389) is reduced when comparing to the initial condition (0.1789).

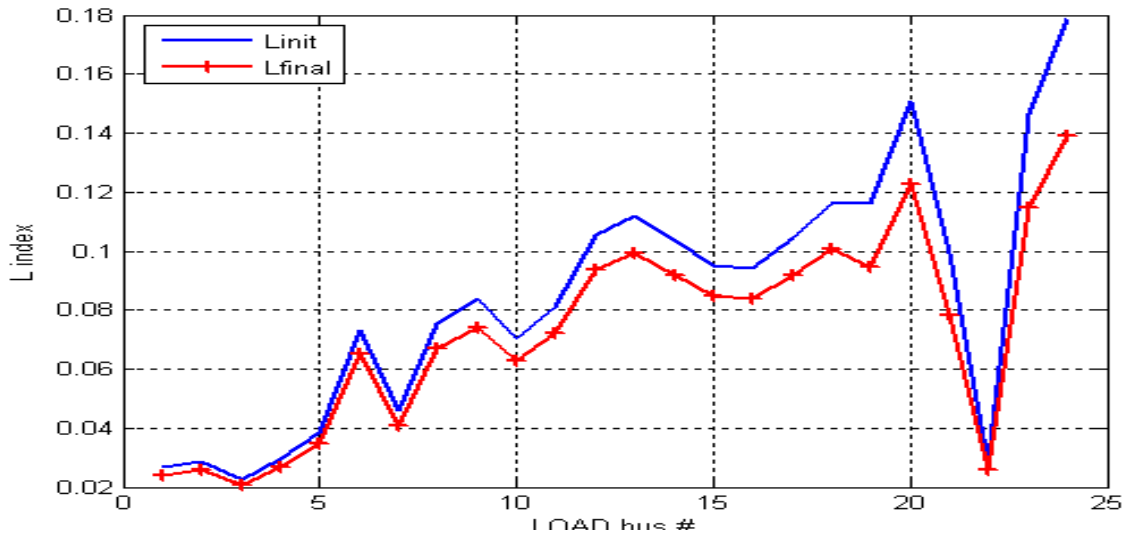


Figure 5-25: L_indicator of the “30 bus IEEE power system” before and after re-adjustment.

Case 2: A line tripped off

Second case is done when a line between buses 23 and 24 is tripped off. Figure 5-26 and Figure 5-27 show the effect of this control strategy.

From Figure 5-26, shows the voltage magnitudes of 30 bus IEEE power system before and after readjusting the controlled variables. The blue line corresponds to original voltages, and the red line is related to final voltages after readjusting control variables. From the figure, we could see that the system voltages are improved and lain into the desired range from 0.95(pu) to 1.1(pu).

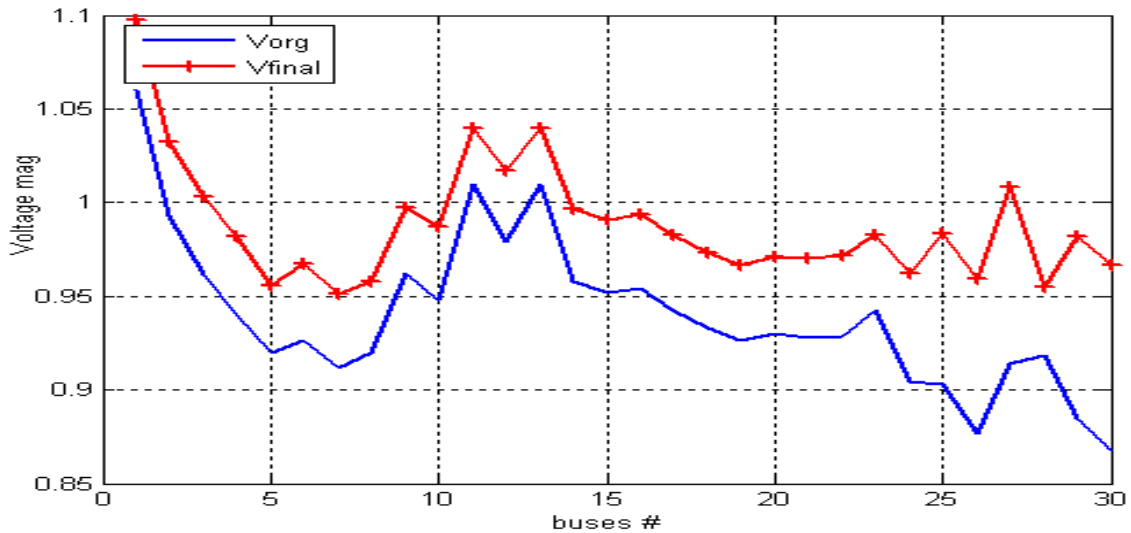


Figure 5-26: Voltages of the “30 bus IEEE power system” before and after re-adjustment.

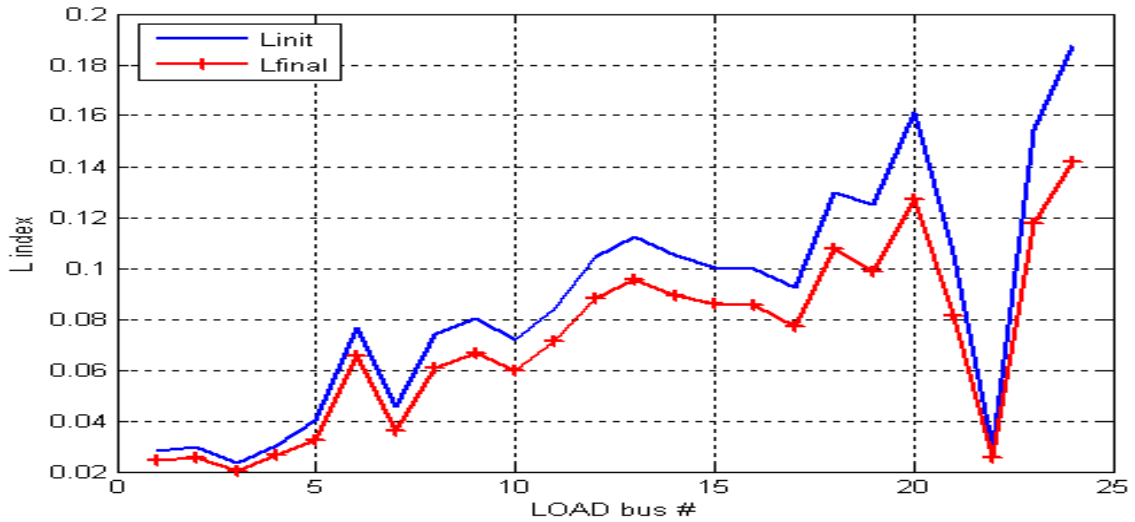


Figure 5-27: L_index of the “30 bus IEEE power system” before and after re-adjustment.

The L_index of both cases before and after adjustment controlled variables are plotted in Figure 5-27, we could see that the L_index (0.1419) is reduced when comparing to the initial condition (0.1878).

5.3.2.4 Application for “Nordic Power System”

At initial operating condition, there are nine buses that have voltage magnitudes lower than 0.95(pu), and one bus has voltage magnitude bigger than 1.1(pu). The final goal is to minimize changes of controlled variables in order to maintain the voltage profile into the desired range from 0.95(pu) to 1.1(pu). There are two available shunt capacitors with 50 MVar and 100 MVar at bus 46 and 4022 (bus numbers 4th and 26th in Figure 5-28.). The results of initial and final condition are listed in Table 5-6.

Table 5-6: List of controlled variables before and after adjustment for the “Nordic power system”.

a: voltage of generators and added shunt.

Bus	V_G (pu)		Q_G (pu)		Added Shunt(MVAr)
	Initial	Final	Initial	Final	
11	1.0897	1.08	-8.4717	33.0042	
12	1.076	1.08	-38.231	-14.9235	
13	1.0792	1.08	-59.728	-70.8898	
14	0.986	1	29.2828	15.0471	
15	0.9924	0.99	114.8431	100.5745	
17	1.0337	1	118.4373	125.5333	
18	0.9659	0.95	86.3658	38.4748	
22	1.0324	1	91.0092	135.5227	
23	1.01	1.01	917.5739	704.4855	
24	0.9873	0.98	-135.812	-92.477	
25	0.9823	0.972	95.0982	55.7116	
27	0.9725	0.95	128.9231	111.3874	
29	0.99	0.98	297.7095	213.8199	
30	0.9721	0.96	333.9246	282.8919	
35	1.0071	1	433.4727	358.5429	
36	1.02	1	298.4977	326.3028	
38	1.0037	1	103.1967	95.4344	
39	1.003	1	135.516	115.3507	
40	1.0048	1.01	125.7512	110.7391	
41	1.0059	1.01	190.8534	178.0179	
3					50
26					100

b: Tap position.

From bus	To bus	Old tap	New tap
1	29	1	1.0065
2	30	1	1.0184
3	31	1	1.0006
4	34	1	1.0107
5	35	1	1.009
6	36	1	1.0012
7	37	1	1
8	38	1	0.9978
9	39	1	0.999
10	23	1.12	1.1
11	24	1.12	1.12
15	26	1.07	1.05
19	32	1	1.008
20	33	1	1.0302
21	27	1.05	1.03

Voltage profiles of system before and after adjustment are shown in Figure 5-28, in which the blue line corresponds to original voltages, and the red line is related to final voltages after readjusting control variables. From this figure, we could observe that voltage of system is effectively improved. There are two buses where the voltage magnitudes are a little lower than 0.95(pu)- buses 43 and 4022 (bus number 3th and 26th in Figure 5-28.).

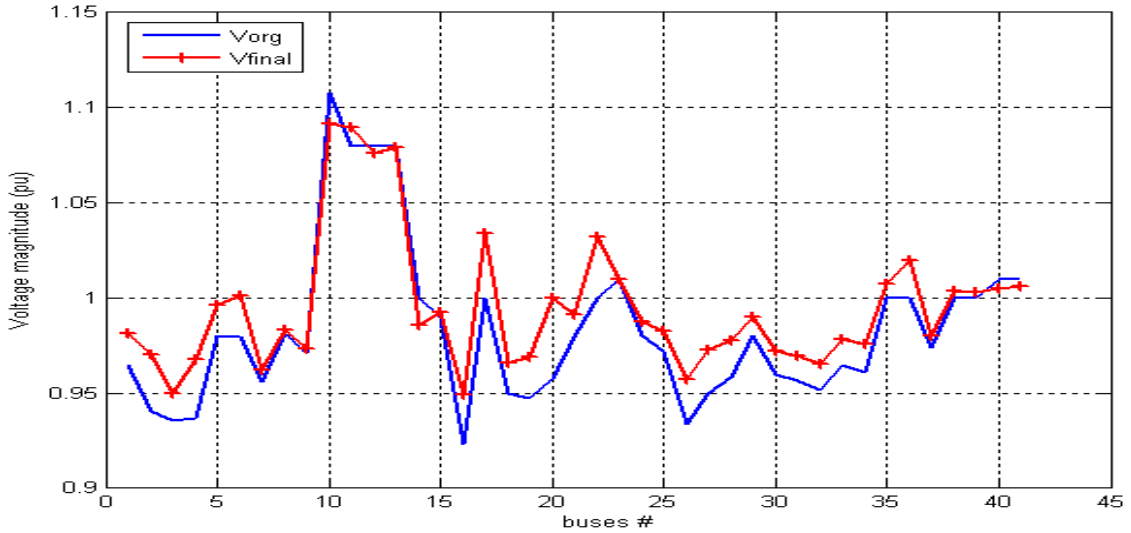


Figure 5-28: Voltage profile of the “Nordic power system” before and after re-adjustment.

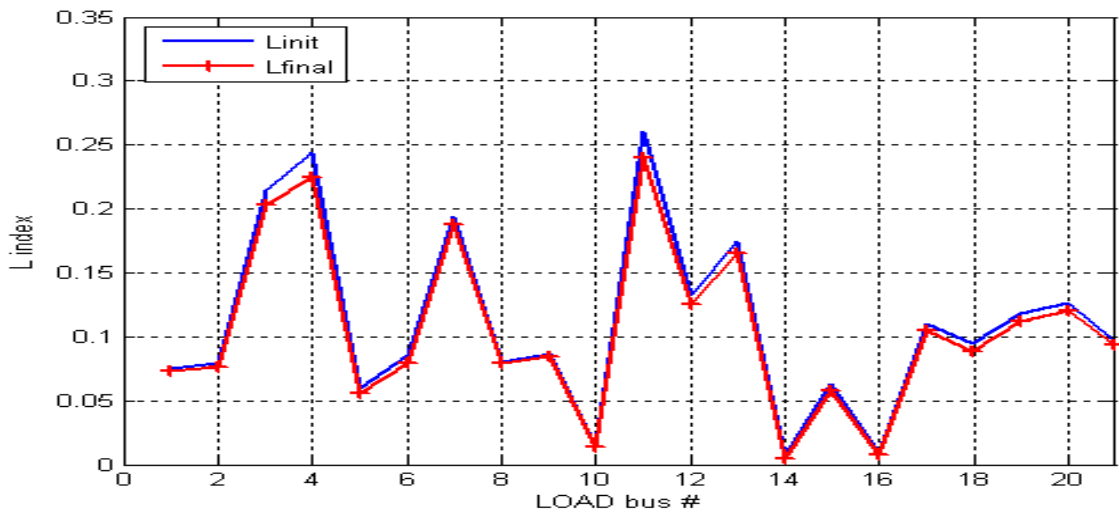


Figure 5-29: L_indicator of the “Nordic power system” before and after re-adjustment.

The L_indicator of both cases before and after adjustment of the controlled variables are plotted in Figure 5-29. From this figure, we could see that the L_indicator is reduced when comparing to the initial condition from $L=0.2712$ to $L=0.2423$. That means the risk of voltage instability or voltage collapse also is reduced.

5.3.3 Dynamic Simulation

In order to illustrate the effectiveness of above control strategy, two dynamic simulations are done for both cases: without adjustment controlled variables and with adjustment controlled variables.

Scenario 1

A line between bus 4021 and bus 4032 is tripped off at $t=5(s)$ and generator at bus 4021 is tripped off 0.1(s) later (Similar as scenario 1 in section 5.2.2)

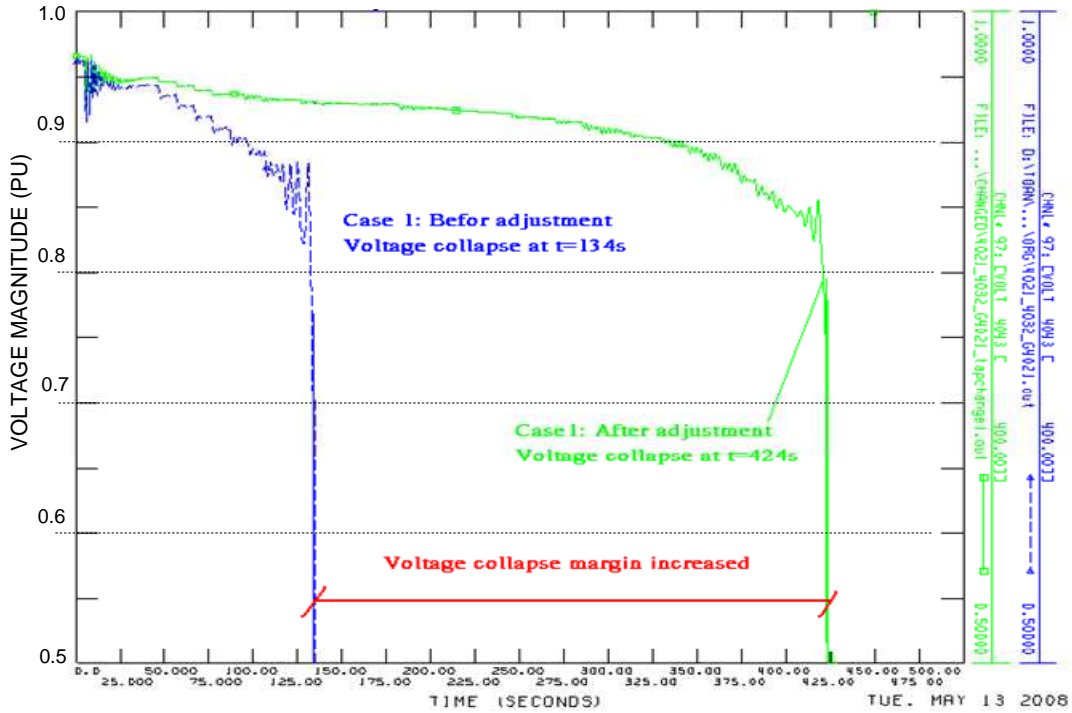


Figure 5-30: Scenario 1: Voltage profile of bus 4043 before and after adjustment.

Figure 5-30 shows voltage magnitude of bus 4043 for both cases, by adjustment controlled variables, time for voltage collapse in case 2 is about 424s seconds, longer than in case 1 (about 275(s)).

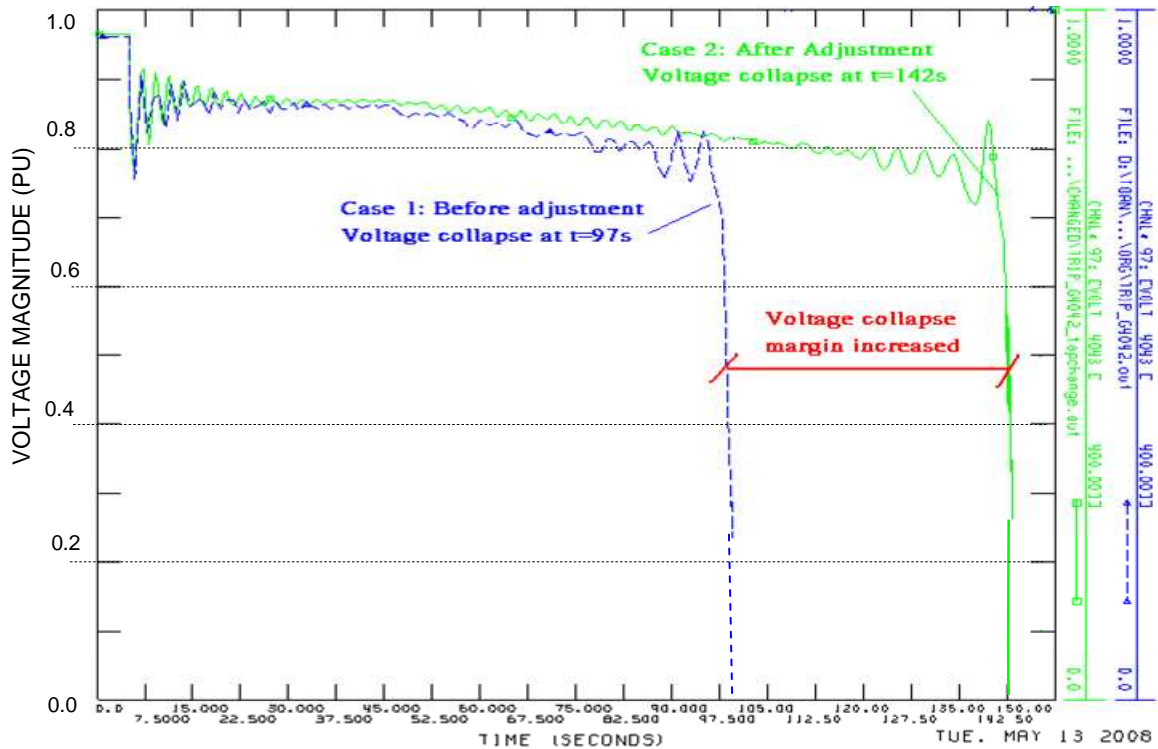


Figure 5-31: Scenario 2: Voltage profile of bus 4043 before and after adjustment.

Scenario 2

A generator at bus 4042 is tripped off at $t = 5$ (s) (similar as scenario 3 in section 5.5.2).

Figure 5-31 shows voltage magnitude of bus 4043 for both cases, by adjustment controlled variable, time for voltage collapse in case 2 is also longer than in case 1 (about approximately 42(s)).

The “Nordic power system” presented here has highly loaded and very high tap references, therefore, the power system is actually operating closer to its secure limit, and very vulnerable to any severe disturbance such as loss of a generator or very important transmission line. With only changing terminal voltage of generators and changing tap references of transformer with ULTC could not prevent totally power system voltage collapse after such above severe contingencies. However, the power system has larger margin to collapse, furthermore, power system operators have more time to act or decide urgent corrective actions.

5.4 CORRECTIVE METHOD BY USING UNDERVOLTAGE LOAD SHEDDING

In case of less serious disturbances, or there is enough reactive power reserve, the preventive methods could avoid the collapse. However, in case of critical contingencies or there is unavailability of both active and reactive power support, the effectiveness of preventive methods are normally to delay the voltage collapse in some minutes. In these situations, corrective method must be implemented in order to eliminate the voltage collapse. The corrective actions always affect generators and/or loads, hence are acceptable only in the presence of very severe disturbances. Many corrective methods have been mentioned in

chapter 2, one of the effective methods is the use of undervoltage load shedding (UVLS) relay. The UVLS relay has been proven a viable and effective method of providing protection to avoid power system voltage collapse. Many UVLS schemes have been studied for a long time, and they are still a very interested issue.

The major goals of these methods concentrated on three purposes as follows:

- 1) To minimize the amount of load to shed
- 2) Determine the location where load is to be shed
- 3) The timing of load shedding is expected as short as possible while considering oscillation problem.

However, almost methods are theoretical solutions that related to solve the optimal mathematic problems. Furthermore, a globe optimization that needs modeling of all dynamic devices such as generators, loads, induction motors, OELs, ULTCs, FACTS, HVDC, protection systems in so complicated phenomena as voltage collapse is a very difficult task. Almost methods are actually dealing with offline studies. Some of them may not be applicable in reality because voltage collapse may occur in very short period. In contrarily, several experiential and practical methods in designing UVLS relay applied in some real electrical utilities have been proven working effectively and reliability to avoid voltage collapse as listed in references [57], [116], [126]. For example, C. W. Taylor in [57] proposed a concept for UVLS used in Puget Sound area utilities (area of the Pacific Northwest) that has been using following rules:

- 5% of load shed at voltage 10% below lowest normal voltage with 3.5 seconds time delay.
- 5% of load shed at voltage 8% below lowest normal voltage with 5 seconds time delay.
- 5% of load shed at voltage 8% below lowest normal voltage with 8 seconds time delay.

The authors in [116] discussed a UVLS scheme applied in the Hydro-Québec system as basis rules bellow:

- 400 MW (R1) of load shed if voltage is below 0.94(pu) with 11 seconds time delay.
- 400 MW (R1) of load shed if voltage is below 0.92(pu) with 9 seconds time delay.
- 700 MW (R1) of load shed if voltage is below 0.90(pu) with 6 seconds time delay.

The following additional criteria have been used in various schemes [127].

- Rate of change of voltage magnitude (TEPCO)
- Inverse time undervoltage (South Africa)
- Current supervision of undervoltage (to prevent operation due to voltage depression caused by short circuits) (TVA)
- Wide area voltage measurement and reactive power reserve (BC Hydro, and Entergy)
- Wide area voltage measurement and system topology (Saudi Arabia).
- Wide area multi-measurement of system state, real and reactive power sources and interconnections with supervision by memorized underfrequency (Florida, FALS)

In term of control and monitoring point of views, there are two types of UVLS schemes that have being applied in some power utilities around the world: a decentralized or distributed scheme (used in Puget Sound utilities) and a centralized scheme (used in Hydro Quebec, New Mexico utilities [128], [129]).

A decentralized or distributed scheme has each protective relay closely coupled to a segment of load to be shed. As voltage conditions at a relay enter the region where collapse is predicted, load assigned to that relay is shed. This philosophy is very similar to common underfrequency load shedding schemes. In the near future, there will be much interest in the demand side management, we could not only control but also monitor even the customer load- the so-called intelligent load. The customer load will be flexible and intelligent in term of being against voltage collapse. Therefore, this scheme will be more desirable because of some advantages given below:

- The reliability of the decentralized/distributed scheme is increased by diversification. Failure of one component of the distributed system will not directly or detrimentally affect the operation of other components of the load shedding system. The centralized scheme depends on the reliability of only a few relays, or one relay. Failure of the centralized system results in complete failure of the scheme, and could result large blocks of load being unnecessarily shed or failure of the scheme to shed load when required.
- In a decentralized/distributed system, load shedding is concentrated and localized to the areas where the effects of the instability are felt most strongly. With a centralized system, load is shed when the centralized decision is made, whether or not the voltage at the load delivery point is low.
- The decentralized /distributed model does not depend on communications facilities for its operation. The local relays and breakers are operable, load shedding will occur even if communications facilities fail. The centralized scheme is heavily dependent upon communications facilities, both for making the shedding decision, and for implementing it. This can make the scheme more expensive than a distributed scheme. If communications are required anyway for load restoration by supervisory control, then this advantage of the distributed scheme is not as prominent.

A centralized scheme has measurements taken at one or more key busses within the area, and trip signals transmitted to shed the load at various locations within the area. Since voltage instability may be recognized by low voltages across the region, the basis of centralized measurement lies in the notion that if the voltage is low at certain key locations, it is likely to be also low throughout the area. This scheme requires communications and may use parameters other than voltage to initiate load shedding. This scheme also has some advantages as follows.

- In a centralized system, the location of the undervoltage measuring relay is not constrained to be near a suitable load. The voltages to be monitored may be selected at strategic locations, purely on the basis of being the most appropriate point on the system. Usually, the important supply busses are monitored, where the voltage level is tightly regulated under normal conditions. Small voltage depressions can be used to indicate voltage instability more reliably than similar voltage depressions at a less stiff bus where the voltage has a wider range of variation under normal conditions.

- By means of communications between key locations, with a centralized system it can be established that low voltages exist throughout the region before a decision is taken to shed load. This avoids load shedding due to voltage depressions caused by local disturbances not associated with imminent regional voltage collapse.
- The reliability of the centralized system can be increased by using other indicators from any part of the system in addition to voltage level to predict the approach of voltage instability.
- Short time delays associated with small voltage depressions are more likely to coordinate with fault clearing devices at stiff busses than at less stiff busses. Thus it may be easier to achieve useful and secure settings with centralized relays at centralized busses.

In this part, a rule for UVLS that could be used to avoid voltage collapse is proposed in accordance with the assumption of intelligent directly controlled load. The new scheme based on the advantages of both rules discussed above. The “Nordic power system” is considered the test case and PSS/E is used for long-term dynamic simulation.

5.4.1 Choosing Thresholds for UVLS Relay

For a particular power system, there is a particular voltage security criterion regarding to the system characteristics. In general, a typical desired operating voltage range varies from 0.95(pu) to 1.05(pu) as in Figure 5-32. Choosing thresholds for UVLS relay is always depended on each specific power system. This task requires a full understanding about the investigated power system. The thresholds for UVLS relay must be chosen in order to avoid voltage collapse in case of voltage decays too low leading voltage collapse and to remain loads in case of normal low voltage situations.

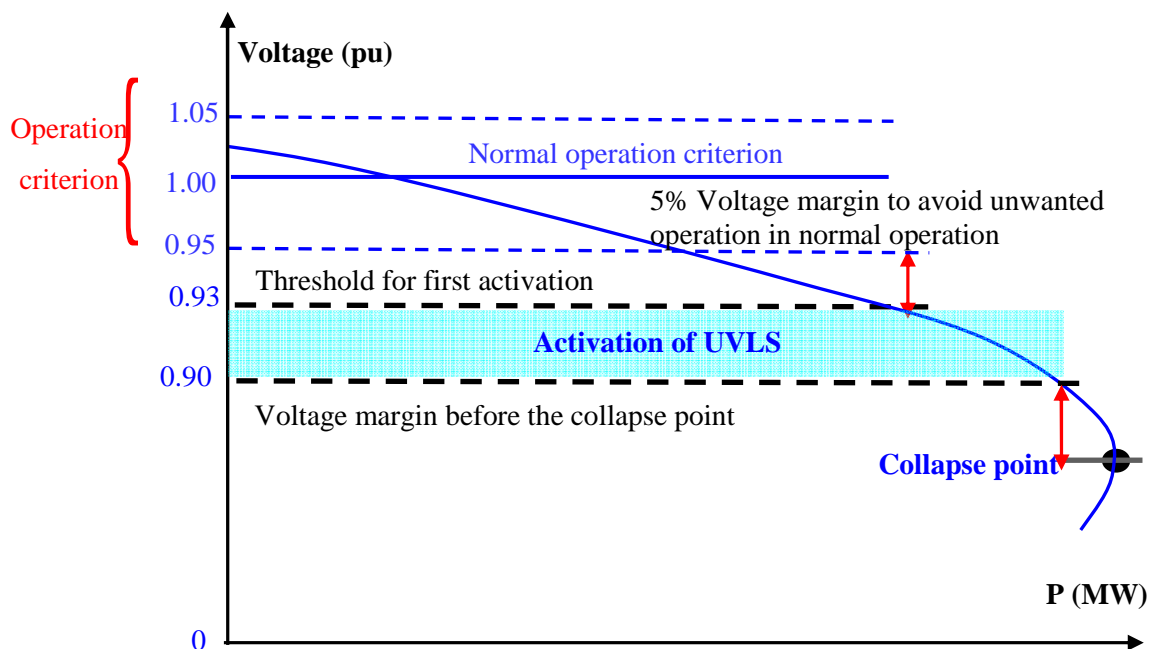


Figure 5-32: Threshold voltage magnitude for setting UVLS relay.

Following the rule proposed by C. W. Taylor [57], the thresholds may be too low for first activation of UVLS relay in term of prevent voltage collapse. In practice, many power systems are operating in highly loaded conditions that may have their voltage magnitude too close to the smallest voltage value as 0.95(pu) (then the first threshold for UVLS relay is chosen as 8% below the lowest voltage or about 0.874(pu) may be too low). Consequently, power system could be collapse when their bus voltages magnitudes are lower than 0.9(pu). Therefore, thresholds for UVLS chosen by this method may be too low to avoid voltage collapse.

A dynamic voltage collapse simulation with UVLS as the rule of C. W. Taylor [57] is done for the “Nordic power system” in this section. The lowest normal operating voltage is 0.9605 (pu) at bus 1041. Then, the thresholds for activations of UVLS relays are chosen as follows:

- 5% of load shed at voltage 10% below lowest normal voltage or at 0.86445 (pu) with 3.5 seconds time delay.
- 5% of load shed at voltage 8% below lowest normal voltage or at 0.88366 (pu) with 5 seconds time delay.
- 5% of load shed at voltage 8% below lowest normal voltage or at 0.88366 (pu) with 8 seconds time delay.

Figure 5-33 plots voltage profile of bus 42 corresponding to voltage collapse scenario: tripping off one transmission line between buses 4011 and 4032, and generator G1022 is tripped off 0.1s latter. From Figure 5-33, the chosen thresholds for UVLS are too low, therefore, even with the presence of UVLS, the voltage is still collapse.

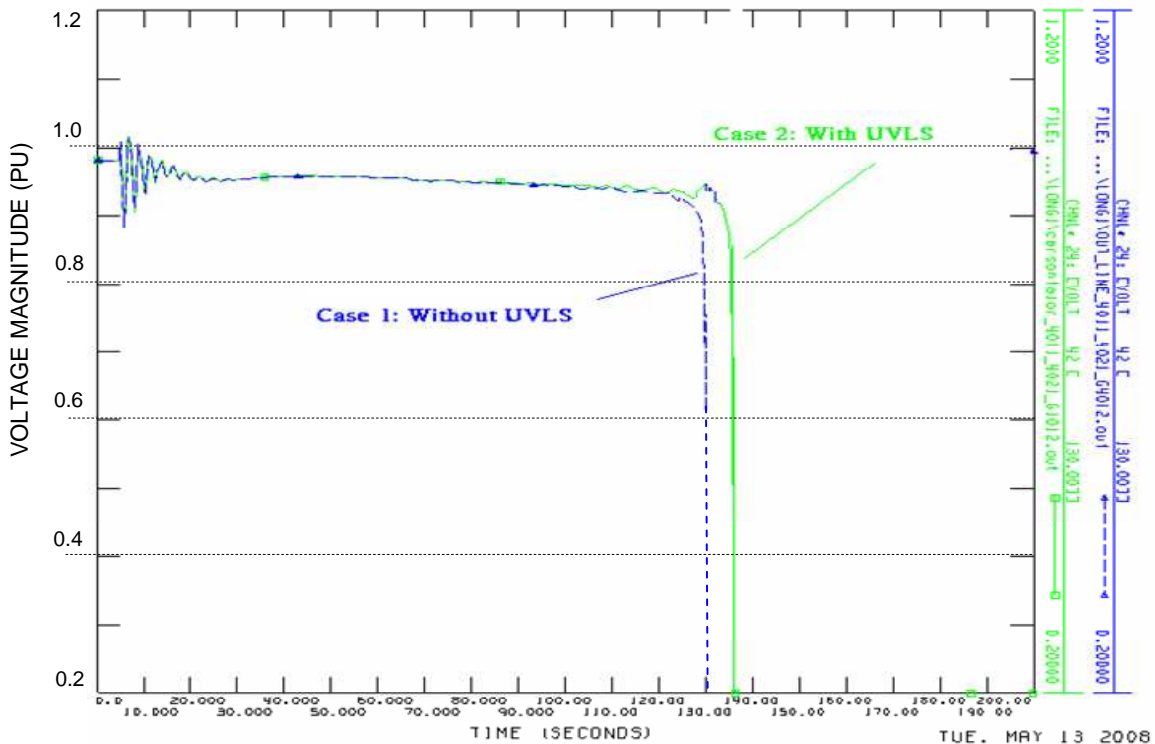


Figure 5-33: Voltage profile of bus 42 when applying the rule C. W. Taylor [57].

Following the rule proposed by the authors in [116], if the thresholds for UVLS relays are fixed as 0.94(pu), 0.92(pu) and 0.90(pu) respectively, the value for first activation of UVLS may be too high to maintain load in service. In some case, after experiencing transient period, voltage magnitude may decay lower than 0.94(pu) in a period longer than the first time delay of the first threshold (11 seconds), therefore UVLS may not active selectively in long-term voltage collapse. Two dynamic simulations are done following this rule.

The first simulation is done to present the case of voltage collapse: tripping off a generator at bus 4042 at $t=5$ seconds. Figure 5-34 plots the voltage profile of bus 42 corresponding to voltage collapse scenario. When there is no UVLS (the green line), the voltage is collapse after 130 seconds. In case 2 corresponding to the presence of UVLS (the blue line), the effect of avoiding voltage collapse is illustrated clearly by dynamic simulation. However, the first threshold for UVLS is too high that UVLS is activated before activation of ULTC and OEL. This may not be effective in term of remaining loads in service if there is no voltage collapse.

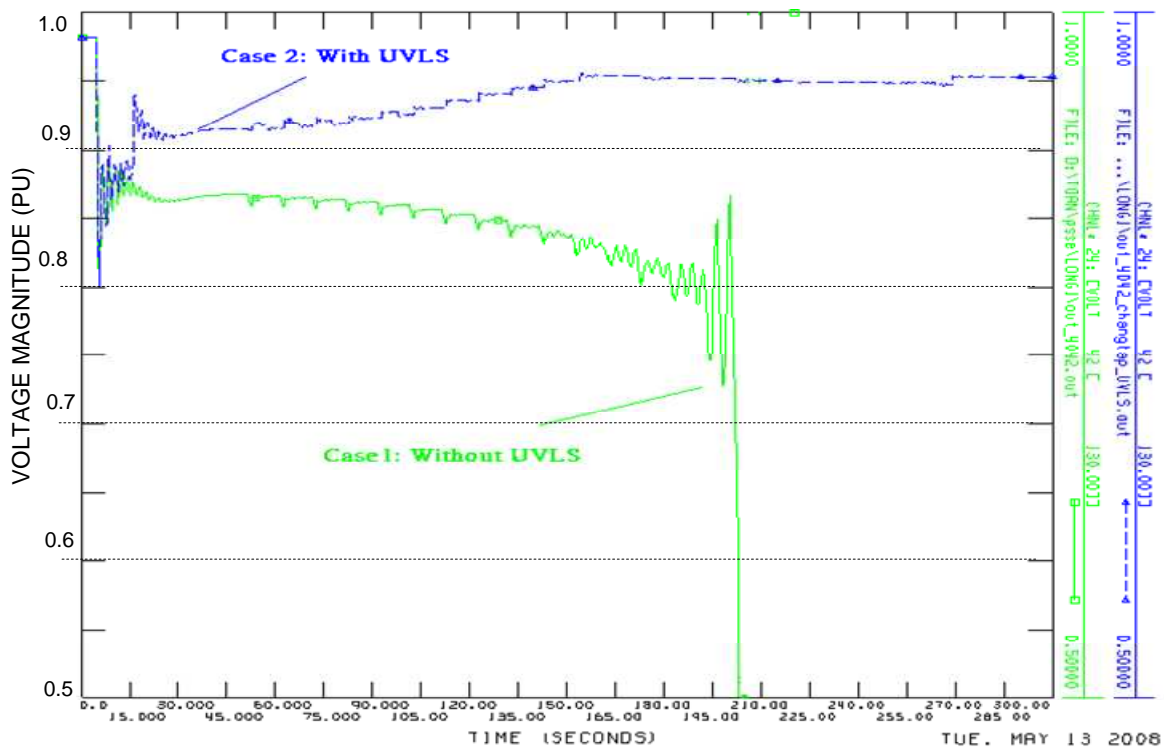


Figure 5-34: Voltage profile of bus 42 when applying rule of authors in [116].

The second scenario was created to present the case without voltage collapse: tripping a generator at bus 5051 at $t= 5$ seconds. Figure 5-35 shows the voltage profile of bus 41 corresponding to the scenario. When there is no UVLS (the green line), after 500 seconds of simulation, the voltages of power system are stable at the value of little bigger than 0.94(pu). In case 2, when applying UVLS, there are 5% of loads shed when transient time is over the 11 seconds and voltage magnitudes are lower than 0.94(pu). That means, UVLS scheme is not working effectively in term of remaining continuously loads in serviced. (Note: this problem may be related to the context of short-term voltage instability that was discussed by J. A. Diaz de Leon II in the reference [130]).

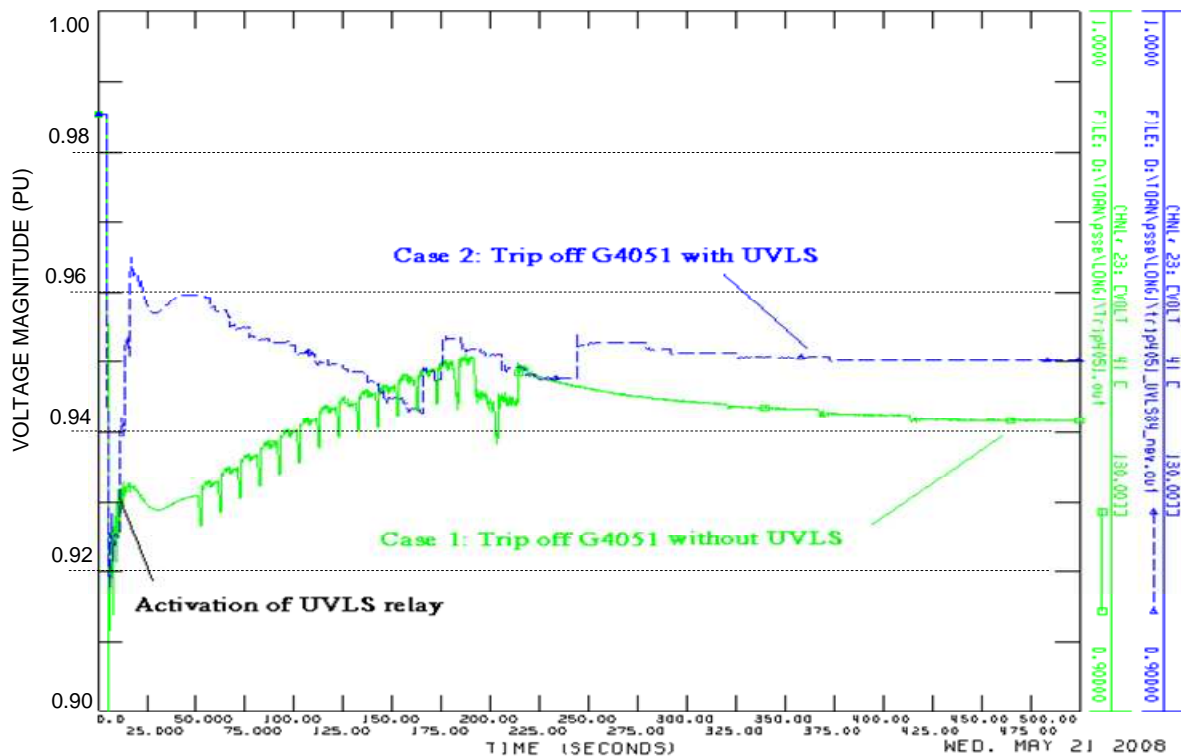


Figure 5-35: Voltage profile of bus 41 when applying rule of authors in [116].

We propose a method that takes into account the advantages of both methods discussed above to choose thresholds for UVLS as follows.

- First activation of UVLS relay if voltage is below 0.93(pu).
- Second activation of UVLS relay if voltage is below 0.92(pu).
- Third activation of UVLS relay if voltage is below 0.9(pu)

Justification of proposed method is investigated through dynamic simulation in the next section.

5.4.2 Choosing Amount of Load Shed

The amount of load needed to shed in order to avoid voltage collapse should be chosen carefully. This amount of load shed depends upon on the specific power system. C. W Taylor [57] did not discussed a procedure for choosing optimal amount of load shed but this choice is done on the basis of the practical operation of Puget Sound power system. The quantity of load shed for each step may vary from 5% to 8% and cumulated load shed may reach from 15% to 20% total load. The authors in [116] also proposed a UVLS scheme with fixed amount of load shed. In the past, the system operators normally control the loads that are supplied by several medium voltage (MV) feeders, which are outgoing from the substation, but they could not control the load at the final customer. Whenever UVLS is performed, the system operators have to trip at least one or two feeders in order to ovoid the voltage collapse. Consequently, the whole feeder loads will be lost. The Figure 5-36 illustrates the centralized UVLS scheme where UVLS relay is placed at the High Voltage busbar.

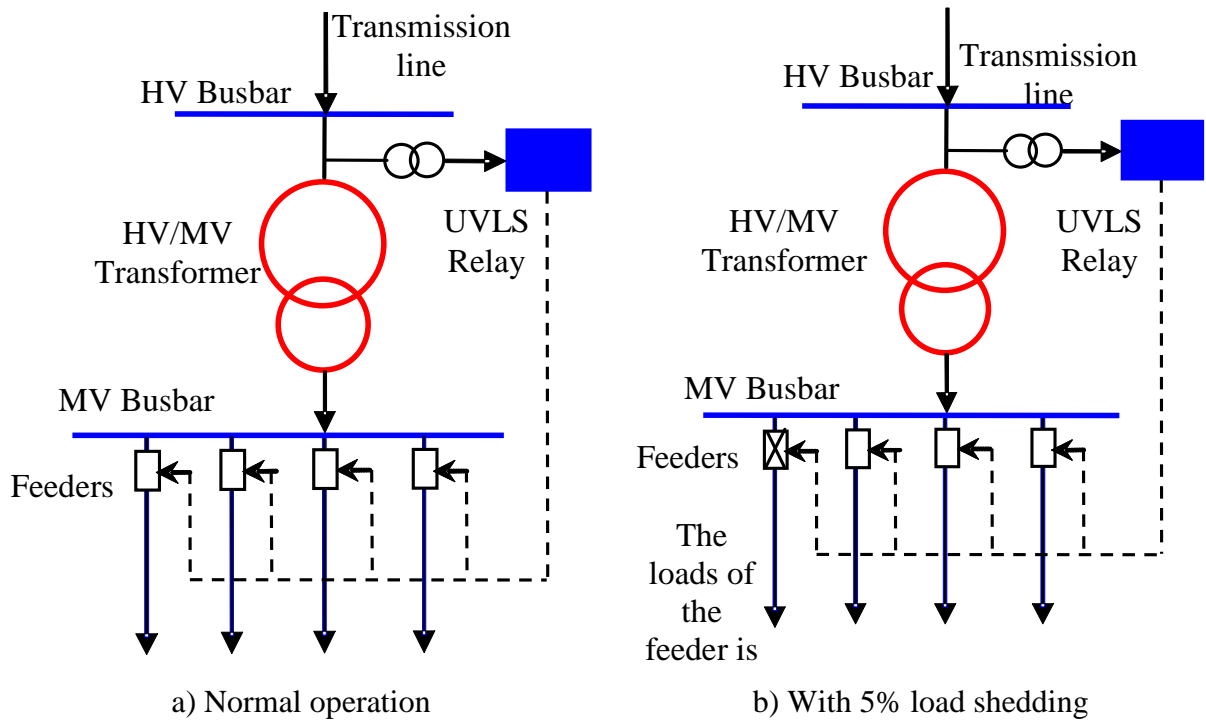


Figure 5-36: Centralized UVLS scheme.

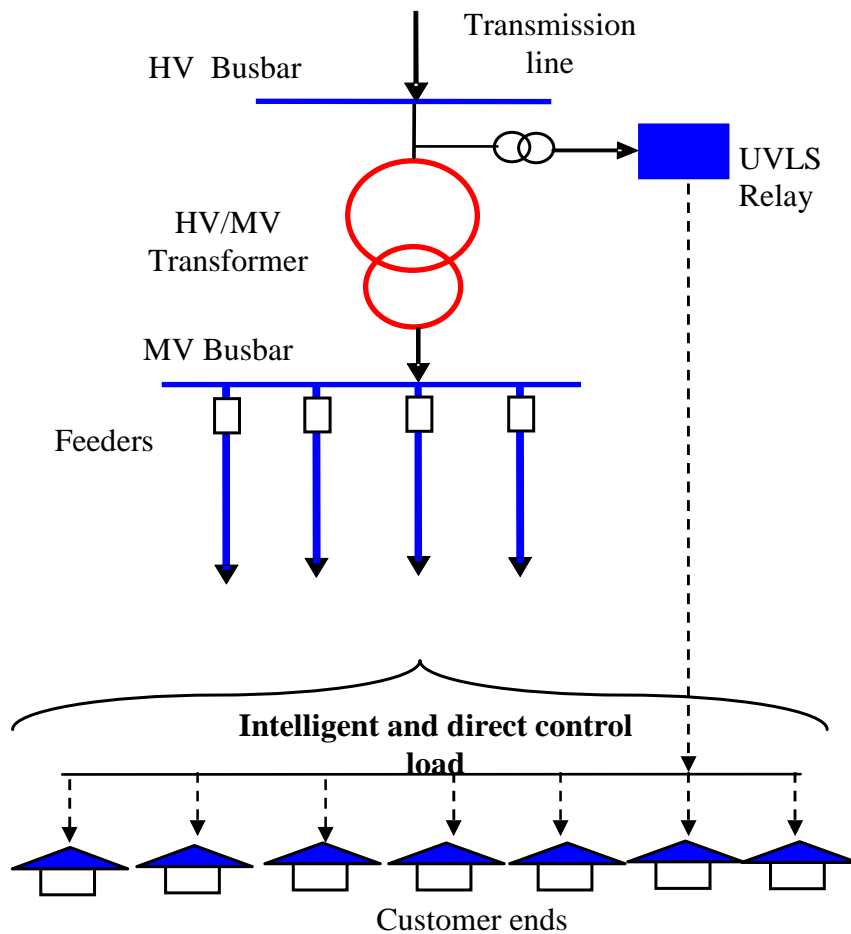


Figure 5-37: New UVLS scheme with direct load control context.

With the new trend in developing intelligent loads that could be adaptive to customer profile, the loss of several percent of load may not have any influence on the customer comfort. Therefore, the output signals of UVLS relays will be transmitted directly to the customer. At the customer's, the control signal is converted into new control signal corresponding to new set-point for radiators, or air-conditioners. The intelligent loads will be controlled to reduce the several percent of total customer load in order to prevent voltage collapse [131]. In this part, the rule of C. W. Taylor proposed in [57] is adopted as criterion for choosing amount of load need to be shed in the new context mentioned above. The effectiveness of this method could be observed through dynamic simulation in the next section. The Figure 5-37 illustrates the new context of using UVLS scheme.

5.4.3 Choosing Time for Activation and Time Steps of UVLS

5.4.3.1 Determination of the Time Steps of UVLS

The time steps of UVLS are expected as small as possible that reduces risk of voltage collapse. However, these values depend on many factors such as the circuit breakers, duration of transmitting decision control signal through communication facilities, selective and coordination requires. Transient stability when shedding load is also considered while choosing the time steps. These values must be chosen dependently on the specific power system. In this section, a rule of a rule of C. W. Taylor [57] is adopted here as major rule:

- 5% of load shed if voltage is below 0.9(pu) with 3.5 seconds time delay.
- 5% of load shed if voltage is below 0.92(pu) with 5 seconds time delay.
- 5% of load shed if voltage is below 0.92(pu) with 8 seconds time delay.

5.4.3.2 Determination of the Time for Activation of UVLS

As analyzed in chapter 4, ULTC and OEL are factors that play very important roles in voltage collapse. In practice, activation of ULTC and OEL are major causes of voltage collapses leading totally power system blackouts. Therefore, when choosing time for activation of UVLS, much attention of the ULTC and OEL setting time must be taken into account. In general, time for first activation of ULCT is about 30 seconds, and 5 seconds for moving one tap (in OLTC1 model in the software PSS/E, 10 seconds is time for two taps moving). In cases of disturbance without voltage collapse, ULTC is activated to restore controlled bus voltage as before contingency after some movements of tap position; therefore, time for activation of UVLS should be bigger than 30 seconds. In practice, the initial tap position is set near the zero position, with +16 forward positions and -16 backward positions. Then, the maximum movement is about 16 tap positions for each direction. Therefore, the maximum time is about $16 \times 10 = 160$ seconds whenever ULTC changes its tap positions. In order to prevent voltage collapse because of activation of ULTC, the time for activation of UVLS should be smaller than 160 seconds.

In cases of disturbance causing voltage collapse, power system voltage is normally going to very dangerous conditions or voltage collapse only after OELs are activated to protect rotor winding (after 120s) [68]. Therefore, time for activation of UVLS is chosen not bigger than

120s. In this section, time for first activation of UVLS is chosen as equal to 120s after the disturbance.

5.4.4 Validation of UVLS by Dynamic Simulation

The UVLS scheme base on the advantages of both methods discuss above and the new context of using direct load control is summarized as follows

Activation of UVLS 120 seconds after the contingency.

- 5% of load shed if voltage is below 0.9(pu) with 3.5 seconds time delay.
- 5% of load shed if voltage is below 0.92(pu) with 5 seconds time delay.
- 5% of load shed if voltage is below 0.93(pu) with 8 seconds time delay.

The effectiveness of this scheme is illustrated by simulation of some training voltage collapse scenarios for the “Nordic power system” as follows:

5.4.4.1 Scenario 1

Scenario 1 is proposed as follows: A transmission line in the “North area”, between buses 4011-4021 is tripped at $t=5(s)$ and generator at bus 4012 (loss a generating unit with 600 MW) is tripped off 0.1(s) latter (similar as scenario 1 in section 5.2).

The Figure 5-38 shows the voltage profile of bus 41 for two cases: with and without UVLS. The blue line is the voltage profile of bus 41 when there is no UVLS. The voltage is collapse at about 130 seconds after the contingency. The green line is the voltage profile of bus 41 when there is UVLSs. The system voltages are kept stable at about 0.95 (pu).

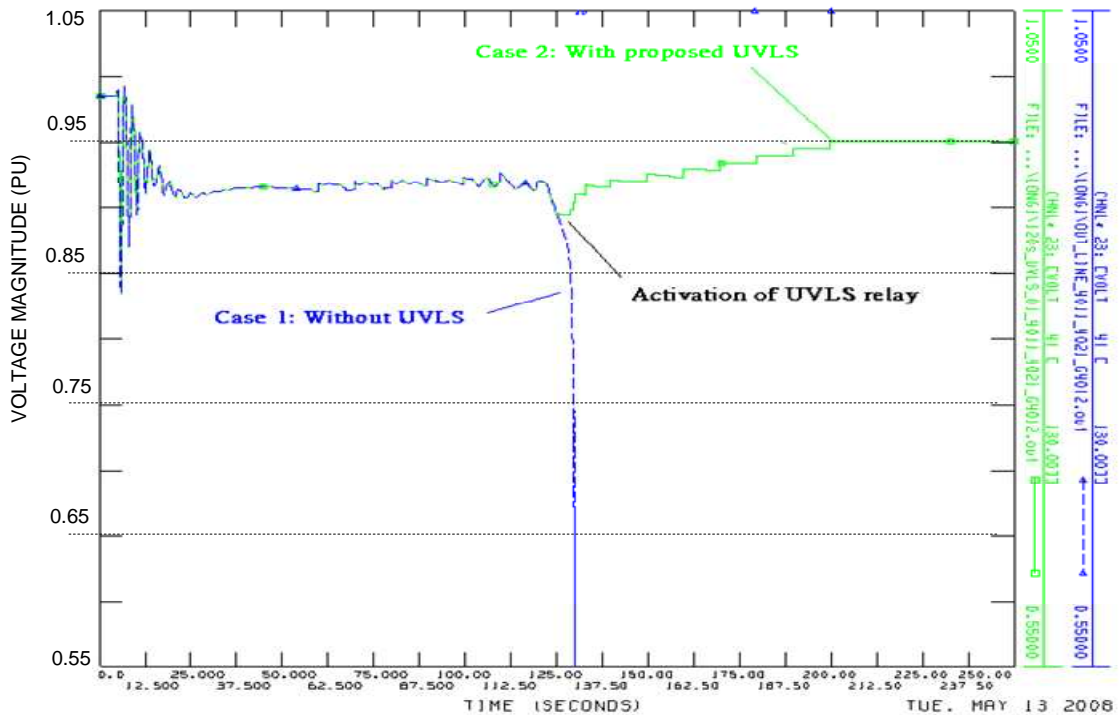


Figure 5-38: Scenario 1-Voltage profile of bus 41 with the proposed UVLS scheme.

5.4.4.2 Scenario 2

Scenario 2 is proposed as follows: Trip off a generator at bus 4047 in Central area as loss of a generator with 540 MW active power and 152 MVAR reactive power (similar as scenario 2 in section 5.2).

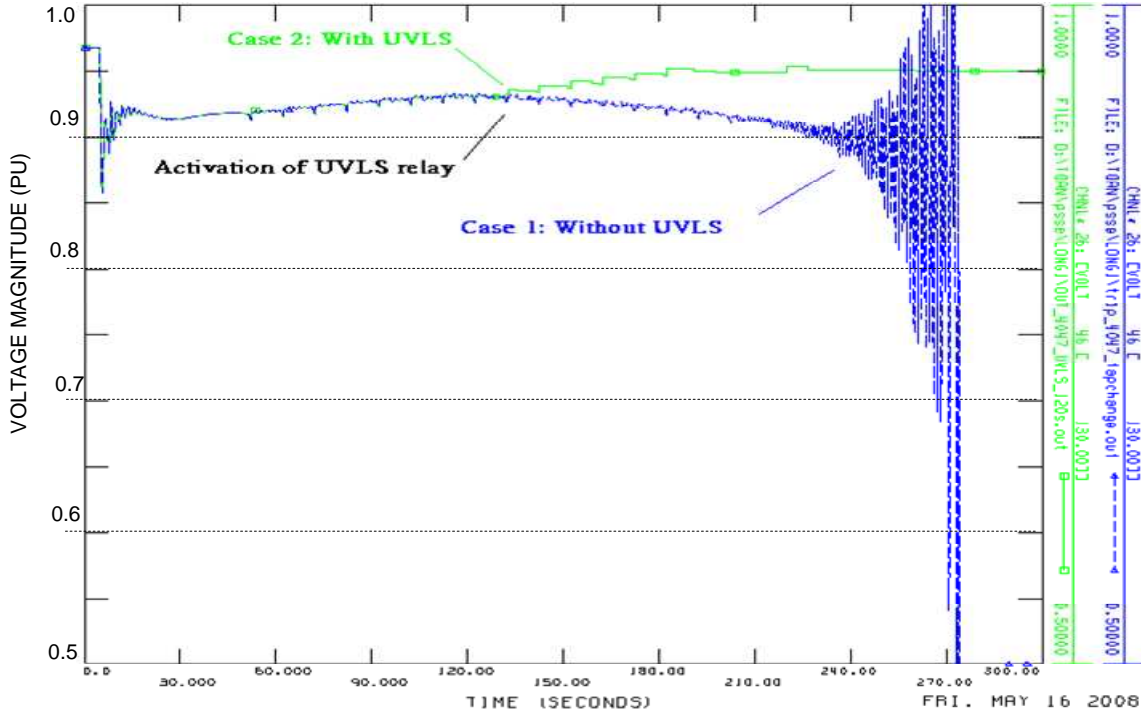


Figure 5-39: Scenario 2-Voltage profile of bus 46 with the proposed UVLS scheme.

Figure 5-39 shows the voltage profile of bus 46 for two cases: with and without UVLS. The blue line is the voltage profile of bus 46 when there is no UVLS. The voltage is collapse at about 270 seconds after the contingency. The green line is the voltage profile of bus 46 when there is UVLSs. The system voltages are kept stable at about 0.95 (pu) at t=300 seconds.

5.4.4.3 Scenario 3

Scenario 3 is proposed as follows: a generator at bus 4042 in the “Centralarea” is tripped at t=5(s) as loss of 630 MW active power and 265 MVAR reactive power (similar as scenario 3 in section 5.2).

Figure 5-40 shows the voltage profile of bus 42 for two cases: with and without UVLS. The blue line is the voltage profile of bus 42 when there is no UVLS. The voltage is collapsed at about 200 seconds after the contingency. The green line is the voltage profile of bus 42 when there is UVLSs. The system voltages are stable at about 0.9 (pu).

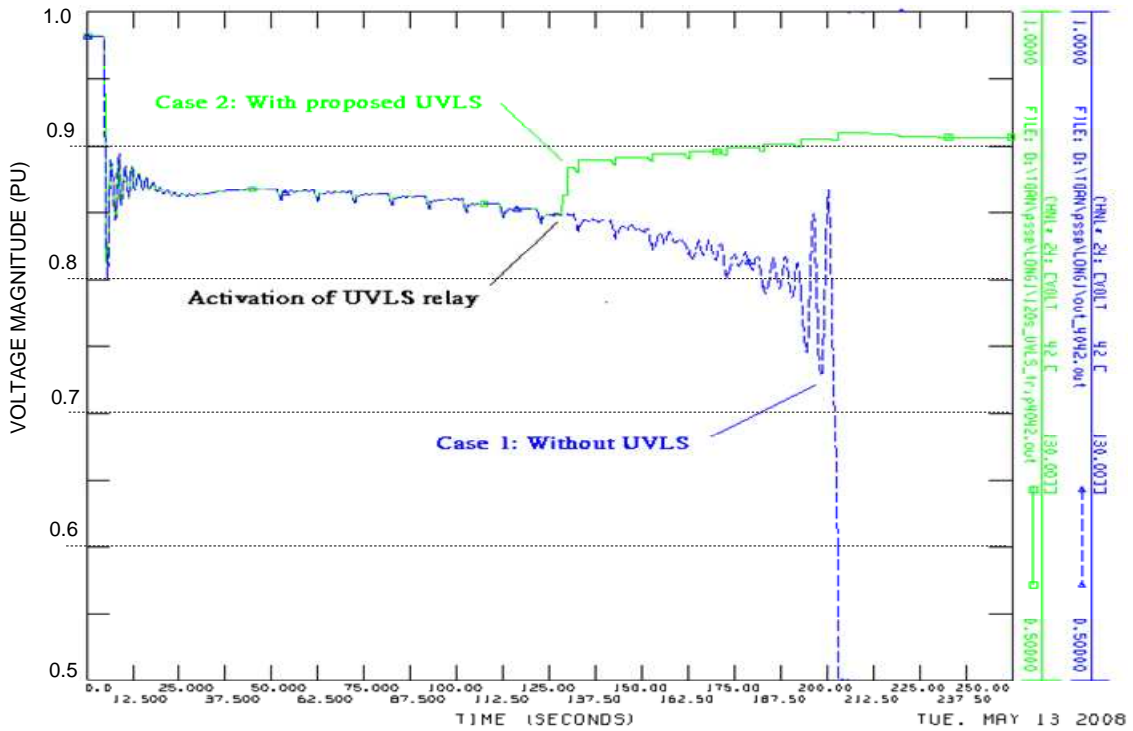


Figure 5-40: Scenario 3-Voltage profile of bus 42 with the proposed UVLS scheme

5.4.4.4 Scenario 4

Scenario 3 is proposed as follows: An interconnection transmission line between North and South areas: 4031-4041 is tripped at $t=5(s)$ and generator at bus 4031(loss of 310 MW and 113 MVar) is tripped off 0.5(s) latter.

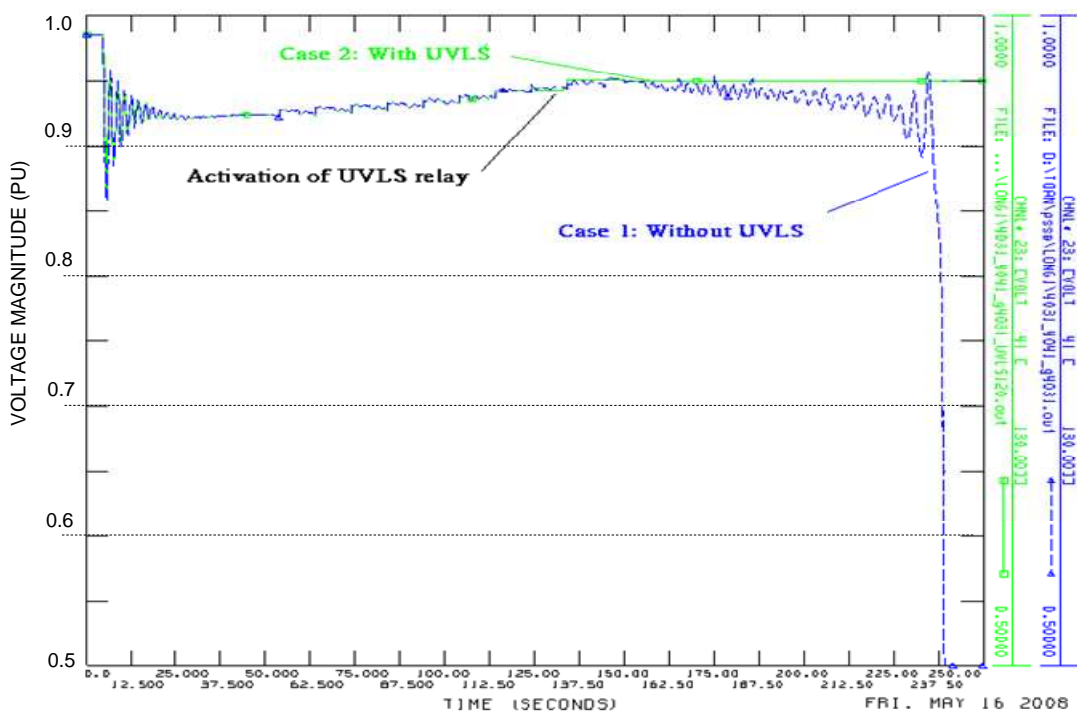


Figure 5-41: Scenario 4-Voltage profile of bus 41 with the proposed UVLS scheme.

Figure 5-41 shows the voltage profile of bus 41 for two cases: with and without UVLS. The blue line is the voltage profile of bus 41 when there is no UVLS. The voltage is collapse at about 200 seconds after the contingency. The green line is the voltage profile of bus 41 when there is UVLSs. The system voltages are stable at about 0.95 (pu).

From the validation results above, with differently proposed long-term voltage collapse scenarios, we could observe the proposed UVLS scheme could prevent power system from being voltage collapse after some severe contingencies.

5.4.4.5 Scenario 5

In order to illustration the effective of this UVLS scheme in the case of there is no voltage collapse, a non-collapse scenario is proposed as follows: an interconnection transmission line between North and South areas: 4032-4044 is tripped at $t=5s$.

In this case, because voltage magnitudes of buses are still greater than the threshold, that mean there is no threat of voltage collapse. Then even being activated at $t=125(s)$, the UVLS relays do not perform load shedding.

From the above simulations, the proposed UVLS scheme is operated effectively in term of voltage collapse prevention.

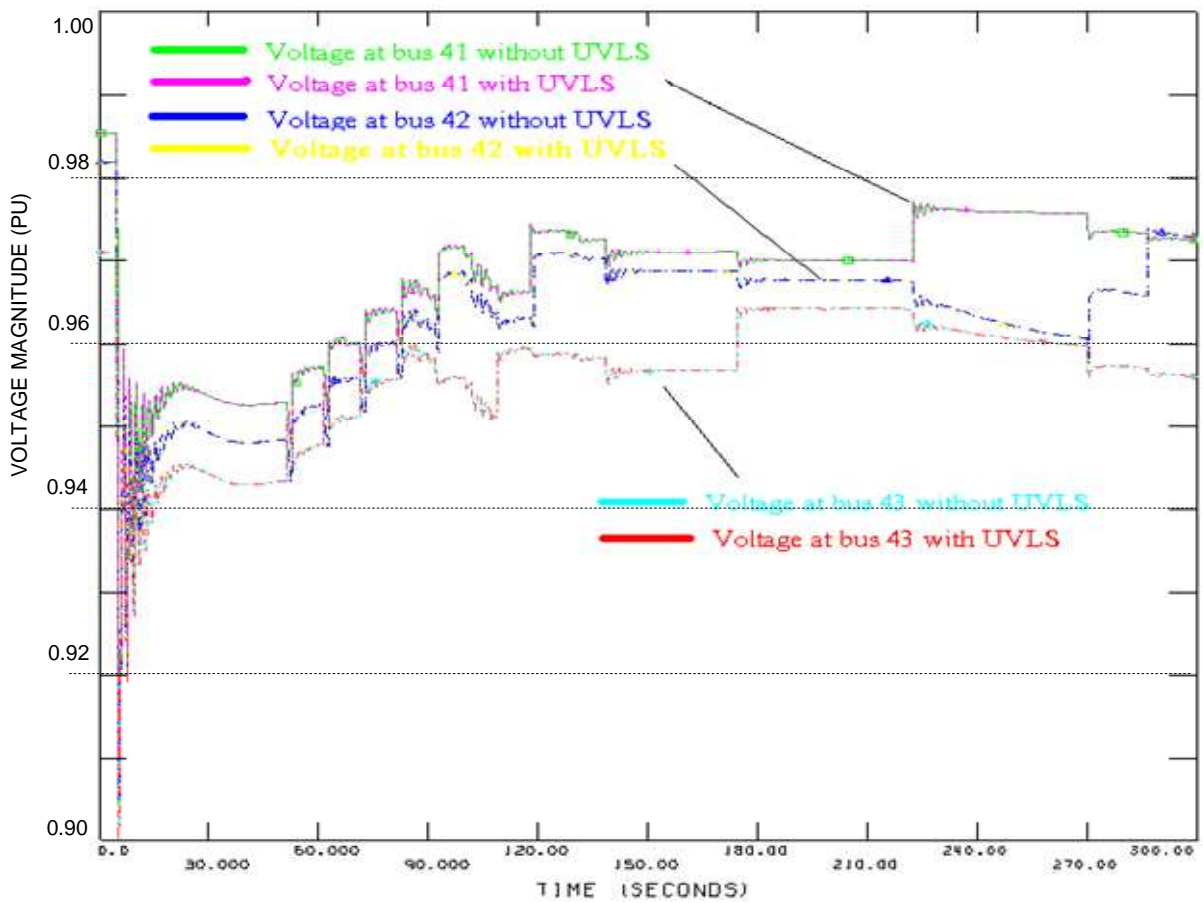


Figure 5-42: Scenario 5-Voltage profile of buses 41, 42, 43 with the proposed UVLS scheme.

5.5 CONCLUSIONS

In this section, factors influencing on voltage collapse were investigated by using dynamic simulation for the BPA system and the Nordic power system.

Influences of static and dynamic load models on investigating voltage collapse were discussed in detail. The influence of static load modeling on voltage collapse depends on the variation of load with respect to voltage. Constant power loads have the worst influence on voltage collapse because when the voltage reduces, the constant loads still try to recover full rated value and the load is independent of voltage magnitude. As the result, voltage magnitude will be reduced further. Constant impedance loads have the least influence on voltage collapse because when voltage reduces, loads also reduce its value proportionally to the square of the voltage magnitude. Dynamic load plays an important role in voltage collapse; especially for induction motor load, since the induction motor loads is a major cause for voltage collapse.

Influence of ULTC and OEL are direct causes for voltage collapse. The impact of ULTC and OEL on voltage collapse as well as dynamic behavior of these automatic devices during long-term dynamic simulation were also investigated.

Some scenarios that are suitable for investigation of voltage collapse were proposed and simulated for two power systems: the BPA and Nordic power systems. Long-term dynamic simulations show that voltage collapse was the total results of a complicated dynamic process where many automatic voltage regulation devices involved.

In this chapter, major problems concerning voltage collapse preventions were discussed.

From preventive actions point of view, a static voltage collapse indicator was used for voltage collapse assessment firstly. The purpose is to answer the question: how close the system is to voltage collapse point? And then, a preventive control strategy was proposed. The major advantages of this proposed control strategy are not only easy to implement in practical system but also provide a quick control decision. This only requires a conventional load flow calculation program, and a quadratic optimal algorithm, this prevention control strategy meets the requirements of quickly identifying how critical the state of the power system is and which controller variable should be used to avoid voltage collapse. Dynamic simulation shown the effectiveness of proposed method, even in some very critical power system, the proposed method may not prevent power system from voltage collapse but we have more time to act urgent corrective actions.

From the corrective action point of view, an undervoltage load shedding scheme under new concept of directly controlled load was proposed and tested with the “Nordic power system”. In some very urgent situations, when voltage is going to collapse, UVLS is the viable solution that could save power system from collapsing. In this part, the UVLS scheme was not considering optimal decision problems such as optimal load amount of load shed, but it can easily used in real power systems. Because the time period of voltage collapse is normally very short, the goal of keeping power system stability is more important than the goal of optimal load shedding. In this chapter, the proposed UVLS were worked effectively with some different voltage collapse scenarios.

CHAPTER 6

CONCLUSIONS AND PERSPECTIVES

6.1 CONCLUSIONS

This dissertation has presented some original contributions to analyze the recent power system blackouts. By learning the lessons from past power system blackouts, some contributions to prevent future power system blackout were provided. First of all, major general suggestions about power system blackouts were summarized in accordance with the international experience. Main contributions to the improvement of rotor angle stability and voltage stability is discussed next. Some specific conclusions are made as below:

6.1.1 Major Suggestions to Preventing Power System Blackouts

Power system blackouts are mainly related to complicated phenomena, which have many diversity causes. They are always related to critical contingencies, equipment failures or poor coordination between control centers. Power system blackouts are normally the final result of successively interrelated events that would otherwise be manageable if they appeared alone. Therefore, some suggestions from the system management point of view in order to prevent power system blackout are listed as follows:

The improvement of existing substations and other equipment through refurbishing, constant inspection, and maintenance, and replacement of critical components, investing new power system facilities (new transmission lines, or new power plant) is vital to the prevention of cascading events.

Normal planning studies cannot capture all of the possible scenarios due to the vast number of possible uncertainties and operating actions. Therefore, reliability standards applied in power system studies should be constantly evolving in accordance to the requirements of the grid and international state-of-the-art practices and technological developments. In designing and planning state, N-m (with $m \geq 2$) criterion should be considered for critical contingency analyses, especially for interconnected power system.

The use and enhancement of special protection systems can be quite effective at times in preventing cascading outages. The application of automatic controls such as automatic voltage regulators, and where applicable power system stabilizers, should be mandatory for generators.

It is of vital importance to enforce and constantly encourage training programs for system operators. The lessons learned from past mistakes must be incorporated into new procedures as well as using such lessons learned to help develop new and improved technologies for system control and monitoring.

Another big challenge is to ensure the redundancy and reliability of remote control and telecommunication devices. Their interactions with control systems should also be

investigated. This plays especially important role in coordination between control centers and performs urgent preventive and corrective actions.

Rapid system restoration is extremely important in order to minimize the impact of a blackout on society. System operators should be given regular refresher training and live drills on system restoration to ensure that they remain familiar with restoration procedures and best practices. Some researches should be devoted to restoration procedures; there are very few contributions on that topic in the present literature.

6.1.2 Contribution to Improving Small Signal Stability

In this dissertation, an energy-based method for the optimal placement of controllers/sensors (or equivalent to selection of inputs/outputs) with the goal of improving controllability and observability gramians was proposed as one of preventive method to improve small signal angle stability.

This heuristic method is based on various scenarios reflecting different set-points or failure situations. This important characteristic introduces some robustness in decision making with respect to system nonlinearities and failure scenarios of power system. This is not provided by any of the existing methods used for optimal location of controllers/sensors in power systems. The method also employed a model reduction technique in order to deal with the dominant modes of the large-scale power system.

6.1.3 Contribution to Improving Angle Transient Stability

In this dissertation, some major factors influencing on transient stability such as fault clearing time, fault location, or load level of generators were investigated in detail by using a time-domain simulation method.

From the transient stability prevention point of view, the critical clearing time of generators is considered as a measure for transient stability improvement. The dissertation proposed a preventive strategy that redispatches active power output of generator while increases the critical clearing time greater than a predefined threshold.

The linear relationship between CCTs and generator output has been utilized for choosing the total shifted power. The idea of using controllability gramian for partitioning the total shifted to candidate generators was firstly introduced.

The effectiveness of transient stability improvement was achieved without solving any differential equation.

6.1.4 Contribution to Improving Voltage Stability

Major factors influencing voltage collapse have been investigated. Particularly, behavior of load characteristics, transformer equipped with underload tap changer, and overexcitation limiters have been investigated in detail by long-term dynamic simulations.

From the preventive action point of view, a static voltage collapse indicator (L) was firstly used for voltage stability assessment. The indicator helps power system operator to know how far the system is from the collapse point. A preventive method with the goal on maintaining a

desirable voltage profile was also proposed. The method only requires conventional loadflow computation, therefore; it could not only implement easily in the practical power system, but also provide some quick control decision. This prevention method meets the requirements of quickly identify how critical the state of the power system is and which controller variable should be used to avoid the risk voltage collapse.

From the corrective action point of view, undervoltage load shedding is the ultimate solution that could save the power system in very urgent situations. In this dissertation, an undervoltage load shedding scheme based on the assumption of using the intelligent and direct load control was proposed and tested with the “Nordic power system”. The new scheme firstly determines the amount of load shed for the necessary situations (preventive or corrective situation), then, tripping signal will be sent directly to the customer. The commands will be converted into new reference control input of load. The load will be reduced several percent to avoid voltage collapse but without violating the customer’s comfort. Even the scheme has not considered the optimal load shedding problem, but it till have many advantages such as simple to implement in real power system, and could be used as intelligent preventive method.

6.2 PERSPECTIVES

6.2.1 Perspectives Concerning the Research

From the dissertation results, some perspectives and research directions need to be further investigated as follows:

The use of controllability gramians is opening some great promised applications in large-scale power systems. For example, this method could be used for optimal placement of FACTS devices as well as choosing suitable control inputs in order to improve overall power system performance and robustness. When dealing with the problem of secondary voltage control, this method could be further study for choosing control signals such as terminal voltage of generators, changing tap position of transformers equipped with ULTC in order to prevent power system blackout. In order to prevent transient angle instability, researchers and operators are still looking for the effective prevention methods. It is evident that the implementation of corrective methods are always more difficult in term of time frame and application. The use of controllability gramian could easily identify and partition power generation output. This is a new direction in term of transient stability prevention and need further studying in order to have most effective application.

In practice, there has been introduced and applied some new control structure in power system- or Wide Area Measurement Systems-WAMS, such as the use of Phasor Measurement Units. The problem of optimal placement of PMU in a system with thousands of buses could be solved effectively by using observability gramian and integer-programming.

The use of controllability/observability gramians could open a new approach that not only ensuring both the design of optimal control architecture and the tuning of the resulting controllers

When dealing with voltage collapse problems, load shedding is a medial and necessary way for saving the power system. This task requires exactly dynamic simulations corresponding to the particular case in order to have right setting values and correct location UVLS relays. Dynamic shedding is a large-scale mixed programming problem that is hardly solvable by existing optimization methods. Some researches should be conducted to propose exact real-time load shedding schemes, rather than heuristic methods such as the here-proposed one. In a near future, the loads become more intelligent and active. They could also be controlled and adjusted smoothly. By effectively controlling and managing the load, we could prevent power system blackout without violating the customer comfort.

6.2.2 General Perspectives

The problem power system blackout is one of the most difficult problems in electrical engineering. This catastrophe involves many factors such as planning and designing, operating stage, maintenance duty as well as unforeseen and fatal contingencies. Therefore, it is necessary to conduct more researches focusing on each specific aspect in order to find effective preventive and corrective methods for preventing power system blackout in the future. Some general perspectives related to power system blackout prevention is suggested as following:

In order to propose effectively blackout prevention methods, it is necessary to investigate and study carefully the mechanisms and root causes of such complicated phenomena from both physical and mathematical points of view. Lessons from the past power system blackouts must be comprehended and trained cautiously through exact simulation tools. Exact models of generators, controllers and protective devices are also mandatory in monitoring and analyzing tools. Therefore, we need for improving simulation and Computer Aided Decision tools (CAD).

We need to define new control schemes in order to take into account the nonlinear dynamics for example: a fault-tolerant control scheme. The use of Information Communication Technology (ICT) should be applied in order to take advantage of distributed control for a better coordination of subsystem, or take into account the communication constraints (for example the latency or lost of information).

The new context of intelligent directed controlled load opens very promising tendency for power system blackout prevention not only as preventive but also as corrective methods. We need more research in order to perform the new idea into the real power system.

Appendix A

The Branch and Bound Method for Integer Programming

The method branch and bound applies to the resolution of combinatorial optimization problems with a large number of solutions. It is to divide the initial problem into several sub-problems and then eliminate some sub-problems with a system majorant and minorant

Consider an integer programming cost function as follows:

$$\begin{aligned} \min z &= C.x \\ \text{constraint } A.x &\leq b \\ x_j &= 0, \text{ or } 1 \quad (j=1, \dots, n) \end{aligned} \tag{A-1}$$

where:

z represents the cost function,

A is a matrix with dimension of $m \times n$

C is one vector with dimension of $1 \times n$

B is one vector with dimension of $m \times 1$

This problem has a finite number of solutions n vectors (because x can not anyway take 2^n possible values). The problem is to find one of these options as the optimal solution. But if the list is too big, when $n > 50$, it takes centuries to get the solution.

The Branch and Bound method consists in enumerating these solutions in an intelligent manner. This method allows finding the optimal solution among all its solutions without having to examine them all and avoid the listing of large classes of bad solutions. In a good algorithm by Branch and Bound method, only potentially good solutions are listed.

A.1: Principle of Building a Branching Tree

The principle of building decision tree is summarized as follows:

1. Let S is all n vectors whose components have the value 0 or 1. We will build a tree (called decision tree) subsets of the S form a partition S .
2. At each iteration of the building of the tree, we choose one component of the vector x_i . A branch will correspond to the subset of vectors with $x_i = 1$ or $x_i = 0$.

To explain the algorithm Branch and Bound, we chose the following example with three variables in integer ($n = 3$).

$$\begin{aligned} \text{Min } f &= -4x_1 + x_2 - 2x_3 \\ \text{constraint } : 0 &\leq x \leq 1 \quad (i=1, \dots, 3) \end{aligned} \tag{A-2}$$

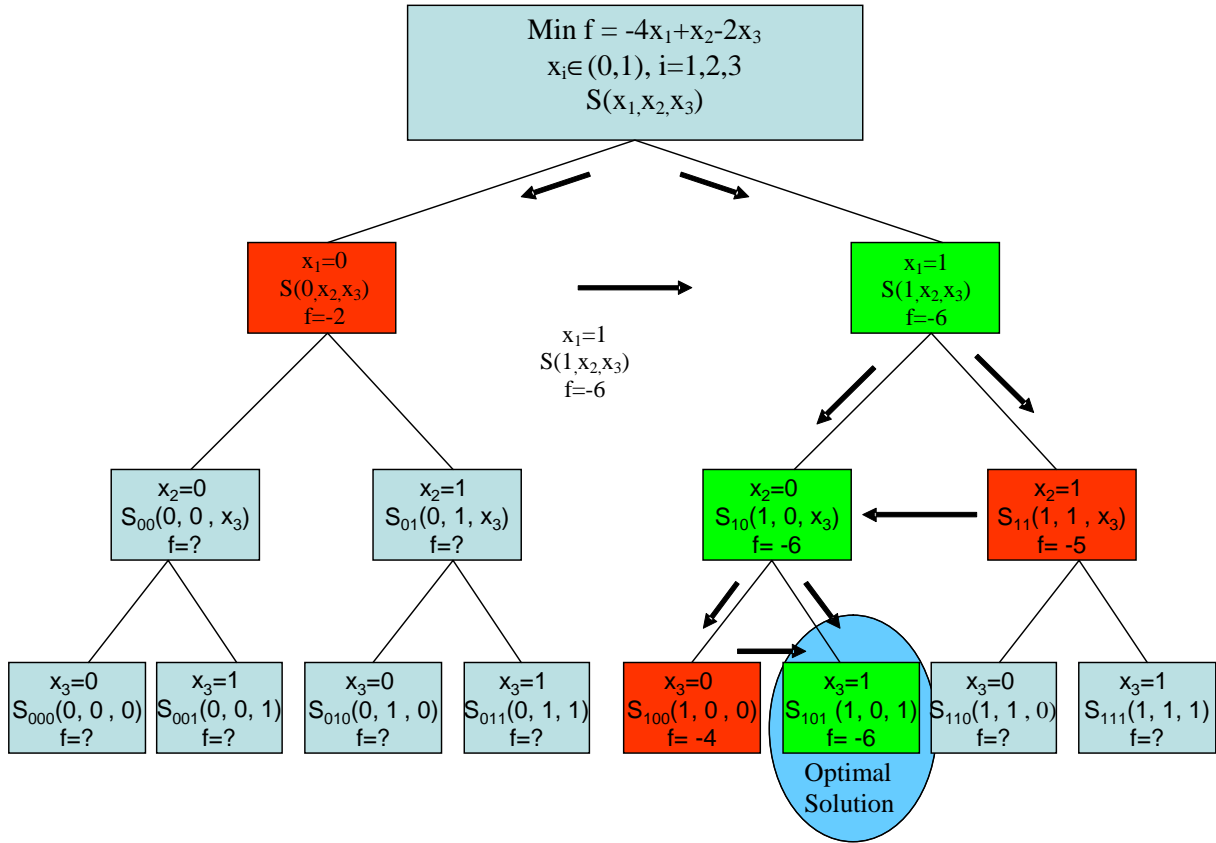


Figure A-6-1: Principle of Branch and Bound method.

In this case, the principle of building a branching tree includes three layers as in Figure A-6-1.

- For the first layer: the set of S is separated into two sub-set $S_0(0, x_2, x_3)$ with $x_1=0$ and $S_1(1, x_2, x_3)$ avec $x_1=1$ ($S = S_0 \cup S_1$).
- For the second layer: the sub-set $S_0(0, x_2, x_3)$ is separated into two sub-set $S_{00}(0, 0, x_3)$ with $x_2=0$ and $S_{01}(0, 1, x_3)$ with $x_2=1$ ($S_0 = S_{00} \cup S_{01}$). The same procedure is done for the sub-set $S_1(S_1 = S_{10} \cup S_{11})$.
- For the third layer, the sub-set $S_{00}(0, x_2, x_3)$ is still separated into two sub-set $S_{000}(0, 0, 0)$ with $x_3=0$ and $S_{001}(0, 0, 1)$ with $x_3=1$ ($S_{00} = S_{000} \cup S_{001}$). The same procedure is done for the sub-set ($S_{01} = S_{010} \cup S_{011}$), S_{10} ($S_{10} = S_{100} \cup S_{101}$), S_{11} ($S_{11} = S_{110} \cup S_{111}$).
- Finally, we have 8 (2^3) combinations.

Note: When a node, with non-optimal solution is determined in the tree search (see evaluation part), it is unnecessary to carry out the separation of its space solutions

A.2: Principle of Evaluation of Bound

The evaluation of a node of decision tree aims to determine the optimum of all the solutions associated with the node in question, or to prove mathematically that this set does not contain a solution of the problem.

For example, in the assessment phase, it is assumed that the programming non-linear Fmincon (in optimization toolbox of the program Matlab) is used to evaluate the objective function f .

- For the first layer, it requires two independent evaluations by Fmincon. The value of the function f evaluated by Fmincon gives $f = -2$ for $x_1 = 0$ ($S_0(0, x_2, x_3)$) and $f = -6$ for $x_1 = 1$ ($S_1(1, x_2, x_3)$), respectively. Subset $S_1(1, x_2, x_3)$ will be retained to continue the evaluation. By against the subset $S_0(0, x_2, x_3)$ and the road from this subset will be eliminated.
- For the second layer, the values of f evaluated by Fmincon gives $f = -6$ for $x_2 = 0$ ($S_{10}(1, 0, x_3)$) and $f = -5$ for $x_2 = 1$ ($S_{11}(1, 1, x_3)$), respectively. Subset $S_{10}(1, 0, x_3)$ will be retained to continue the evaluation. By against the subset $S_{11}(1, 1, x_3)$ and the road from this subset will be eliminated.
- The method continues on a heuristic for the next layer. Finally, the optimal solution is a subset $S_{101}(1, 0, 1) = 1$ with $x_1=1, x_2 = 0, x_3 = 1$ and $f = -6$.
- Finally, for $n = 3$ a procedure for 6 evaluations (2×3) must be done instead of 8 (2^3) (For $n = 10$, we would have about 20 evaluations instead of $1024 = 2^{10}$).

In practical system, the Branch and Bound could be applied to optimal selection of controllers/sensor in power system as efficient suboptimal solutions.

Appendix B

The “Two-Area Power System” and “39 Bus New England Power System”

B.1: Data of the “Two-Area Power System”

Load flow data: $S_{base}=100MVA$

Table B-1: Bus data of the “Two area power system”.

No Bus	Bus Name	Base (kV)	Bus Type	Shunt (MVar)	$V_{Scheduled}$ (pu)	Angle (degree)	Pload (MW)	Qload (MVar)
1	'GEN 1'	230.000	2	0.000	1.01000	9.8124	0	0
2	'GEN 2'	230.000	2	0.000	1.01000	-0.0789	0	0
3	'GEN 3'	230.000	3	0.000	1.01000	-6.8000	0	0
4	'GEN 4'	230.000	2	0.000	1.01000	-16.803	0	0
7	'BUS 7'	230.000	1	200	1.00167	-7.9414	1367	100
8	'BUS 8'	230.000	1	0.000	1.00452	-16.405	0	0
9	'BUS 9'	230.000	1	350.0	1.00754	-24.697	1367	100

Table B-2: Generators load flow data of the “Two area power system”.

No Bus	Gen Name	Base (kV)	Pgen (MW)	Qgen (MVar)	Sbase (MVA)	Qmin (MVar)	Qmax (MVar)	Internal Transformer Reactance (pu)
1	GEN 1	230.0000	700	-11.60	900	-300	500	0.01670
2	GEN 2	230.0000	700	166.00	900	-300	500	0.01670
3	GEN 3	230.0000	700	-10.00	900	-300	500	0.01670
4	GEN 4	230.0000	700	110.00	900	-300	500	0.01670

Table B-3: Branch data of the “Two area power system”.

From Bus	To bus	ID	R (pu)	X (pu)	B (pu)
1	2	'1'	0.0025	0.02500	0.04375
2	7	'1'	0.0010	0.0100	0.0175
3	4	'1'	0.0025	0.0250	0.04375
4	9	'1'	0.0010	0.0100	0.0175
7	8	'1'	0.0110	0.1100	0.1925
8	9	'1'	0.0110	0.1100	0.1925

Dynamic data:

Table B-4: Generators dynamic data of the "Two area power system".

Model	G1	G2	G3	G4
	GENROE	GENROE	GENROE	GENROE
X_d	1.8	1.8	1.8	1.8
X_q	1.7	1.7	1.7	1.7
X_l	0.02	0.02	0.02	0.02
X'_d	0.3	0.3	0.3	0.3
X'_q	0.55	0.55	0.55	0.55
X''_d	0.25	0.25	0.25	0.25
X''_q	0.25	0.25	0.25	0.25
R_a	0.0025	0.0025	0.0025	0.0025
T'_{do}	0.4	0.4	0.4	0.4
T'_{qo}	0.4	0.4	0.4	0.4
T''_{do}	0.03	0.03	0.03	0.03
T''_{qo}	0.05	0.05	0.05	0.05
H	6.5	6.5	6.175	6.175
D	0.0	0.0	0.0	0.0

Table B-5: Excitation dynamic data of the "Two area power system".

Model	G1	G2	G3	G4
	EXST1	EXST1	EXST1	EXST1
K_A	200	200	200	200
T_A	0.01	0.01	0.01	0.01
T_B	1	1	1	1
T_C	1	1	1	1
T_R	0.01	0.01	0.01	0.01
V_{Rmax}	6.43	6.43	6.43	6.43
V_{Rmin}	-6	-6	-6	-6
T_F	1	1	1	1
K_F	0	0	0	0

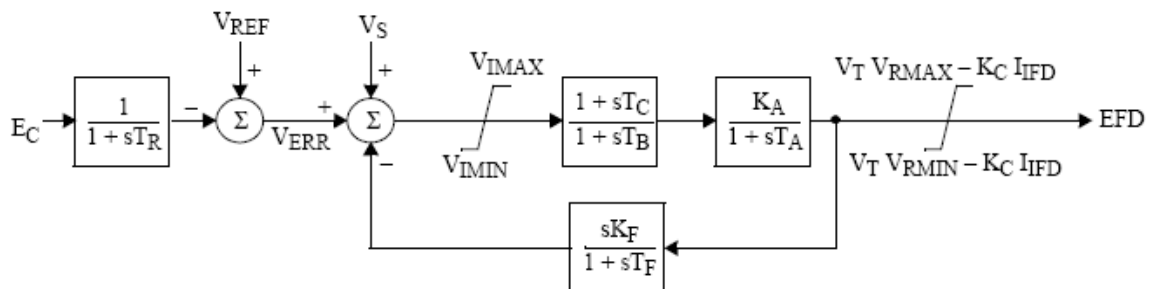


Figure B-6-2: Bloc diagram of the EXST1 model.

Table B-6: PSS data of the “Two area power system”.

Model	G1	G2	G3	G4
	STAB1	STAB1	STAB1	STAB1
K/T	20	20	20	20
T	10	10	10	10
T1/T3	2.238	2.238	2.238	2.238
T3	0.021	0.021	0.021	0.021
T2/T4	5.55	5.55	5.55	5.55
T4	5.4	5.4	5.4	5.4
H _{LIM}	0.2	0.2	0.2	0.2

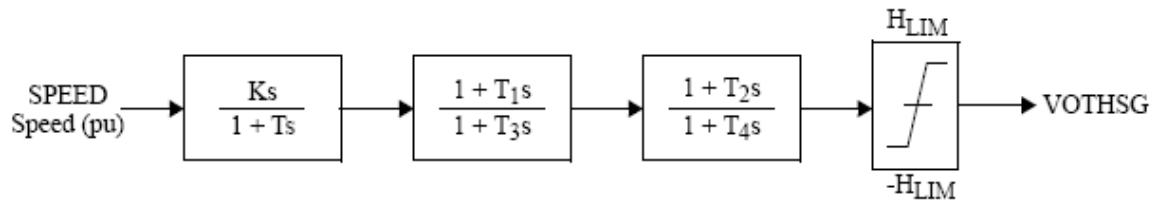


Figure B-6-3: Bloc diagram of the STAB1 power system stabilizer model.

B.2: Data of the “39 Bus New England Power System”

Load flow data: Sbase=100MVA

Table B-7: Bus data of the “39 bus New England System”.

Bus	Bus Type	Shunt (MVar)	V _{Scheduled} (pu)	Angle (degree)	Y-Load (MW)	Y_Qload (MVar)
1	1	0.000	1.04745	-8.9831	0.000	0.000
2	1	0.000	1.04879	-6.3842	0.000	0.000
3	1	0.000	1.03334	-9.1910	301.558	-2.248
4	1	0.000	1.01443	-10.0971	485.880	-178.804
5	1	0.000	1.02154	-9.0707	0.000	0.000
6	1	0.000	1.02519	-8.4191	0.000	0.000
7	1	0.000	1.01329	-0.5326	227.708	-81.811
8	1	0.000	1.01160	-1.0133	510.100	-171.988
9	1	0.000	1.03464	-10.7729	0.000	0.000
10	1	0.000	1.02770	-5.9701	0.000	0.000
11	1	0.000	1.02558	-6.8076	0.000	0.000
12	1	0.000	1.01198	-6.7861	8.300	-85.928
13	1	0.000	1.02451	-6.6372	0.000	0.000
14	1	0.000	1.02073	-8.1883	0.000	0.000
15	1	0.000	1.01903	-8.3176	308.158	-147.338
16	1	0.000	1.03302	-6.7963	308.678	-30.268
17	1	0.000	1.03350	-7.9320	0.000	0.000
18	1	0.000	1.03211	-8.8401	148.322	-28.162
19	1	0.000	1.05016	-1.6349	0.000	0.000
20	1	0.000	0.99121	-2.6258	639.193	-104.836
21	1	0.000	1.03252	-4.3923	257.012	-107.870
22	1	0.000	1.05003	0.0540	0.000	0.000
23	1	0.000	1.04501	-0.1441	226.638	-77.469
24	1	0.000	1.03841	-6.6766	286.193	85.506
25	1	0.000	1.05551	-4.9675	201.060	-42.366
26	1	0.000	1.04260	-6.2648	127.874	-15.639
27	1	0.000	1.03257	-8.2024	263.554	-70.813
28	1	0.000	1.02837	-2.8475	194.790	-26.098
29	1	0.000	1.02458	-0.0267	270.062	-120.885
30	2	0.000	1.04700	-3.9634	9.540	-4.770
31	2	0.000	0.98200	-1.5868	1040.626	-235.649
32	2	0.000	0.98300	1.9442	0.000	0.000
33	2	0.000	0.99700	3.5835	0.000	0.000
34	2	0.000	1.01200	2.5663	301.558	-2.248
35	2	0.000	1.04900	5.0160	485.880	-178.804
36	2	0.000	1.06300	7.7115	0.000	0.000
37	2	0.000	1.02700	1.8339	0.000	0.000
38	2	0.000	1.01000	7.1285	227.708	-81.811
39	3	0.000	1.03000	0	510.100	-171.988

Table B-8: Generators load flow data of the “39 bus New England System”.

No Bus	Pgen (MW)	Qgen (MVAr)	Sbase (MVA)	Qmin (MVAr)	Qmax (MVAr)
30	250	142	1000	-500	800
31	541	324	1000	-500	800
32	650	155	1000	-500	800
33	632	106	1000	-500	800
34	508	163	1000	-500	800
35	650	208	1000	-500	800
36	560	98	1000	-500	800
37	540	5.8	1000	-500	800
38	810	76	1000	-500	800
39	1000	61	1000	-500	800

Table B-9: Branch data of the “39 bus New England System”.

From Bus	To Bus	R (pu)	X (pu)	B (pu)	From Bus	To bus	R (pu)	X (pu)	B (pu)
1	2	0.00350	0.04110	0.69870	13	14	0.00090	0.01010	0.17230
1	39	0.00100	0.02500	0.75000	14	15	0.00180	0.02170	0.36600
2	3	0.00130	0.01510	0.25720	15	16	0.00090	0.00940	0.17100
2	25	0.00700	0.00860	0.14600	16	17	0.00070	0.00890	0.13420
3	4	0.00130	0.02130	0.22140	16	19	0.00160	0.01950	0.30400
3	8	0.00110	0.01330	0.21380	16	21	0.00080	0.01350	0.25480
4	5	0.00080	0.01280	0.13420	16	24	0.00030	0.00590	0.06800
4	14	0.00080	0.01290	0.13820	17	18	0.00070	0.00820	0.13190
5	-6	0.00020	0.00260	0.04340	17	27	0.00130	0.01730	0.32160
5	8	0.00080	0.01120	0.14760	21	22	0.00080	0.01400	0.25650
6	7	0.00060	0.00920	0.11300	22	23	0.00060	0.00960	0.18460
6	11	0.00070	0.00820	0.13890	23	24	0.00220	0.03500	0.36100
7	8	0.00040	0.00460	0.07800	25	26	0.00320	0.03230	0.51300
8	9	0.00230	0.03630	0.38040	26	27	0.00140	0.01470	0.23960
9	39	0.00100	0.02500	1.20000	26	28	0.00430	0.04740	0.78020
10	11	0.00040	0.00430	0.07290	26	29	0.00570	0.06250	1.02900
10	13	0.00040	0.00430	0.07290	28	29	0.00140	0.01510	0.24900

Table B-10: Transformer data of the “39 bus New England System”.

From Bus	To bus	R (pu)	X (pu)	TAP	From Bus	To bus	R (pu)	X (pu)	TAP
2	30	0.000	0.0181	1.025	19	33	0.0007	0.0142	1.007
31	6	0.000	0.0250	0.90	20	34	0.0009	0.018	1.009
10	32	0.000	0.020	1.07	22	35	0.00000	0.0143	1.025
12	11	0.00160	0.0435	1.006	23	36	0.00050	0.0272	1.00
12	13	0.00160	0.0435	1.006	25	37	0.00060	0.02320	1.025
19	20	0.0007	0.0138	1.006	29	38	0.00080	0.01560	1.025

Dynamic data: As in [27]

Power system stabilizers models - STAB1

Table B-11: Power system stabilizers data of the “39 bus New England System”.

Model	K/T	T	T1/T3	T3	T2/T4	T4	H_{LIM}
STAB1	10	10	5	0.02	5	0.1	0.2

Appendix C

The “BPA Power System” and “Nordic Power System”

C.1: Data of the “BPA power system”

Load flow data: $S_{base}=100MVA$

Table C-12: Bus data of the “BPA power system”.

No Bus	Bus Name	Base (kV)	Bus Type	Shunt (MVA)	$V_{Scheduled}$ (pu)	Angle (degree)	Pload (MW)	Qload (MVA)
1	'GEN 1'	13.8000	3	0.000	0.98000	0.0000	0	0
2	'GEN 2'	13.8000	2	0.000	0.96400	-8.3710	0	0
3	'GEN 3'	13.8000	2	0.000	1.0400	-26.4296	0	0
5	'BUS 5'	500.000	1	100.000	1.08799	-3.9654	0	0
6	'BUS 6'	500.000	1	100.000	1.06304	-12.2425	0	0
7	'BUS 7'	500.000	1	963.000	1.02337	-30.2168	0	0
8	'BUS 8'	13.8000	1	700.000	0.94072	-36.5965	3359	1044
9	'BUS 9'	115.0000	1	400.000	0.93775	-36.2825	0	0
10	'BUS10'	230.000	1	0.000	0.88961	-43.3881	0	0
11	'BUS11'	13.8000	1	100.000	0.91255	-45.7697	3486	0

Table C-13: Generators load flow data of the “BPA power system”.

No Bus	Gen Name	Base (kV)	Pgen (MW)	Qgen (MVA)	Sbase (MVA)	Qmin (MVA)	Qmax (MVA)
1	'GEN 1'	13.8000	4162.494	1166.611	9999	-5000	5000
2	'GEN 2'	13.8000	1736.000	672.133	2200	-200	725
3	'GEN 3'	13.8000	1155.000	653.724	1600	-200	700

Table C-14: Branch data of the “BPA power system”.

From Bus	To bus	ID	R (pu)	X (pu)	B (pu)
5	6	'1'	0.00000	0.00400	0.0000
6	7	'1'	0.00150	0.02880	1.17300
6	7	'2'	0.00150	0.02880	1.17300
6	7	'3'	0.00150	0.02880	1.17300
6	7	'4'	0.00150	0.02880	1.17300
6	7	'5'	0.00150	0.02880	1.17300
9	10	'1'	0.00100	0.00300	0.00000

Table C-15: Transformer data of the “BPA power system”.

From Bus	To bus	R (pu)	X (pu)	TAP	TAP Min	TAP Max	Vmin (pu)	Vmax (pu)	No of TAP	Type
1	5	0.000	0.00200	0.8857	0.9	1.1	0.9	1.1	33	Fixed
2	6	0.000	0.00450	0.8857	0.9	1.1	0.9	1.1	33	Fixed
3	7	0.000	0.00625	0.9024	0.9	1.1	0.9	1.1	33	Fixed
7	8	0.000	0.00300	1.06640	0.9	1.1	0.9	1.1	33	Fixed
7	9	0.000	0.00260	1.0800	0.9	1.1	0.9	1.1	33	Fixed
10	11	0.000	0.00100	0.9750	0.9	1.1	0.9	1.1	33	ULTC

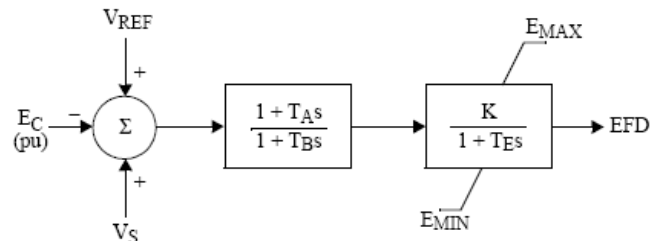
Dynamic data:

Table C-16: Generators dynamic data of the “BPA power system”.

Model	G1	G2	G3
	GENCLS	GENROU	GENROU
Xd	0	2.070	2.070
Xq	0	1.9900	1.9900
Xl	0	0.1550	0.1550
X'd	0	0.2800	0.2800
X'q	0	0.4900	0.4900
X''d	0	0.2150	0.2150
X''q	0	0.2150	0.2150
T'do	0	4.1000	4.1000
T'qo	0	0.5600	0.5600
T''do	0	0.0330	0.0330
T''qo	0	0.0620	0.0620
S(1.0)	0	0.1000	0.1000
S(1.2)	0	0.4000	0.4000
H	999.00	2.0900	2.0900
D	0.0000	0.0000	0.0000

Table C-17: Excitation dynamic data of the “BPA power system”.

Model	G2	G3
	SEXS	SEXS
T _A /T _B	0.1	0.1
T _B	10	10
K	400	400
T _E	0.02	0.02
E _{max}	6	6
E _{min}	0	0



Over-Excitation Limiter (OEL) model: MAXEX2

Under-Load Tap Changer (ULTC) model: OLTC1

Dynamic Motor Model: CIM5

C.2: Data of the “NORDIC power system”

Load-flow and dynamic data available at [122]

Generator models:

 Hydro generator models: GENSAL

 Thermal generator models: GENROU

Excitation system models: Simplified Excitation System: SEXS

Governor models: HYGOV

Power System Stabilizers: STAB1

Over-Excitation Limiter models: MAXEX2:

Under-Load Tap Changer models: OLTC1

Bibliography

- [1] Prabha Kundur, *Power System Stability and Control*. New York: McGraw-Hill, 1994.
- [2] Carson. W. Taylor, *Power System Voltage Stability*. New York: McGraw-Hill, 1994.
- [3] Sami Repo, "On-Line Voltage Stability Assessment of Power System – An Approach of Black-Box Modelling," Doctoral thesis at Tampere University of Technology, available at website:http://butler.cc.tut.fi/~repo/Julkaisut/SR_thesis.pdf, 2001.
- [4] Brant Eldridge, "August 2003 Blackout Review," available at website:<http://www.indiec.com/Meeting%20Schedule/2004/IEC%20Program%20Agenda%202004.html>.
- [5] "2003 North America Blackout," available at website:<http://www.answers.com/topic/2003-North-america-blackout>.
- [6] S. Corsi and C. Sabelli, "General Blackout in Italy Sunday September 28, 2003, h. 03:28:00," *IEEE Power Engineering Society General Meeting*, vol. 2, pp. 1691-1702, June 2004.
- [7] A. Berizzi, "Security Issues Regarding the Italian Blackout," in *Presentation at the IEEE PES General Meeting*, Milano, Italia, June 2004.
- [8] A. Allegato, "Report on Events of September 28th, 2003," Italia April 2004.
- [9] "Resources for Understanding Electric Power Reliability," Available at website:http://www.pserc.wisc.edu/Resources.htm#European_Blackout.htm.
- [10] R. G. Farmer and E. H. Allen, "Power System Dynamic Performance Advancement from History of North American Blackouts," *IEEE PES Power Systems Conference and Exposition*, pp. 293-300, 2006.
- [11] M. Schlöpfer, "Comparative Case Studies on Recent Blackouts " in *Workshop on Interdependencies and Vulnerabilities of Energy, Transportation and Communication 22 – 24 September 2005 Zurich, Switzerland* available at website:<http://pforum.isn.ethz.ch/docs/BAAF270D-65B0-58E9-217BE9DF3A540E24.pdf>, 2005
- [12] D. Novosel, "System Blackouts: Description and Prevention," in *IEEE PSRC System Protection RC, WG C6 "Wide Area Protection and Control", Cigre TF38.02.24 Defense Plans* November 2003.
- [13] G. Andersson et al, "Causes of the 2003 Major Grid Blackouts in North America and Europe, and Recommended Means to Improve System Dynamic Performance," *IEEE Transactions on Power Systems*, vol. 20, no 4, pp. 1922-1928, November 2005.

-
- [14] "U.S-Canada Power System Outage Task Force Final Report on the August 14, 2003 Blackout in the United States and Canada: Causes and Recommendations," *Available at website: <http://www.nerc.com>*, 2004.
- [15] S. Larsson and E. Ek, "The Black-out in Southern Sweden and Eastern Denmark, September 23, 2003," *IEEE Power Engineering Society General Meeting*, 2004
- [16] C. D. Vournas, V. C. Nikolaidis, and A. Tassoulis, "Experience from the Athens Blackout of July 12, 2004," in *IEEE Power Tech Russia*, 2005.
- [17] UCTE, "Final Report System Disturbance on 4 November 2006," *available at website: <http://www.ucte.org/library/otherreports/Final-Report-20070130.pdf>*.
- [18] Jean-LucThomas, "Rapport D'enequête de la Commission de Régulation de L'énergie sur la Panne D'électricité du Samedi 4 Novembre 2006, Commssion de Régulation de L'énergie- L'enquête réalisée par la CRE a été menée avec l'appui technique de Monsieur Jean-LucThomas, Professeur Titulaire de la Chaire d'Électrotechnique au Conservatoire national desarts et métiers (CNAM)," Paris, 7 février 2007.
- [19] S. Paduraru, "The Leap Forward Raising the Functionality and Impact of the Synchrophasor Measurement Systems on Power Systems Stability-A presentation at: International Conference on Synchrophasor Measurement Applications," Rio de Janeiro BRASIL, June 2006.
- [20] Prabha Kundur et al, "Definition and Classification of Power System Stability- IEEE/CIGRE Joint Task Force on Stability Terms and Definitions," *IEEE Transactions on Power Systems*, vol. 19, no 3, pp. 1387-1401, May 2004.
- [21] D. N. Kosterev, C. W. Taylor, and W. A. Mittelstadt, "Model Validation for the August 10,1996 WSCC System Outage," *IEEE Transactions on Power Systems*, vol. 14, no 3, pp. 967-979, August 1999.
- [22] L. Rouco, "Eigenvalue-Based Methods for Analysis and Control of Power System Oscillations," *IEE Colloquium on Power System Dynamics Stabilisation (Digest No 1998/196 and 1998/278)*, vol. 7, February 1998.
- [23] J. Persson, "Using Linear Analysis to find Eigenvalues and Eigenvectors in Power Systems," *available at website: <http://www.stri.se/metadot/index.pl?id=2426&isa=Category&op=show>*
- [24] L. Rouco and I. J. Perez-Arriaga, "Multi-Area Analysis of Small Signal Stability in Large Electric Power Systems by SMA," *IEEE Transactions on Power Systems*, vol. 8, no 3, pp. 1257-1265, August 1993.

-
- [25] P. Kundur, M. G. Rogers, D. Y. Wong, L. Wang, and M. G. Lauby, "A Comprehensive Computer Program Package for Small Signal Stability Analysis of Power Systems," *IEEE Transactions on Power Systems*, vol. 5, no 4, pp. 1076-1083, November 1990.
- [26] N. Martins, "The Dominant Pole Spectrum Eigensolver," *IEEE Transactions on Power Systems*, vol. 12, no 1, pp. 245-254, February 1997.
- [27] M. A. Pai, *Energy Function Analysis for Power System Stability*: Kluwer Academic Publishers, 1989.
- [28] C.-W. Liu and J. S. Thorp, "A Novel Method to Compute the Closest Unstable Equilibrium Point for Transient Stability Region Estimate in Power Systems," *IEEE Trans on circuits and systems*, vol. 44, no 7, pp. 630-635, July 1997.
- [29] G. D. Irisarri, G. C. Ejebe, J. G. Waight, and W. F. Tinney, "Efficient Solution for Equilibrium Points in Transient Energy Function Analysis," *IEEE Transactions on Power Systems*, vol. 9, no 2, pp. 693-699, May 1994.
- [30] D. Ruiz-Vega and M. Pavella, "Transient Stability: Assessment and Control," in *Chapter 7 of the book "Electric Power System"*, M. Crappe, Ed.: Wiley 2008.
- [31] E. Z. Zhout, O. P. Malik, and G. S. Hope, "Theory and Method for Selection of Power System Stabilizer Location," *IEEE Transactions on Energy Conversion*, vol. 6, no 1, pp. 170-176, March 1991.
- [32] K. Lakmeharan and M. L. Coker, "Optimal Placement and Tuning of Power System Stabilisers," in *Proceeding of IEEE AFRICON Cape Town, South Africa, 1999*.
- [33] M. Klein, G. J. Rogers, S. Moorty, and P. Kundur, "Analytical Investigation of Factors Influencing Power System Stabilizers Performance," *IEEE Transactions on Energy Conversion*, vol. 7, no 3, pp. 382-390, September 1992.
- [34] A. J. A. Simoes-Costa, F. D. Freitas, and H. E. Peiia, "Power Systems Stabilizer Design via Structurally Constrained Optimal Control," *Electric Power System Research*, vol. 33, no 1, pp. 33-40, April 1995.
- [35] F. D. Freitas and A. S. Costa, "Computationally Efficient Optimal Control Methods Applied to Power Systems," *IEEE Transactions on Power Systems*, vol. 14, no 3, pp. 1036-1045, August 1999.
- [36] S. S. Ahmed, "A Robust Power System Stabiliser for an Overseas Application," in *IEE Colloquium on Generator Excitation Systems and Stability London, UK, Feb 1996*.

-
- [37] M. M. Farsangi, Y. H. Song, and K. Y. Lee, "Choice of FACTS Device Control Inputs for Damping Interarea Oscillations," *IEEE Transactions on Power Systems*, vol. 19, no 2, pp. 1135-1143, May 2004.
- [38] N. Mithulananthan, C. A. Canizares, J. Reeve, and G. J. Rogers, "Comparison of PSS, SVC, and STATCOM Controllers for Damping Power System Oscillations," *IEEE Transactions on Power Systems*, vol. 18, no 2, pp. 786-792, May 2003.
- [39] L. Zhang, F. Wang, Y. Liu, M. R. Ingram, S. Eckroad, and M. L. Crow, "FACTS/ESS Allocation Research for Damping Bulk Power System Low Frequency Oscillation," in *Proceeding of IEEE Power Electronics Specialists Conference*, 2005.
- [40] P. Vuorenpää, T. Rauhala, P. Järventausta, and T. Käsälä, "On Effect of TCSC Structure and Synchronization Response on Subsynchronous Damping," *the International Conference on Power Systems Transients (IPST'07) in Lyon, France* June 4-7, 2007.
- [41] I. Dobson, T. Van Cutsem, C. Vournas, C.L. DeMarco, M. Venkatasubramanian, T. Overbye, and C.A. Canizares, "Basic Theoretical Concepts- Chapter 2 from: Voltage Stability Assessment: Concepts, Practices and Tools," *IEEE Power Engineering Society-Power System Stability Subcommittee Special Publication*, August, 2002.
- [42] V. Ajjarapu and B. Lee, "Bibliography on Voltage Stability," *IEEE Transactions on Power Systems*, vol. 13, no 1, pp. 115-125, February 1998.
- [43] Q. Wang and V. Ajjarapu, "A Critical Review on Preventive and Corrective Control Against Voltage Collapse," *Electrical Power Components and Systems*, vol. 29, December 2001.
- [44] T. V. Cutsem, "Voltage Instability: Phenomena, Countermeasures, and Analysis Methods," *Proceeding of The IEEE*, vol. 88, February 2000.
- [45] T. J. Overbye and I. Dobson, "Q-V Curve Interpretations of Energy Measures for Voltage Security," *IEEE Transactions on Power Systems*, vol. 9, no 1, pp. 331-340, February 1994.
- [46] B. H. Chowdhury and C. W. Taylor, "Voltage Stability Analysis: V-Q Power Flow Simulation Versus Dynamic Simulation," *IEEE Transactions on Power Systems*, vol. 15, no 4, pp. 1354-1359, November 2000.
- [47] Y. Tamura, H. Mori, and S. Iwamoto, "Relationship between Voltage Instability and Multiple Load Flow Solutions in Electric Power Systems," *IEEE Transactions on Power Apparatus and Systems*, vol. PAS-102, no 5, pp. 1115-1125, May 1983.

-
- [48] K. P. Basu, "Power Transfer Capability of Transmission Line Limited by Voltage Stability: Simple Analytical Expressions," *IEEE Power Engineering Review*, vol. 20, no 9, pp. 46-47, September 2000.
- [49] A. M. Chebbo, M. R. Irving, and M. J. H. Sterling, "Reactive Power Dispatch Incorporating Voltage Stability," in *IEE Proceedings-Generation, Transmission and Distribution* MAY 1992.
- [50] P. A. Lof, T. Smed, G. Anderson, and D. J. Hill, "Fast Calculation of a Voltage Stability Index," *IEEE Transactions on Power Systems*, vol. 7, no 1, pp. 54-64, February 1992.
- [51] B. Gao, G. K. Morison, and P. Kundur, "Voltage Stability Evaluation Using Modal Analysis," *IEEE Transactions on Power Systems*, vol. 7, no 4, pp. 1529-1542, November 1992.
- [52] A. C. Z. de Souza, C. A. Cañizares, and V. H. Quintana, "New Techniques to Speed up Voltage Collapse Computations Using Tangent Vectors," *IEEE Transactions on Power Systems*, vol. 12, no 3, pp. 1380-1387, August 1997.
- [53] A. Teshome and E. Esiyork, "Distance to Voltage Collapse through Second-Order Eigenvalue Sensitivity Technique," *International Journal of Electrical Power & Energy Systems*, vol. 17, no 6, pp. 425-431, December 1995.
- [54] A. Halim, K. Takashi, and B. Kermanshahi, "Dynamical Voltage Stability Analysis Using Lyapunov Function Method," in *Proceeding of The 8th international Conference on Harmonics and Quality of Power*, Greece, October 1998.
- [55] T. J. Overbye and C. L. Demarco, "Voltage Security Enhancement Using Energy Based Sensitivities," *IEEE Transactions on Power Systems*, vol. 6, no 3, pp. 1196-1202, August 1991.
- [56] T. J. Overbye, "Use of Energy Methods for Online Assessment of Power System Voltage Security," *IEEE Transactions on Power Systems*, vol. 8, no 2, pp. 452-458, May 1993.
- [57] C. W. Taylor, "Concepts of Undervoltage Load Shedding for Voltage Stability," *IEEE Transactions on Power Delivery*, vol. 7, no 2, pp. 480-488, April 1992.
- [58] T. V. Cutsem, "An Approach to Corrective Control of Voltage Instability Using Simulation and Sensitivities," *IEEE Transactions on Power Systems*, vol. 10, no 2, pp. 616-622, May 1995.

-
- [59] J. V. Hecke, N. Janssens, J. Deuse, and F. Promel, "Coordinated Voltage Control Experience in Belgium," *available at website: http://www.eurostag.be/download/TVC_BE_E.pdf*.
- [60] H. Lefebvre, D. Fragnier, J. Y. Boussion, P. Mallet, and M. Bulot, "Secondary Coordinated Voltage Control System: Feedback of EDF," *IEEE Power Engineering Society Summer Meeting*, vol. 1, pp. 290-295, 2000.
- [61] M. M. Begovic and A. G. Phadke, "Control of Voltage Stability Using Sensitivity Analysis," *IEEE Transactions on Power Systems*, vol. 7, no 1, pp. 114-123, February 1992.
- [62] C. Vournas and M. Karystianos, "Load Tap Changers in Emergency and Preventive Voltage Stability Control," *IEEE Transactions on Power Systems*, vol. 19, no 1, pp. 492-498, February 2004.
- [63] T. Quoc-Tuan, C. Praing, R. Feuillet, J. C. Sabonnadière, U. La-Van, and C. Nguyen-Duc, "Improvement of Voltage Stability on the Vietnam Power System," *IEEE Power Engineering Society Winter Meeting*, vol. 2, pp. 1513-1518 2000.
- [64] T. V. Menezes, L. C. P. d. Silva, and V. F. d. Costa, "Dynamic VAR Sources Scheduling for Improving Voltage Stability Margin," *IEEE Transactions on Power Systems*, vol. 18, no 2, pp. 969-971, May 2003.
- [65] Y. Su, S. Cheng, J. Wen, and Y. Zhang, "Reactive Power Generation Management for the Improvement of Power System Voltage Stability Margin," in *Proceeding of the 6th World Congress on Intelligent Control and Automation*, Dalian China, June 2006.
- [66] X. Wang, G. C. Ejebe, J. Tong, and J. G. Waight, "Preventive/Corrective Control for Voltage Stability Using Direct Interior Point Method," *IEEE Transactions on Power Systems*, vol. 13, no 3, pp. 878-883, August 1998.
- [67] Z. Feng, V. Ajjarapu, and D. J. Maratukulam, "A Comprehensive Approach for Preventive and Corrective Control to Mitigate Voltage Collapse," *IEEE Transactions on Power Systems*, vol. 5, no 2, pp. 791-797, May 2000.
- [68] T. V. Cutsem and C. D. Vournas, "Emergency Voltage Stability Controls: an Overview," *IEEE Power Engineering Society General Meeting*, pp. 1-10, June 2007.
- [69] M. K. Pal, "Assessment of Corrective Measures for Voltage Stability Considering Load Dynamics," *International Journal of Electrical Power & Energy Systems*, vol. 17, no 5, pp. 325-334, October 1995.

-
- [70] B. Otomega, V. Sermanson, and T. V. Cutsem, "Reverse-logic control of load tap changers in emergency voltage conditions," in *Proceeding of IEEE Power Tech Confonference*, Bologna, June 2003.
- [71] T. Q. Tuan, J. Fandino, and J. C. Sabonnadière, "Calculation of Load Shedding Using Sensitivities in Order to Avoid Voltage Collapse," in *Proceeding of the 27th Universities Power Engineering Conference, UPEC92*, University of Bath, 1992, pp. 161-164.
- [72] T. Q. Tuan, J. Fandino, N. Hadjsaid, J. C. Sabonnadière, and H. Vu, "Emergency Load Shedding to Avoid Risks of Voltage stability Using Indicators," *IEEE Transactions on Power Systems*, vol. 9, no 1, pp. 341-351, February 1994.
- [73] R. Balanathan, N. C. Pahalawaththa, U. D. Annakkage, and P. W. Sharp, "Under-Voltage Load Shedding to Avoid Voltage Instability," in *IEE Proceedings on Generation, Transmission and Distribution*, March 1998.
- [74] C. Moors, D. LeCebvre, and T. V. Cutsem, "Design of Load Shedding Schemes Against Voltage Instability," *IEEE Power Engineering Society Winter Meeting*, vol. 2, pp. 1495-1500, 2000.
- [75] J. E. Dagle, "Data Management Issues Associated with the August 14th, 2003 Blackout Investigation," *IEEE Power Engineering Society General Meeting* vol. 2, pp. 1680-1684, June 2004.
- [76] J. F. Hauer, N. B. Bhatt, K. Shah, and S. Kolluri, "Performance of WAMS East in Providing Dynamic Information for the North East Blackout of August 14, 2003," *IEEE Power Engineering Society General Meeting*, vol. 2, pp. 1685-1690, June 2004.
- [77] P. Kundur, "Power System Security in the New Industry Environment: Challenges and Solutions," in *IEEE Toronto Centennial Forum on Reliable Power Grids in Canada* available at website:<http://www.ewh.ieee.org/r7/toronto/events/oct0303/prabha.ppt>, 3 October 2003.
- [78] A. G. Phadke and J. S. Thorp, "Improved Control and Protection of Power Systems though Synchronized Measurements," *Control and Dynamic Systems*, Academic Press, vol. 43, 1991.
- [79] A. Phadke and J. Thorp, "History and Application of Phasor Measurements," available at website: http://www.ieee.org/portal/cms_docs_pes/pes/subpages/meetings-folder/PSCE/PSCE06/panel13/Panel-13-1_History_and_Applications.pdf, 2006.
- [80] E. Martin et al, "IEEE Standard for Synchrophasors for Power Systems " *IEEE Transactions on Power Delivery*, vol. 13, no 1, pp. 73-77, January 1998.

-
- [81] J. V. Milanovic and A. C. S. Duque, "The Use of Relative Gain Array for Optimal Placement of PSSs," *IEEE Power Engineering Society Winter Meeting*, vol. 3, pp. 992-996, 2001.
- [82] A. R. Messina, O. Begovich, J. H. López, and E. N. Reyes, "Design of Multiple FACTS Controllers for Damping Inter-area Oscillations: A Decentralised Control Approach," *International Journal of Electrical Power and Energy Systems*, vol. 26, no 1, pp. 19-29, January 2004.
- [83] E. Kreindler and P. E. Sarachik, "On the Concept of Controllability and Observability of Linear Systems," *IEEE Transactions on Automatic and Control*, vol. 9, no 2, pp. 129- 136, April 1964.
- [84] R. W. Brockett, *Finite Dimensional Linear Systems*. New York: Wiley, 1970.
- [85] B. C. Moore, "Principle Component Analysis in Linear Systems: Controllability, Observability and Model Reduction," *IEEE Transactions on Automatic and Control*, vol. 26, no 1, pp. 17- 32, February 1981.
- [86] J. Hahn and T. F. Edgar, "An Improved Method for Nonlinear Model Reduction Using Balancing of Empirical Gramians," *Elsevier, Computer & Chemical Engineering*, vol. 26, 2002.
- [87] J. Hahn and T. F. Edgar, "Balancing Approach to Minimal Realization and Model Reduction of Stable Nonlinear Systems," *Industrial & Engineering Chemistry Research*, vol. 41, no 9, pp. 2204-2212 2002.
- [88] J. Hahn, T. F. Edgar, and W. Marquardt, "Controllability and Observability Covariance Matrices for the Analysis and Order Reduction of Stable Nonlinear Systems," *Journal of Process Control*, vol. 13, no 2, pp. 115-127, March 2003.
- [89] J. J. Sanchez-Gasca, J. H. Chow, and R. Galarza, "Reduction of Linearized Power Systems for the Study of Inter-area Oscillations," in *IEEE Proceedings of the 4th Conference on Control Applications*, New York- USA, September 1995.
- [90] M. A. Wicks and R. A. Decarlo, "An Energy Approach to Controllability," in *Proceedings of the 27th Conference on Decision and Control*, Texas, December 1988.
- [91] D. Georges, "The Use of Observability and Controllability Gramians or Functions for Optimal Sensor and Actuator Location in Finite-Dimensional Systems," in *Proceedings of the 4th Conference on Decision and Control*, New Orleans-USA, 1995, pp. 3319-3324.

-
- [92] S. Leleu, H. Abou-Kandil, and Y. Bonnassieux, "Piezoelectric Actuators and Sensors Location for Active Control of Flexible Structures," *IEEE Transactions on Instrumentation and Measurement* vol. 50, no 6, pp. 1577-1582, December 2001.
- [93] A. Arbel, "Controllability Measures and Actuator Placement in Oscillatory Systems," *International Journal of Control*, vol. 33, no 3, pp. 565-574, 1981.
- [94] A. Hac and L. Liu, "Sensor and Actuator Location in Motion Control of Flexible Structures," *Journal of Sound and Vibration*, vol. 167, no 2, pp. 239-261, 1993.
- [95] H. D. Chiang, J. S. Thorp, J. C. Wang, J. Lu, and B. Aubert, "Optimal Controller Placements in Large-Scale Linear Systems," in *IEE Proceedings in Control Theory and Applications*, January 1992.
- [96] D. T. Nguyen, D. Georges, and Q. T. Tran, "An Energy Approach to Optimal Selection of Controllers/Sensors in Power System," *Accepted for publication in the International Journal of Emerging Electric Power Systems*.
- [97] "PSS/E 29 Online Documentation," PTI, INC, October 2002.
- [98] IEEE Std 421.5TM-2005, "Recommended Practice for Excitation System Models for Power System Stability Studies."
- [99] "Techniques for Power System Stability Limit Search," *IEEE PES, TP-138-0*.
- [100] M. L. Scala, M. Trovato, and C. Antonelli, "On-Line Dynamic Preventive Control: An Algorithm for Transient Security Dispatch," *IEEE Transactions on Power Systems*, vol. 13, no 2, pp. 601-610, May 1998.
- [101] D. H. Kuo and A. Bose, "A Generation Rescheduling Method to Increase the Dynamic Security of Power Systems," *IEEE Transactions on Power Systems*, vol. 10, no 1, pp. 68-76, February 1995.
- [102] A. A. Fouad and T. Jianzhong, "Stability Constrained Optimal Rescheduling of Generation," *IEEE Transactions on Power Systems*, vol. 8, no 1, pp. 105-112, February 1993.
- [103] Y. Katoh, H. Takada, and S. Iwamoto, "Transient Stability Preventive Control Using Kinetic and Critical Clearing Time," in *Proceedings of International Conference on Power System Technology*, Perth, WA, Australia, 2000.
- [104] Y. Kato and S. Iwamoto, "Transient Stability Preventive Control for Stable Operating Condition with Desired CCT," *IEEE Transactions on Power Systems*, vol. 17, no 4, pp. 1154-1161, November 2002.

-
- [105] J. Takeue, K. Takahashi, T. Ohtaka, and S. Iwamoto, "Transient Stability Preventive Control Using Critical Clearing Time Sensitivity," in *IEEE/PES Transmission and Distribution Conference and Exhibition 2002 Asia Pacific*, 2002.
- [106] W. Li and A. Bose, "A Coherency Based Rescheduling Method for Dynamic Security," *IEEE Transactions on Power Systems*, vol. 13, no 3, pp. 810-815, August 1998.
- [107] H. Takada, Y. Kato, and S. Iwamoto, "Transient Stability Preventive Control Using CCT and Generation Margin," *IEEE Power Engineering Society Summer Meeting*, vol. 2, pp. 881-886, 2001.
- [108] D. T. Nguyen, D. Georges, and Q. T. Tran, "Power Generation Redispatching to Improve Transient Stability in Power Systems using Controllability and Observability Gramians," in *The 43rd International Universities Power Engineering Conference – UPEC 2008*, Padova, Italy, 1-4 September, 2008.
- [109] D. T. Nguyen and D. Georges, "Controllability Gramian for Optimal Placement of Power System Stabilizers in Power Systems," in *the IEEE Asia Pacific Conference on Circuits and Systems, APCCAS*, 2006.
- [110] D. T. Nguyen and D. Georges, "Optimal Selection of Control Inputs in Power Systems," in *Proceeding of European Control Conference*, Kos, Greece, July 2-5, 2007.
- [111] N. D. Toan and D. Georges, "An Energy Approach to Optimal Selection of Controllers/Sensors in Power System," in *The 8th International Power Engineering Conference – IPEC2007* Singapore, 2007.
- [112] Tran Quoc Tuan, "Analyses et Outils pour La Proposion De Parades Contre Les Risques D'instabilité De Tension Dans Les Grands Réseaux De Transport et D'interconnexion," in *Laboratoire Génie Electrique-Institute National Polytechnique De Grenoble*. vol. Docteur, 24, February 1993.
- [113] R. A. Schlueter, M. W. Chang, and A. Costi, "Loss of Voltage Controllability As a Cause of Voltage Collapse," in *Proceeding of Proceedings of the Conference on Decision and Control*, December 1988.
- [114] P. A. Chamorel and A. J. Germond, "An Efficient Constrained Power Flow Technique Based On Active-Reactive Decoupling And The Use of Linear Programming," *IEEE Transactions on Power Apparatus and Systems*, vol. 101, no 1, pp. 158 - 168, January 1982.

-
- [115] G. Yesuratnam and D. Thukaram, "Optimum Reactive Power Dispatch and Identification of Critical On-load Tap Changing (OLTC) Transformers," *Taylor & Francis: Electric Power Components and Systems*, vol. 35, no 6 pp. 655 - 674 June 2007 , pages 655 - 674
- [116] D. Lefebvre, S. Bernard, and T. V. Cutsem, "Undervoltage Load Shedding Scheme for The Hydro-Québec System," *IEEE Power Engineering Society General Meeting*, vol. 2, pp. 1619-1624, June 2004.
- [117] "The CIGRE TF 38-02-08 BPA Test System Voltage Collapse," *available at website: http://www.eurostag.epfl.ch/users_club/cases/bpa/bpa.html*, December 1995.
- [118] "Load Representation for Dynamic Performance Analysis-IEEE Task Force on Load Representation for Dynamic Performance " *IEEE Transactions on Power Systems*, vol. 8, no 2, pp. 472-482, May 1993.
- [119] "Standard Load Models for Power Flow and Dynamic Performance Simulation-IEEE Task Force on Load Representation for Dynamic Performance," *IEEE Transactions on Power Systems*, vol. 10, no 3, pp. 1302-1313, August 1995.
- [120] C. D. Vournas and G. A. Manos, "Modelling of Stalling Motors During Voltage Stability Studies," *IEEE Transactions on Power Systems*, vol. 13, no 3, pp. 775-781, August 1998.
- [121] I. Dobson and L. Lu, "Voltage Collapse Precipitated by the Immediate Change in Stability When Generator Reactive Power Limits are Encountered " *IEEE Transactions on circuits and systems-I: Fundamental Theory and Applications*, vol. 39, no 9, pp. 762-766, September 1992.
- [122] "CIGRE TF 38-02-08: Long Term Dynamics Phase II," 1995.
- [123] C. A. Aumuller and T. K. Saha, "Investigating the Impact of Powerformer on Voltage Stability by Dynamic Simulation," *IEEE Transactions on Power Systems*, vol. 18, no 3, pp. 1142-1148, August 2003.
- [124] P. Kessel and H. Glavitsch, "Estimating The Voltage Stability of a Power System," *IEEE Transactions on Power Delivery*, vol. PWRD-1, no 3, pp. 346-354, July 1986.
- [125] "Power Systems Test Case Archive," *available at website: <http://www.ee.washington.edu/research/pstca/>*.
- [126] S. Kolluri and T. He, "Design and Operating Experience with Fast Acting Load Shedding Scheme in the Entergy System to Prevent Voltage Collapse," *IEEE Power Engineering Society General Meeting* vol. 2, pp. 1625-1630, June 2004.

- [127] IEEE PES Power System Relaying Committee, "Working Group C-13, System Protection Subcommittee- Undervoltage Load Shedding Protection," vol. Draft 4.1, available at website: <http://www.pes-psrc.org/c/>.
- [128] S. Imai, "Undervoltage Load Shedding Improving Security as Reasonable Measure for Extreme Contingencies," *IEEE Power Engineering Society General Meeting*, vol. 2, pp. 1754-1759, June 2005.
- [129] M. Begovic et al, "Summary of System Protection Voltage Stability," *IEEE Transactions on Power Delivery*, vol. 10, no 2, pp. 631-638, April 1995.
- [130] J. A. Diaz de Leon II and C. W. Taylor, "Understanding and Solving Short-Term Voltage Stability Problems," *IEEE Power Engineering Society Summer Meeting*, vol. 2, pp. 745-752, July 2002.
- [131] Le Ky, "Gestion optimale des consommations d'énergie dans les bâtiments." vol. Thèse pour obtenir le degré Docteur: Laboratoire Génie Electrique-Institute National Polytechnique De Grenoble, 10, Juillet 2008.

Personal Publications

- 1) D. T. Nguyen, D. Georges, and Q. T. Tran, "*Power Generation Redispatching to Improve Transient Stability in Power Systems using Controllability and Observability Gramians*" in The 43rd International Universities Power Engineering Conference - UPEC2008, Padova, Italy, 1-4 September, 2008.
- 2) D. T. Nguyen, D. Georges, and Q. T. Tran, "*An Energy Approach to Optimal Selection of Controllers/Sensors in a Power System,*" accepted for publication in the International Journal of Emerging Electric Power Systems - IJEEPS.
- 3) N. D. Toan and D. Georges, "*An Energy Approach to Optimal Selection of Controllers/Sensors in Power System,*" in The 8th International Power Engineering Conference – IPEC2007, Singapore, 2007.
- 4) D. T. Nguyen and D. Georges, "*Optimal Selection of Control Inputs in Power Systems,*" in Proceeding of European Control Conference, Kos, Greece, July 2-5, 2007.
- 5) D. T. Nguyen and D. Georges, "*Controllability Gramian for Optimal Placement of Power System Stabilizers in Power Systems,*" in the IEEE Asia Pacific Conference on Circuits and Systems, APCCAS-Singapore, December 2006.

TITRE

Contributions à l'analyse et à la prévention des blackouts de réseaux électriques

Résumé

Le réseau électrique joue un rôle important en tant qu'infrastructure majeure dans chaque pays. Toutefois, avec l'accroissement de la pression économique et environnementale, les systèmes électriques deviennent plus étendus, plus complexes et fonctionnant plus près de leur limite de stabilité. Les blackouts de réseau électrique qui se sont produits dans le monde ces dernières années sont la conséquence de cette situation. Cette thèse a pour objectif de fournir des solutions permettant de prévenir les blackouts de réseaux électriques. Une analyse des phénomènes de blackouts passés est tout d'abord proposée afin de comprendre leurs principales causes et leurs mécanismes. Sur la base de cette analyse, il est établi que les principales causes de blackouts sont directement liées aux problèmes de la stabilité, tels que la stabilité angulaire et la stabilité de tension. Afin de pouvoir prévenir les pannes du réseau causées par les problèmes de stabilité, une nouvelle approche énergétique fondée sur l'utilisation des grammiens de commandabilité et d'observabilité a été proposée. La méthode permet la meilleure sélection de contrôleurs/capteurs afin de pouvoir améliorer l'amortissement des oscillations électriques. Les résultats pourraient être appliqués à grande échelle aux systèmes électriques, afin de construire une nouvelle structure de commande robuste. Dans ce mémoire, cette approche énergétique a également été appliquée afin de maîtriser la stabilité transitoire. Il s'agit d'une méthode heuristique utilisant le gramien de commandabilité comme moyen de choisir les générateurs qui sont utilisés pour replanifier la production d'électricité afin d'améliorer la stabilité transitoire de plus en plus critique lors d'un blackout. Enfin, les principaux facteurs influençant l'écroulement de tension ont été pris en compte à long terme grâce à une approche par simulation dynamique. Une stratégie de contrôle préventif fondée sur un « power flow » optimal a été également proposée. Du point de vue de la prévention, le problème du délestage de charges en cas de sous-tension a été discuté et évalué.

Mots-clés: blackout électrique, stabilité « petits signaux », grammiens de contrôlabilité et d'observabilité, stabilité transitoire, écroulement de tension, délestage de charges.

TITLE

Contributions to analysis and prevention of power system blackouts

Abstract

The electrical power system plays an important role as the major infrastructure in any country. However, with the increases in economic and environment pressures, power systems now become large-scale, more complex and operating closer to their stability limit. Some power system blackouts occurred around the world in recent years are consequence of that situation. The main objective of this dissertation is to find some preventive solutions to avoid future power systems blackout. Some major analyses of past blackout phenomena were firstly investigated in order to understand the main causes and mechanism. From these analyses, the major reasons for power system blackouts are directly related to the stability problems, such as angle and voltage stability. In order to prevent power system from blackout caused by small signal stability, a novel energy approach based on controllability and observability gramians has been proposed. The method was applied to choosing the optimal selection of inputs in order to add damping to reduce power system oscillations. The results could be applied to large-scale power systems in order to build a new control structure with robustness properties. In this dissertation, this energy approach was also applied to prevent transient stability. The approach employs a heuristic method combination with controllability gramians to choose generators which are used to resdispatch power generation output in order to improve transient stability by mean of increasing critical clearing time. Finally, major factors influenced on voltage collapse have been taken into account through long-term dynamic simulation. One preventive control strategy based on optimal power flow has also been proposed. From the prevention point of view, some major discussions of undervoltage load shedding based on intelligent and directly controlled load have been given and tested.

Keywords: Power system blackout, small signal stability, controllability and observability gramians, transient stability, voltage collapse, undervoltage load shedding.
